SYNTHESIS AND REACTIONS OF HALOGENATED STILBENES MEDIATED BY LEWIS ACID AND QSAR STUDIES OF STILBENE ANALOGUES

MOHD FADZLI MD DIN

THESIS SUBMITTED IN FULFILMENT OF THE REQUIREMENTS FOR THE DEGREE OF DOCTOR OF PHILOSOPHY

FACULTY OF SCIENCE
UNIVERSITY OF MALAYA
KUALA LUMPUR

2016

UNIVERSITY OF MALAYA

ORIGINAL LITERARY WORK DECLARATION

Name of Candidate: **MOHD FADZLI BIN MD DIN** (

Registration/ Matric No: **SHC 080042**

Name of Degree: **Doctor of Philosophy**

Title of Project Paper/Research Report/Dissertation/Thesis ("this work"):

SYNTHESIS AND REACTIONS OF HALOGENATED STILBENES MEDIATED BY LEWIS ACID AND QSAR STUDIES OF STILBENE ANALOGUES

Field of Study: **ORGANIC CHEMISTRY**

I do solemnly and sincerely declare that:

(1)   I am the sole author/writer of this Work;
(2)   This Work is original;
(3)   Any use of any work in which copyright exists was done by way of fair dealing and for permitted purposes and any excerpt or extract from, or reference to or reproduction of any copyright work has been disclosed expressly and sufficiently and the title of the Work and its authorship have been acknowledged in this Work;
(4)   I do not have any actual knowledge nor do I ought reasonably to know what the making of this work constitutes an infringement of any copyright work;
(5)   I hereby assign all and every rights in the copyright to this Work to the University of Malaya ("UM"), who henceforth shall be owner of the copyright in this Work and that any reproduction or use in any form or by any means whatsoever is prohibited without the written consent of UM having been first had and obtained;
(6)   I am fully aware that if in the course of making this Work I have infringed any copyright whether intentionally or otherwise, I may be subject to legal action or any other action as may be determined by UM.

Candidate's Signature   Date: 18/4/2016

Subscribed and solemnly declared before,

Witness's Signature   Date: 18/4/2016

Name:
Designation: Professor Dr. Khalijah Awang
                        Department of Chemistry,
                        Faculty Science, University Malaya,
                        50603 Kuala Lumpur.

ABSTRACT

A total of nine halogenated stilbenes have been produced by Heck coupling method. Five halogenated stilbenes were then subjected to cytotoxicity test on five cancer cell lines and one normal human cell lines. (*E*)-*N*-(2-(3-fluorostyryl)phenyl)acetamide **98** displayed good antiproliferative on some of the cancer cell lines. Moreover, all the stilbenes did not show any cytotoxicity on the normal human cell line. Investigation on Lewis acid reactions; $FeCl_3$ and $SnCl_4$, were pursued on the halogenated stilbenes and produced imines for the former and indolines for the latter. Products conceived from these reactions were discussed thoroughly. Quantitative structure activity relationship (QSAR) study was done on several stilbene analogues to relate the bioactivity of the estrogen- insensitive breast cancer line with the molecular structure of the stilbene analogues. Three types of QSAR applied on these stilbene analogues were 2D QSAR, 3D QSAR and 3D QSAR pharmacophore. 3D QSAR pharmacophore showed the most promising model in predicting activity of new ligands.

ABSTRAK

Sembilan stilbena terhalogen telah dihasilkan melalui kaedah penggandingan Heck. Lima stilbena terhalogen telah diuji ketoksikan ke atas lima sel kanser dan satu sel normal. (*E*)-*N*-(2-(3-fluorostiril)fenil)asetamida **98** telah menunjukkan kesan antiproliferatif ke atas beberapa sel kanser. Demikian juga kesemua stilbena terhalogen tidak menunjukkan sifat toksik ke atas sel normal. Penyelidikan ke atas tindakbalas asid Lewis; $FeCl_3$ dan $SnCl_4$, telah dijalankan ke atas stilbena terhalogen bagi menghasilkan produk imina bagi $FeCl_3$ dan produk indolina bagi $SnCl_4$. Produk yang terhasil daripada tindakbalas ini telah dibincangkan dengan terperinci. Kajian Hubungan Struktur Aktiviti Kuantitatif (QSAR) telah dijalankan ke atas beberapa analog stilbena untuk menghubungkan bioaktiviti sel kanser payudara yang tak sensitif estrogen dengan struktur molekul analog stilbena. Tiga jenis QSAR telah dijalankan ke atas analog stilbena ini ialah 2D QSAR, 3D QSAR and 3D QSAR farmakofor. 3D QSAR farmakofor menunjukkan bahawa model ini adalah yang paling memberangsangkan dalam meramal activiti bagi ligan yang baharu.

Acknowledgements

Alhamdullillah, all praise to Allah for helping me through my PhD studies. I would like to thank Prof . Dr. Khalijah Awang for her guidance, encouragement and all the discussion that we had together. A big thank you to Dr Leong for his assistance in the QSAR studies. To the late Associate Prof. Dr. Mat Ropi Mukhtar for his support. Thank you to Associate Prof. Dr. Ibrahim Noorbatcha for his help on the computational part and Prof. Marilyn Olmstead for the crystal structure.

A special thank you to Kak Nor, Encik Nordin, Fateh and Kak Fiono for their help on the NMR machine.To Pak Din and Rafly, thank you for the help in maintaining the lab. A great thank you to my friends, Kee and Ang for all your help in the lab and all the discussion that we had together. Thank you to Chong, Aimi, Azmi, Nana, Azeana, Momo, Joey, Chan, Ahmad Kaleem, Omar, Faizah, Remy and all the phytochemistry members for your support and help.

I am grateful for the scholarship provided by MOE and Universiti Malaya to undertake this PhD programme.

A big hug and thank you to my mum and dad for all your support and love. All the advice and prayers that you give me.

To my love, my wife, Siti Balkis, thank you for being there for me and supporting me.

Contents

List of Schemes

List of Figures

List of Tables

ABBREVIATIONS

dppf	1,1'-Bis(diphenylphosphino)ferrocene
AIBN	2,2'-azobisisobutyronitrile
NMR	Nuclear Magnetic Resonance
COSY	Correlation Spectroscopy
DMSO	Dimethylsulfoxide
DNA	Deoxyribonucleic Acid
HMBC	Heteronuclear Multiple-Bond Correlation
HMQC	Heteronuclear Multiple-Quantum Coherence
HSQC	Heteronuclear Single-Quantum Correlation spectroscopy
NOE	Nuclear Overhauser Effect
s	singlet
d	Doublet
t	Triplet
q	Quartet
m	multiplet
IR	Infrared spectroscopy
MS	Mass Spectrometry
THF	Tetrahydrofuran
DMF	Dimethylformamide
TLC	Thin Layer Chromatography
UV	Ultraviolet spectroscopy
HPLC	High-Pressure Liquid Chromatography

Chapter 1

Introduction And Background

1.1   Stilbenoids

Stilbenes can be characterized as compounds with two phenyl ring connected to each other by an olefinic bridge. It is commonly found in a planar conformation and exist in two isomers. The first is the *E* type or *trans* stilbene **1** and the second is the *Z* type or *cis* stilbene **2**. It was first mentioned in a book manual written by Fownes in 1869.[1]

1   **2**
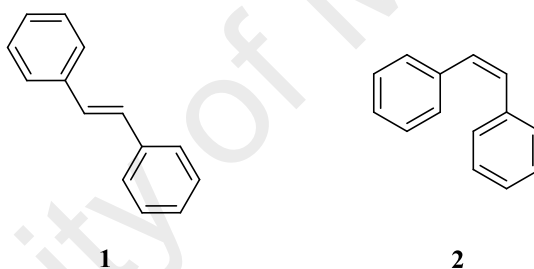
The first stilbene discovered from nature was by Takaoka, a Japanese scientist from the *Veratrum grandiflorum* plant in 1939 and was named resveratrol **3**. Resveratrol contained two hydroxyl group on one ring and one hydroxyl group on the other. Resveratrol was known for its pharmacological properties and the same goes for other resveratrol analogues such as pterostilbene **4**, isorhapontigenin **5** and piceatannol **6** as shown in Figure 1.1.[2,3] Due to their various pharmacological properties such as anticancer, antioxidant and antimitotic, stilbenes are widely synthesized and studied on their activities by researchers worldwide.[4,5,6]
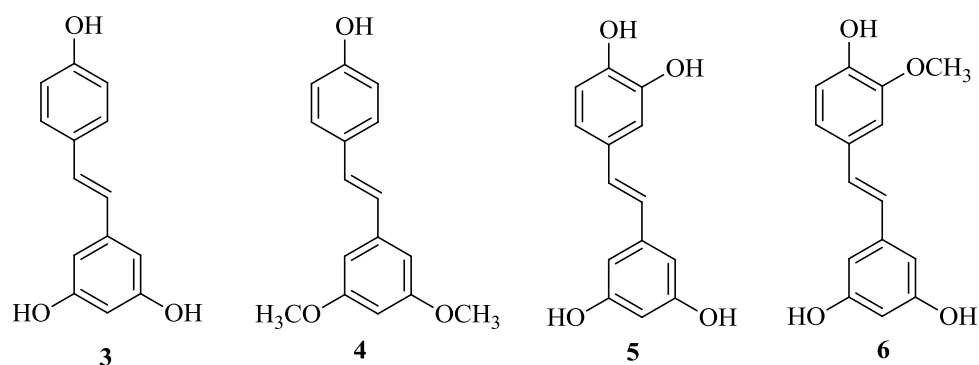
Figure 1.1 : Well-known pharmacologically active stilbenes.

Stilbenes act as precursors to the synthesis of natural oligostilbenoids. Oligostilbenoids are also attracting immense attention due to their significant biological activities and complex structures.[7] Exquisite examples of the complexity of their structures can be seen in the octameric vateriaphenol A **7** which was isolated from *Vateria indica*, hopeaphenol **8** was the first isolated oligostilbenoid, and originated from *Hopea odorata* in 1951 in Malaysia by Coggon[8] and elucidated through X-ray analysis in 1970,[9] and α-viniferin **9** which is abundant in plants from Vitacea family.[10]

Apart from medicinal and health application, stilbenes are used as an organic dye in the operation of the dye laser.[11] Stilbenes are also used in the hole-transporting agent for the photoreceptor which act as a function in the electrophotographic.[12] In LED, stilbenes are used as substituents for pendafluor bulbs mainly for its energy saving properties. Stilbenes also proved to be good copolymers in the composite for LED.[13,14]

There are many ways to synthesize stilbenes. Likhtenshtein (2010) have written a comprehensive classic synthetic method on the synthesis of stilbenes and their application in chemistry[15] and Velu (2012) have recently written a review on making stilbenes and stilbenes role as a precursor in producing oligostilbenoids via
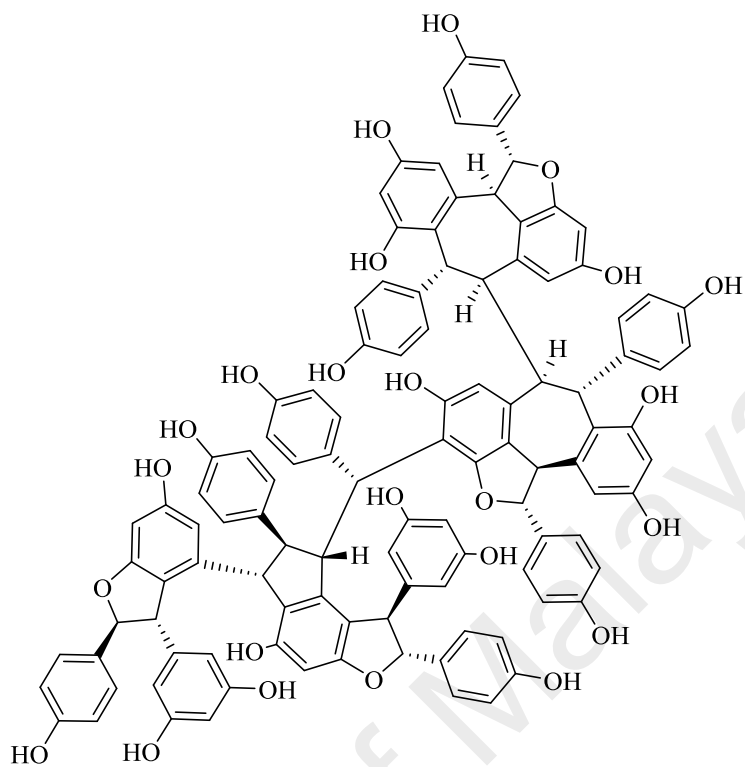
7
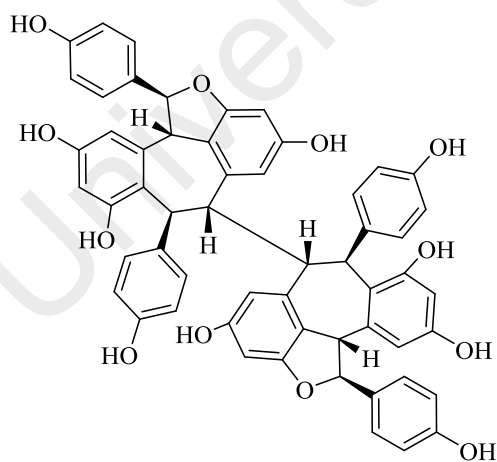
8
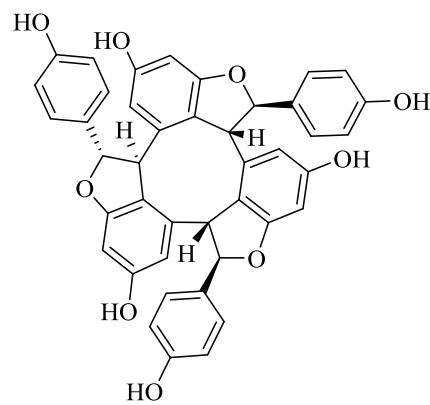
9

biotransformation and through chemical reactions.[16] In general, the method can be divided into two i) palladium mediated coupling and ii) non-palladium coupling which uses other type of metal promoted coupling of stilbenes and non-metals such as phosphine. One of the most popular methods in generating stilbenes is the Heck-Mizoroki method which uses palladium catalyst. This invention has led to the 2010 Nobel Prize being awarded to Heck, Negishi and Suzuki.[17]

1.2   Stilbenes Reaction with Lewis Acid

The studies of stilbenes reaction with Lewis acid provide the insight into the radical mechanism behind it and also the possible synthetic routes to other oligomeric stilbenes. Among the earliest reaction between stilbenes and Lewis acid was conducted by Heiba in 1968.[18] *Trans* stilbene **1** was reacted with manganese (III) acetate in acetic acid at 135 °C with added potassium acetate to raise the temperature of the solution to yield γ-butyrolactones **10** in 16% yield (Scheme 1.1).

Reaction involving stilbenes and Lewis acid started to gain attention in the years to come. Engler who have written some interesting papers on stilbene reactions with Lewis acid published a study in 1995 in which stilbene was reacted with benzoquinones in a Lewis acid promoted reaction at −78 °C in CH_2Cl_2 to attain benzofurans **A** and new phenyl substituted stilbenes **B** (Scheme 1.2).[19]
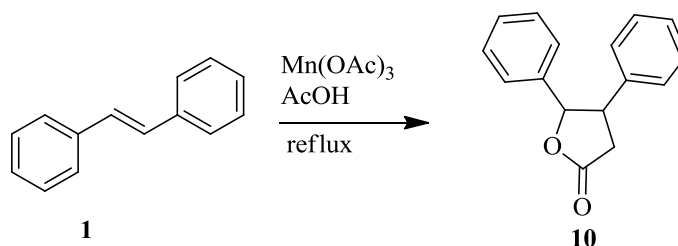
Scheme 1.1: Synthesis of γ-butyrolactones **10** from stilbene **1**.
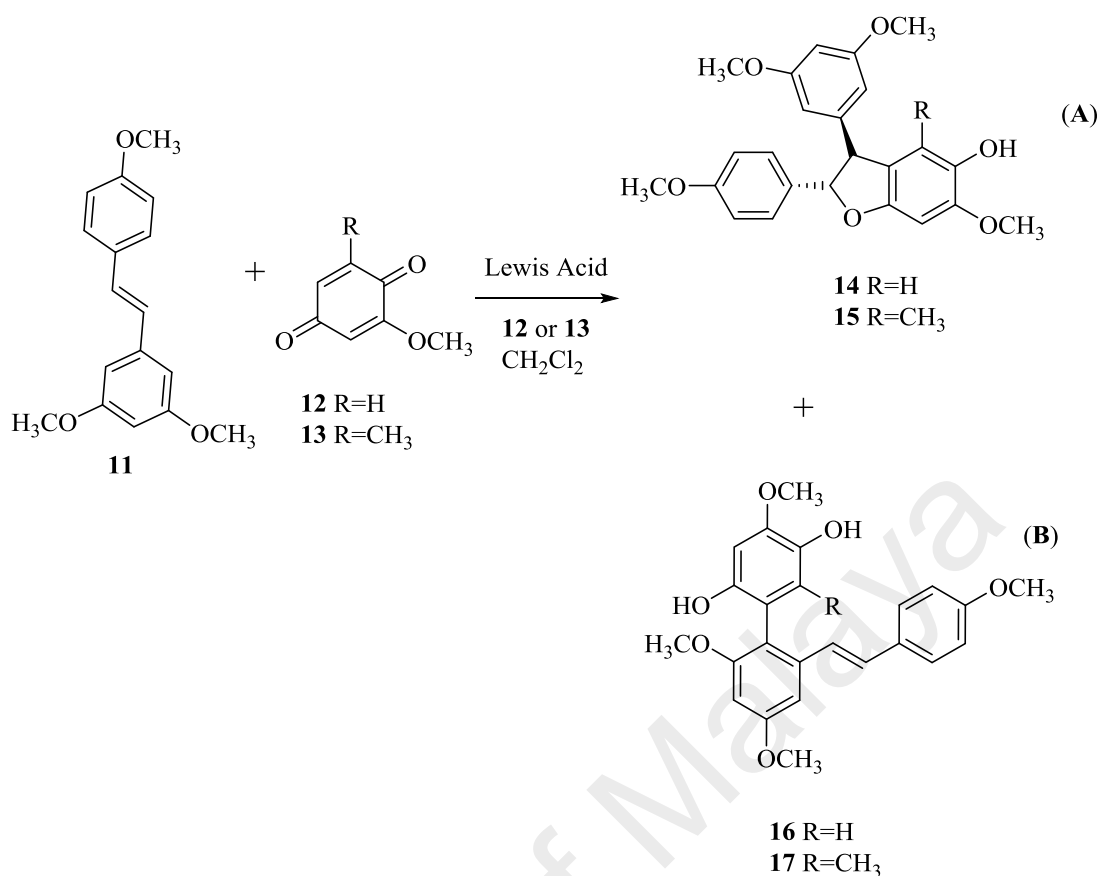
Scheme 1.2: Stilbene **11** reaction with Lewis acid.

Inspired by the isolation of natural occurring oligostilbenoid from the plant *Neobalanocarpus heimii* by Weber,[20] Thomas in 2002 have succeeded in producing dihydronaphthalene **19** from stilbene **18** which are electron rich by reaction with $FeCl_3$ in dichloromethane.[21] The formation of dihydronaphthalene **19** was discussed extensively through pericyclic transformation of the stilbene (Scheme 1.3). Our group was the first to study the reaction mechanism between acetamido stilbenes and Lewis acid ($FeCl_3$). Then after a decade, our group published a paper on the study of various groups attached to the amide and the mechanism involved in the creation of the bisindoline dimers and indolines through $FeCl_3$ promoted reaction, it was thoroughly investigated by Kee.[22]

5
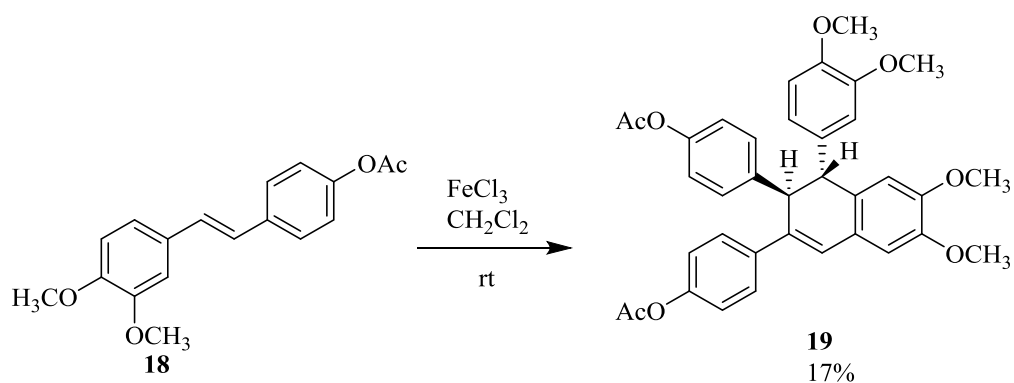
Scheme 1.3 : Reaction of stilbene **18** with Lewis acid yielding dihydronaphthalene **19**.

1.3   Computational Chemistry

The immense works on the syntheses of stilbenes have led to the evaluation of the biological activities of the synthesized compounds. The amounts of biological data from the vast array of stilbenes have intrigued scientist to think of ways to find relationships between structural features of compounds and the biological activities. One of the approaches is to analyze the skeletal type and functional groups. For example, Ruan have designed a series of resveratrol acrylamide amine derivatives and tested on three cancer cell lines.[23] From the data, it was observed that aromatic amine derivatives were better than the fatty amine derivatives against human chronic myelocytic leukemia cell (K562), human hepatoma (HuH-7) and human lung carcinoma (A549). Then scientists move further in trying to interpret the relationship mathematically hence to develop a model description that could predict the activity of a compound towards a biological cell, that's how QSAR (Quantitave Structure Activity Relationship) was borne. 2D-QSAR was carried out by Tripathi on 24 stilbene derivatives of resveratrol for their affinity to aryl hydrocarbon receptor (AhR).[24] AhR regulate the biological response towards the planar aromatic hydrocarbons. Statistical method that was applied was the multi linear regression model (MLR) in Systat 7.0

software. By using this model, the strength of the stilbenes towards AhR could be predicted. It was concluded from the study that the structural parameter (the *trans* geometry in the stilbene) and the hydrophobicity positively influenced the activity.

1.4   Problems to be Addressed

Over the years, biomimetic syntheses of oligostilbenoids were based on the coupling or cyclization of resveratrol and its derivatives. The endeavour was mostly pursued through biotransformation and the use of inorganic salt. Previously our group have started studies on Lewis acid mediated reaction on amide stilbenes which are the first attempt on non-resveratrol based stilbene in yielding oligostilbenoid. This attempt resulted in the formation of bisindoline, indoline and an indolo stilbene dimer. For this study, halogenated acetamido stilbenes are used because no halogen bearing stilbenes have ever been attempted before in the reaction with Lewis acid. Whether these halogenated acetamido stilbenes will follow previous reaction pathway of amido stilbenes with Lewis acid yielding indoline based product will be revealed later in the thesis. The pharmacological effect of the amido stilbenes on biological assay is extensively elaborated in computational studies through QSAR (Quantitative Structure Activity Relationship).

1.5   Objectives of This Study

In view of the biological importance of stilbenes and interesting products produced from reactions of stilbenes with Lewis acid, our group initiated the study on acetamido stilbenes. Previous works were focussed on stilbenes substituted with electron donating groups such as methoxyl and acetoxyl, while in this work attention is

given on stilbenes substituted with electron-withdrawing groups, in particular the halogens; F, Cl and Br. The specific objectives of this study are as follows.

1) To synthesize halogenated acetamido stilbenes by palladium catalyst coupling and investigate its cytotoxic activities.

2) To study the chemistry of the electron deficient halogenated acetamido stilbenes reaction with Lewis acids; $FeCl_3$ and $SnCl_4$, and the products of the reactions.

3) To perform Quantitative Structure Activity Relationship (QSAR) studies in order to relate the relationship between stilbene structures and cytotoxic activity.

1.6   Scope

In this study, the halogenated acetamido stilbenes were produced through Heck coupling and submitted to Lewis acid ($FeCl_3$ and $SnCl_4$) mediated reaction. From this, we hope to understand the mechanism governing this reaction. Furthermore, the understanding of the biological properties of stilbene analogues is obtained through QSAR studies.

1.7   Significance of Research

Through the Lewis acid mediated reaction of amido stilbenes, a better comprehension of the mechanistic pathway obtained from this study will lead to synthesizing other forms of oligostilbenoids. In addition, an improved pharmacologically design of stilbene would be made possible from outcome of the QSAR models.

1.8   References

1   G. Fownes, *A Manual on Elementary Chemistry, Theoratical and Practical*, Henry C. Lea, Philadelphia, 1869.

2   R. Maurya, A. B. Ray, F. K. Duah, D. J. Slatkin and P. L. Schiff, *J. Nat. Prod.*, 1984, **47**, 179.

3   D. Lee, M. Cuendet, J. S. Vigo, J. G. Graham, F. Cabieses, H. H. S. Fong, J. M. Pezzuto and A. D. Kinghorn, *Org. Lett.*, 2001, **3**, 2169.

4   A. H. Hasiah, A. R. Ghazali, J. F. Weber, S. Velu, N. F. Thomas and S. H. Inayat Hussain, *Hum. Exp. Toxicol.*, 2011, **30**, 138.

5   C. J. Lion, C. S. Matthews, M. F. G. Stevens, and A. D. Westwell, *J. Med. Chem.*, 2005, **48**, 1292.

6   M. A. Reddy, N. Jain, D. Yada, C. Kishore, J. R. Vangala,; P. S. Reddy, A. Addlagatta, S. V. Kalivendi and B. Sreedhar, *J. Med. Chem.*, 2011, **54**, 6751.

7   K. Xiao, H.-J. Zhang, L. J. Xuan, J. Zhang, Y. M. Xu and D. L. Bai, in *Studies in Natural Products Chemistry*, ed. A. Rahman, Elsevier, London, 2008, vol. 34, p. 453.

8   P. Coggon, N. F. Janes, F. E. King, T. J. King, R. J. Molyneux, J. W. W. Morgan and K. Sellars, *J. Chem. Soc.*, 1965, 406.

9   P. Coggon, A. T. McPhail and S. C. Wallwork, *J. Chem. Soc. B: Phys. Org.*, 1970, 884.

10   R. J. Pryce and P. Langcake, *Phytochemistry*, 1977, **16**, 1452.

11   W. Rettig, B. Strehmel and W. Majenz, *Chem. Phys.*, 1993, **173**, 525.

12   *US Pat.*, US7977020, 2011.

13   *US Pat.*, US20050017629A1, 2005.

14   U. Mitschke and P. Bauerle, *J. Mat. Chem.*, 2000, **10**, 1471.

15   G. Likhtenshtein, *Stilbenes : Applications in Chemistry, Life Sciences and Materials Science*, Wiley, Weinheim, 2010.

16   S. S. Velu, N. F. Thomas and J. F. F. Weber, *Curr. Org. Chem.*, 2012, **16**, 605.

17   C. C. C. Johansson Seechurn, M. O. Kitching, T. J. Colacot and V. Snieckus, *Angew. Chem. Int. Ed.*, 2012, **51**, 5062.

18   E. I. Heiba, R. M. Dessau and W. J Koehl, *J. Am. Chem. Soc.*, 1968, **90**, 5905.

19   T. A. Engler, G. A. Gfesser and B. W. Draney, *J. Org. Chem.*, 1995, **60**, 3700.

20   J. F. F. Weber, I. Abdul Wahab, A. Marzuki, N. F. Thomas, A. Abdul Kadir, A. H. A. Hadi, K. Awang, A. Abdul Latiff, P. Richomme and J. Delaunay, *Tetrahedron Lett.*, 2001, **42**, 4895.

21   N. F. Thomas, K. C. Lee, T. Paraidathathu, J. F. F. Weber, K. Awang, D. Rondeau and P. Richomme, *Tetrahedron*, 2002, **58**, 7201.

22   C. H. Kee, A. Ariffin, K. Awang, I. Noorbatcha, K. Takeya, H. Morita, C. G. Lim and N. F. Thomas, *Molecules*, 2011, **16**, 7267.

23   B. F. Ruan, S. Q. Wang, X. L. Ge and R. S. Yao, *Lett. Drug Des. Discov.*, 2014, **11**, 2.

24   T. Tripathi and A. Saxena, *Med. Chem. Res.*, 2008, **17**, 212.

Chapter 2

Synthesis And Lewis Acid Mediated Reactions Of Stilbenes

Methods on producing diverse stilbene molecules that are regularly employed by chemist are through the merging of two aromatic rings. These couplings of rings are frequently performed by utilising Heck, Suzuki, Wittig, Horner-Wadsworth-Emmons couplings and Perkins condensation. Studies on the effect of Lewis acid on stilbenes normally utilize these range of Lewis acid; $Mn(OAc)_3$, $FeCl_3$, $SnCl_4$ and $TiCl_4$.

2.1   Stilbene Synthesis

The syntheses of stilbenes have attracted immense interest and various methods have been developed. Here, the syntheses are categorised into two major methods which are:

i)   Palladium catalyzed syntheses of stilbenes

ii)   Non-palladium catalyzed syntheses of stilbenes

2.1.1 Palladium Catalyzed Syntheses of Stilbenes

The procedure in synthesizing stilbenes by palladium catalyst was first reported by Richard Heck in 1969 using arylmercuric halide and palladium (II) acetate in reaction with propylene.[1] Heck improvised the method by including a base, a hindered amine *tri-n*-butylamine (*n*-Bu$_3$N) and replaced the arylmercuric chloride with aryl halide **20** and styrene **21**.[2]

Independently, Mizoroki also investigated on the catalytic function of palladium, and palladium(II) chloride was chosen with potassium acetate as base in methanol for coupling of aryl halide **20** and styrene **21**.[3] Both Heck and Mizoroki produced stilbene **1** in 75% and 90% yield as shown in Scheme 2.1.
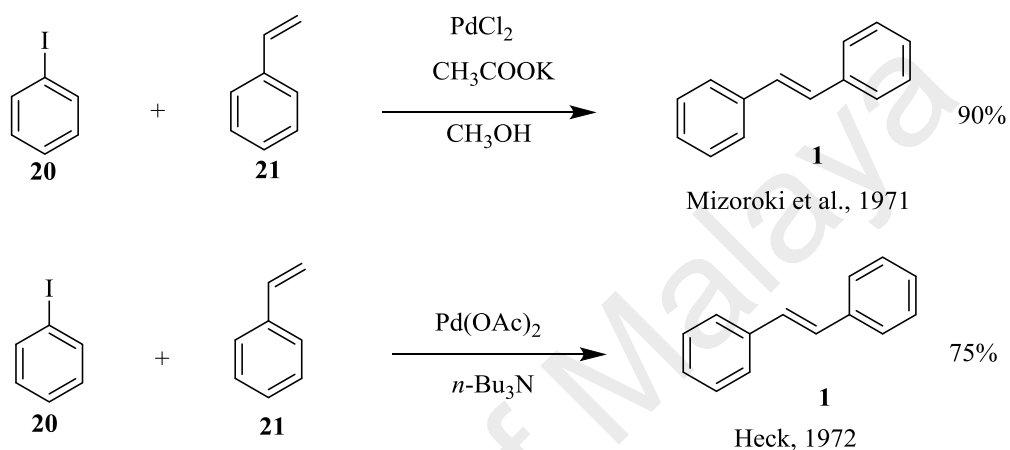
Scheme 2.1 : The synthesis of stilbene using the Heck-Mizoroki method.

Morales-Morales have created another palladium based catalyst which is highly efficient with turnover of 10^6 for reactions with bromo and iodo benzenes.[4] The palladium phosphino-thioether P–S chelate complex catalyst assisted in the coupling of 2-chloro bromobenzene **22** with styrene 2**1** and with sodium carbonate as base yielded an excellent 96% yield of stilbene **23** as shown in Scheme 2.2.

Studies on the solid support of the Heck method were pursued by Hamza by adding iodobenzene **20** with styrene 2**1** catalyzed by silica sol−gel encaged $PdCl_2(PPh_3)_2$ in the presence of Pr_3N base resulting in 84% of stilbene **1** being produced.[5] The costly palladium catalyst was recycled back and did not lose any catalytic activity (Scheme 2.3).
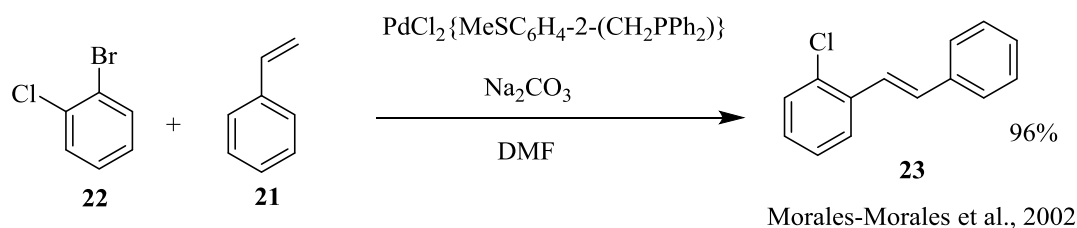
Scheme 2.2 : Morales-Morales produced an excellent yield of stilbene **23** using palladium phosphino-thioether P–S chelate complex.
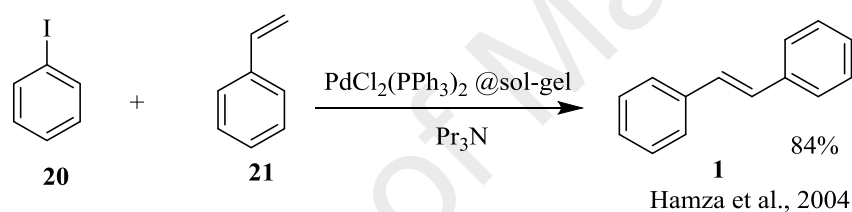
Scheme 2.3 : Synthesis of stilbene **1** using the recycled silica sol−gel encaged PdCl$_2$(PPh$_3$)$_2$.

Albert reported the versatile catalytic reaction of palladium (II) acetate when hydroxystyrene **24** reacted with halo benzene **25** in the presence of triethanolamine at 100 °C to yield various hydroxylated stilbenes **26** as shown in Scheme 2.4.[6]
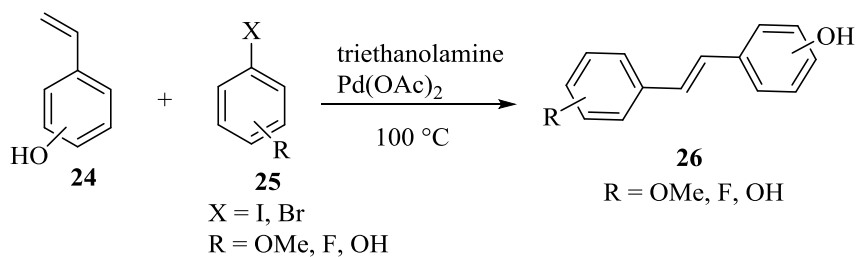
Scheme 2.4 : Albert's synthesized hydroxylated stilbenes **26**.

In 2010, Luo showed the stereoselective synthesis of the *trans* 2**8** and *cis* **29** stilbenes in Scheme 2.5 using palladium catalyzed reduction of alkynes **27** in the presence of HSiEt₃ and dppf (1,1'-Bis(diphenylphosphino)ferrocene).[7] CuSO₄ played a stereoselective role in transforming the *cis* to *trans* stilbene in moderate yield.
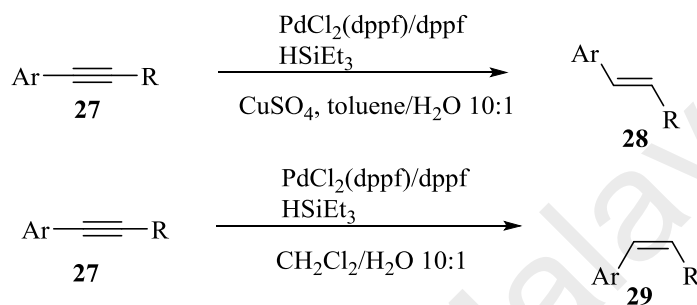
Scheme 2.5 : Luo's stereoselective synthesis of *trans* **28** and *cis* **29** stilbenes.

An excellent review on the synthesis of stilbene via Heck reactions was produced by Le Bras by the intermolecular dehydrogenative reaction[8] and the use of metal organic framework (MOF) by Dhakshinamoorthy.[9] Velu et al., (2012) wrote a review on the syntheses of oligostilbenoids using biotransformation, metal catalyzed synthesis and electrochemical reactions.[10]

2.1.2 Non-Palladium Catalyzed Syntheses of Stilbenes

Non-palladium catalyzed reaction of stilbene have also been reported. Warren used titanium (III) chloride to synthesized stilbene **31** from aldehyde **30** without the need for arylhalide and styrene.[11] The process gave a symmetrical stilbene **31** in 95% yield (Scheme 2.6).
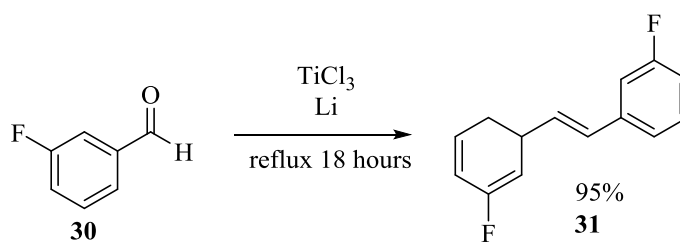
Scheme 2.6 : Warren's synthesis of symmetrical stilbene **31**.

Kabalka have reported an efficient and without the use of expensive palladium catalyst to produce symmetrical stilbene in an economical method **33**.[12] By reacting with lithium *tert*-butoxide, they homocoupled an aryl aldehyde tosylhydrazones **32**. Lithium tosylate precipated out from this process. Trimethyl borate was added to prevent the lithium tosylate from reacting with the aryl carbene intermediate (Scheme 2.7).

X=H,F,Cl,Br,Me,OMe,CN,NO$_2$
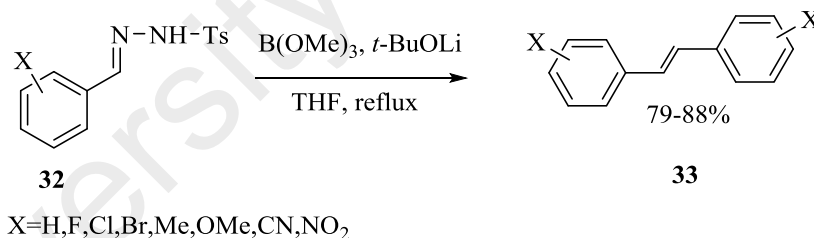
Scheme 2.7 : An inexpensive method of generating stilbene **33** by Kabalka (2001).

Synthesizing stilbenes through *in-situ* Ramberg−Bäcklund Rearrangement was reported by Soderman.[13] 1,2-Dibromotetrachloroethane BrC(Cl$_2$)CBr(Cl$_2$) as the halogenation agent was chosen as it was inexpensive and a non-ozone depleting substances (ODS), was reacted with sulfones **34** in the presence of a strong base KOH-Al$_2$O$_3$. The mixture was dissolved in *t*-BuOH/THF and reacted at room temperature to produce various stilbenes **35** in great yield (Scheme 2.8).
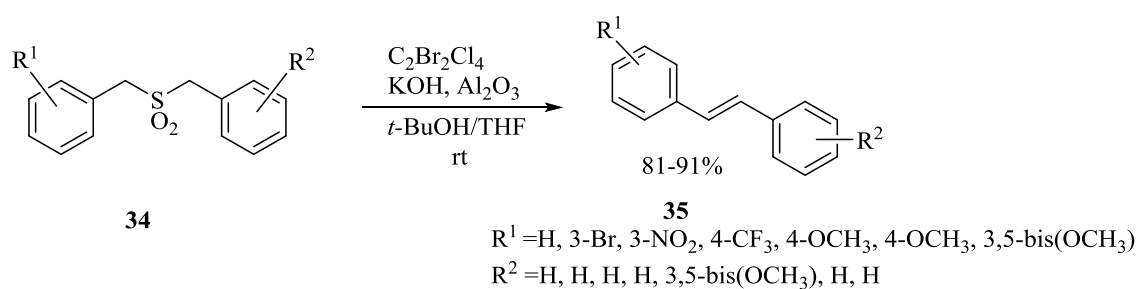
Scheme 2.8 : Soderman's synthesis of stilbenes **35** from sulfones **34.**

The use of phosphonate in preparing stilbene was reported by Chakrapani via the Horner-Wadsworth-Emmons reaction whereby prenylated benzaldehyde **36** and geranylated phosphonate **37** were reacted in the presence of t-BuOK.[14] This resulted in good amount of the prenylated and geranylated stilbene **38** (Scheme 2.9).
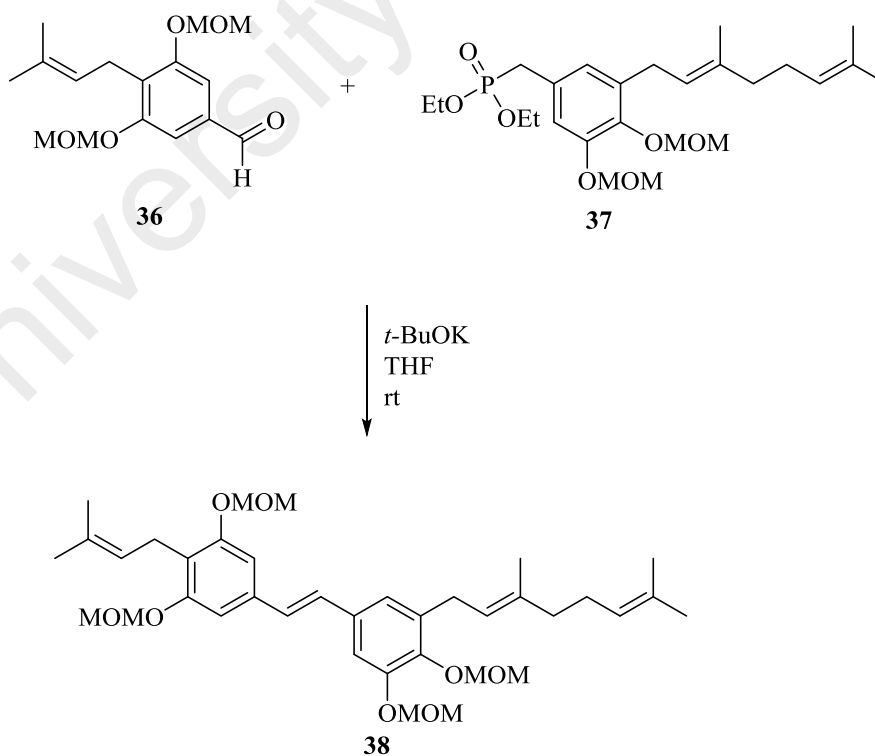
Scheme 2.9 : Prenylated and geranylated stilbene **38** by Chakrapani et al. (2010).

While palladium has been extensively used for the coupling of stilbene, rhodium catalyzed reaction is gaining ground in the C-H bond activation cross-coupling of various stilbenes. Patureau showed various olefination of unactivated acetanilides by rhodium catalyzed coupling.[15] Different substituted acetanilides **39** were reacted with various styrenes **40** via a low loading rhodium catalyst [RhCp*Cl$_2$]$_2$ in the presence of an oxidant Cu(OAc)$_2$. This *ortho*-olefination of acetanilides gave stilbenes **41** in good amount for electron rich or halogenated groups (Scheme 2.10).
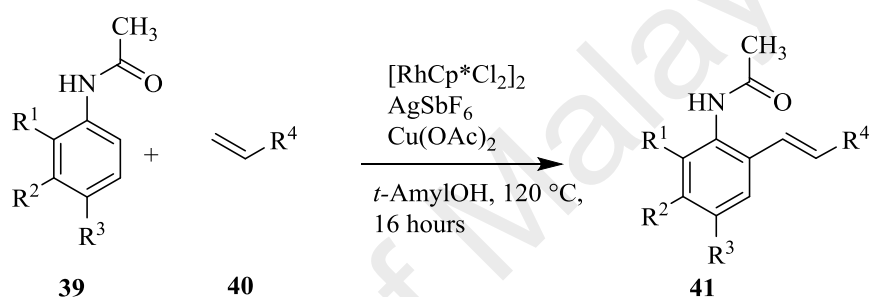
Scheme 2.10 : Patureau's rhodium catalysed stilbenes **41.**

2.2 Stilbene Reactions Through Radical Pathway

Free radical was first reported in 1815 by heating mercuric cyanide to form cyanogen (the dimer of •CN).[16] Turning to the 1900's, the earliest physical method in the detection carbon based radical cation was achieved by using the cathode ray in the gas phase. In normal temperature, viable free radicals as reactive intermediates in organic reaction solution were beginning to be accepted in general through the article written by Walling.[17] With the advent of time-resolved EPR (TREPR) and time-resolved NMR (CIDNP) provide a great understanding of the mechanistic of radical chemistry.[18,19]

The mechanistic and detection of carbon centered free radicals and radical cations have been neatly described by Forbes.[16] A dimeric hexaketone (chrysohermidin)

43 was formed through the transient-blue anion radical while establishing the C-C bond in the autooxidation of *Mercurialis perennis L.* plant alkaloid hermidin **42** as seen in Scheme 2.11.[20] Lewis acid such as manganese acetate is known to be involved in the radical oxidation reaction.
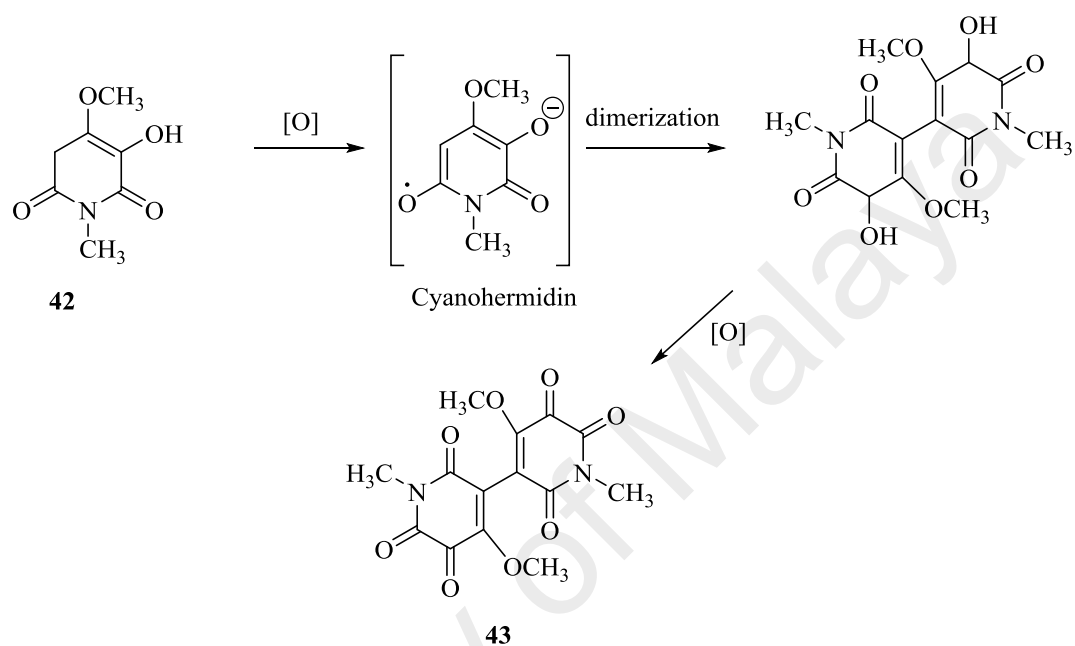
Scheme 2.11 : Synthesis of chrysohermidin **43** through radical dimerization.

2.2.1 Stilbenes Reactions Mediated by Lewis Acid

Reaction of unsaturated β-ketoester **44** with manganese (III) acetate (Lewis acid), it gave the electrophilic enol radical **45** which then formed the nucleophilic tertiary radical **46**. After a few steps, it reacted with cupric acetate,[21] to give bicyclo[3.2.1]octane **47** in Scheme 2.12.[22] An excellent monograph on manganese(III) based free-radical cyclization was written by Snider gave a wider understanding on metal radical relationship.[23]
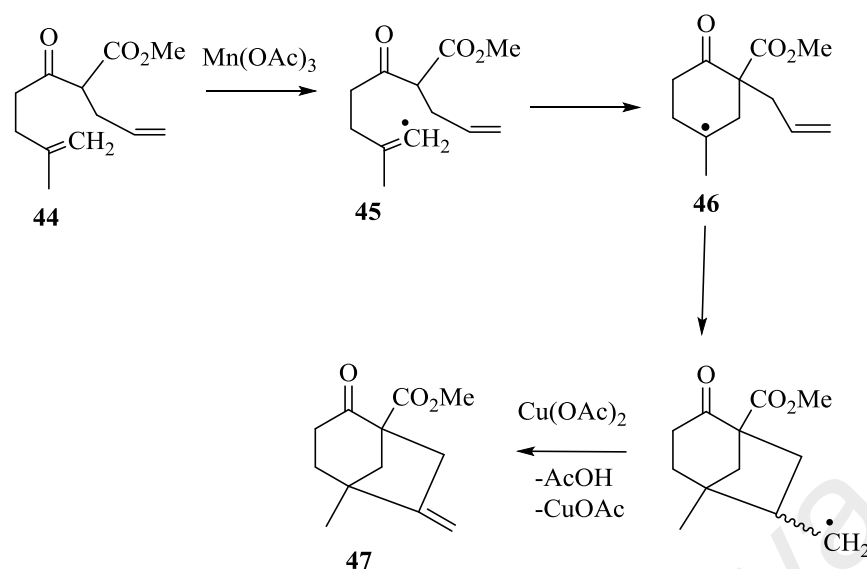
Scheme 2.12: Synthesis of octane **47** through radical cyclization.

Using vinyl sulfonate tethering chain **48**, intramolecular free radical ipso substitution reaction could be used in the synthesis of stilbene **49** as shown in Scheme 2.13.[24] Another Lewis acid, AgOAc was used by Sako to produce dehydrodimer **50** by reacting it with resveratrol **3** via radical oxidative dimerization through single electron transfer from resveratrol to the silver(I) cation as shown in Scheme 2.14.[25]
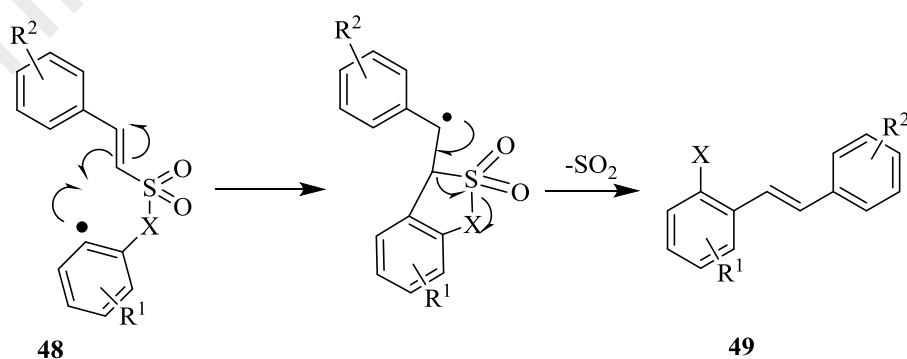
Scheme 2.13 : Godfrey's intramolecular free radical reaction of vinyl sulfonate into

stilbenes **49**.
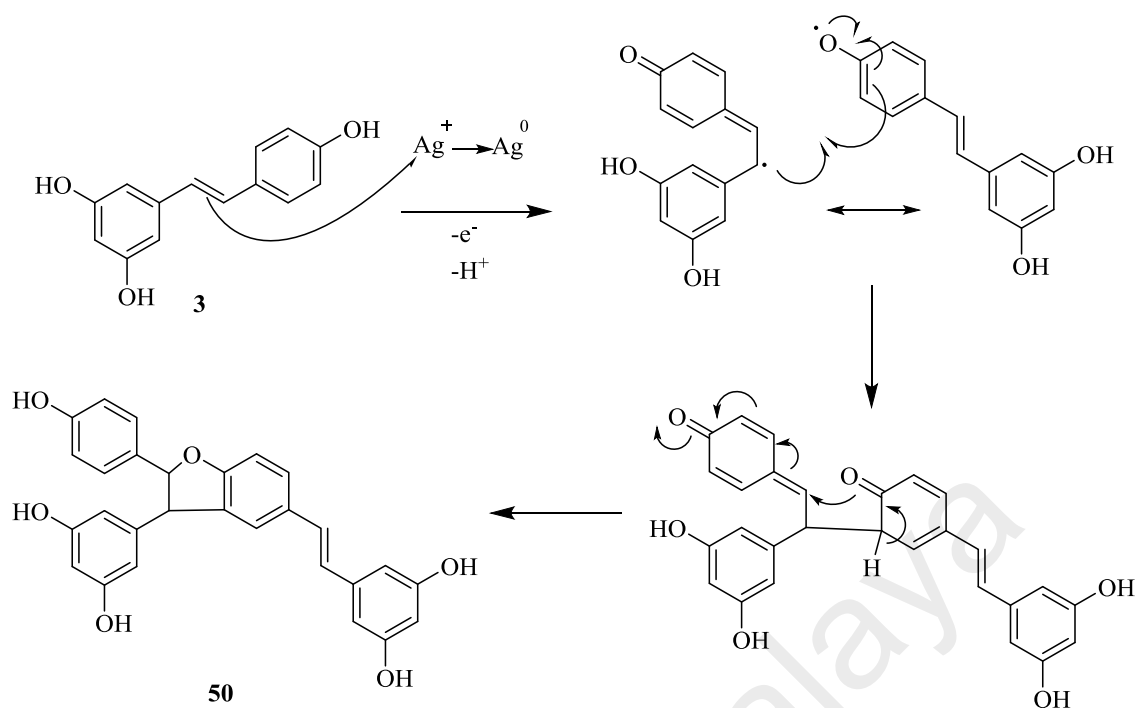
Scheme 2.14 : Sako's dehydrodimer **50** through radical reaction.

2.3   Indoline

Construction of indoles and indolines from stilbenes have gain rapid interest from the synthetic chemists. The first reported synthesis of indoles **52** by cyclization of stilbene **51** was by Sundberg when *o*-nitrostilbene **53** was reacted with triethyl phosphite at 160 °C to produce indole **54** in 71% yield and bisindole **55** in small amount via deoxygenation of the nitro groups on the stilbene (Scheme 2.15).[26]

R=C$_6$H$_5$, CH$_3$, CH$_3$CH$_2$CH$_2$, CH$_3$CO, C$_6$H$_5$CO, C$_2$H$_5$OCO
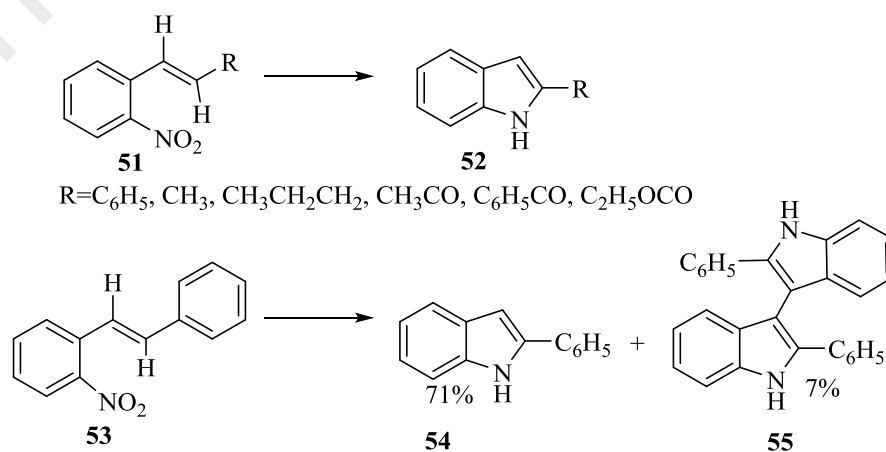
Scheme 2.15 : Cyclization of stilbenes to indoles by Sundberg in 1965.

Gilmore have shown the construction of indoline **58** in a metal free environment by reacting *N*-carbamoyl dehydroalanine esters **56** with silyl aryl triflates **57** via the [3+2] cycloaddition in the presence of tetrabutylammonium difluorotriphenylsilicate (TBAT) and THF as solvent with yield in modest amount (Scheme 2.16).[27] Attaining indoline from indoles has been one of the most straight forward reactions to chemists. Gribble have proved that indole can be reduced to indoline by reacting indole **59** with sodium cyanoborohydride NaBH₃CN and acetic acid AcOH to give indoline **60** in excellent yield of 88%.[28] The mechanism of the reaction was performed by deuterated experiment (Scheme 2.17).
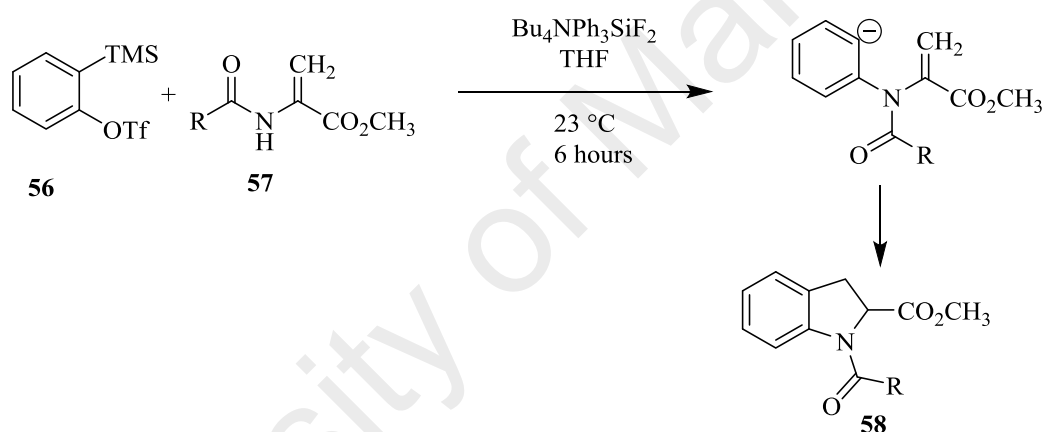
Scheme 2.16 : Gilmore's synthesis of indoline **58**
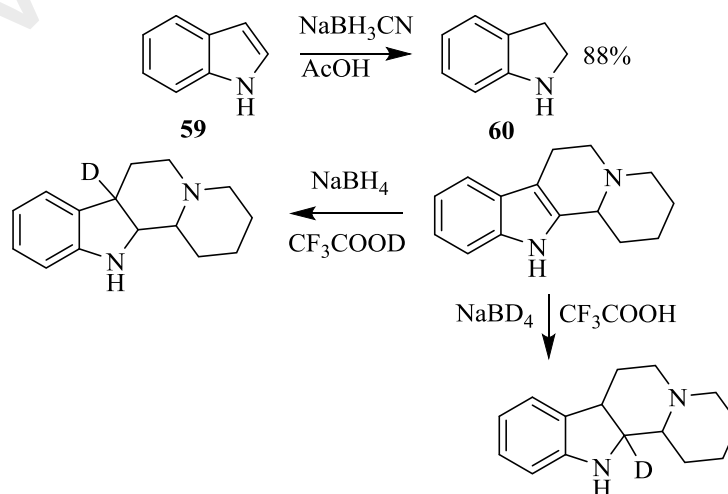
Scheme 2.17 : Gribble's reduction of indole **59** to indolines **60.**

Synthesized indoline by metal catalyzed process was reported by Neumann through the activation of C(sp^3)-H bond activation/C-N bond formation cascade without the use of nitrenes.[29] The various anilides **60** were reacted with palladium (II) acetate as a catalyst, AgOAc as the oxidant with Na_2CO_3 as the base and dissolved in mesitylene to produced indoline **61** in various amount (Scheme 2.18).
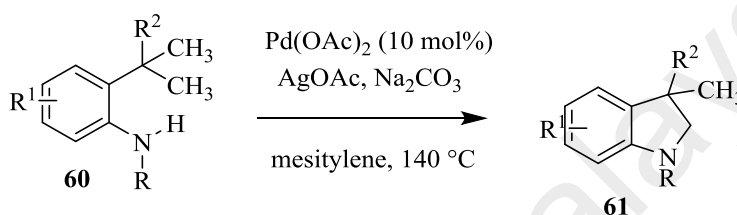
Scheme 2.18 : Neumann's intramolecular reaction to form indoline **61.**

Kang reported the asymmetric synthesis of *trans*-2,3-disubstituted indolines by employing the Mitsunobu intramolecular cyclization.[30] Cyclodehydration of various amino alcohols **62** using PBu_3 and diethyl azodicarboxylate (DEAD) afforded the *trans* indolines **63** in good yield (Scheme 2.19).
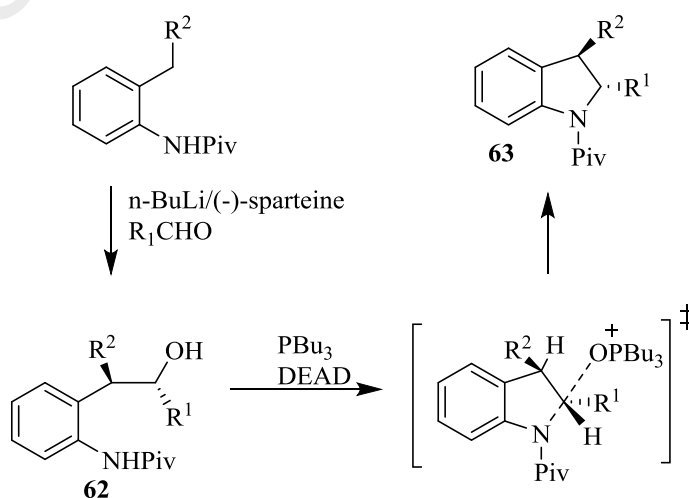
Scheme 2.19 : Synthesis of indoline **63** by Kang et al. (2013).

Rahm et al. have successfully cyclized an amino-tethered bis-alkynyl carbene complexes **64** to generate the two rings of the indoline **65** via a 1,4-diradical intermediate in the presence of a hydrogen source (1,4-cyclohexadiene) with the addition of acetic anhydride and Et$_3$N to give good yield of indoline (Scheme 2.20).[31]
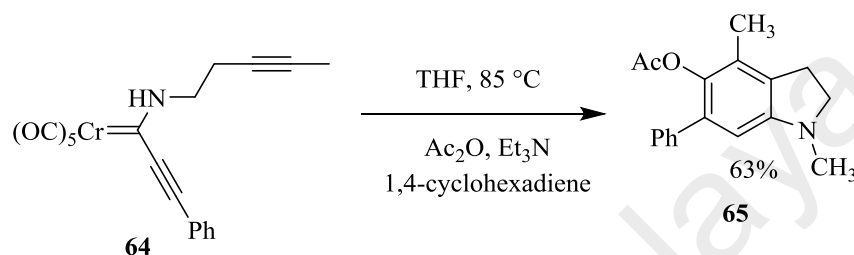
Scheme 2.20 : Cyclization of amino-tethered bis-alkynyl carbene complexes **64** to indoline **65**.

Azobisisobutyronitrile (AIBN), a very popular radical initiator was used in producing indolines was reported by Johnston.[32] It started with *o*-bromophenethylamine **66** reacted with ketones in the presence of tributyltin hydride *n*-Bu$_3$SnH with the AIBN at 80 °C in benzene and afforded indolines **67** in good yields (Scheme 2.21). In a one pot synthesis, Noji et al. had successfully synthesized indoline via benzyne mediated from carbamate **68** using Mg(TMP)$_2$·2LiCl as base with different electrophiles to give indoline **69** in good yield (Scheme 2.22).[33]

Akazome used PdCl$_2$(PPh$_3$)$_2$ as a catalyst and tin(II) chloride SnCl$_2$ as an additive for the reduction of *N*-heterocyclization of 2-Nitrostyrenes **70** at 100 °C under 20 kgcm^{-2} of carbon monoxide pressure to obtained various indoles **71** in good yield.[34] Carbon monoxide acted as a deoxygenating agent of the nitro group. The changed of SnCl$_2$ to SnCl$_4$ resulted in low yield of indole (Scheme 2.23).
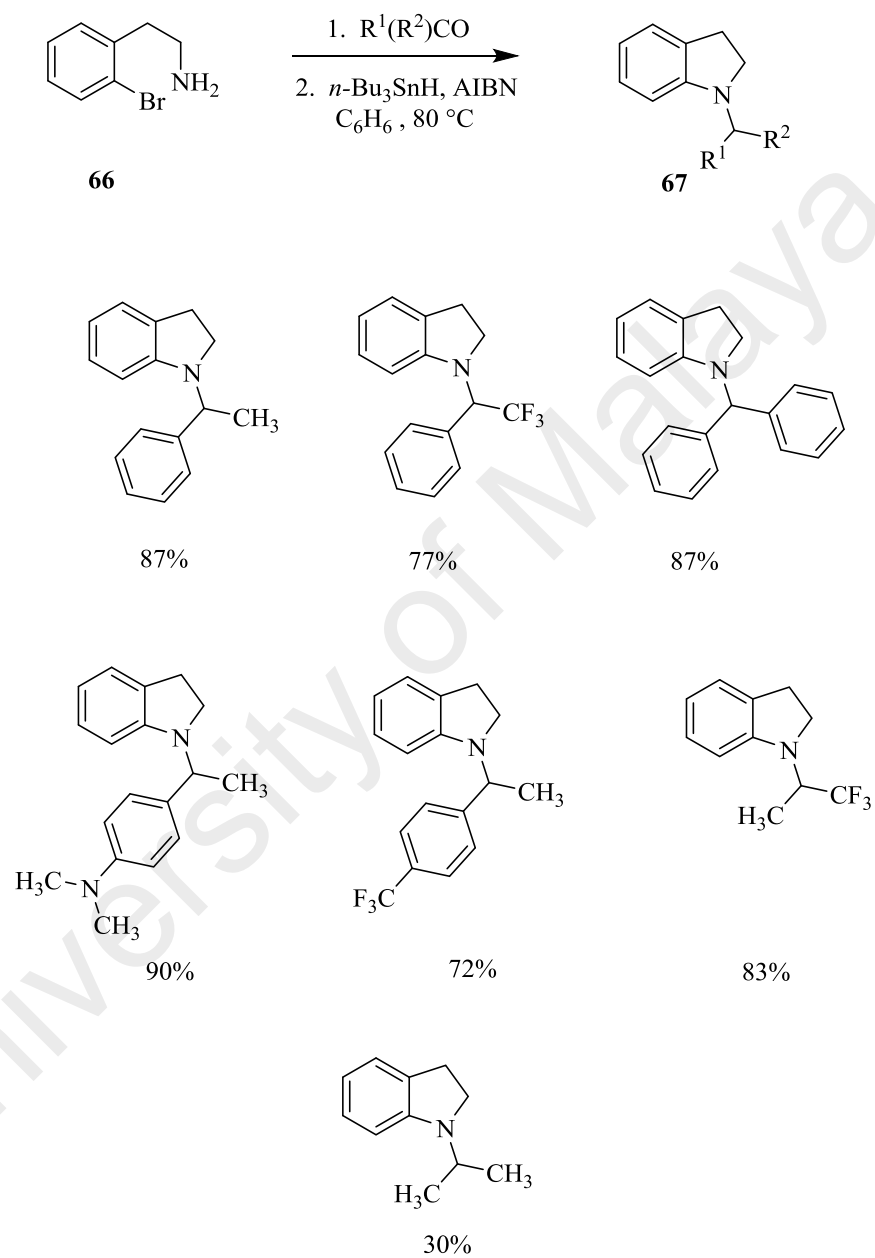
Scheme 2.21 : Johnston's radical cyclization of various indolines 67.
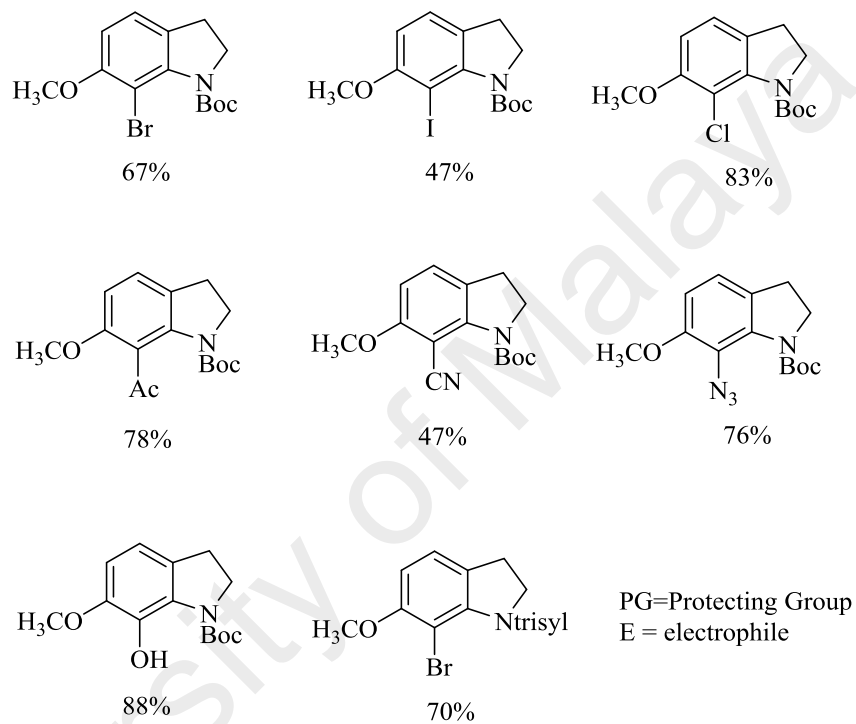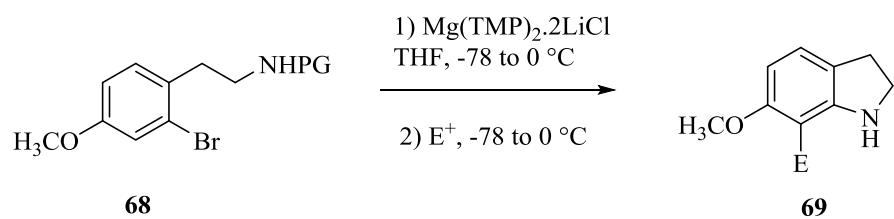
Scheme 2.22 : Synthesis of indolines **69** by Noji et al. (2013).
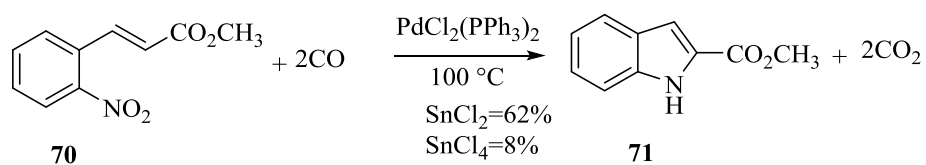
Scheme 2.23 : Synthesis of indoles **71** from *N*-heterocyclization of 2-Nitrostyrenes.

Du reported to electrosynthesize *o*-nitrostilbene **72** into 1*H*-indoles **73** without the harsh chemical reagents. *o*-nitrostilbene **72** was reduced at carbon cathode in DMF with tetramethylammonium tetrafluoroborate electrolyte (TMABF$_4$) as supporting electrolyte.[35] Reaction was observed at room temperature and provided 1*H*-indoles **73** in moderate to good yield (Scheme 2.24).
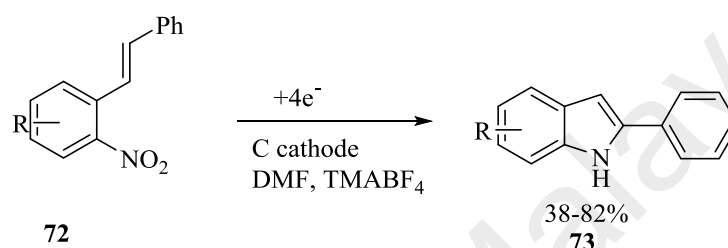
Scheme 2.24 : Du's electrosynthesis of indoles **73**.

The *N*-heterocyclization of 2-Nitrostilbene **74** into indoles **75** with the presence of sulphur and trimethylamine in DMF.[36] The reaction was done under 30 atm pressure at 150 °C for 24 hours to produce indoles **75** in moderate to good yields (Scheme 2.25).
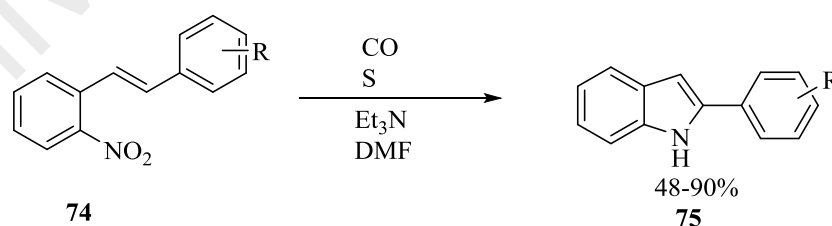
Scheme 2.25 : *N*-heterocyclization of 2-Nitrostilbene **74** into indoles **75**.

2.4   Previous Studies on Stilbene Reactions with Lewis Acid

The work on stilbene reactions with Lewis acid in our group was prompted by the discovery of a natural oligostilbenoid from *Neobalanocarpus heimii* called Heimiol A, a dimeric stilbenoid.[37] Through the discovery of Heimiol A, our group started studies on Lewis acid mediated reaction on stilbenes in 2002 by reacting stilbene **76a** and **76b** with manganese (III) acetate with the former giving **77** and the latter producing **78a** and 78**b** of lactones, (Scheme 2.26).[38] We also used FeCl$_3$ as the Lewis acid which resulted in two dimers (**19** and **79**) being formed from stilbene **18** (Scheme 2.27).[39]
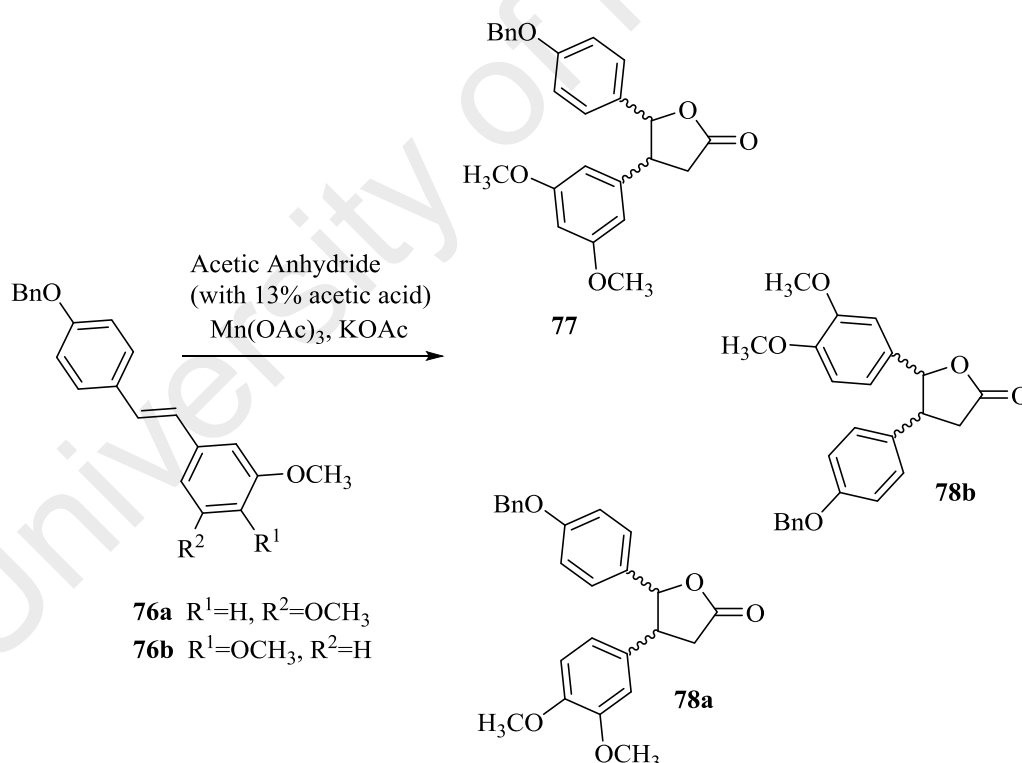
Scheme 2.26 : Cyclization of stilbene into lactones **77**, **78a** and **78b**.
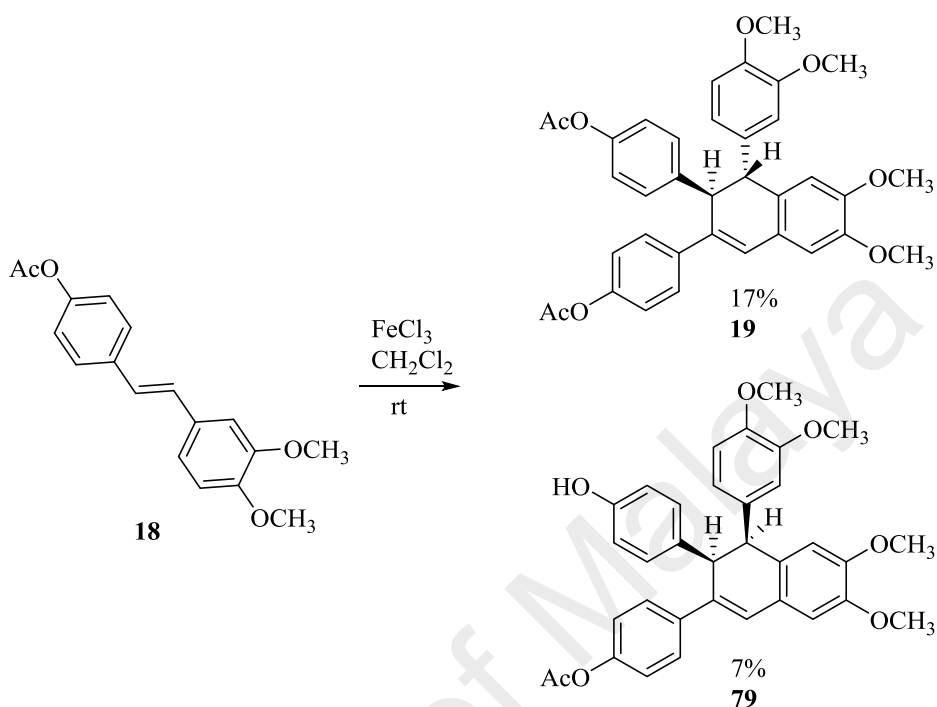
Scheme 2.27 : Dimerization of stilbene **18**.

In 2004, our group published a study on the FeCl$_3$ reaction on a different kind of stilbene that is an acetamido stilbene with methoxy groups at position C-3 and C-4, **80**, and it gave indoline **81** and bisindoline **82** (Scheme 2.28).[40] In 2009, a study on the 3,5-dimethoxy acetamido stilbene **83** reaction with FeCl$_3$, was communicated. It resulted in the formation of indolostilbenes containing chlorine (**84** and **85)**, stilbene incorporated with two chlorine atoms **86** and aldehyde **87** (Scheme 2.29).[41] The absence of a *para* methoxy and only *meta* methoxy substituent group on amido stilbene suggested that the *para* methoxy plays an important role in determining the formation of the indoline and bisindoline.
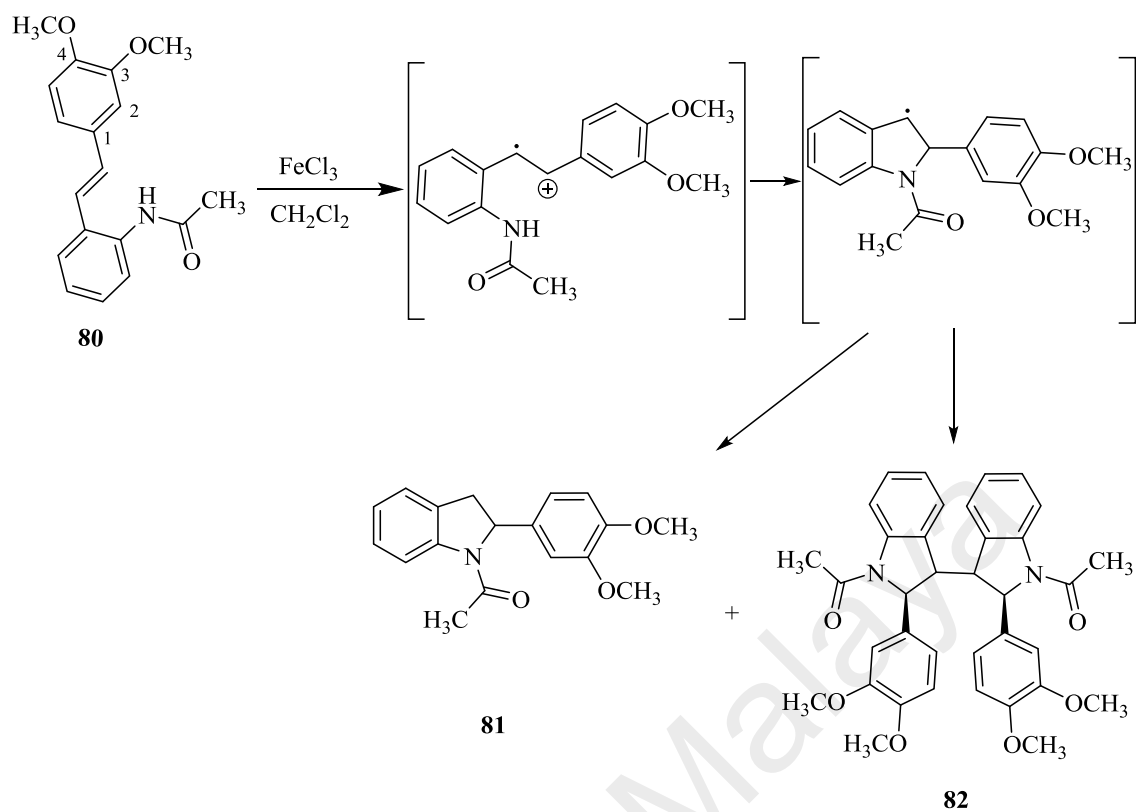
Scheme 2.28 : Formation of indoline **81** and bisindoline **82**.
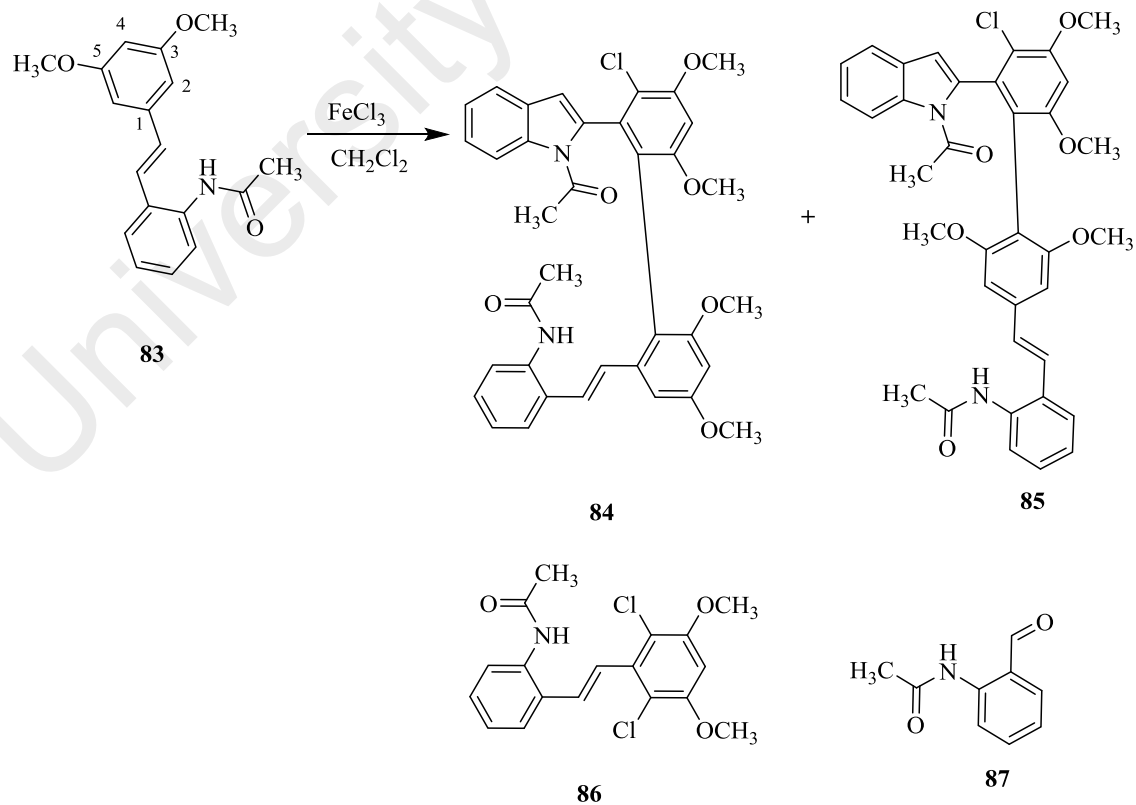
Scheme 2.29 : Stilbene with indole linkage **84** and **85**.

The formation of indolostilbenes **84** and **85** started with the cyclization of stilbene **83** to indole with an electrophilic chlorination preceded onto the indole. Unlike the bisindoline **82** where dimerization occurred between the carbons (C-3) in the indoline ring, the indolostilbenes **84** and **85** were formed through linkages between position C-2 for the former and position C-4 for the latter in stilbene **83** with the indole. The formation started with the indole and stilbene radicalised with Fe(III) abstracting an electron from the methoxy group in the indole and from the olefinic bridge in the stilbene. In the presence of the radical cation stilbene, the radicalised indole connected with the stilbene at different position on the stilbene to give different indolostilbenes **84** and **85** as shown in Scheme 2.30.

In Kee's reported paper, a study on different substituent on the amide group in stilbene **86** was conducted and its effect on the formation of various indolines **87(a-h)** and bisindolines **88(a-h)** (Scheme 2.31).[42] The *n*-propyl group of R^4 on stilbene **86a** gave both the indoline **87a** and bisindoline **87b** while stilbene **86b** with R^4 is *iso*propyl gave only the indoline **87b**. Stilbene **86** that contained a furanyl group on R^4 produced indoline and bisindoline **88g** and **88h** if there is a methoxy group on R^3 while other furanyl containing stilbene **86** only gave indoline **87** and no bisindoline.
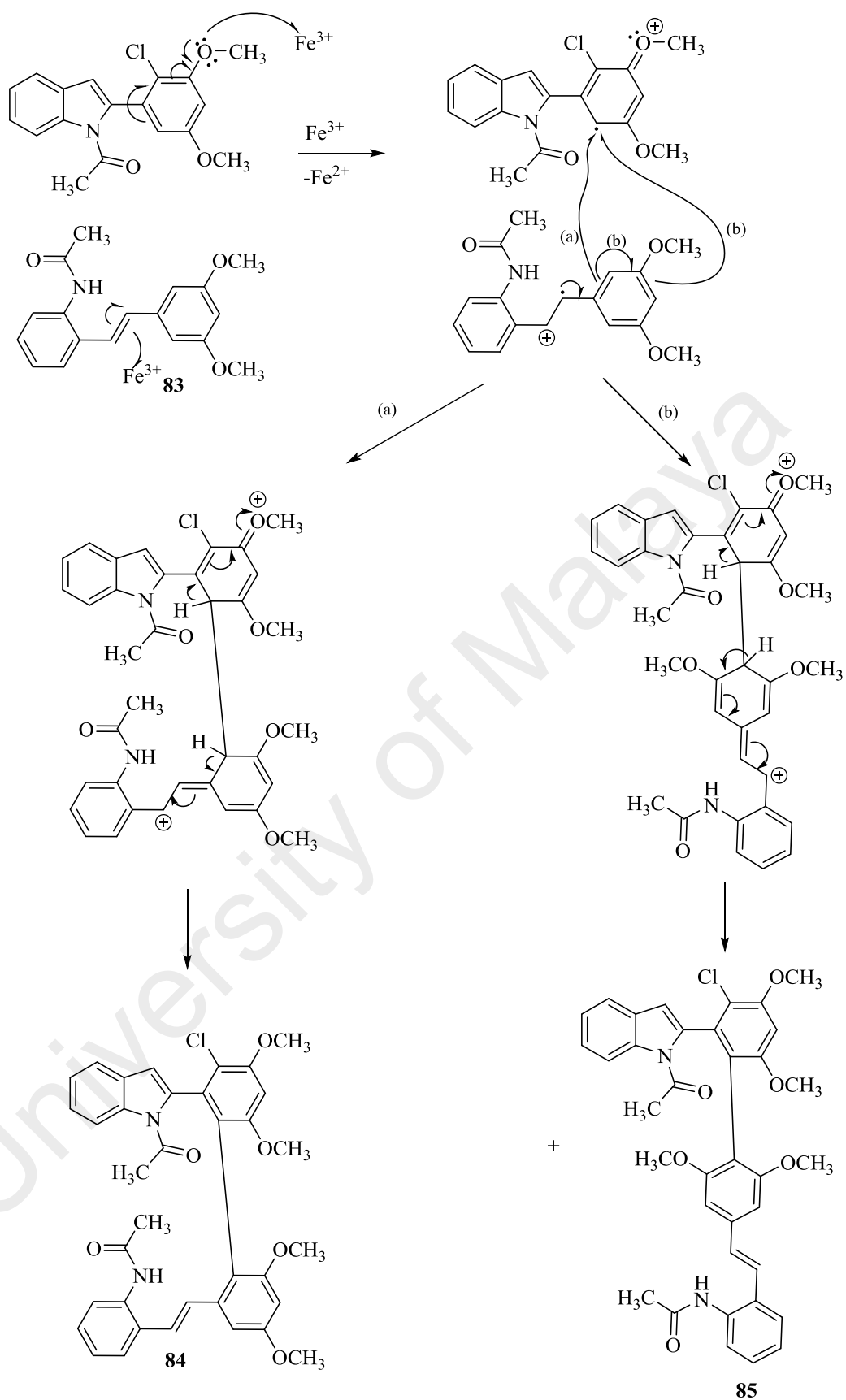
Scheme 2.30 : Proposed mechanism for the formation of indolostilbenes **84** and **85**.

a = R^1=H, R^2=OCH$_3$, R^3=OCH$_3$,
    R^4=*n*-propyl
b = R^1=H, R^2=OCH$_3$, R^3=OCH$_3$,
    R^4=*iso*propyl
c = R^1=H, R^2=OCH$_3$, R^3=OCH$_3$,
    R^4=phenyl
d = R^1=H, R^2=OCH$_3$, R^3=OCH$_3$,
    R^4=cyclohexyl
e = R^1=OCH$_3$, R^2=H, R^3=H,
    R^4=furanyl
f = R^1=H, R^2=OCH$_3$, R^3=H,
    R^4=furanyl
g = R^1=H, R^2=OCH$_3$, R^3=OCH$_3$,
    R^4=furanyl
h = R^1=H, R^2=H, R^3=OCH$_3$,
    R^4=furanyl

a = R^1=H, R^2=OCH$_3$, R^3=OCH$_3$,
    R^4=*n*-propyl
b = R^1=H, R^2=OCH$_3$, R^3=OCH$_3$,
    R^4=*iso*propyl
c = R^1=H, R^2=OCH$_3$, R^3=OCH$_3$,
    R^4=phenyl
d = R^1=H, R^2=OCH$_3$, R^3=OCH$_3$,
    R^4=cyclohexyl
e = R^1=OCH$_3$, R^2=H, R^3=H,
    R^4=furanyl
f = R^1=H, R^2=OCH$_3$, R^3=H,
    R^4=furanyl
g = R^1=H, R^2=OCH$_3$, R^3=OCH$_3$,
    R^4=furanyl
h = R^1=H, R^2=H, R^3=OCH$_3$,
    R^4=furanyl

a = R^1=H, R^2=OCH$_3$, R^3=OCH$_3$,
    R^4=*n*-propyl
g = R^1=H, R^2=OCH$_3$, R^3=OCH$_3$,
    R^4=furanyl
h = R^1=H, R^2=H, R^3=OCH$_3$,
    R^4=furanyl

Scheme 2.31 : Kee's synthesized indolines **87** and bisindolines **88.**

2.5 References

1   R. F. Heck, *J. Am. Chem. Soc.*, 1969, **91**, 6707.
2   R. F. Heck and J. P. Nolley, *J. Org. Chem.*, 1972, **37**, 2320.
3   T. Mizoroki, K. Mori and A. Ozaki, *Bull. Chem. Soc. Jpn.*, 1971, **44**, 581.
4   D. Morales-Morales, R. Redón, Y. Zheng and J. R. Dilworth, *Inorg. Chim. Acta*, 2002, **328**, 39.
5   K. Hamza, R. Abu-Reziq, D. Avnir and J. Blum, *Org. Lett.*, 2004, **6**, 925.
6   S. Albert, R. Horbach, H. B. Deising, B. Siewert and R. Csuk, *Bioorg. Med. Chem.*, 2011, **19**, 5155.
7   F. Luo, C. Pan, W. Wang, Z. Ye and J. Cheng, *Tetrahedron*, 2010, **66**, 1399.
8   J. Le Bras and J. Muzart, *Chem. Rev.*, 2011, **111**, 1170.
9   A. Dhakshinamoorthy, A. M. Asiri and H. Garcia, *Chem. Soc. Rev.*, 2015, **44**, 1922-1947.
10 S. S. Velu, N. F. Thomas and J. F. F. Weber, *Curr. Org. Chem.*, 2012, **16**, 605.
11 S. Warren and P. Wyatt, *Tetrahedron: Asymmetry*, 1996, **7**, 989.
12 G. W. Kabalka, Z. Wu, Z. and Y. Ju, *Tetrahedron Lett.*, 2001, **42**, 4759.
13 S. C. Söderman and A. L. Schwan, *J. Org. Chem.*, 2012, **77**, 10978.
14 L. Chakrapani, E. M. Jung and Y. R. Lee, *Helv. Chim. Acta*, 2010, **93**, 829.
15 F. W. Patureau and F. Glorius, *J. Am. Chem. Soc.*, 2010, **132**, 9982.
16 M. D. E. Forbes, *Carbon-Centered Free Radicals and Radical Cations*, Wiley, New Jersey, 2010.
17 C. Walling, *Free Radicals in Solution*. Wiley, New York, 1957.
18 G. L. Closs and R. J. Miller, *Rev. Sci. Instrum.*, 1981, **52**, 1876.
19 M. D. E. Forbes, *Photochem. Photobiol.*, 1997, **65**, 73.
20 Z. V. Todres, *Ion-Radical Organic Chemistry: Principles and Applications*. Taylor & Francis Group, Boca Raton, 2009.
21 J. K. Kochi, *Science*, 1967, **155**, 415.
22 B. B. Snider and B. O. Buckman, *Tetrahedron*, 1989, **45**, 6969.
23 B. B. Snider, *Chem. Rev.*, 1996, **96**, 339.
24 C. R. A. Godfrey and P. Hegarty, *Tetrahedron Lett.*, 1998, **39**, 723.
25 M. Sako, H. Hosokawa, T. Ito and M. Iinuma, *J. Org. Chem.*, 2004, **69**, 2598.
26 R. J. Sundberg, *J. Org. Chem.*, 1965, **30**, 3604.
27 C. D. Gilmore, K. M. Allan and B. M. Stoltz, *J. Am. Chem. Soc.*, 2008, **130**, 1558.
28 G. W. Gribble, P. D. Lord, J. Skotnicki, S. E. Dietz, J. T. Eaton and J. Johnson, *J. Am. Chem. Soc.*, 1974, **96**, 7812.
29 J. J. Neumann, S. Rakshit, T. Dröge and F. Glorius, *Angew. Chem. Int. Ed.*, 2009, **48**, 6892.
30 K. H. Kang, Y. Kim, C. Im and Y. S. Park, *Tetrahedron*, 2013, **69**, 2542.
31 A. Rahm and W. D. Wulff, *J. Am. Chem. Soc.*, 1996, **118**, 1807.
32 J. N. Johnston, M. A. Plotkin, R. Viswanathan and E. N. Prabhakaran, *Org. Lett.*, 2001, **3**, 1009.
33 T. Noji, H. Fujiwara, K. Okano and H. Tokuyama, *Org. Lett.*, 2013, **15**.1946.
34 M. Akazome, T. Kondo and Y. Watanabe, *J. Org. Chem.*, 1994, **59**, 3375.
35 P. Du, J. L. Brosmer and Peters, D. G., *Org. Lett.*, 2011, **13**, 4072.
36 R. Umeda, Y. Nishimoto, T. Mashino and Y. Nishiyama, *Heterocycles*, 2013, **87**, 1241.
37 J. F. F. Weber, I. Abdul Wahab, A. Marzuki, N. F. Thomas, A. Abdul Kadir, A. H. A. Hadi, K. Awang, A. Abdul Latiff, P. Richomme and J. Delaunay, *Tetrahedron Lett.*, 2001, **42**, 4895.

38 N. F. Thomas, K. C. Lee, T. Paraidathathu, J. F. F. Weber and K. Awang, *Tetrahedron Lett.*, 2002, **43**, 3151.

39 N. F. Thomas, K. C. Lee, T. Paraidathathu, J. F. F. Weber, K. Awang, D. Rondeau and P. Richomme, *Tetrahedron*, 2002, **58**, 7201.

40 N. F. Thomas, S. S. Velu, J. F. F. Weber, K. C. Lee, A. H. A. Hadi, P. Richomme, D. Rondeau, I. Noorbatcha and K. Awang, *Tetrahedron*, 2004, **60**, 11733.

41 K. Ahmad, N. F. Thomas, M. R. Mukhtar, I. Noorbatcha, J. F. F. Weber, M. A. Nafiah, S. S. Velu, K. Takeya, H. Morita, C. G. Lim, A. H. A. Hadi and K. Awang, *Tetrahedron*, 2009, **65**, 1504.

42 C. H. Kee, A. Ariffin, K. Awang, I. Noorbatcha, K. Takeya, H. Morita, C. G. Lim and N. F. Thomas, *Molecules*, 2011, **16**, 7267.

Chapter 3

Results And Discussion

The proposal was to synthesized halogenated acetamido stilbenes utilising the Heck method. Previously, the amido stilbenes produced from the author's group contained electron-donating group (OMe) while this study concentrated on electron-withdrawing group (F, Cl, Br) on the stilbenes. It was reported that these amido stilbenes (electron-donating group) when reacted with Lewis acid ($FeCl_3$), produced indoles or indolines product accompanied with bisindoline. Therefore, it is rather interesting to see if the halogenated acetamido stilbenes will follow this pattern when reacted with Lewis acid.

3.1   Synthesis of Halogenated Acetamido Stilbenes

Producing the stilbenes was done by applying the Heck method by which an aryl iodide coupled with a styrene catalyzed by palladium salt. But first, the aryl iodide **89** (2-Iodoaniline) was acetylised using acetic anhydride with the help of a base (NaH) in DMF and afforded *N*-(2-Iodophenyl)acetamide **90** in 71% yield (Scheme 3.1).[1] Acetylisation of 2-Iodoaniline can proceed without NaH due to the acidic proton of the amine but it will give a lower yield.
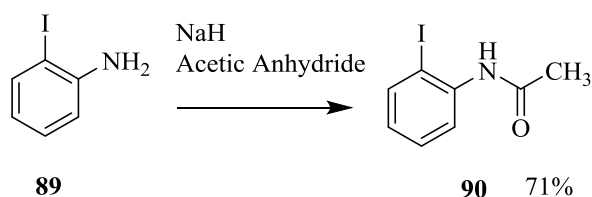
Scheme 3.1 : Synthesis of 2-Iodoacetamide.

The coupling of the *N*-(2-Iodophenyl)acetamide **90** with various halogenated styrenes **91** catalyzed by Pd(OAc)$_2$ with Et$_3$N as base in DMF yielded the *trans* halogenated acetamido stilbenes **92** in low yield (34-45%) (Table 3.1) (Scheme 3.2).[1-2]
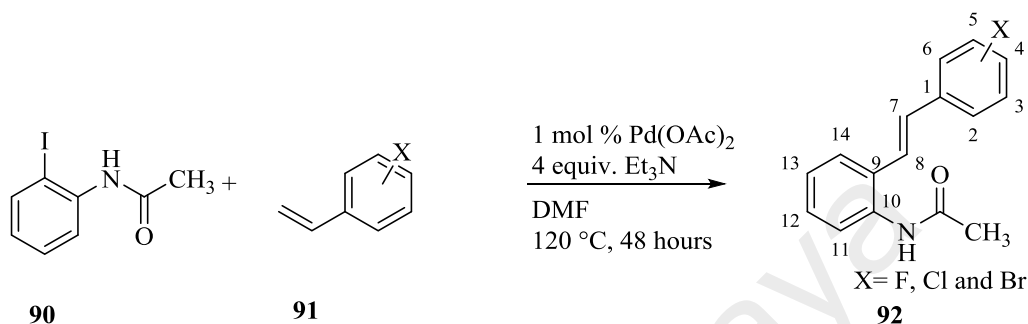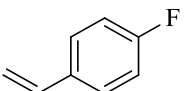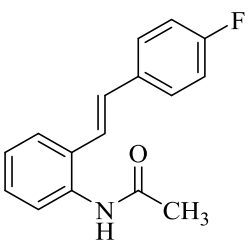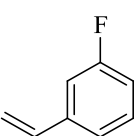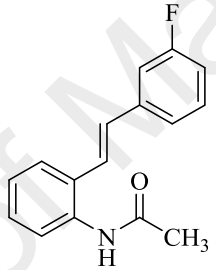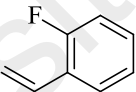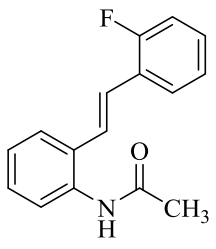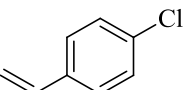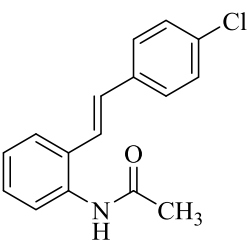
Scheme 3.2 : Synthesis of halogenated acetamido stilbenes **92**.

The low yield of the afforded *trans* halogenated acetamido stilbenes are due to the isomerization of the *trans* to *cis* stilbene.[3] While the *trans* isomer exist in solid form, the *cis* isomer is in liquid form.[4] The *cis* isomer was obtained in small amount and, it is difficult to isolate the *cis* and *trans* mixture, resulted in reduced yield of the isolated *trans* stilbene **92**. The Heck method also known to produce diphenylethylene **94** type product as seen in previous report by Ahmad and Kee which contributed to the low yield of the *trans* stilbene (Scheme 3.3).[5,6,7] Previous reported synthesis of amido stilbenes from our group were afforded in low yield (<50%).[1,5,7]
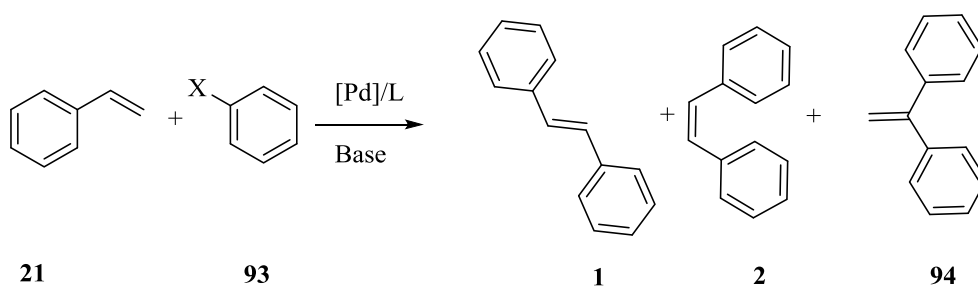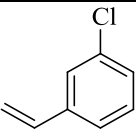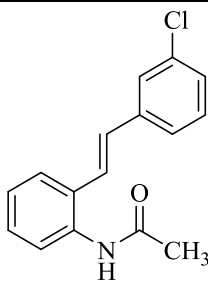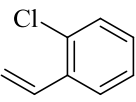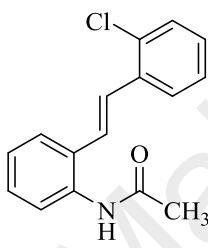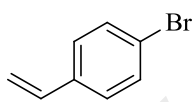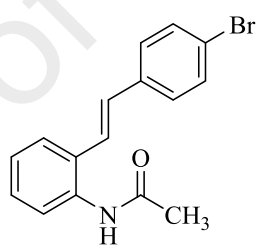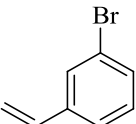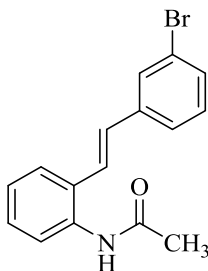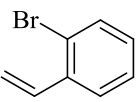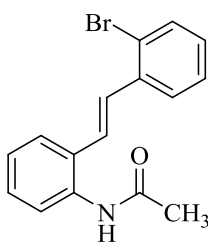
Scheme 3.3 : Common products from Heck Coupling (Ferre-Filmon et al.).[6]

Table 3.1 : Halogenated acetamido stilbenes synthesized from halogenated

styrenes

Entry	Styrene	Stilbene	Yield (%)
1	**95**	**96**	39
2	**97**	**98**	43
3	**99**	**100**	37
4	**101**	**102**	45

Table 3.1 : (continued)

Entry	Styrene	Stilbene	Yield (%)
5	**103**	**104**	44
6	**105**	**106**	36
7	**107**	**108**	40
8	**109**	**110**	37
9	**111**	**112**	34

3.2   The Proposed Mechanism for the Formation of *trans* Stilbenes

The proposed mechanistic pathway for the formation of halogenated acetamido stilbenes is shown in Scheme 3.4. The Pd(OAc)$_2$ was activated with the reduction of the Pd(II) to Pd(0) through the addition of Et$_3$N. Later, oxidative addition of *N*-(2-Iodophenyl)acetamide **90** to Pd(0) will form two new bonds to afford the complex intermediate Pd^{II}Ar(Et$_3$N)$_2$I **113**. The intermediate will then undergo a *syn* insertion with the styrene in what is called carbopalladation to give **114**.[8]

A C-C bond rotation internally will position an sp^3 hydrogen in *syn* towards the palladium atom. The split of HPd(II)(Et$_3$N)$_2$I **115** through *syn* β-hydride elimination gave the desired *trans* halogenated acetamido stilbene **92**. The HPd(II)(Et$_3$N)$_2$I **115** underwent a reductive oxidation to give back the active Pd(0).[9] The Pd(0) will start the catalytic cycle again.[10]
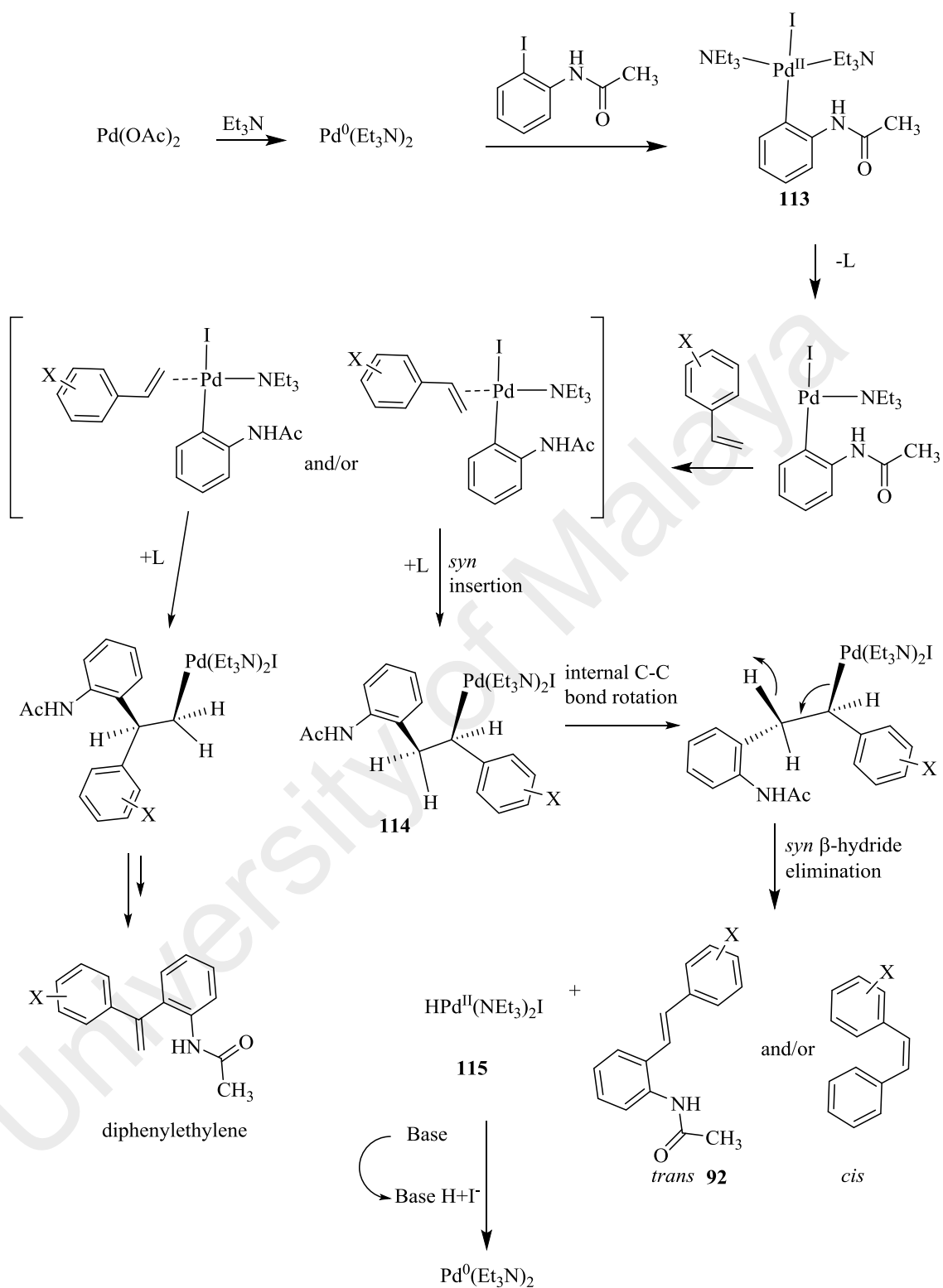
Scheme 3.4 : Proposed mechanism for the formation of *trans* stilbenes **92**.

3.3   Reactions of Halogenated Acetamido Stilbenes Mediated by Lewis Acid

3.3.1   Reactions of Halogenated Acetamido Stilbenes with FeCl₃

As reported in the author's group previous literature, acetamido stilbenes reaction mediated by $FeCl_3$ resulted in the formation of indoline **81** or bisindoline **82** (Scheme 2.28). Even with different substituent on the amide group of the stilbenes, indoline or bisindoline was still prevalent in the final product (Scheme 2.31). Only when the methoxy group on the 3,5 position rather the 4 or 3,4 position of the aromatic ring on the acetamido stilbene that it gave an indolostilbene (**84** and **85**) (Scheme 2.30).

As all the amido stilbenes contained electron-donating group (OMe), the author will study the effect of electron-withdrawing group, mainly halogens (F, Cl, Br) on the amido stilbenes when reacted with $FeCl_3$. Niu reported the homocoupling of 2-arylindoles **116** with $FeCl_3$ as the catalyst and O_2 as oxidant giving bisindoles **117** (Scheme 3.5).[11] The similarity of bisindole and bisindoline would suggest that these halogenated acetamido stilbenes when reacted with $FeCl_3$ will produce bisindoline.
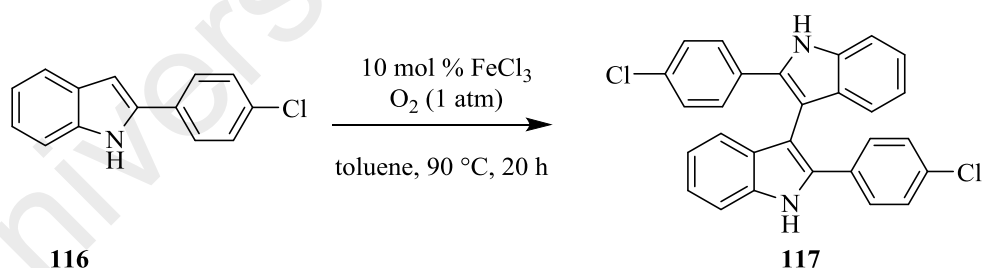
Scheme 3.5 : Niu's synthesis of bisindole **117**.

As the author tried to use the same condition reported in Ahmad's paper, no indolines **118** or bisindoline **119** were afforded.[5]   Different ratio of $FeCl_3$ was then applied on the stilbenes (Table 3.2). A lesser equivalent of 3 compared to 5 equivalents of $FeCl_3$ stated in Ahmad's paper resulted in the formation of imine **120** in very small amount and a lot of spots on the TLC. When the amount of $FeCl_3$ was further reduced to

2.5 equivalent, yield of imine **120** was increased to 38%. But at 2 equivalents of FeCl$_3$, only trace amount of imine **120** can be seen and this due to the longer reaction time (36 hours) for the stilbene to be fully consumed. FeCl$_3$ are hygroscopic and overtime will absorb moisture, forming HCl as the reaction set up is not moisture proof. HCl will then hydrolyse the imine product resulting in more by-products.[12] The best condition (Entry 3, Table 3.2) was then applied on different halogen at different position giving various yields (Table 3.3). All of the stilbene gave one diastereomer product except one stilbene (**110**) which gave two diastereomers.

Table 3.2 : Synthesis of imine **120** mediated by FeCl$_3$
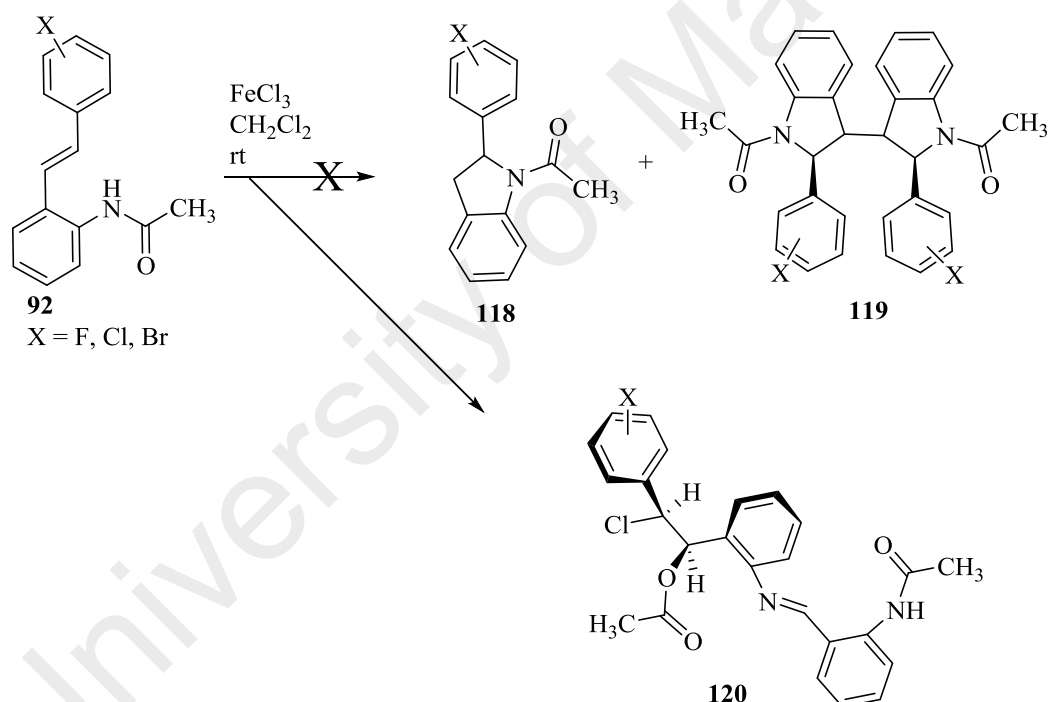
Entry	FeCl$_3$ (equiv)	Time (hour)	Yield (%)[a]
1	5	1	0
2	3	7	3
3	2.5	16	38
4	2	36	trace

- General procedure: Stilbene (0.31 mmol), 6 ml dichloromethane.
- Reaction stopped when all the stilbene have been consumed (monitored by TLC).
- [a]Isolated yield.

Table 3.3 : Synthesis of imines using various halogenated acetamido stilbenes mediated by FeCl₃ (2.5 equivalents).
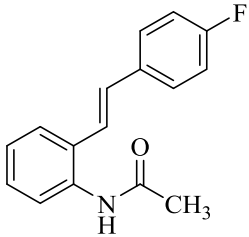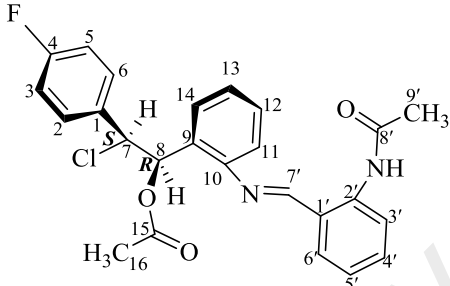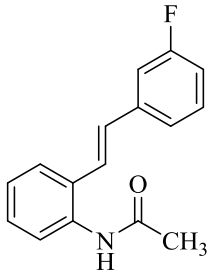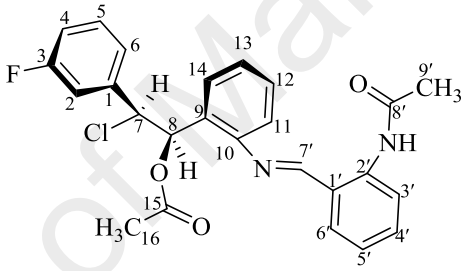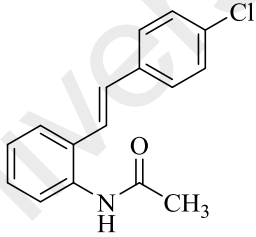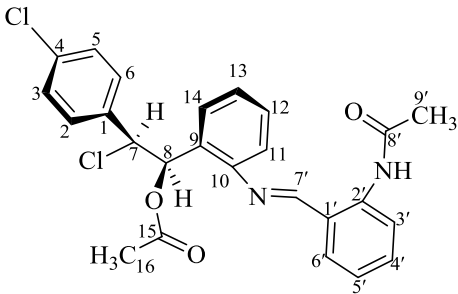
Entry	Stilbene	Product	Yield (%)
1	 **96**	 **121**	37
2	 **98**	 **122**	39
3	 **102**	 **123**	35

Table 3.3 (continued)
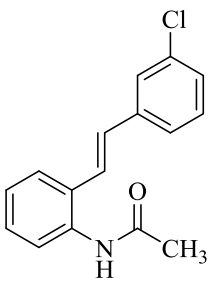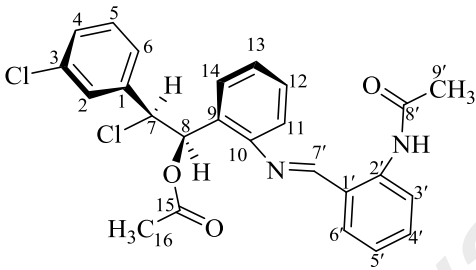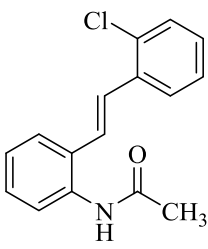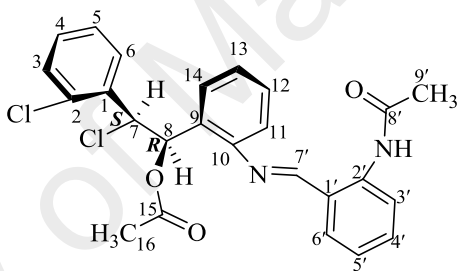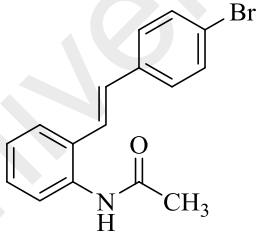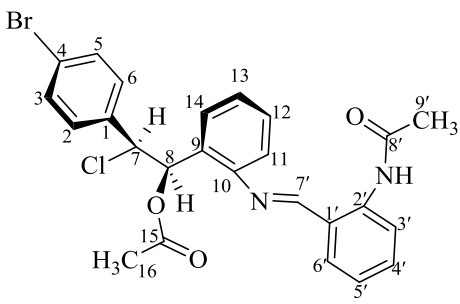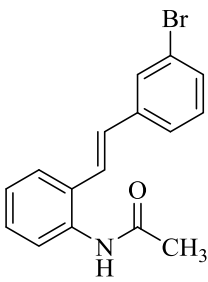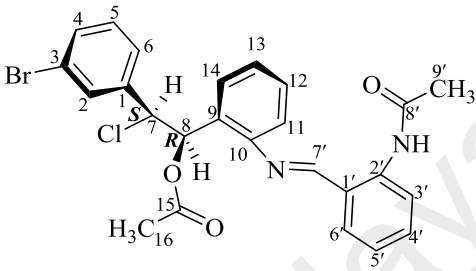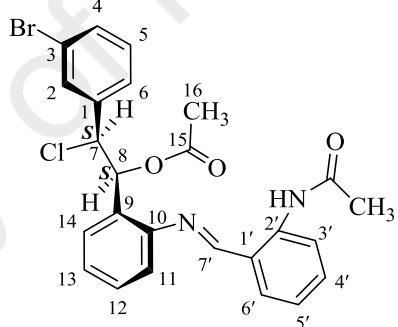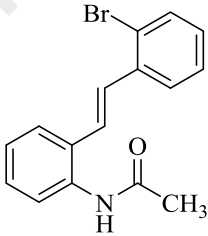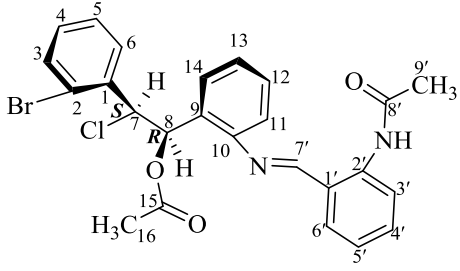
Entry	Stilbene	Product	Yield (%)
4	**104**	**124**	40
5	**106**	**125**	36
6	**108**	**126**	38

Table 3.3 (continued)

Entry	Stilbene	Product	Yield (%)
7	**110**	**127**	32
		128	15
8	**112**	**129**	38

3.3.2 The Proposed Mechanism for the Formation of Imines from Halogenated Acetamido Stilbenes Reaction Mediated by Ferric Chloride

The mechanism for the creation of the imine **120** is through the linkage of 2-acetamidobenzaldehyde **132** with stilbene **92**. Firstly, the formation 2-acetamidobenzaldehyde **132** started with the oxidation process of stilbene **92** to a radical cation **130** through the abstraction of an electron from the π olefinic bond of stilbene with the help of $FeCl_3$ (Scheme 3.6). $FeCl_3$ is a strong Lewis acid and a known single electron transfer (SET) oxidant.[13] Fe(III) ion is reduced to Fe(II) ion when abstracting an electron from stilbene **92**. The formation of 2-acetamidobenzaldehyde **132** in this study is similar to the one proposed by Ahmad et al. in 2009.[5] The radical cation **130** will then be attacked by H_2O and subsequently form a diol **131** and cleaved to give 2-acetamidobenzaldehyde **132** and halide benzaldehyde **133**,[14] whereby compound **133** will oxidize to carboxylic acid and dissolved during the workup.[15]
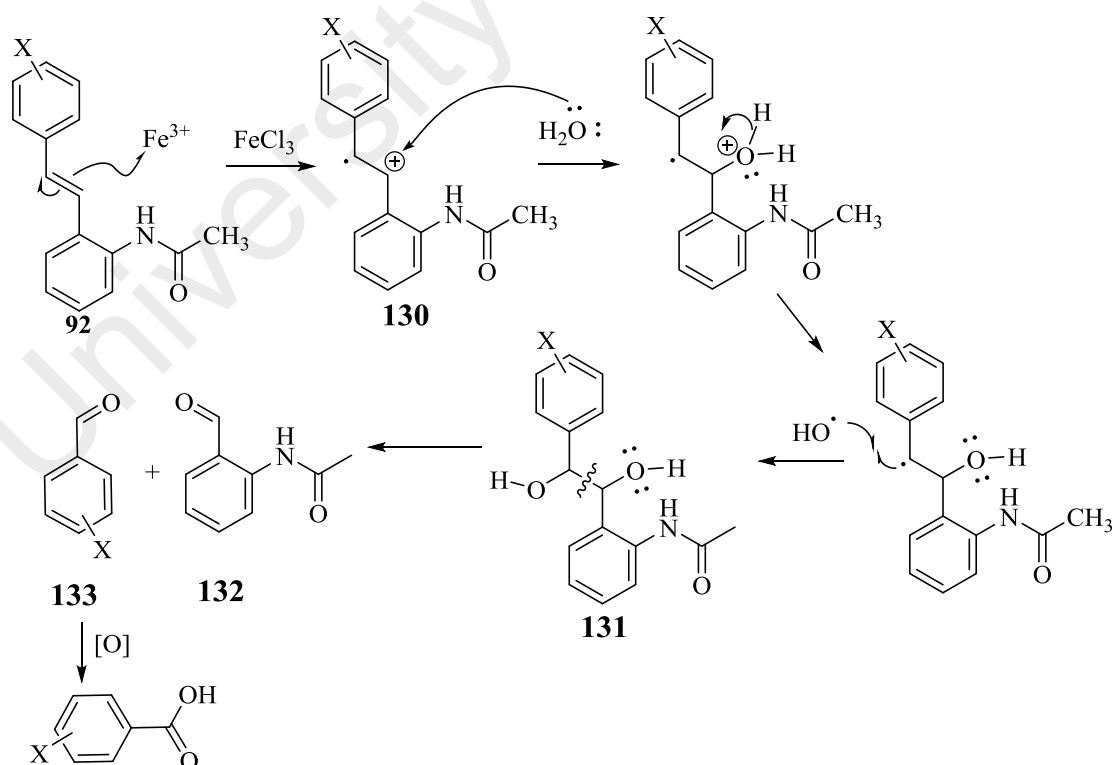
Scheme 3.6 : Proposed mechanism for the formation of 2-acetamidobenzaldehyde **132**

Another proposal on the production of 2-acetamidobenzaldehyde **132** is through the formation of stilbene radical cation **130** by reaction of stilbene with molecular oxygen which exist in diradical state (Scheme 3.7).[16] The stilbene radical cation will again react with diradical oxygen and formed the intermediate dioxetane **134** which decomposes to 2-acetamidobenzaldehyde **132** and halide benzaldehyde **133**.[17,18,19] The halide benzaldehyde **133** will oxidise to carboxylic acid.[15]
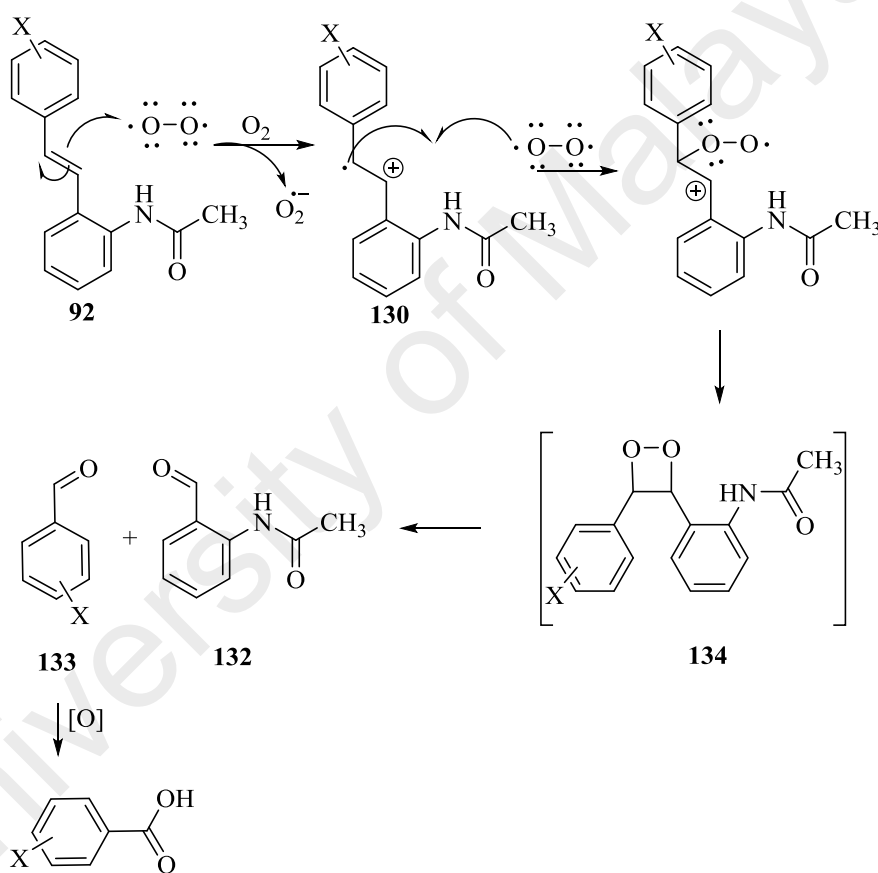
Scheme 3.7 : Proposed mechanism for the formation of 2-acetamidobenzaldehyde **132** through dioxetane **134** intermediate.

The second step in the formation of imine **120** (Scheme 3.6) also start with the generation of stilbene radical cation **130** by single electron transfer from stilbene to Fe(III) (Scheme 3.8).[5] The stilbene radical cation **130** formed a bond with chlorine radical. Togo et al. (2004) showed that the chlorine radical is derived from $FeCl_3$.[20] An intramolecular cyclization occurred when the lone pair of electron on the oxygen attacked the carbocation forming a bond. During the workup, the water molecule attack and this lead to a cleaved of the C-N bond forming the ester group and the amine group **135.** The aromatic amine act as a nucleophile and attacked the electrophilic carbon of 2-acetamidobenzaldehyde **132**, and generate a C=N bond which lead to the formation of imine **120**.
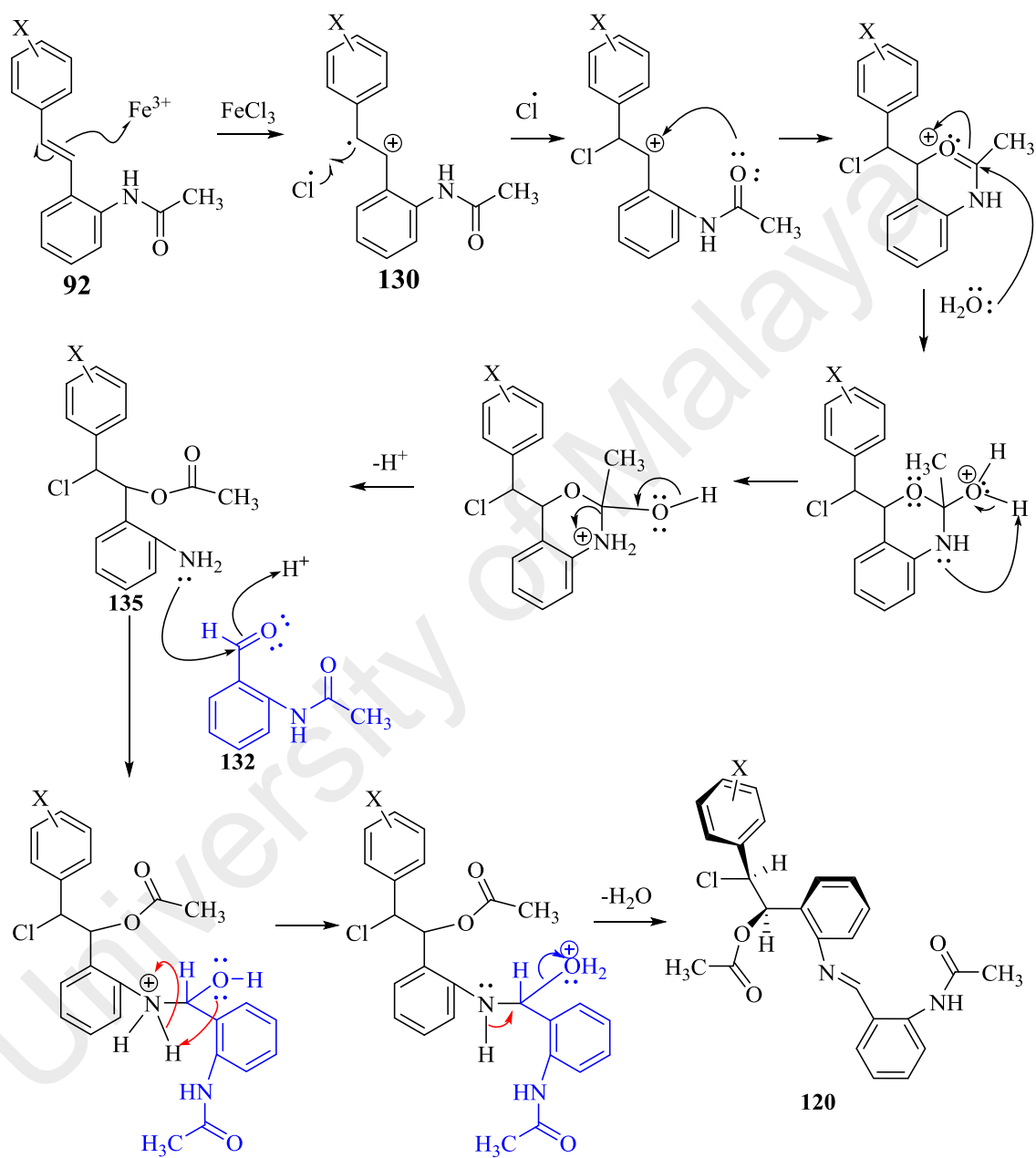
Scheme 3.8 : Proposed mechanism for the formation of imine **120**.

3.3.3 Reactions of Halogenated Acetamido Stilbenes with SnCl₄

We continued our study on Lewis acid mediated reaction of halogenated acetamido stilbene with SnCl₄. 4-Methoxy acetamido stilbene **136** was chosen as we expect it to react faster with SnCl₄.Various temperature was tested and yielded indoline **137** in various percentage with full conversion of stilbene **136** (Scheme 3.9) (Table 3.4).[21]
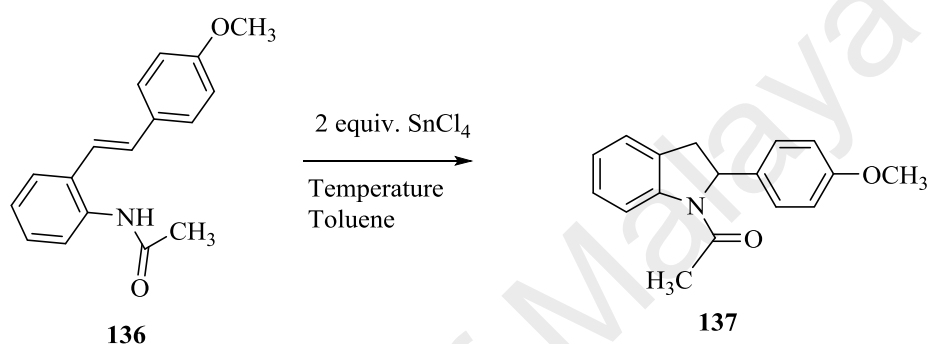
Scheme 3.9 : SnCl₄ mediated reaction of stilbene **136**.

Table 3.4 : Reaction of stilbene **136** with SnCl₄ at various temperature

Entry	Temperature (°C)	Yield (%)
1	-70	0
2	-10	0
3	0	0
4	5	0
5	10	20
6	18	34
7	23	55
8	rt (29-31)	47

The indoline **137** was obtained in moderate yield at 23 °C but the yield decreased when the temperature increased to room temperature. The same condition was applied to 4-Cl-stilbene **102** but no indoline was observed. The increase in temperature and ratio of the $SnCl_4$ seemed not to improve the yield. Different solvents (THF and DMF) were used instead of toluene, however no indoline was formeed. 4-Methoxy stilbene **136** containing the methoxy group activated the ring and conjugated system, making it easier for the stilbene to cyclize into indoline. A halogen group on the stilbene made the ring less active and hard to cyclize to indoline. In normal reflux in toluene, 4-Cl-stilbene **102** seemed to fly off from the flask and cling to the wall of the condenser, unable to react with $SnCl_4$ in the flask. A pressure tube was used to contain the 4-Cl-stilbene **102** in the solution to complete the reaction. High amounts of $SnCl_4$, increased in temperature and longer period of time were required to obtain a reasonable yield of indoline (Table 3.5). When the temperature was raised to 110 °C, the yield decreased and this was possibly attributed to the degradation of the $SnCl_4$ (b.p. 114 °C) at that temperature. Thus the optimum conditions for the cyclization of 4-Cl stilbene **102** to indoline **140** (Entry 16, Table 3.5) was found to be at 90 °C with 30 equivalent of $SnCl_4$ in toluene were then applied on various halogenated acetamido stilbenes **92** to obtain indolines **138** and the results are tabulated in Table 3.6.

Table **3.5** : Reaction between SnCl$_4$ and 4-Cl stilbene **102** in various condition

102 → **140**
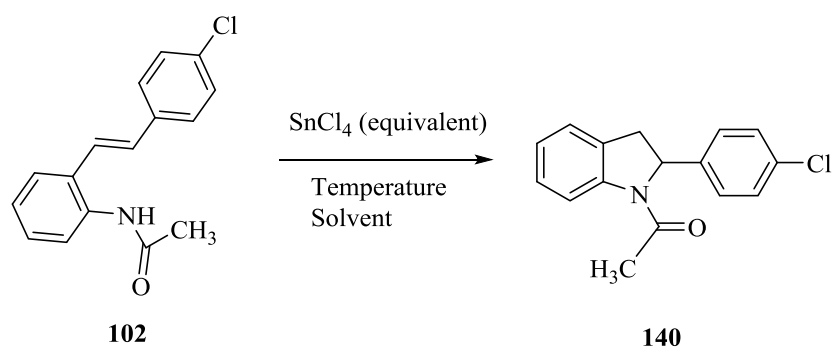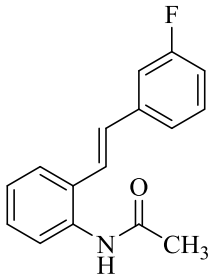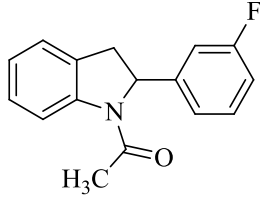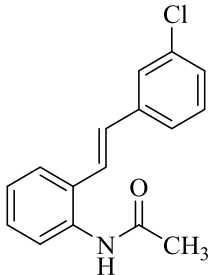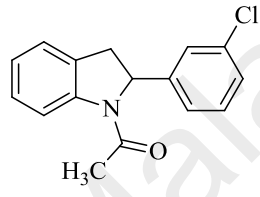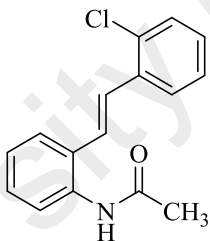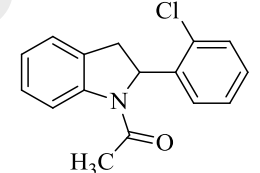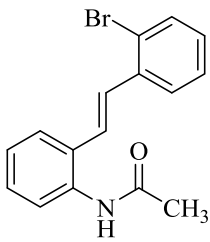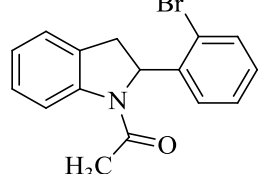
Entry	SnCl$_4$ (equiv.)	Solvent	Temperature (°C)	Time (hours)	Yield (%)
1	2	Toluene	rt	2	0
2	2	Toluene	50	2	0
3	2	Toluene	70	2	0
4	2	Toluene	80	4	0
5	2	Toluene	100	4	0
6	4	Toluene	50	6	0
7	4	Toluene	80	6	0
8	10	Toluene	70	6	0
9	10	Toluene	90	6	5
10	10	Toluene	100	6	0
11	10	THF	60	6	0
12	10	DMF	70	6	0
13	10	Toluene	60	2[a]	0
14	10	Toluene	90	10[a]	7
15	20	Toluene	90	20[a]	20
16	30	Toluene	90	36[a]	36
17	30	Toluene	110	20[a]	5

[a]pressure tube, rt = room temperature (29-31 °C)

Table 3.6 : Reaction of halogenated acetamido stilbenes under this optimum conditions

i) 30 equivalents SnCl$_4$ ii) 90 °C iii) Toluene iv) 36 hours
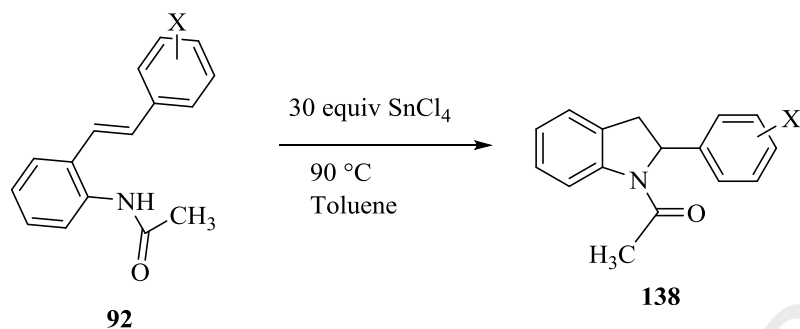
Entry	Stilbene	Product	Yield (%)
1	**96**	**139**	32
2	**102**	**140**	36
3	**108**	**141**	28

Table 3.6 continued

Entry	Stilbene	Product	Yield (%)
4	**98**	**142**	35
5	**104**	**143**	33
6	**106**	**144**	35
7	**112**	**145**	32

3.3.4 The Proposed Mechanism for the Formation of Indolines from Halogenated Acetamido Stilbenes Reaction with SnCl₄

When SnCl$_4$ was added to stilbene **92** it undergoes a radical oxidation to give radical cation of stilbene **130**. Okamoto et al., (2001) have shown that SnCl$_4$ was used for the aryl-aryl radical coupling of naphthol.[22] The stilbene radical cation **130** cyclizes to form the cation indoline **146** and the radical anion of $^{-•}$SnCl$_4$ formed HSnCl$_4$ with hydrogen from the amine.[23,24] Hydrogen was then inserted on the carbocation and formed indoline **138**. Stilbene with the methoxy group at *para* position requires less energy and time to form the indoline compared to stilbene with halogen because the methoxy group stabilise the carbon cation on stilbene **130** better than halogen. Because of this it requires a lot more SnCl$_4$ and energy to complete the reaction (Scheme 3.10).
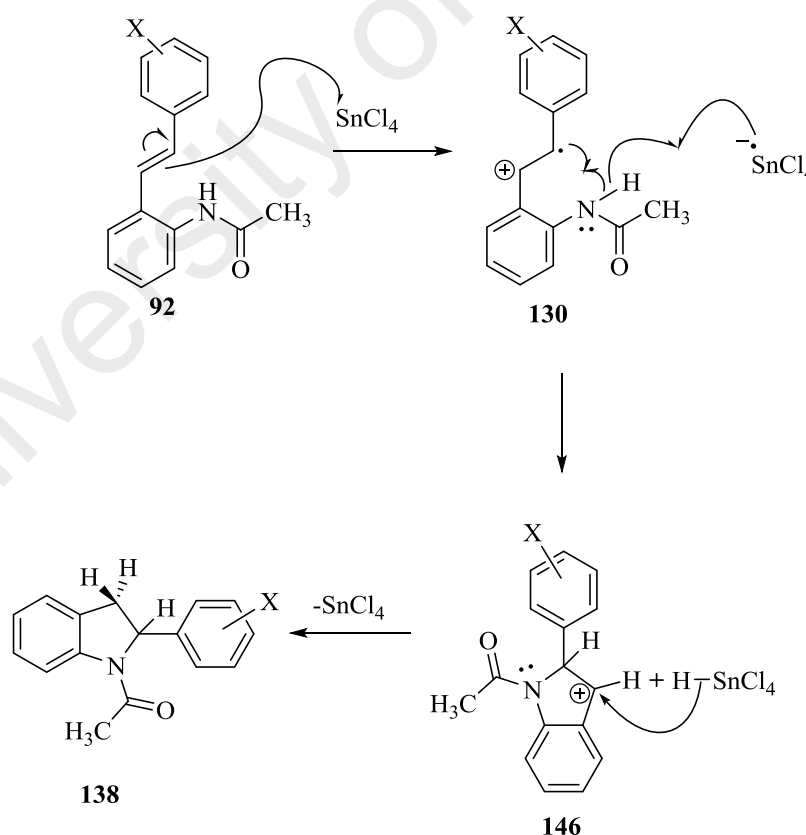
Scheme 3.10 : Proposed mechanism for the formation of indolines **138** mediated by SnCl$_4$

3.4 Structure Elucidation on Selected Stilbene, Imine and Indoline

3.4.1 Stilbene : (*E*)-*N*-(2-(4-fluorostyryl)phenyl)acetamide
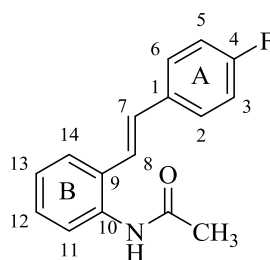
96

Compound **96** was afforded as a white amorphous. The mass spectrum showed a molecular ion peak M^+ at *m/z* 255.9151 (calcd. 255.1059) corresponding to the molecular formula of $C_{16}H_{14}FNO$. IR spectrum showed peaks at 3259 cm^{-1} and 1659 cm^{-1} due to the stretching of secondary amine NH and C=O stretching respectively.

^{1}H NMR spectrum displayed eight aromatic proton signals, a methyl singlet CH$_3$ at δ 2.18 that is bonded to the acetamide and two olefinic protons. Two sets of doublets were apparent at δ 6.95 and δ 7.05 with a coupling constant of 16.5 Hz corresponded to the *trans* olefinic protons of H-7 and H-8 respectively, which is the characteristic feature of this compound. The most deshielded aromatic proton H-11, resonated at δ 7.68 (d, *J* = 7.6 Hz) followed by H-14 at δ 7.53 (d, *J* = 7.6 Hz). Four protons of a *para* substituted phenyl ring of ring A appeared at δ 7.47 and δ 7.08 respectively attributable to H-2, H-6 and H-3, H-5 respectively. Other aromatic protons, H-12 and H-13, gave signals at δ 7.26 (t, *J* = 7.6 Hz) and δ 7.19 (t, *J* = 7.6 Hz) respectively.

From the ^{13}C NMR spectrum, 13 carbon signals were detected corresponded to 16 carbons; eight aromatic carbons, two olefinic carbons, four quartenary, one carbonyl and one *sp^3* carbon. The most deshielded carbon that was found was the carbonyl at δ 168.6 that formed the amide group. The second most deshielded carbon, C-4 was

detected at δ 161.2 (*para* position) which is attached to the very electronegative fluorine. As fluorine atom have the spin quantum number I of ½ , same as carbon, it coupled with carbon to give splitting of a doublet ($^1J_{cf}$ = 250.0 Hz). The symmetrical carbons, C-3 and C-5 were observed at δ 115.7 and displayed a doublet ($^2J_{cf}$ = 22.0 Hz), as it coupled with fluorine while another symmetrical two carbons, C-2 and C-6 resonated at δ 128.4 ($^3J_{cf}$ = 9.5 Hz). Other values of the ^{1}H and ^{13}C NMR is stated in Table 3.7.

^{1}H-^{1}H COSY spectrum showed correlation between H-7 with H-8. There were no other correlations for these protons which indicated that both H-7 and H-8 do not have any neighbouring protons thus indicating an isolated olefinic system. Other correlations were evident between the aromatic protons of ring A and B; H-11/H-12, H-13/H-14, H-2/H-3 and H-5/H-6 respectively.

The HMBC spectrum showed correlation spots between H-8 and C-9 while H-7 correlated with C-1, thus indicating that the olefinic group is connected to ring A through C-1 while connection to ring B is through C-9. From HMBC, C-10 correlated with H-14 and quartenary C-9 correlated with H-11. Other important signal that was detected is the correlation of C-8 with H-14. Furthermore, C-4 correlated with H-3 and H-5 in the ring A area. While C-9 correlated with H-11.

Thorough analysis of all 2D spectrums established the structure of compound **96**. Complete assignment of all ^{13}C and ^{1}H are listed in Table 3.7. HMBC correlations are shown in Figure 3.1.
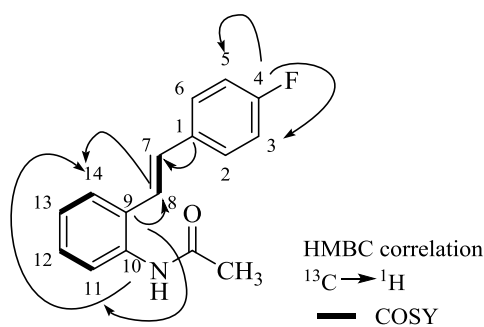
Figure 3.1: Main HMBC correlation of **96**

Compounds **98** and **100** differed only in the position of F atom. The fluorine atom is attached to C-3 (*meta*) in **98** while in **100** was attached to C-2 (*ortho*). Both compound **98** and **100** have similar proton data on ring B with **96** except for ring A, which is different due to the position of the fluorine (see spectrum of **98** and **100** in Appendix).

Table 3.7 : ^{1}H and ^{13}C NMR values of compound **96**

Position	[1]H (ppm)	[13]C (ppm)
1	-	133.1
2	7.47 (m)	128.4 (d, $J = 9.5$ Hz)
3	7.08 (m)	115.7 (d, $J = 22.0$ Hz)
4	-	161.2 (d, $J = 250.0$ Hz)
5	7.08 (m)	115.7 (d, $J = 22.0$ Hz)
6	7.47 (m)	128.4 (d, $J = 9.5$ Hz)
7	6.95 (d, $J = 16.5$ Hz)	131.0
8	7.05 (m)	123.2
9	-	130.4
10	-	134.4
11	7.68 (d, $J = 7.6$ Hz)	124.5
12	7.26 (t, $J = 7.6$ Hz)	128.1
13	7.19 (t, $J = 7.6$ Hz)	125.6
14	7.53 (d, $J = 7.6$ Hz)	126.6
C=O	-	168.6
CH$_3$	2.18 (s)	24.1
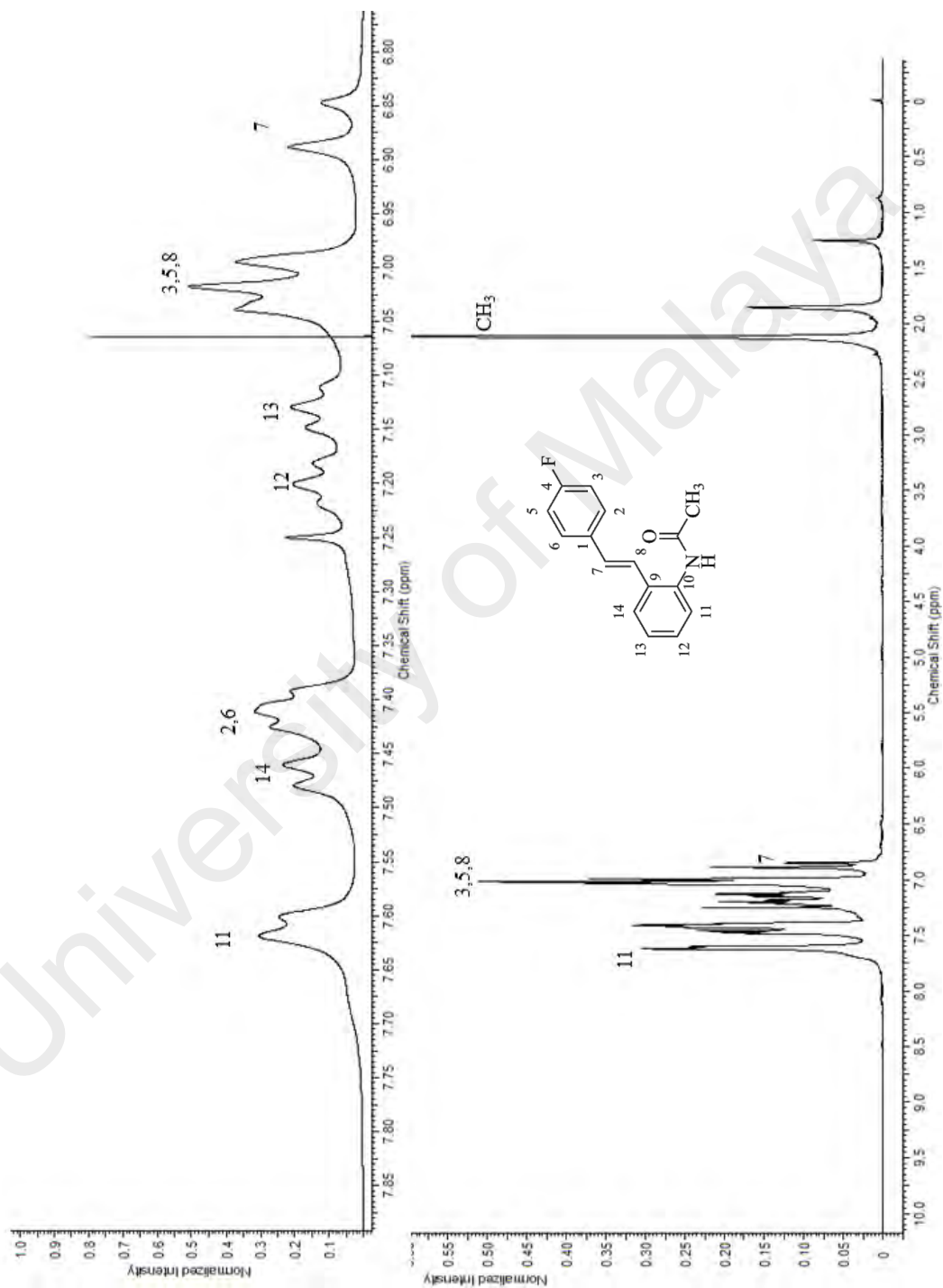
Figure 3.2 : ^{1}H NMR (CDCl$_3$, 400 MHz) spectrum of compound **96**
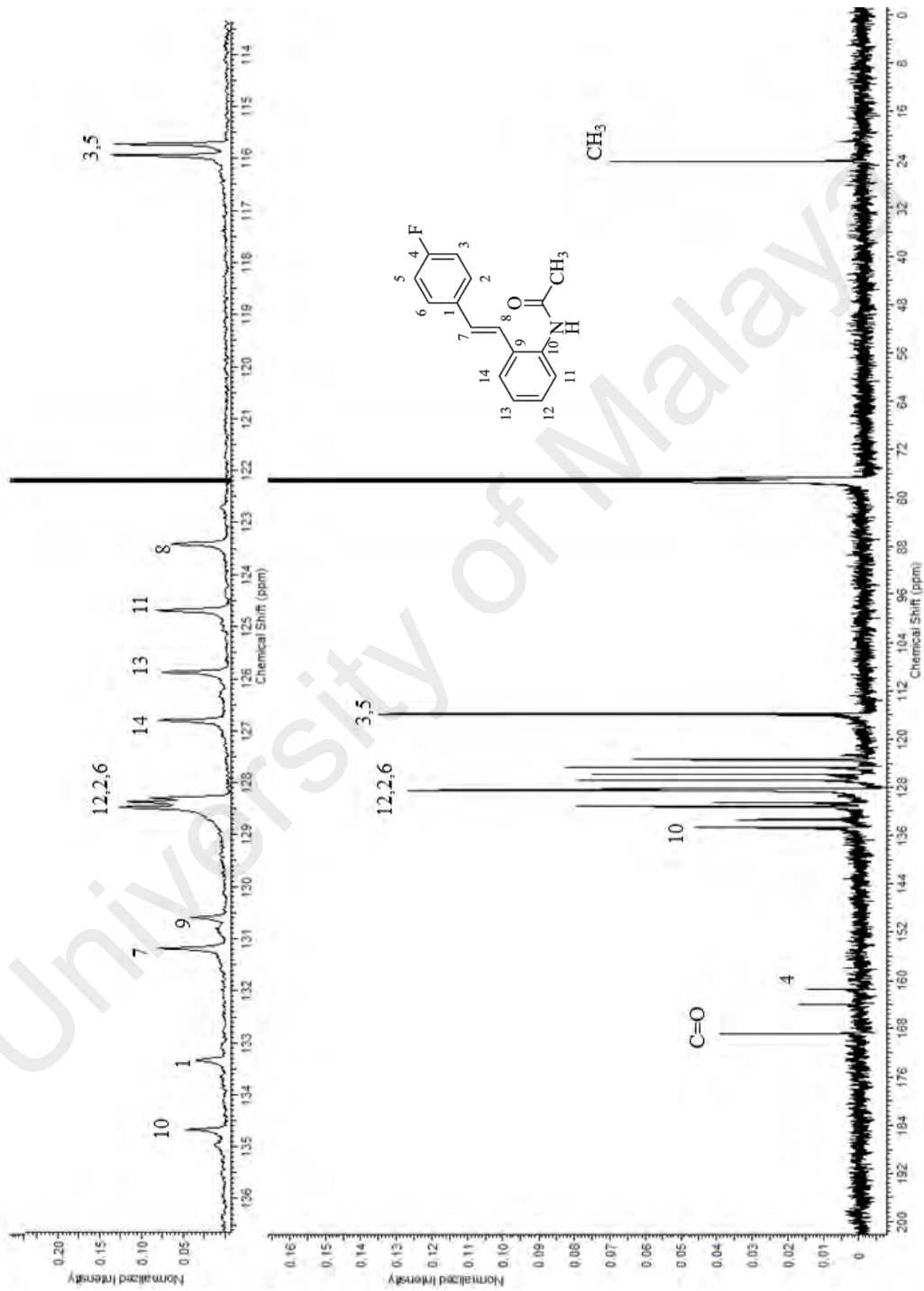
Figure 3.3 : ^{13}C NMR (CDCl$_3$, 100 MHz) spectrum of compound **96**
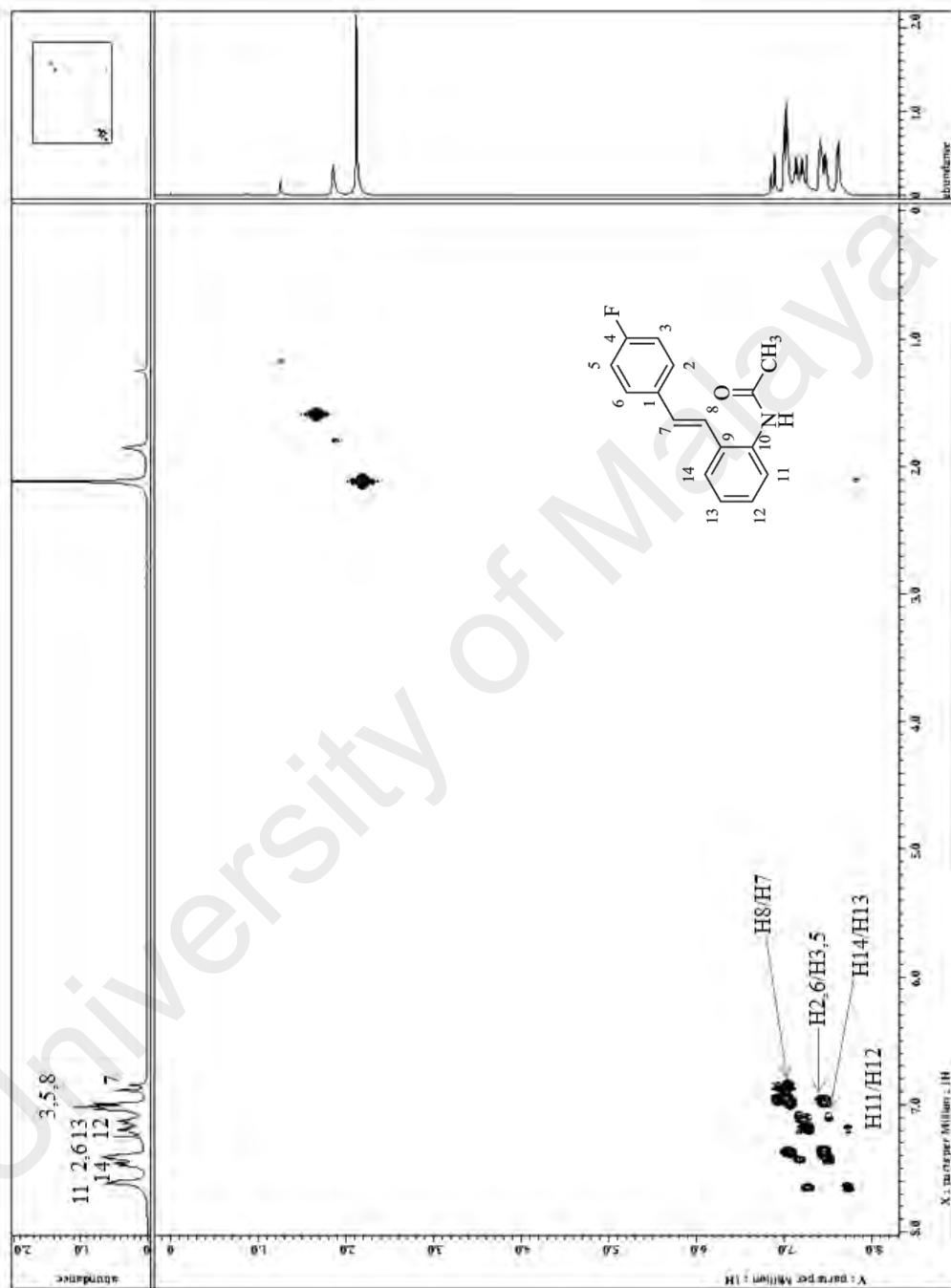
Figure 3.4 : COSY (CDCl$_3$, 400 MHz) spectrum of compound **96**
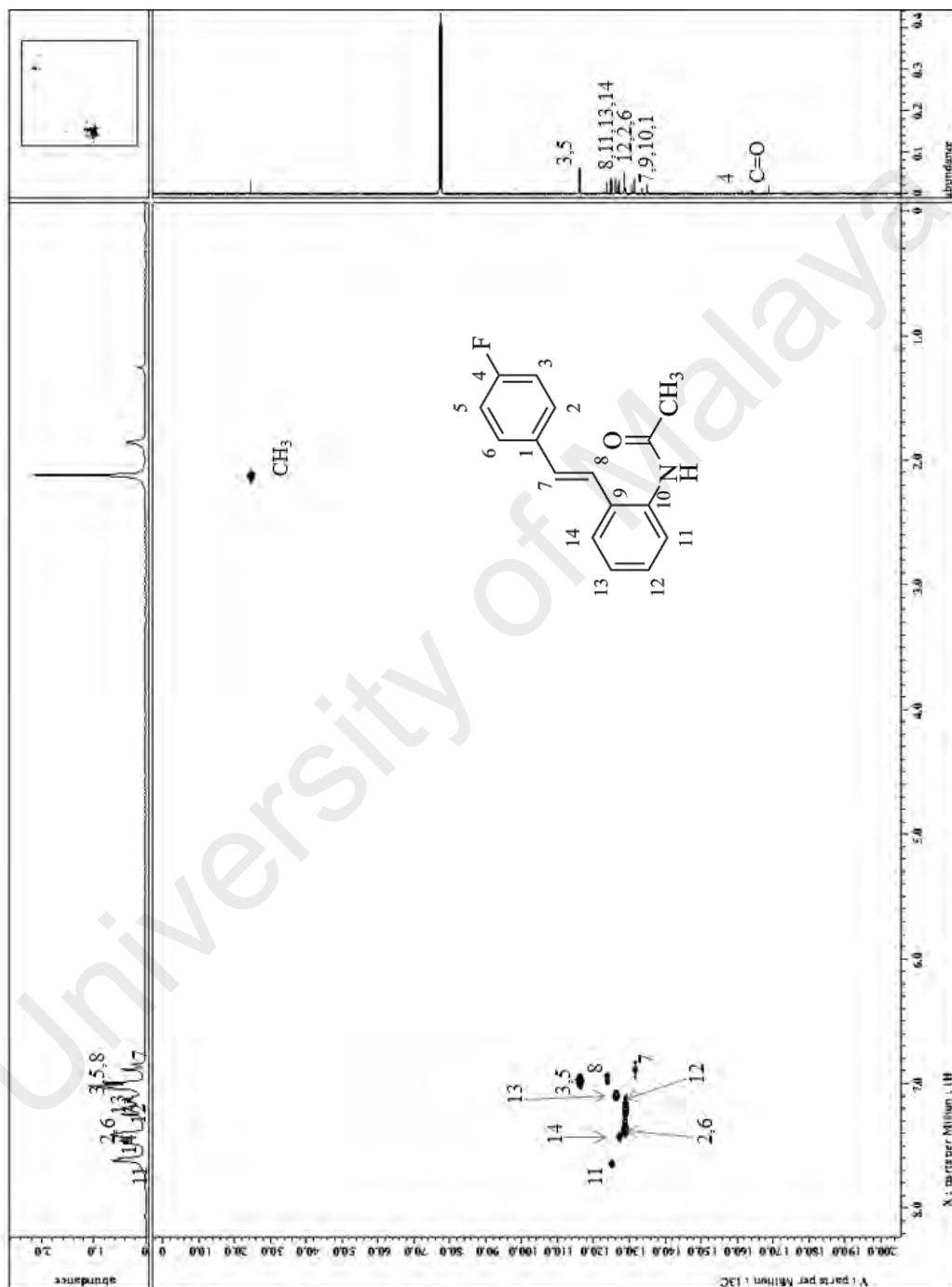
Figure 3.5 : HSQC (CDCl₃, 400 MHz) spectrum of compound **96**
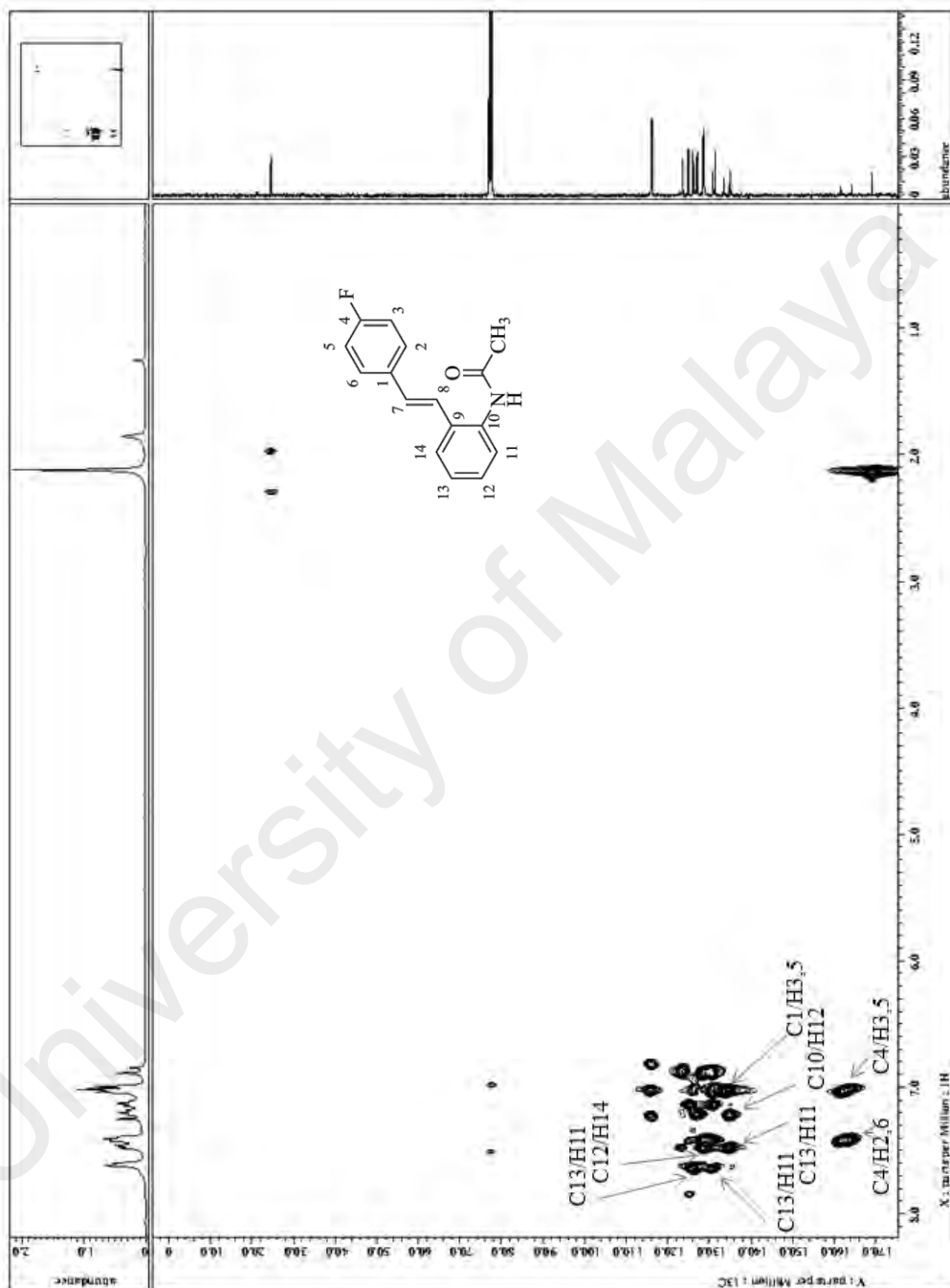
Figure 3.6 : HMBC (CDCl$_3$, 400 MHz) spectrum of compound **96**

3.4.2   Imine : (*1R,2S*)-1-(2-(((*E*)-2-acetamidobenzylidene)amino)phenyl)-2-(3-bromophenyl)-2-chloroethyl acetate and (*1S,2S*)-1-(2-(((*E*)-2-acetamidobenzylidene)amino)phenyl)-2-(3-bromophenyl)-2-chloroethyl acetate

127 (32%)   **128** (15%)
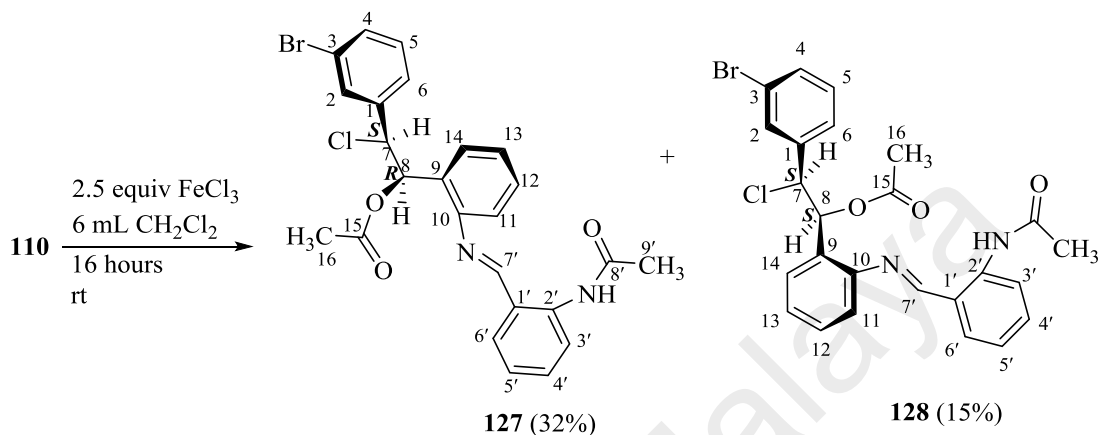
Two products **127** and **128** with similar spectroscopic characteristic were obtained. The only difference is the dihedral angle at H-7 and H-8.
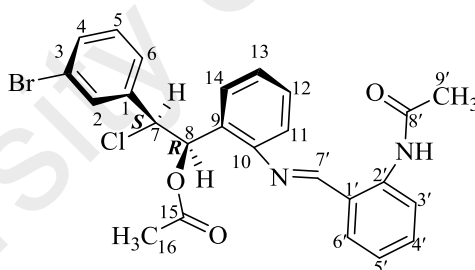
127

Compound **127** was afforded as a white amorphous. The mass for **127** was determined from HRESIMS with a value of $[M+H]^+$ of *m/z* 513.0581 (calcd. 513.0581). The mass value of compound **127** corresponded to the molecular formula of $C_{25}H_{23}BrClN_2O_3$. As compound **127** contained 2 halogens that are chlorine and bromine with chlorine has 2 isotopes ^{35}Cl and ^{37}Cl while bromine also has 2 isotopes ^{79}Br and ^{81}Br. From the mass spectra we observed an isotope pattern where *m/z* 513.0581, 515.0563 and 517.0549 were displayed and the intensities of isotope peaks showed that

[M+H+2]$^+$ peak is 130% the length of [M+H]$^+$ peak (*m/z* 513.0581) and [M+H+4]$^+$ peak is 30% the length of [M+H]$^+$ thus confirming the presence of one Cl and one Br in the structure of **127** and **128**.[25] The spectrum also showed [M+Na]$^+$ peak (*m/z* 535.0403), [M+Na+2]$^+$ (*m/z* 537.0387) and [M+Na+4]$^+$ (*m/z* 539.0367) portraying the same isotope pattern as before. In addition, 15 degree of unsaturation was deduced from the molecular formula which suggested the possible presence of 3 aromatic rings.

In the ^{1}H NMR spectrum, a total of 22 proton signals were found. Twelve were aromatic protons, six methyl protons, two aliphatic protons, one NH and one attached to a sp^2 carbon (CN). The absence of the *trans* coupling was replaced by a pair of doublet signals at δ 4.99 (d, *J* = 8.2 Hz) and δ 6.57 (d, *J* = 8.2 Hz) which were assigned to H-7 and H-8 respectively. These two aliphatic proton signals were rather deshielded as they were in proximity to two electronegative atoms, Cl and O. H-7′ signal at δ 7.74 is link to the imine. NH proton signal was observed at δ 12.03 which was more deshielded and the nitrogen was attached to C-2′. In ring A, a singlet at δ 7.18 was evident and ascribed to H-2. The most deshielded aromatic proton resonated at δ 8.87 and was attributed to H-3′. Another two singlets were observe on the upfield part at δ 2.21 and δ 2.32 and corresponded to H-16 and H-9′ respectively.

^{13}C NMR displayed 25 carbon signals. 18 were aromatic carbons, two aliphatic sp^3 carbons, two carbonyls, two methyls and one sp^2 carbon (CN). Two carbonyl signals appeared at δ 169.9 and δ 170.4 were assignable to C-15 and C-8′ respectively. Interestingly the two olefinic signals present in the starting material, stilbenes, were not detected. Instead two downfield sp^3 carbon signals were detected at δ 64.8 and δ 73.5, therefore indicating that the carbons are attached to electronegative heteroatoms, O and Cl. In addition a downfield sp^2 methane carbon signal appeared at δ 164.6 thus implying

the existence of an imine carbon (C-7′).The ^{1}H and ^{13}C values of **127** is shown in Table 3.8.

In light of the complex structure, 2D NMR experiments were executed to confirm the structure. HSQC-TOCSY experiment was applied on the compound and gave three ^{1}H-^{1}H spin system that help in assigning the atom. It was found that H-4, H-5, H-6 form a spin system, H-11, H-12, H-13, H-14 form another spin system and the final spin system was formed by H-3′, H-4′, H-5′ and H-6′. Through COSY NMR, H-14 was found to correlate with H-13 and H-13 showed a splitting of a triplet with a coupling constant of 7.3 Hz same as H-12 (t, J = 7.3 Hz) in the same spin system. Furthermore H-3′ showed correlation to H-4′. Correlation between H-7 and H-8 showed there was no adjacent proton to this aliphatic system.

In addition, HMBC spectrum has shown cross-peaks between C-1 with H-5 and H-7 suggesting a link between ring A and ring B through C-7 and C-8. Correlation between C-10 with H-7′ and C-6 with H-7 showed that there was an imine linkage between ring B and ring C. Signal showing C-15 corresponded with H-8 suggested that there was an ester group attached to C-8 (Figure 3.7). NOESY spectrum showed a correlation between H-7 and H-8 implying that they were near to each other through space.

After thorough analysis of the 1D and 2D NMR we proposed the structure of compound **127** to be (*1R,2S*)-1-(2-((((*E*)-2-acetamidobenzylidene)amino)phenyl)-2-(3-bromophenyl)-2-chloroethyl acetate.
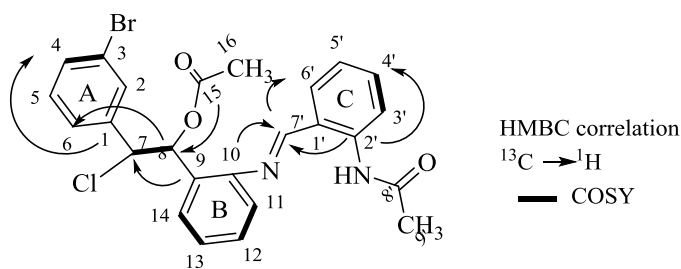
Figure 3.7 : Main HMBC correlation of imine **127** (stereochemistry omitted).

Compound **127** was the major entity while **128** the minor one. Comparison of the ^{1}H and ^{13}C data is shown in Table 3.8 with similar values. It is noted that the coupling constant for H-7 and H-8 was different for compound **127** and **128**. In addition the chemical shifts were also quite different. The H-7 and H-8 resonated in **128** at a slightly lower field than that of **127**. Imine **127** showed a coupling constant of 8.0 Hz while imine **128** showed 4.0 Hz.
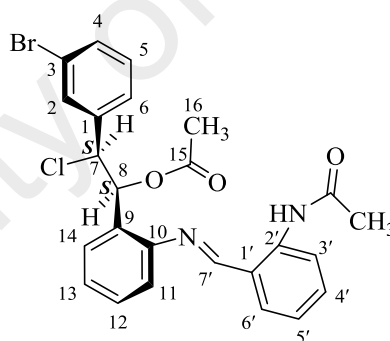
128

According to Karplus equation, 8.0 Hz represent the dihedral angle of H-7 and H-8 with an angle of -37° while 4.0 Hz is equal to -50°.[26] A computational analysis of compound **127** and **128** was performed; the calculation showed that compound **127** have a dihedral angle of -46.1° with enthalpy energy of -300.9668 kJ/mol (Figure 3.8) while compound **128** possessed a dihedral angle of -53.6° with energy of -269.1187 kJ/mol (Figure 3.9). This calculation supports that compound **127** is the major product

with lower enthalpy energy compared to compound **128** implying that the former was more stable.

Compound **126** and **129** have similar spectroscopic features as compound **127** with a similar coupling constant of H-7 and H-8 (8 Hz). The difference observed between the compounds is the coupling pattern of the aromatic protons of ring A (see spectrum of **126**, **129** and **128** in Appendix).

Table 3.8: ^{1}H and ^{13}C values of compound **127** and **128**

Position	^{1}H (ppm) **127**	^{13}C (ppm)	^{1}H (ppm) **128**	^{13}C (ppm)
1	-	130.4	-	128.4
2	7.18 (s)	131.1	7.16 (m)	131.1
3	-	122.0	-	122.1
4	7.23 (d, J = 8.0 Hz)	131.6	7.16 (m)	131.9
5	6.83 (m)	129.5	6.92 (m)	129.5
6	6.98 (d, J = 8.0 Hz)	126.6	7.03 (d, J = 7.7 Hz)	126.6
7	4.99 (d, J = 8.0 Hz)	64.8	5.23 (d, J = 4.0 Hz)	63.4
8	6.57 (d, J = 8.0 Hz)	73.5	6.71 (d, J = 4.0 Hz)	72.6
9	-	138.9	-	138.8
10	-	149.0	-	149.1
11	7.60 (d, J = 7.3 Hz)	126.8	7.50 (m)	128.3
12	7.41 (t, J = 7.3 Hz)	130.3	7.33 (t, J = 8.0 Hz)	126.3
13	7.37 (t, J = 7.3 Hz)	126.8	6.92 (m)	118.4
14	6.81 (m)	118.7	7.45 (m)	130.2
15	-	169.9	-	169.5
16	2.21 (s)	21.0	2.21 (s)	21.0
1′	-	120.4	-	120.4
2′	-	140.2	-	140.1
3′	8.87 (d, J = 7.8 Hz)	120.1	8.82 (d, J = 8.0 Hz)	120.0
4′	7.53 (t, J = 7.8 Hz)	133.0	7.52 (m)	133.0
5′	7.19 (t, J = 7.8 Hz)	122.7	7.16 (m)	122.6
6′	7.32 (d, J = 7.8 Hz)	134.9	7.38 (d, J = 8.0 Hz)	134.7
7′	7.74 (s)	164.6	8.07 (s)	164.6
8′	-	170.4	-	170.2
9′	2.32 (s)	25.6	2.33 (s)	25.6
NH	12.03	-	12.01	-
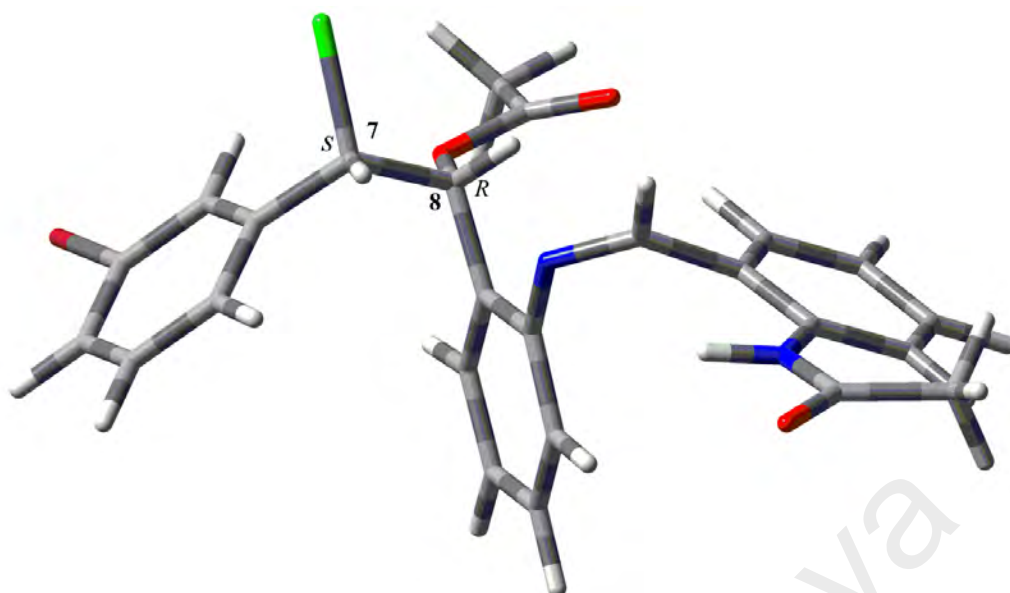
Figure 3.8 : Imine **127** (Optimized 3D model)
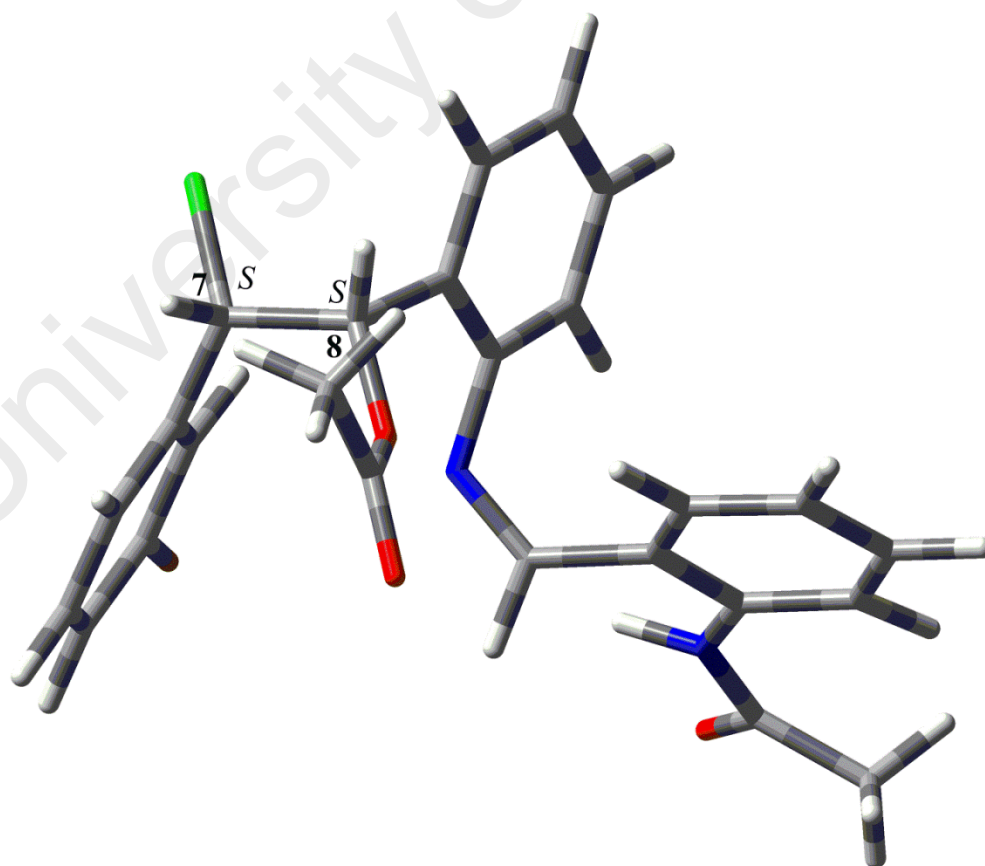
Figure 3.9 : Imine **128** (Optimized 3D model)
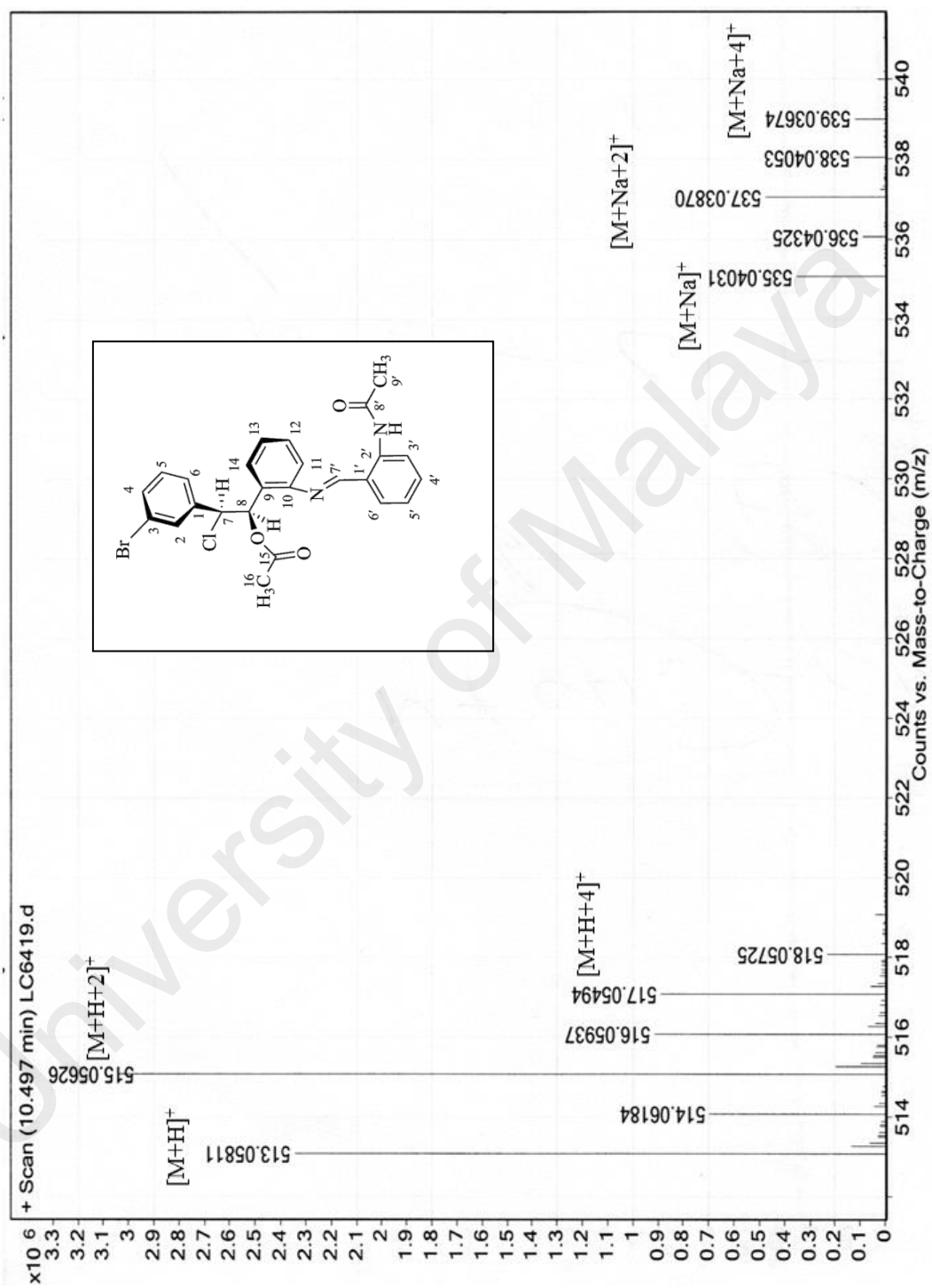
Figure 3.10 : Mass spectrum *m/z* of compound **127**
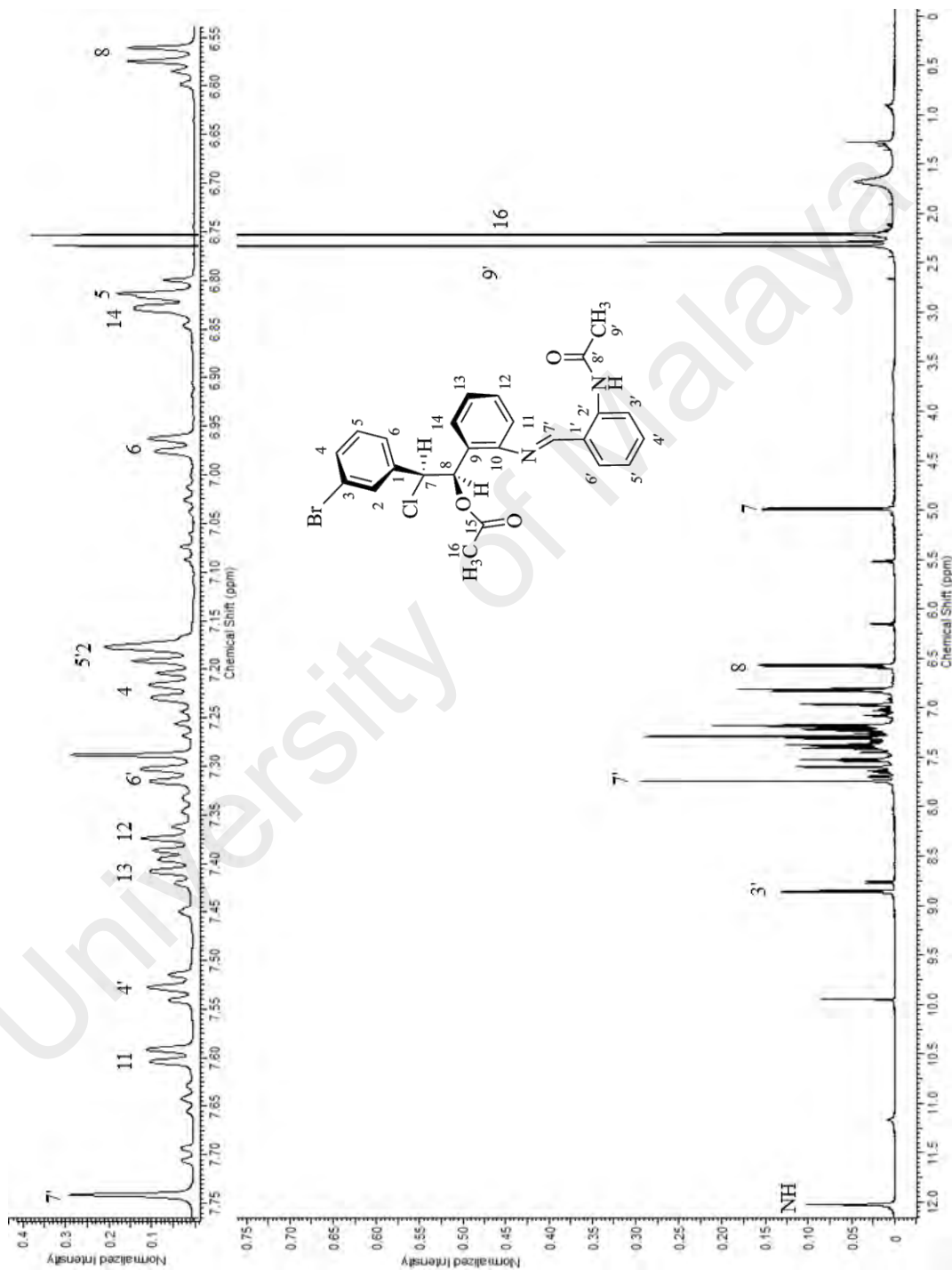
Figure 3.11 : ¹H NMR (CDCl₃, 600 MHz) spectrum of compound **127**
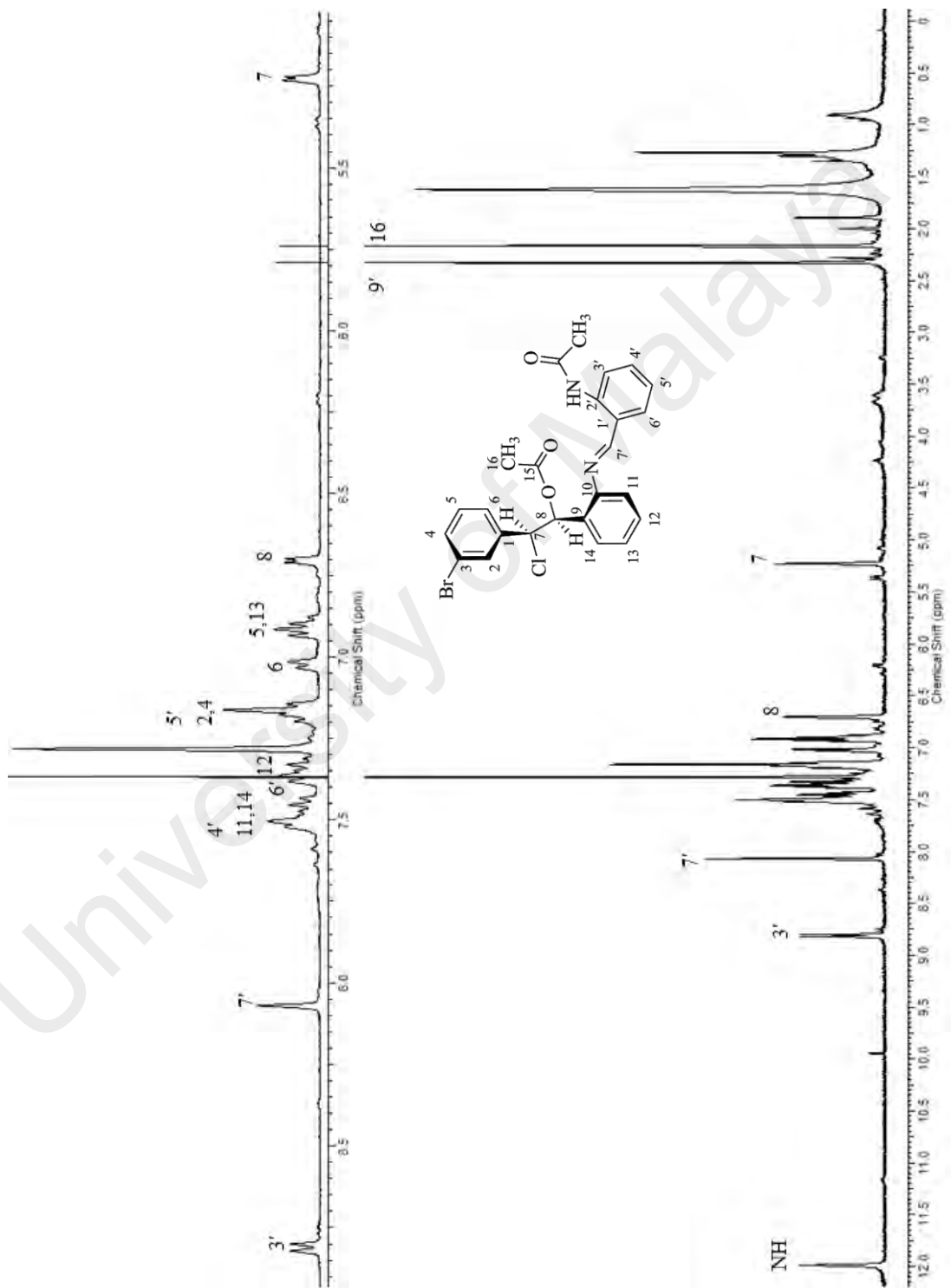
Figure 3.12 : ^{1}H NMR (CDCl$_3$, 400 MHz) spectrum of compound **128**

71
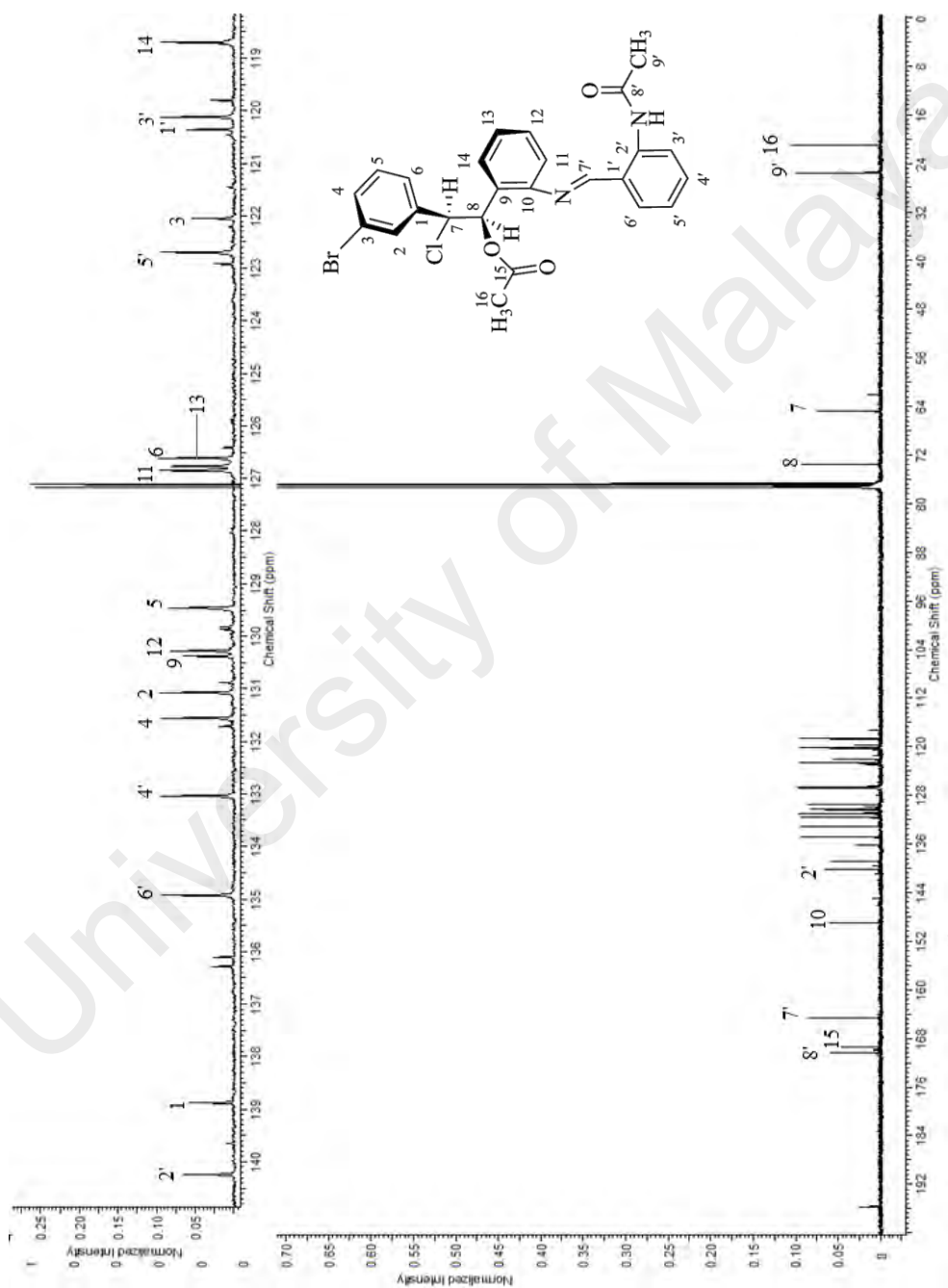
Figure 3.13 : ^{13}C NMR (CDCl$_3$, 150 MHz) spectrum of compound **127**
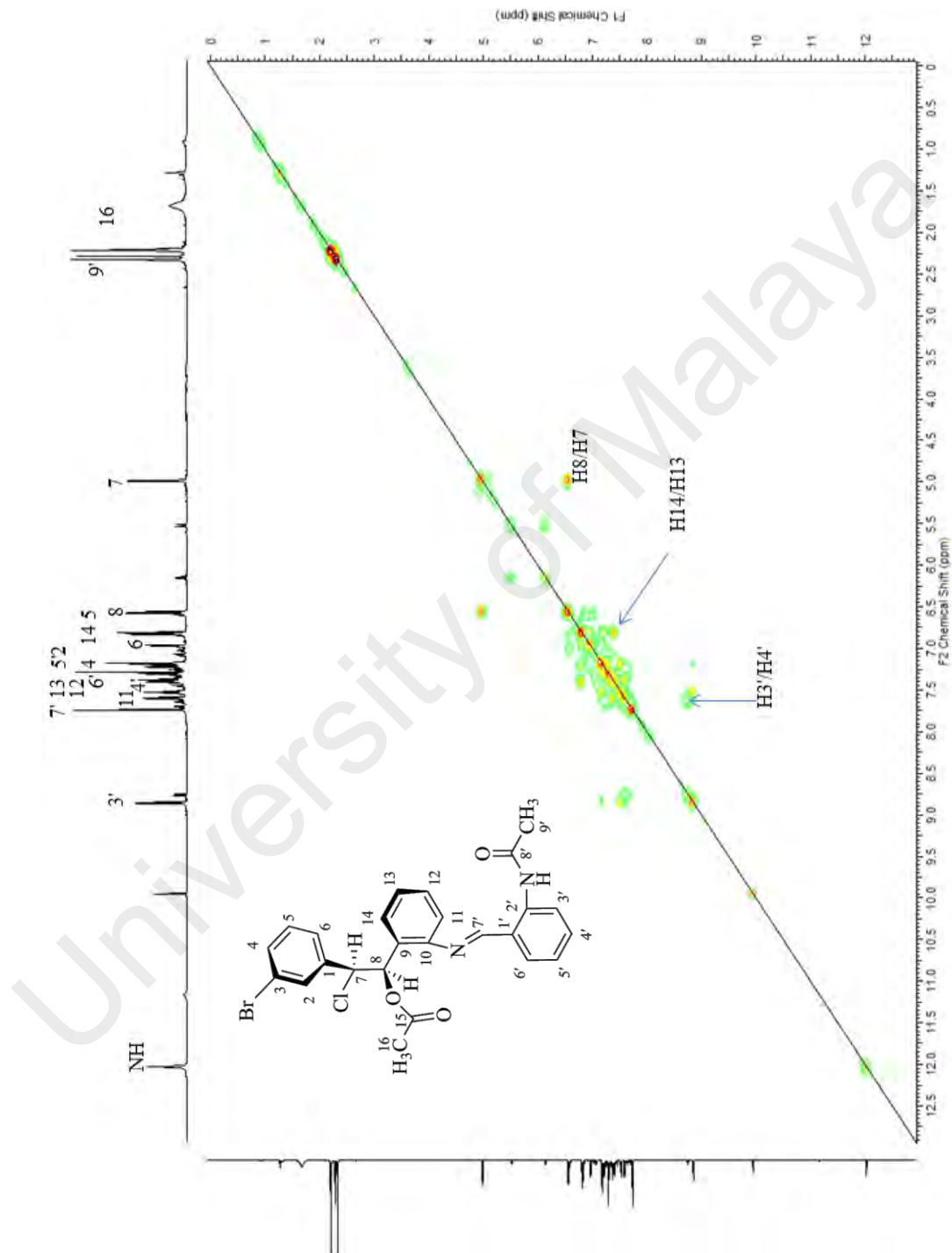
Figure 3.14 : COSY (CDCl₃, 600 MHz) spectrum of compound **127**
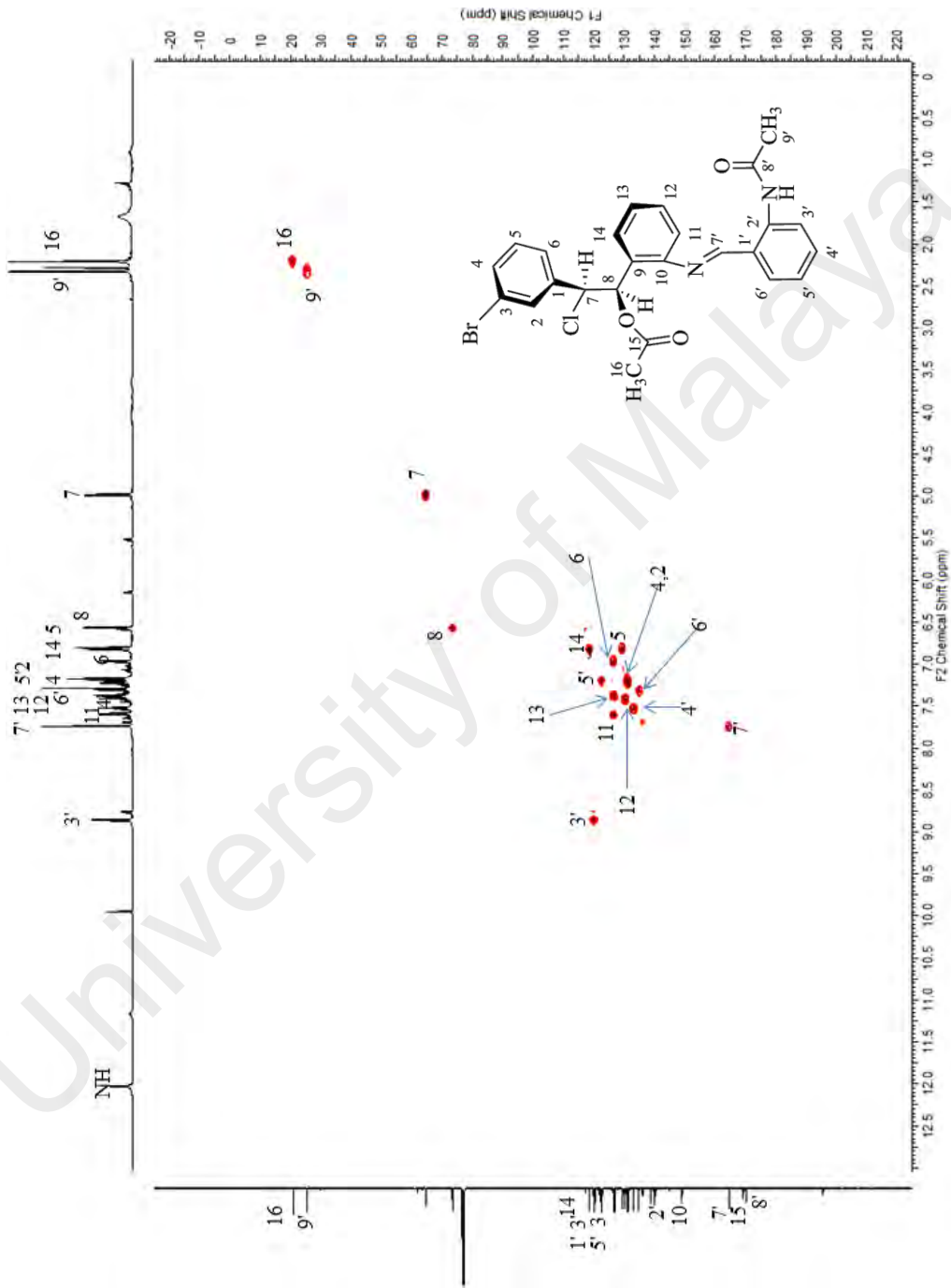
Figure 3.15 : HSQC (CDCl₃, 600 MHz) spectrum of compound **127**
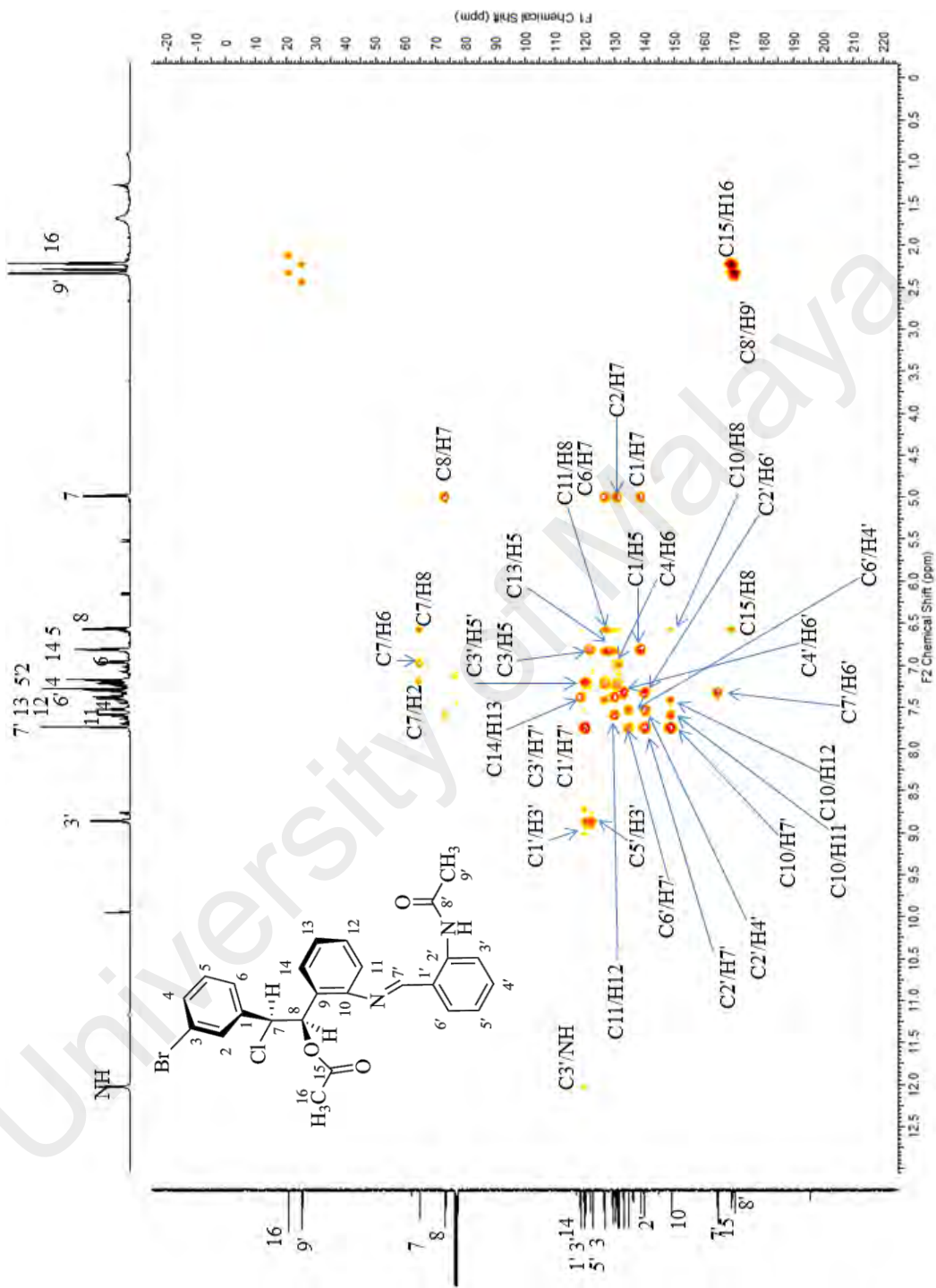
Figure 3.16 : HMBC (CDCl₃, 600 MHz) spectrum of compound **127**
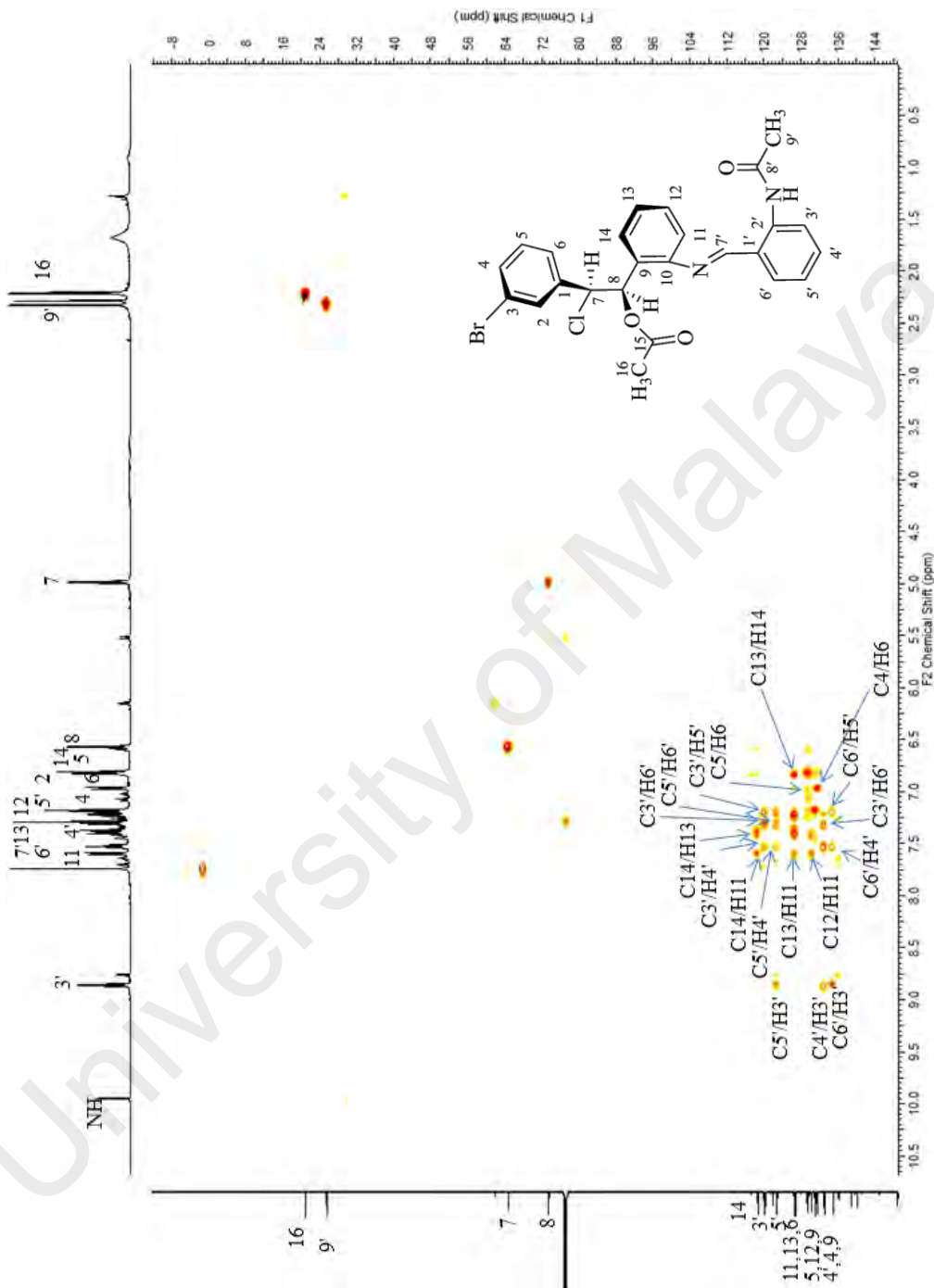
Figure 3.17 : HSQC-TOCSY (CDCl$_3$, 600 MHz) spectrum of compound **127**
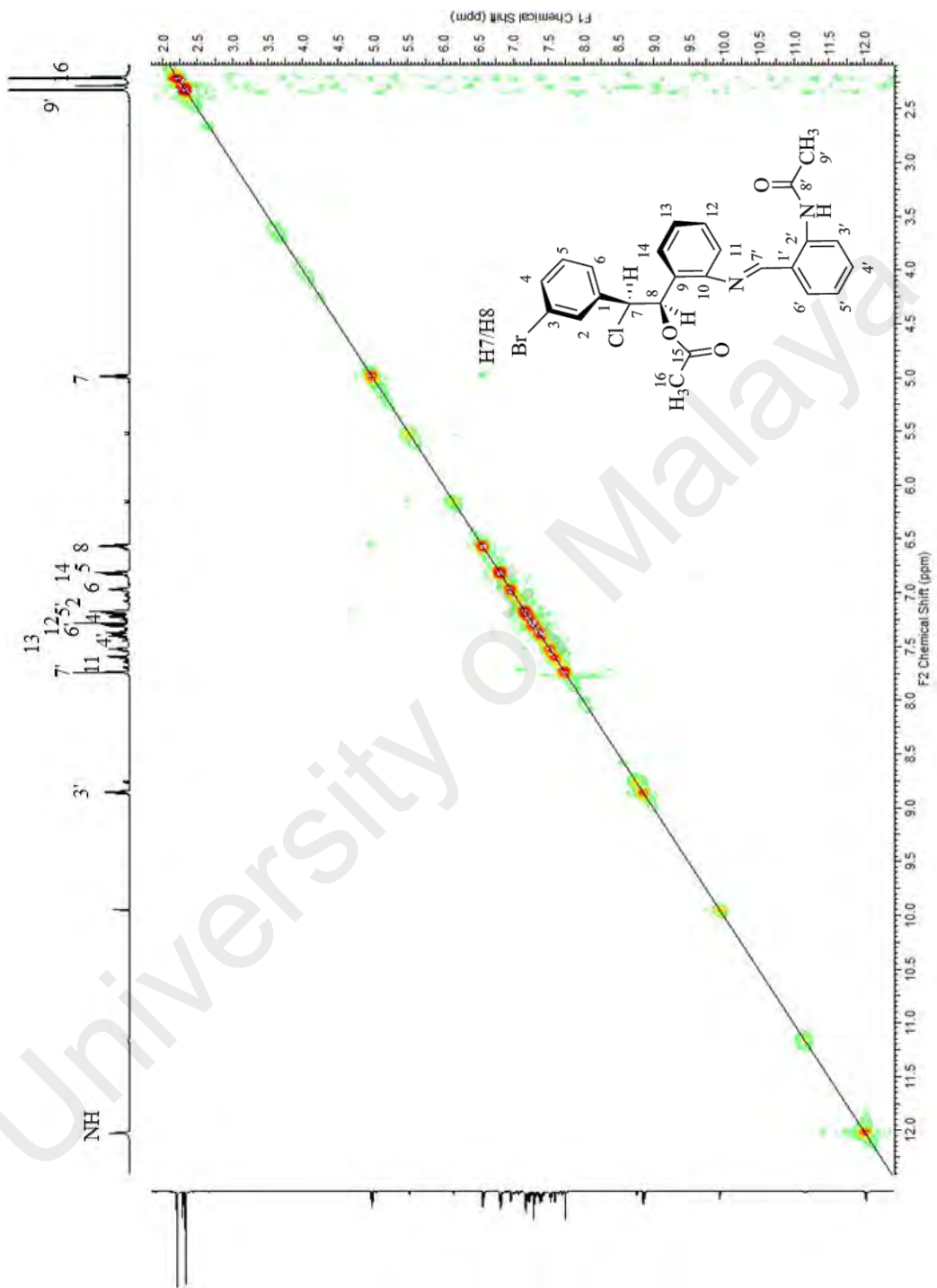
Figure 3.18 : NOESY (CDCl₃, 600 MHz) spectrum of compound **127**

3.4.3 Indoline : 1-(2-(2-chlorophenyl)indolin-1-yl)ethan-1-one
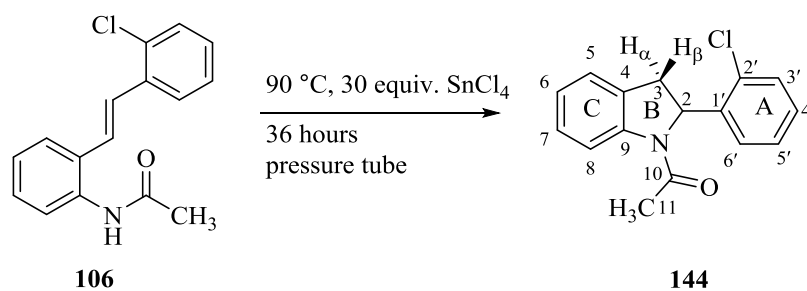
Compound 1**44** was afforded as a white amorphous. The mass was determined by HRESIMS and showed a pseudo molecular ion peak $[M+H]^+$ of m/z 272.0849 and corresponded to the molecular formula of $C_{16}H_{15}ClNO$. As chlorine have two isotopes ^{35}Cl and ^{37}Cl, another mass peak of $[M+H+2]^+$ m/z 274.0828 corresponded to isotope ^{37}Cl which is 32.6% in height of the molecular ion peak.

The ^1H NMR spectrum showed eight aromatic protons, three aliphatic proton signals and a methyl. One methyl peak was detected at δ 2.00 was attached to the amide. The most deshielded proton signal appeared at δ 8.34 in ring C was ascribable to H-8. Other aromatic proton signals for ring B were found at δ 7.13, δ 7.22 and δ 7.28. Aromatic proton signals for ring A were detected at δ 7.06, δ 7.05, δ 7.16 and δ 7.43. A crucial CH_2 peak appeared at δ 2.94 (d, J = 16.1 Hz) and δ 3.85 (dd, J = 16.1 and 9.0 Hz) were attributed to H-3α and H-3β suggested that this structure is an indoline and not an indole as reported by Ahmad et al. in 2009.[5] Furthermore, a doublet was observed at δ 5.77 (d, J = 9.0 Hz) and assigned to H-2, added further support that **144** is an indoline.

Spectrum of ^{13}C NMR showed 16 carbon signals with 12 aromatic carbons, two aliphatic carbons, a methyl and one carbonyl. The two aliphatic carbon signals were very important as it showed the pattern of an indoline and were observed at δ 60.6 and δ 37.5 ascribable to C-2 and C-3 respectively. A methyl peak was present at δ 23.7 and attributed to C-11. C-4 and C-2′ signals were overlapped and exhibited at δ 131.3.

Carbonyl peak can be seen at δ 169.4 and assigned to C-10. Other aromatic carbon signals were shown in Table 3.9.

COSY showed the correlation of H-8 and H-7 and also cross-peak of H-2 with H-3α and H-3β. HMBC spectrum assisted in confirming the structure whereby a cross-peak of C-9 with H-5 and H-3α suggested ring B and C are fused together. Signals of C-1′ with H-3α and H-3β were observed linking ring A and B. Other correlation such as between C-6 with H-3α/3β and H-8 were present in the spectrum (Figure 3.18).

Thorough study of the 1D and 2D NMR data with mass spectra and based on the literature,[7] it is conclusive that compound **144** is 1-(2-(2-chlorophenyl)indolin-1-yl)ethan-1-one.
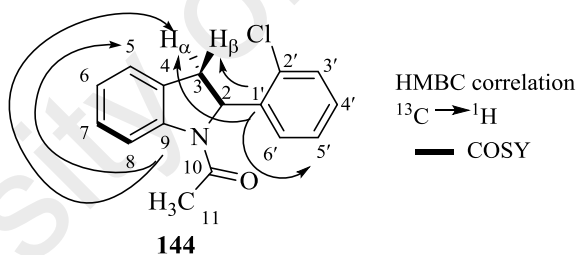
Figure 3.19 : Main HMBC correlation of indoline **144**

Table 3.9: ^{1}H and ^{13}C NMR data of compound **144**

Position	^{1}H (ppm)	^{13}C (ppm)
1	-	-
2	5.77 (d, J = 9.0 Hz)	60.6
3α	2.94 (d, J = 16.1 Hz)	37.5
3β	3.85 (dd, J = 16.1 and 9.0 Hz)	37.5
4	-	131.3
5	7.13 (d, J = 7.7 Hz)	125.0
6	7.22 (t, J = 7.7 Hz)	129.0
7	7.28 (t, J = 7.7 Hz)	127.8
8	8.34 (d, J = 7.7 Hz)	117.1
9	-	143.2
10	-	169.4
11	2.00 (s)	23.7
1'	-	140.2
2'	-	131.3
3'	7.06 (d, J = 7.6 Hz)	124.3
4'	7.05 (dt, J = 7.6 and 1 Hz)	125.8
5'	7.16 (t, J = 7.6 Hz)	127.7
6'	7.43 (d, J = 7.6 Hz)	129.9
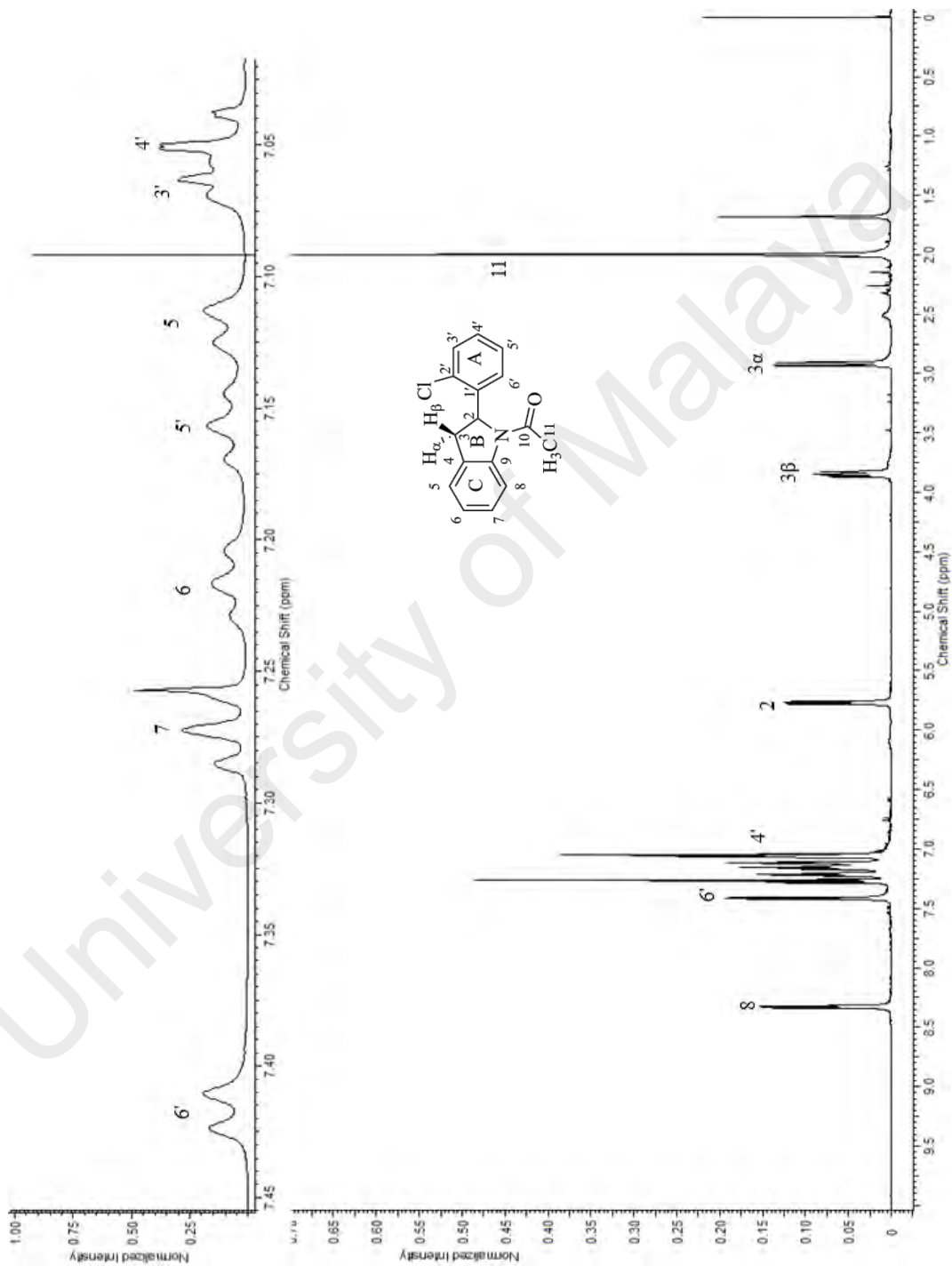
Figure 3.20 : ^{1}H NMR (CDCl$_3$, 600 MHz) spectrum of compound **144**
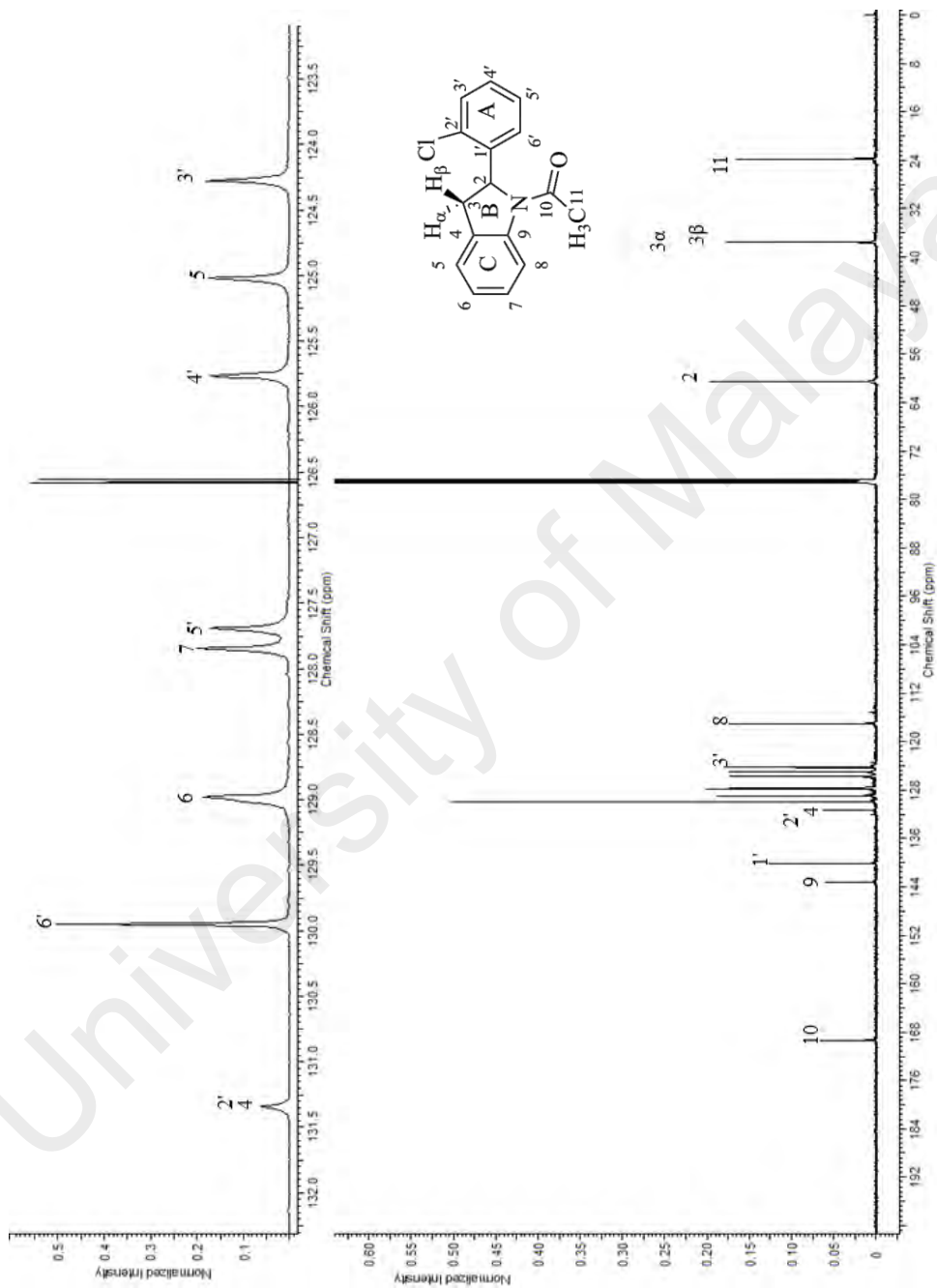
Figure 3.21 : ^{13}C NMR (CDCl$_3$, 150 MHz) spectrum of compound **144**
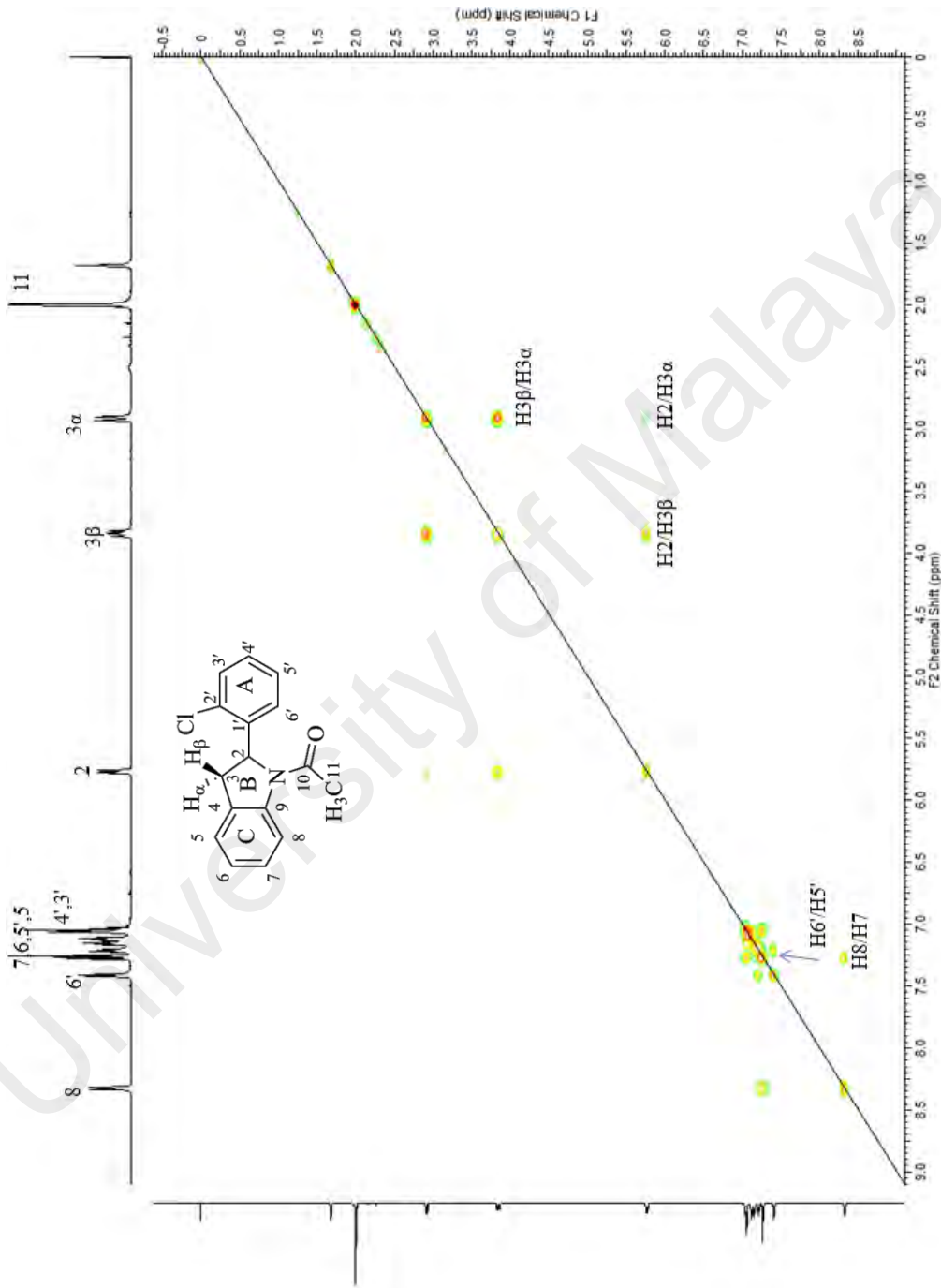
Figure 3.22 : COSY (CDCl₃, 600 MHz) spectrum of compound **144**
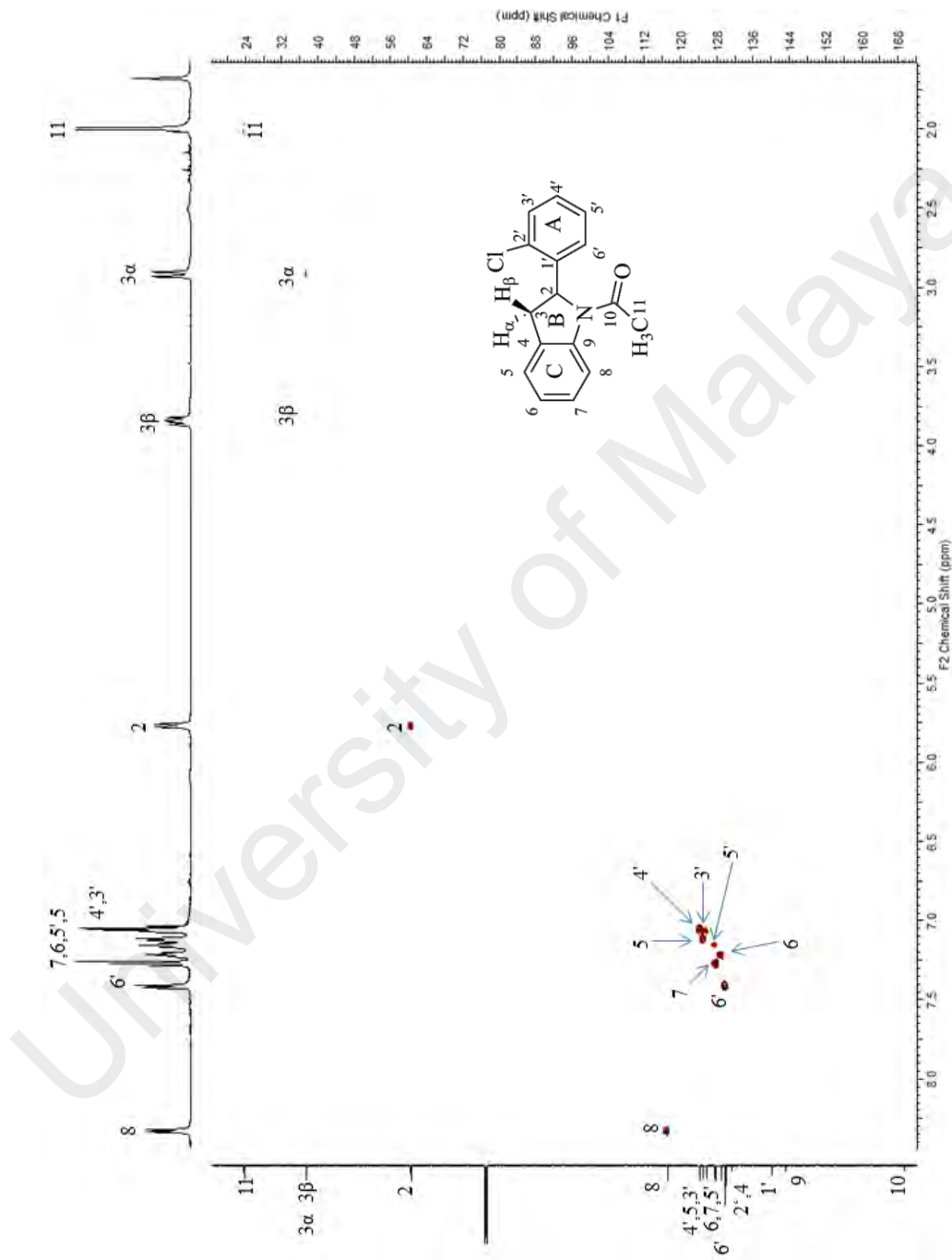
Figure 3.23 : HSQC (CDCl₃, 600 MHz) spectrum of compound **144**
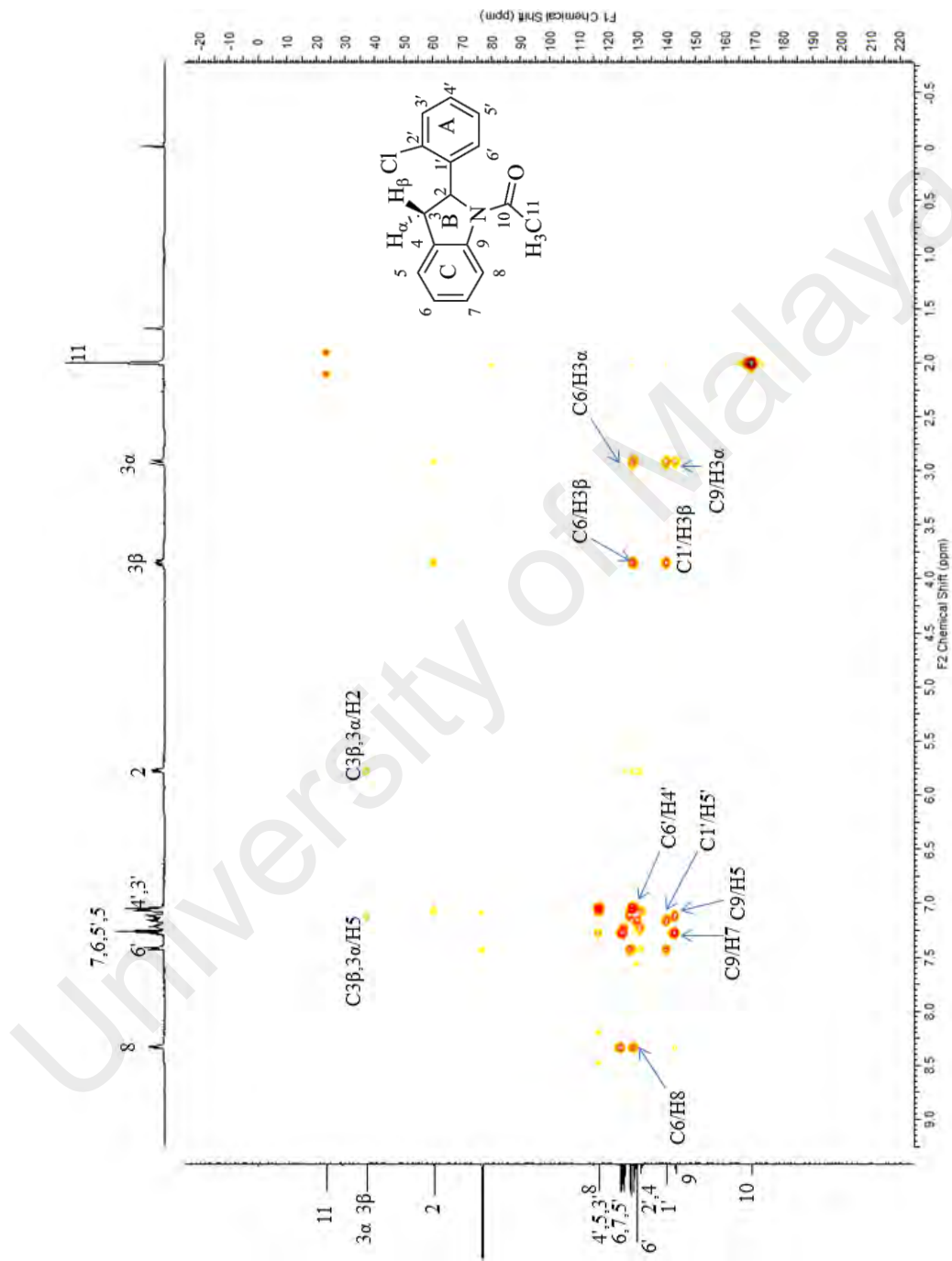
Figure 3.24 : HMBC (CDCl$_3$, 600 MHz) spectrum of compound **144**

3.5 Conclusion

Synthesis of halogenated acetamido stilbenes were done by the coupling of 2-Iodoacetamide with halogenated styrenes through the Heck coupling which afforded nine stilbenes (**96, 98, 100, 102, 104, 106, 108, 110, 112**). The stilbenes were then subjected to Lewis acid (FeCl₃, SnCl₄) mediated reaction.

Reaction between $FeCl_3$ and the halogenated acetamido stilbenes resulted in the formation of imines (**121, 122, 123, 124, 125, 126, 127, 128, 129**) which clearly are different products (indoline and bisindoline) from our group previous studies with $FeCl_3$.[5,27] The imines were produced with the loss of ring A of stilbene **92**, ring B which was 2-acetamidobenzaldehyde **132** coupled with the uncleaved stilbene **135** linking through the imine bond is commonly seen in the production of Schiff base. The insertion of chlorine into the stilbene replacing the *trans* bond of stilbene **92** probably comes from $FeCl_3$ as can be seen in Ahmad et al. (2009) work.[5] Only stilbene **110** gave 2 isomers (**127** and **128**) while the other halogenated acetamido stilbenes **92** gave one isomer. This study shows that electron-withdrawing group does have an effect in the radical cation oxidative reaction of stilbene with Lewis acid.

$SnCl_4$ reaction with the halogenated acetamido stilbenes produced indolines (**139, 140, 141, 142, 143, 144, 145**) which are similar with products (indoline) we attained from previous group studies with $FeCl_3$. Harsh reaction condition (higher temperature and higher ratio of $SnCl_4$) were required due to the halogen withdrawing properties that required more energy compared with indoline **137** that have electron-donating group (methoxy) which required less time and energy for the cyclization of stilbene **136** to complete. No dimerization of the stilbenes was observed from the $SnCl_4$ reaction.

3.6   Experimental Section

All reagents were purchased from company and used without further purification. Column chromatography purification was done using Merck 60 silica gel. Thin layer chromatography (TLC) and preparative TLC was performed on Aluminium backed TLC Merck silica gel 60 F_{254} and visualized under UV light 254 nm and Merck preparative TLC glass backed 20 x 20 cm F_{254}. Infra-red (IR) were recorded on a Perkin Elemer FTIR Spectrum RX-1 spectrometer. Nuclear Magnetic Resonance (NMR) experiments were conducted on a Bruker Avance III 600 MHz, Bruker Avance II 400 MHz, Jeol ECA 400 MHz and Jeol Lambda 400 MHz. Proton chemical shifts are reported in ppm (δ) relative to tetramethylsilane (TMS) with the solvent resonance employed as the internal standard (CDCl$_3$ δ 7.24 ppm; CD$_3$OD δ 3.31 ppm) while ^{13}C chemical shift also reported in ppm (δ) relative to tetramethylsilane (TMS) with the solvent resonance employed as the internal standard (CDCl$_3$, δ 77.1 ppm; CD$_3$OD δ 49.0 ppm). Melting points were determined on Fargo Melting Point Apparatus MP-1D. High Resolution MS experiments were performed on Shimadzu LC-MS Ion Trap TOF and Agilent 6530 Accurate-Mass Q-TOF ESI LC/MS.

3.6.1 Synthesis Of Starting Material

3.6.1.1: *N*-(2-Iodophenyl)acetamide
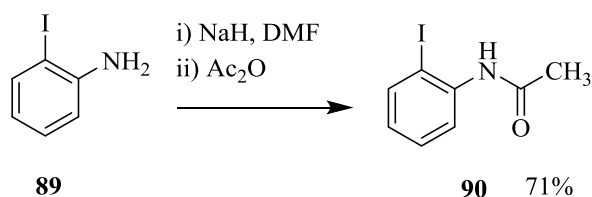
To a cold solution (0–5 °C) of 2-iodoaniline **89** (2.50 g, 11.41 mmol) in 30 mL DMF was reacted with NaH (0.274 g, 11.40 mmol). Acetic anhydride (5.824 g, 57.05

mmol) was later added into the solution and left to stir under nitrogen gas overnight at room temperature. To stop the reaction, saturated ammonium chloride was added into the flask. The mixture was extracted with ethyl acetate (3 x 30 mL) was used to and washed with distilled water. The combined ethyl acetate extracts were dried with anhydrous sodium sulphate and filtered. The solvent was evaporated under reduced pressure to give the crude product and purified by column chromatography (hexane/ethyl acetate, 60:40) to afford *N*-(2-Iodophenyl)acetamide **90** (2.115 g, 71% yield) as a white solid.

^{1}H NMR (CDCl$_3$, 400 MHz) δ: 2.21 (s, 3H, CH$_3$), 7.76 (d, *J* = 7.8 Hz, 1H, H-3), 7.30 (t, *J* = 7.8 Hz, 1H, H-4), 6.82 (t, *J* = 7.8 Hz, 1H, H-5), 8.20 (d, *J* = 7.8 Hz, 1H, H-6) 7.55 (br s, 1H, NH) ; ^{13}C NMR (CDCl$_3$, 100 MHz) : 138.0 (C-1), 90.9 (C-2), 138.5 (C-3), 128.7 (C-4), 126.0 (C-5), 122.8 (C-6), 168.2 (C=O), 24.3 (CH$_3$); HREIMS [M+H]$^+$: found *m/z* 261.9695, C$_8$H$_9$INO requires *m/z* 261.9729.

3.6.2 General Procedure for Syntheses of Stilbenes

3.6.2.1: (*E*)-*N*-(2-(2-fluorostyryl)phenyl)acetamide
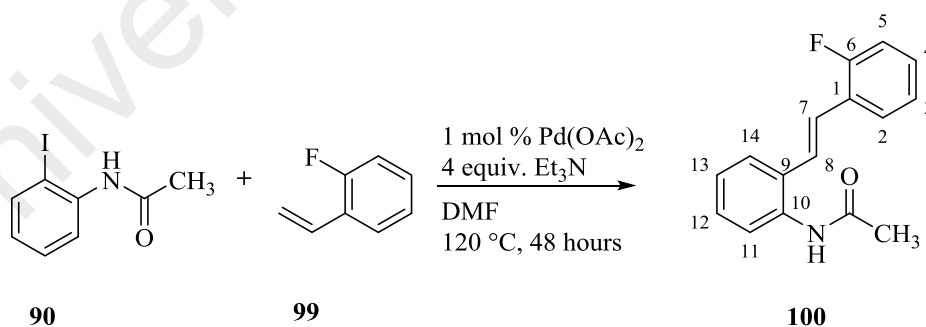
To a solution of compound **90** (0.30 g, 1.15 mmol) in 50 mL dry DMF under nitrogen gas that was heated up to 120 °C for a few minutes was added palladium (II) acetate (2.6 mg, 0.0115 mmol) followed by triethylamine (0.48 mL, 3.45 mmol) into the mixture. Compound **99** (0.12 g, 1.20 mmol) was later added into the reaction flask. The mixture was reflux under nitrogen until full consumption of compound **90** (check via

TLC). The reaction mixture was treated according to the general procedure. The crude product was purified by column chromatography (dichloromethane/ethyl acetate, 97:3) to afford (*E*)-*N*-(2-(2-fluorostyryl)phenyl)acetamide **100** (0.109g, 37% yield) as an off-white solid.

IR (neat): 3265, 1665, 1526, 1452, 1234, 1178, 1036, 755 cm $^{-1}$; ^{1}H NMR (CDCl$_3$, 400 MHz) δ: 2.10 (s, 3H, CH$_3$), 7.05 (dd, *J* = 8.2 and 1.1 Hz, 1H, H-3), 7.25 (m, 1H, H-4), 7.09 (dt, *J* = 8.2 and 1.1 Hz, 1H, H-5), 7.24 (dd, *J* = 8.2 and 1.1 Hz, 1H, H-6), 7.13 (m, 1H, H-7), 7.18 (m, 1H, H-8), 7.71 (d, *J* = 7.6 Hz, 1H, H-11), 7.26 (m, 1H, H-12), 7.53 (m, 1H, H-13), 7.56 (m, 1H, H-14); ^{13}C NMR (CDCl$_3$, 100 MHz) : 125.0 (d, *J* = 11.5 Hz, C-1), 161.7 (d, *J* = 248.2 Hz ,C-2), 116.0 (d, *J* = 22.2 Hz, C-3), 129.3 (d, *J* = 7.7 Hz, C-4), 124.6 (C-5), 126.1 (d, *J* = 5.5 Hz, C-6), 124.3 (C-7), 125.8 (C-8), 130.6 (C-9), 134.7 (C-10), 124.6 (C-11), 128.6 (C-12), 126.8 (C-13), 127.6 (C-14), 168.8 (C=O), 24.1 (CH$_3$); HREIMS [M+H]$^+$: found *m/z* 256.1164, C$_{16}$H$_{15}$FNO requires *m/z* 256.1138.

3.6.2.2: (*E*)-*N*-(2-(3-fluorostyryl)phenyl)acetamide
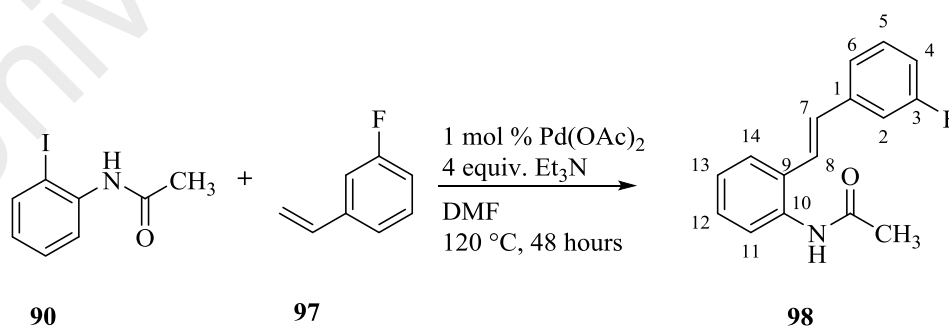
To a solution of compound **90** (0.30 g, 1.15 mmol) in 50 mL dry DMF under nitrogen gas that was heated up to 120 °C for a few minutes was added palladium (II) acetate (2.6 mg, 0.0115 mmol) followed by triethylamine (0.48 mL, 3.45 mmol) into the mixture. Compound **97** (0.12 g, 1.20 mmol) was later added into the reaction flask. The

mixture was heated until full consumption of compound **90** (check via TLC). The reaction mixture was treated according to the general procedure. The crude product was purified by column chromatography (dichloromethane/ethyl acetate, 97:3) to afford (*E*)-*N*-(2-(3-fluorostyryl)phenyl)acetamide **98** (0.126 g, 43% yield) as an off-white solid.

IR (neat): 3281, 1642, 1531, 1299, 951, 803,748 cm $^{-1}$; ^{1}H NMR (CDCl$_3$, 400 MHz) δ: 7.11 (m, 1H, H-2), 6.93 (t, *J* = 8.0 Hz,1H, H-4), 7.25 (m, 1H, H-5), 7.14 (m, 1H, H-6), 6.81 (d, *J* = 16.5 Hz, 1H, H-7), 7.07 (m, 1H, H-8), 7.48 (d, *J* = 7.8 Hz, 1H, H-11), 7.13 (m, 1H, H-12), 7.07 (m, 1H, H-13), 7.43 (d, *J* = 7.8 Hz, 1H, H-14), 2.10 (s, 3H, CH$_3$) 7.97 (br s, 1H, N-H); ^{13}C NMR (CDCl$_3$, 100 MHz) : 139.6 (d, *J* = 7.7 Hz, C-1), 112.9 (d, *J* = 22.0 Hz, C-2), 163.0 (d, *J* = 247.2 Hz, C-3), 114.9 (d, *J* = 21.1 Hz,, C-4), 130.2 (d, *J* = 8.6 Hz, C-5), 122.8 (C-6), 130.0 (C-7), 125.0 (C-8), 130.6 (C-9), 134.8 (C-10), 125.3 (C-11), 128.5 (C-12), 126.0 (C-13), 126.4 (C-14), 169.0 (C=O), 24.0(CH$_3$); HRMS(+ESI) [M + H]$^{+}$: found *m/z* 256.1160, C$_{16}$H$_{15}$FNO requires *m/z* 256.1138.

3.6.2.3: (*E*)-*N*-(2-(4-fluorostyryl)phenyl)acetamide
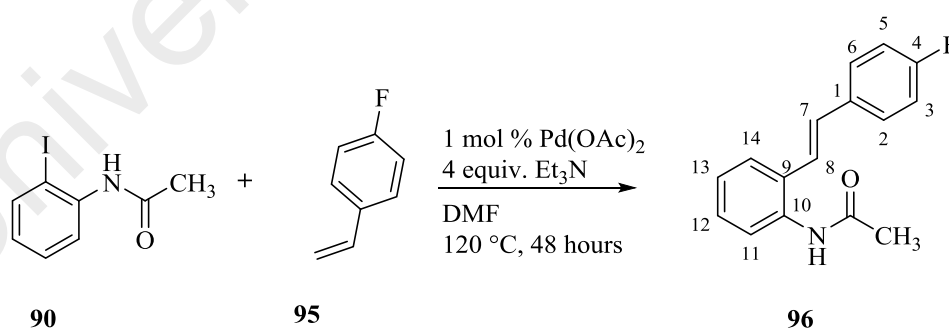
To a solution of compound **90** (0.30 g, 1.15 mmol) in 50 mL dry DMF under nitrogen gas that was heated up to 120 °C for a few minutes was added palladium (II) acetate (2.6 mg, 0.0115 mmol) followed by triethylamine (0.48 mL, 3.45 mmol) into the mixture. Compound **95** (0.12 g, 1.20 mmol) was later added into the reaction flask. The mixture was heated until full consumption of compound **90** (check via TLC). The

reaction mixture was treated according to the general procedure. The crude product was purified by column chromatography (dichloromethane/ethyl acetate, 97:3) to afford (*E*)-*N*-(2-(4-fluorostyryl)phenyl)acetamide **96** (0.114 g, 39% yield) as an off-white solid.

IR (neat): 3259, 1659, 1527, 1297, 963, 818 cm^{-1}; ^{1}H NMR (CDCl$_3$, 400 MHz) δ: 7.47 (m, 2H, H-2 & H-6), 7.08 (d, 2H, H-3 & H-5), 6.95 (d, *J* = 16.5 Hz,1H, H-7), 7.05 (m, 1H, H-8), 7.68 (d, *J* = 7.6 Hz, 1H, H-11), 7.26 (t, *J* = 7.6 Hz, 1H, H-12), 7.19 (t, *J* = 7.6 Hz, 1H, H-13), 7.53 (d, *J* = 7.6 Hz, 1H, H-14), 2.18 (s, 3H, CH$_3$); ^{13}C NMR (CDCl$_3$, 100 MHz) : 133.1 (C-1), 128.1 (d, *J* = 9.5 Hz, C-2), 115.7 (d, *J* = 22.0 Hz, C-3), 161.2 (d, *J* = 250.0 Hz, C-4), 115.7 (d, *J* = 22.0 Hz, C-5), 128.1 (d, *J* = 9.5 Hz, C-6), 131.0 (C-7), 123.2 (C-8), 130.4 (C-9), 134.4 (C-10), 124.5 (C-11), 128.1 (C-12), 125.6 (C-13), 126.6 (14), 24.1 (CH$_3$), 168.6 (C=O); HRMS (+EI) M$^+$: found *m/z* 255. 9151, C$_{16}$H$_{14}$FNO requires *m/z* 255. 1059.

3.6.2.4: (*E*)-*N*-(2-(2-chlorostyryl)phenyl)acetamide
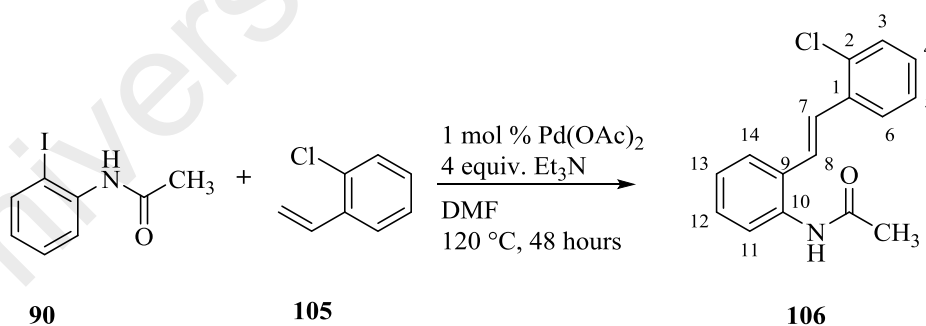
To a solution of compound **90** (0.30 g, 1.15 mmol) in 50 mL dry DMF under nitrogen gas that was heated up to 120 °C for a few minutes was added palladium (II) acetate (2.6 mg, 0.0115 mmol) followed by triethylamine (0.48 mL, 3.45 mmol) into the mixture. Later compound **105** (0.17 g, 1.20 mmol) was added into the reaction flask. The mixture was heated until full consumption of compound **90** (check via TLC). The reaction mixture was treated according to the general procedure. The crude product was

purified by column chromatography (dichloromethane/ethyl acetate, 97:3) to afford (*E*)-*N*-(2-(2-chlorostyryl)phenyl)acetamide **106** (0.113 g, 36% yield) as an off-white solid.

IR (neat): 3270, 1655, 1530, 1299, 954, 752 cm^{-1}; ^{1}H NMR (CD$_3$OD , 400 MHz) δ: 7.30 (m, 1H, H-3), 7.27 (m, 1H, H-4), 7.40 (m, 1H, H-5), 7.37 (m, 1H, H-6), 7.28 (m, 1H, H-7), 7.48 (d, *J* = 16.5 Hz, 1H, H-8), 7.77 (dd, *J* = 7.6 and 2.0 Hz,1H, H-11), 7.29 (m, 1H, H-12), 7.25 (m, 1H, H-13), 7.72 (dd, *J* = 7.6 and 2.0 Hz,1H, H-14), 2.17 (s, 3H, CH$_3$); ^{13}C NMR (CD$_3$OD, 100 MHz) : 132.4 (C-1), 134.9 (C-2), 127.0 (C-3), 126.4 (C-4), 129.4 (C-5), 126.6 (C-6), 126.7 (C-7), 126.0 (C-8), 133.1 (C-9), 135.4 (C-10), 126.5 (C-11), 128.1 (C-12), 128.7(13), 125.9(C-14), 21.8 (CH$_3$), 171.2 (C=O); HRMS (+EI) [M+H]$^{+}$: found *m/z* 272.0865, C$_{16}$H$_{15}$ClNO requires *m/z* 272.0842.

3.6.2.5: (*E*)-*N*-(2-(3-chlorostyryl)phenyl)acetamide
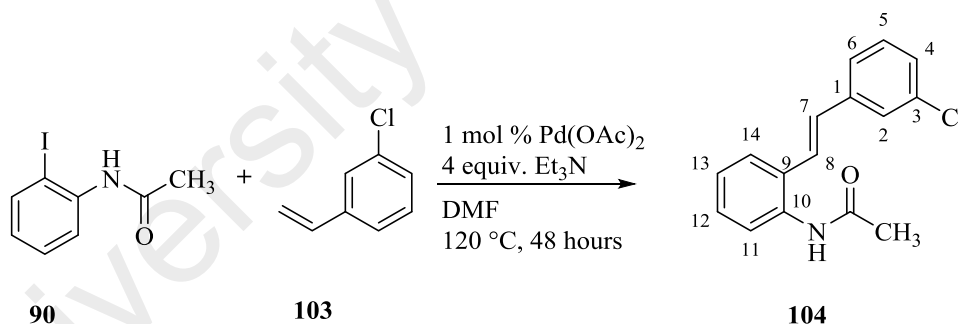
To a solution of compound **90** (0.30 g, 1.15 mmol) in 50 mL dry DMF under nitrogen gas that was heated up to 120 °C for a few minutes was added palladium (II) acetate (2.6 mg, 0.0115 mmol) followed by triethylamine (0.48 mL, 3.45 mmol) into the mixture. Later, compound **103** (0.17 g, 1.20 mmol) was added into the reaction flask. The mixture was heated until full consumption of compound **90** (check via TLC). The reaction mixture was treated according to the general procedure. The crude product was purified by column chromatography (dichloromethane/ethyl acetate, 97:3) to afford (*E*)-*N*-(2-(3-chlorostyryl)phenyl)acetamide **104** (0.138 g, 44% yield) as an off-white solid.

IR (neat): 3281, 1655, 1530, 1298, 951, 773, 749cm^{-1}; ^{1}H NMR (CDCl$_3$, 400 MHz) δ: 7.47 (s, 1H, H-2), 7.32 (m, 1H, H-4), 7.30 (m, 1H, H-5), 7.29 (m, 1H, H-6), 6.92 (d, J = 16.5 Hz, 1H, H-7), 7.15 (d, J = 16.5 Hz, 1H, H-8), 7.73 (d, J = 7.9 Hz, 1H, H-11), 7.25 (m, 1H, H-12), 7.18 (d, J = 7.9 Hz, 1H, H-13), 7.52 (d, J = 7.9 Hz, 1H, H-14), 2.21 (s, 3H, CH$_3$); ^{13}C NMR (CDCl$_3$, 100 MHz) : 139.0 (C-1), 126.9 (C-2), 134.8 (C-3), 125.0 (C-4), 128.8 (C-5), 130.1 (C-6), 130.8 (C-7), 125.1 (C-8), 130.3 (C-9), 134.8 (C-10), 124.8 (C-11), 128.1 (C-12), 125.9 (13), 126.5 (C-14), 24.4 (CH$_3$), 168.8 (C=O); HRMS (+ESI) [M+H]$^+$: found m/z 272.0873, C$_{16}$H$_{15}$ClNO requires m/z 272.0842.

3.6.2.6: (*E*)-*N*-(2-(4-chlorostyryl)phenyl)acetamide
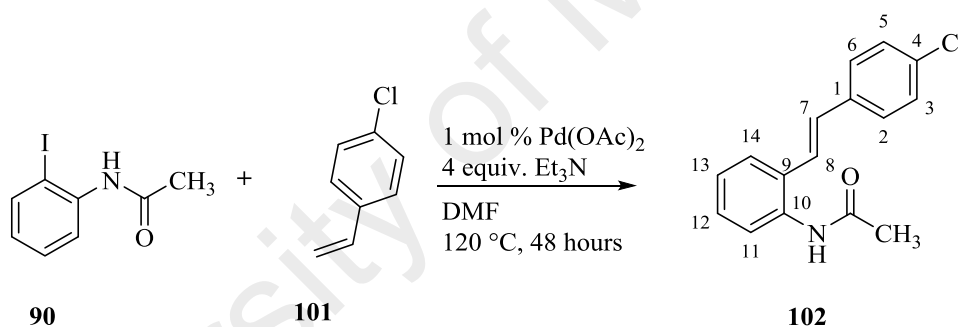
To a solution of compound **90** (0.30 g, 1.15 mmol) in 50 mL dry DMF under nitrogen gas that was heated up to 120 °C for a few minutes was added palladium (II) acetate (2.6 mg, 0.0115 mmol) followed by triethylamine (0.48 mL, 3.45 mmol) into the mixture. Later, compound **101** (0.17 g, 1.20 mmol) was added into the reaction flask. The mixture was heated until full consumption of compound **90** (check via TLC). The reaction mixture was treated according to the general procedure. The crude product was purified by column chromatography (dichloromethane/ethyl acetate, 97:3) to afford (*E*)-*N*-(2-(4-chlorostyryl)phenyl)acetamide **102** (0.141 g, 45% yield) as an off-white solid.

IR (neat): 3281, 1642, 1531, 1299, 951, 803, 748cm^{-1}; ^{1}H NMR (CDCl$_3$, 400 MHz) δ: 7.42 (d, J = 8.4 Hz, 2H, H-2 and H-6), 7.33 (d, J = 8.4 Hz, 2H, H-3 and H-5), 6.95 (d, J

= 16.0 Hz, 1H, H-7), 7.11 (d, J = 16.0 Hz, 1H, H-8), 7.75 (d, J = 7.7 Hz, 1H, H-11), 7.29 (m, 1H, H-12), 7.18 (t, J = 7.7 Hz, 1H, H-13), 7.52 (d, J = 7.7 Hz, 1H, H-14), 2.21 (s, 3H, CH$_3$); ^{13}C NMR (CDCl$_3$, 100 MHz) : 135.5 (C-1), 127.8 (C-2), 128.9 (C-3), 133.7 (C-4), 128.9 (C-5), 127.8 (C-6), 130.9 (C-7), 124.1 (C-8), 130.9 (C-9), 134.6 (C-10), 124.7 (C-11), 128.5 (C-12), 125.8 (C-13), 126.7 (C-14), 24.2 (CH$_3$), 168.6 (C=O); HRMS (+ESI) [M+H]$^+$: found m/z 272.0873, C$_{16}$H$_{15}$ClNO requires m/z 272.0842.

3.6.2.7: (*E*)-*N*-(2-(2-bromostyryl)phenyl)acetamide
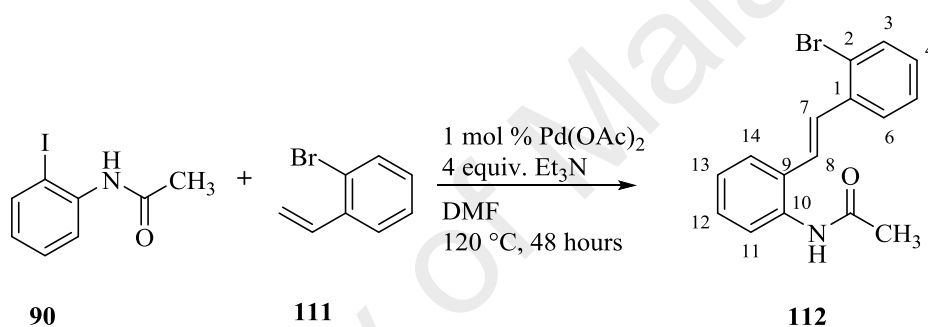
To a solution of compound **90** (0.30 g, 1.15 mmol) in 50 mL dry DMF under nitrogen gas that was heated up to 120 °C for a few minutes was added palladium (II) acetate (2.6 mg, 0.0115 mmol) followed by triethylamine (0.48 mL, 3.45 mmol) into the mixture. Later, compound **111** (0.22 g, 1.20 mmol) was added into the reaction flask. The mixture was heated until full consumption of compound **90** (check via TLC). The reaction mixture was treated according to the general procedure. The crude product was purified by column chromatography (dichloromethane/ethyl acetate, 97:3) to afford (*E*)-*N*-(2-(2-bromostyryl)phenyl)acetamide **112** (0.124 g, 34%) as an off-white solid.[28]

IR (neat): 3257, 1661, 1528, 1298, 1023, 962, 803, 752cm^{-1}; ^{1}H NMR (CDCl$_3$, 400 MHz) δ: 7.62 (dd, J = 8.0 and 1.3 Hz, 1H, H-3), 7.18 (dt, J = 8.0 and 1.3 Hz, 1H, H-4), 7.33 (m, 1H, H-5), 7.66 (dd, J = 8.0 and 1.3 Hz, 1H, H-6), 7.09 (d, J = 16.0 Hz, 1H, H-7), 7.37 (d, J = 16.0 Hz, 1H, H-8), 7.80 (d, J = 7.7 Hz, 1H, H-11), 7.31 (m, 1H, H-12),

7.22 (t, J = 7.7 Hz, 1H, H-13), 7.59 (d, J = 7.7 Hz, 1H, H-14), 2.23 (s, 3H, CH$_3$): ^{13}C

NMR (CDCl$_3$, 100 MHz) : 137.0 (C-1), 124.2 (C-2), 133.1 (C-3), 129.3 (C-4), 127.7

(C-5), 127.1 (C-6), 126.7 (C-7), 131.1 (C-8), 130.1 (C-9), 134.7 (C-10), 124.5 (C-11),

128.8 (C-12), 125.8 (C-13), 127.4 (C-14), 24.4 (CH$_3$), 168.8 (C=O); HRMS (+ESI)

[M+H]$^+$: found m/z 316.0340, C$_{16}$H$_{15}$BrNO requires m/z 316.0337.

3.6.2.8: (*E*)-*N*-(2-(3-bromostyryl)phenyl)acetamide
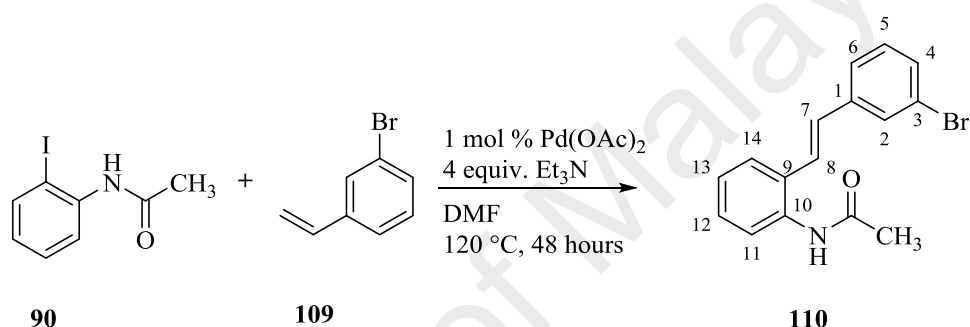
To a solution of compound **90** (0.30 g, 1.15 mmol) in 50 mL dry DMF under

nitrogen gas that was heated up to 120 °C for a few minutes was added palladium (II)

acetate (2.6 mg, 0.0115 mmol) followed by triethylamine (0.48 mL, 3.45 mmol) into the

mixture. Later, compound **109** (0.22 g, 1.20 mmol) was added into the reaction flask.

The mixture was heated until full consumption of compound **90** (check via TLC). The

reaction mixture was treated according to the general procedure. The crude product was

purified by column chromatography (dichloromethane/ethyl acetate, 97:3) to afford (*E*)-

N-(2-(3-bromostyryl)phenyl)acetamide **110** (0.135 g, 37% yield) as an off-white solid.

IR (neat): 3278, 1666, 1526, 1449, 1296, 1079, 800, 758cm^{-1}; ^{1}H NMR (CDCl$_3$, 400

MHz) δ: 7.67 (t, J = 1.6 Hz, 1H, H-2), 7.41 (d, J = 7.9, 2H, H-4), 7.26 (t, J = 7.9 Hz,

1H, H-5), 7.45 (d, J = 7.9 Hz, 1H, H-6), 6.94 (d, J = 16.0 Hz, 1H, H-7), 7.16 (d, J = 16.0

Hz, 1H, H-8), 7.77 (d, J = 7.8 Hz, 1H, H-11), 7.33 (t, J = 7.8 Hz, 1H, H-12), 7.22 (t, J =

7.8 Hz, 1H, H-13), 7.55 (d, J = 7.8 Hz, 1H, H-14), 2.26 (s, 3H, CH$_3$): ^{13}C NMR (CDCl$_3$

, 100 MHz) : 139.1 (C-1), 129.4 (C-2), 123.0 (C-3), 125.3 (C-4), 130.3 (C-5), 131.1 (C-6), 130.9 (C-7), 125.0 (C-8), 130.2 (C-9), 134.7 (C-10), 124.3 (C-11), 128.8 (C-12), 125.9 (C-13), 126.8 (C-14), 24.3(CH$_3$), 168.7(C=O); HRMS (+ESI) [M+H]$^+$: found *m/z* 316.0342, C$_{16}$H$_{15}$BrNO requires *m/z* 316.0337.

3.6.2.9: (*E*)-*N*-(2-(4-bromostyryl)phenyl)acetamide
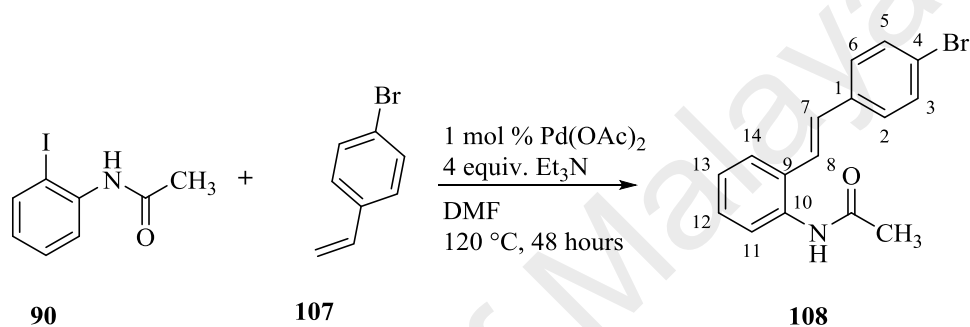
To a solution of compound **90** (0.30 g, 1.15 mmol) in 50 mL dry DMF under nitrogen gas that was heated up to 120 °C for a few minutes was added palladium (II) acetate (2.6 mg, 0.0115 mmol) followed by triethylamine (0.48 mL, 3.45 mmol) into the mixture. Later, compound **107** (0.22 g, 1.20 mmol) was added into the reaction flask. The mixture was heated until consumption of compound **90** (check via TLC). The reaction mixture was treated according to the general procedure. The crude product was purified by column chromatography (dichloromethane/ethyl acetate, 97:3) to afford (*E*)-*N*-(2-(4-bromostyryl)phenyl)acetamide **108** (0.145 g, 40% yield) as an off-white solid.

IR (neat): 3315, 1664, 1557, 1259, 1029, 798, 772cm^{-1}; ^{1}H NMR (CDCl$_3$, 400 MHz) δ: 7.48 (d, *J* = 8.2 Hz, 2H, H-2 and H-6), 7.34 (d, *J* = 8.2 Hz, 2H, H-3 and H-5), 6.91 (d, *J* = 16.5 Hz, 1H, H-7), 7.12 (d, *J* = 16.5 Hz, 1H, H-8), 7.70 (d, *J* = 7.8 Hz, 1H, H-11), 7.27 (d, J = 7.8 Hz, 1H, H-12), 7.17 (t, *J* = 7.8 Hz, 1H, H-13), 7.52 (d, *J* = 7.8 Hz, 1H, H-14), 2.19 (s, 3H, CH$_3$): ^{13}C NMR (CDCl$_3$, 100 MHz) : 136.1 (C-1), 132.0 (C-2), 128.2 (C-3), 121.9 (C-4), 128.2 (C-5), 132.0 (C-6), 130.9 (C-7), 124.3 (C-8), 130.5 (C-

9), 134.7 (C-10), 124.9 (C-11), 128.6 (C-12), 126.0 (C-13), 126.8 (C-14), 24.3 (CH$_3$), 168.9 (C=O); HRMS (+ESI) [M+H]$^+$: found m/z 316.0334, C$_{16}$H$_{15}$BrNO requires m/z 316.0337.

3.6.2.10: (*E*)-*N*-(2-(4-methoxystyryl)phenyl)acetamide
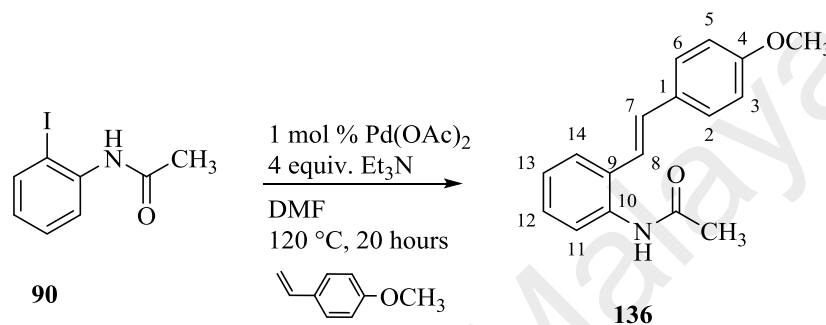
To a solution of compound **90** (0.30 g, 1.15 mmol) in 50 mL dry DMF under nitrogen gas that was heated up to 120 °C for a few minutes was added palladium (II) acetate (2.6 mg, 0.0115 mmol) followed by triethylamine (0.48 mL, 3.45 mmol) into the mixture. Later, 4-methoxystyrene (0.16 g, 1.20 mmol) was added into the reaction flask. The mixture was heated until full consumption of **90** (checked via TLC). The reaction mixture was treated according to the general procedure. The crude product was purified by column chromatography (dichloromethane/ethyl acetate, 97:3) afforded (*E*)-*N*-(2-(4-methoxystyryl)phenyl)acetamide **136** (0.200 g, 65% yield) as an off-white solid. X-ray structure of **136** was reported in Ahmad et al..[29]
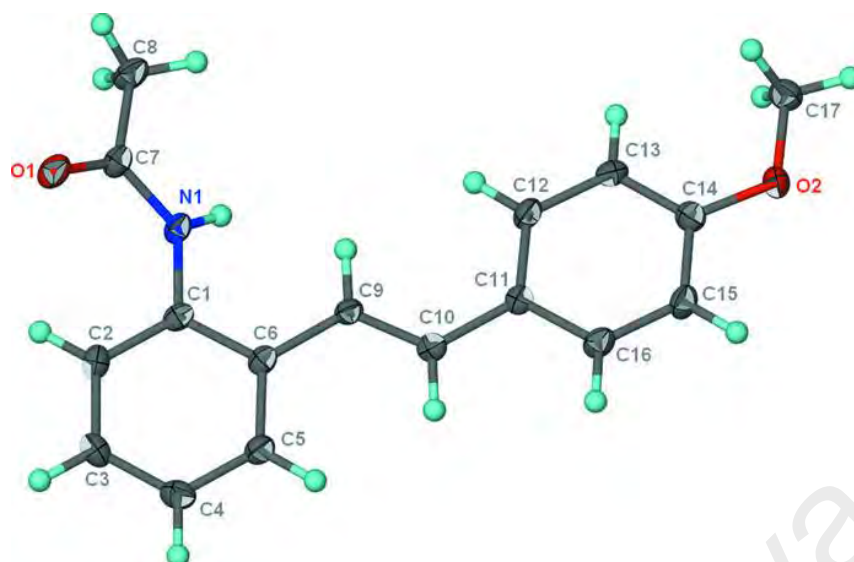
Figure 3.24 : Single crystal X-ray structure of **136**

3.6.3 General Procedure for Syntheses of Imines

3.6.3.1: (*1R,2S*)-1-(2-(((*E*)-2-acetamidobenzylidene)amino)phenyl)-2-chloro-2-(4-fluorophenyl)ethyl acetate
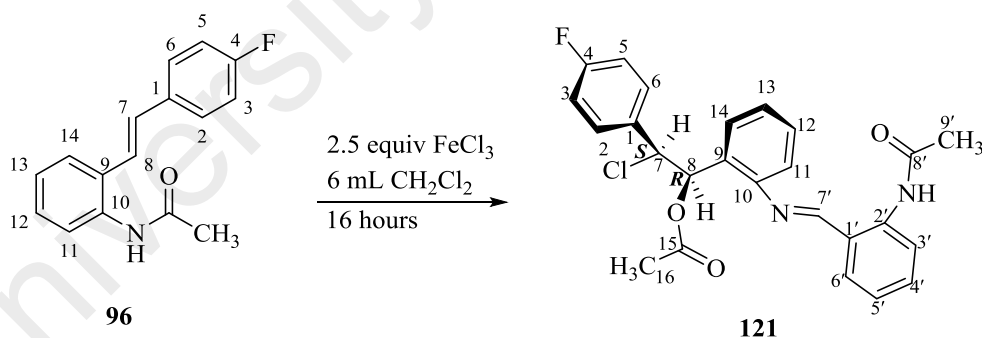
Compound **96** (0.080 g, 0.31 mmol) was dissolved in 6 mL of dichloromethane. Ferric chloride (0.130 g, 0.78 mmol) was added into the solution and capped with a rubber septum. It was left to stir until all **96** were consumed (checked via TLC). Saturated ammonium chloride was added and extracted with dichloromethane. Distilled water was used to wash, and dried over anhydrous sodium sulphate. Later the solution was filtered and dried under reduced pressure to afford the crude product. Purification

of the crude product by column chromatography (ethyl acetate/hexane 20:80) and extra step of separation by preparative TLC of silica backed glass (ethyl acetate/hexane 10:90) to afford (*1R,2S*)-1-(2-(((*E*)-2-acetamidobenzylidene)amino)phenyl)-2-chloro-2-(4-fluorophenyl)ethyl acetate **121** (0.030 g, 37% yield) as a white amorphous.

^{1}H NMR (CDCl$_3$, 600 MHz) δ: 6.94 (dd, *J* = 8.4 and 5.2 Hz, 2H, H-2 and H-6), 6.55 (m, H-3 and H-5), 5.01 (d, *J* = 9.0 Hz, 1H, H-7), 6.50 (d, *J* = 9.0 Hz, 1H, H-8), 7.56 (dd, *J* = 7.3 and 1.7 Hz, 1H, H-11), 7.33 (m, 1H, H-12), 7.35 (m, 1H, H-13), 6.72 (dd, *J* = 7.3 and 1.7 Hz, 1H, H-14), 2.19 (s, 3H, CH$_3$, H-16), 8.84 (d, *J* = 8.1 Hz, 1H, H-3′), 7.50 (t, *J* = 8.1 Hz, 1H, H-4′), 7.18 (t, *J* = 8.1 Hz, 1H, H-5′), 7.24 (m, 1H, H-6′), 7.52 (s, 1H, H-7′), 2.32 (s, 3H, CH$_3$, H-9′), 12.00 (s, 1H, NH): ^{13}C NMR (CDCl$_3$, 125 MHz) : 132.5 (C-1), 129.7 (d, *J* = 7.5 Hz, C-2), 114.8 (d, *J* = 18.1 Hz, C-3), 161.4 (d, *J*= 206.3 Hz, C-4), 114.8 (d, *J*= 18.1 Hz, C-5), 129.7 (d, *J*= 7.5 Hz, C-6), 65.1 (C-7), 73.7 (C-8), 130.5 (C-9), 149.1 (C-10), 126.6 (C-11), 126.7 (C-12), 130.1 (C-13), 118.7 (C-14), 169.4 (C-15), 21.0 (C-16), 120.5 (C-1′), 140.0 (C-2′), 120.0 (C-3′), 133.0 (C-4′), 122.7 (C-5′), 134.6 (C-6′), 164.4 (C-7′), 170.5 (C-8′), 25.5 (C-9′); HRMS (+ESI) [M+H]$^+$: found *m/z* 453.1341, C$_{25}$H$_{23}$ClFN$_2$O$_3$ requires *m/z* 453.1381.

3.6.3.2: (*1R,2S*)-1-(2-(((*E*)-2-acetamidobenzylidene)amino)phenyl)-2-chloro-2-(3-fluorophenyl)ethyl acetate

98   **122**

Compound **98** (0.080 g, 0.31 mmol) was dissolved in 6 mL of dichloromethane. Ferric chloride (0.130 g, 0.78 mmol) was added into the solution and capped with a rubber septum. It was left to stir until all **98** were consumed (checked via TLC). Saturated ammonium chloride was added and extracted with dichloromethane. Distilled water was used to wash, and dried over anhydrous sodium sulphate anhydrous. Later the solution was filtered and dried under reduced pressure to afford the crude product. Purification of the crude product by column chromatography (ethyl acetate/hexane 20:80) and extra step of separation by preparative TLC of silica backed glass (ethyl acetate/hexane 10:90) to afford (*1R,2S*)-1-(2-(((*E*)-2-acetamidobenzylidene)amino)phenyl)-2-chloro-2-(3-fluorophenyl)ethyl acetate **122** (0.031 g, 39% yield) as a white amorphous.

^{1}H NMR (CDCl$_3$, 400 MHz) δ: 6.75 (m, 1H, H-2), 6.74 (m, 1H, H-4), 6.87 (m, 1H, H-5), 6.79 (m, 1H, H-6), 4.98 (d, *J* = 8.2 Hz, 1H, H-7), 6.57 (d, *J* = 8.2 Hz, 1H, H-8), 7.55 (dd, *J* = 9.0 and 2.0 Hz, 1H, H-11), 7.35 (m, 1H, H-12), 7.36 (m, 1H, H-13), 6.77 (m, 1H, H-14), 2.19 (s, 3H, CH$_3$, H-16), 8.85 (d, *J* = 8.0 Hz, 1H, H-3′), 7.51 (t, *J* = 8.0 Hz, 1H, H-4′), 7.17 (dt, *J* = 8.0 and 1.3 Hz, 1H, H-5′), 7.28 (dd, *J* = 8.0 and 1.3 Hz, 1H, H-6′), 7.69 (s, 1H, H-7′), 2.29 (s, 3H, CH$_3$, H-9′) 12.00 (s, 1H, NH): ^{13}C NMR (CDCl$_3$, 100 MHz) : 139.2 (d, *J* = 6.9 Hz, C-1), 115.6 (d, *J* = 20.0 Hz, C-2), 160.8 (d, *J* = 246.6 Hz C-3), 115.1 (d, *J* = 23.0 Hz, C-4), 129.5 (d, *J* = 7.7 Hz, C-5), 123.7 (C-6), 64.1 (C-7), 73.5 (C-8), 130.4 (C-9), 149.1 (C-10), 126.8 (C-11), 126.7 (C-12), 130.2 (C-13), 118.7 (C-14), 169.3 (C-15), 20.9 (C-16), 120.3 (C-1′), 140.2 (C-2′), 120.1 (C-3′), 133.0 (C-4′), 122.6 (C-5′), 134.7 (C-6′), 164.7 (C-7′), 170.4 (C-8′), 25.5 (C-9′); HRMS (+ESI) [M+H]$^+$: found *m/z* 453.1341, C$_{25}$H$_{23}$ClFN$_2$O$_3$ requires *m/z* 453.1381.

3.6.3.3: (*1R,2S*)-1-(2-(((*E*)-2-acetamidobenzylidene)amino)phenyl)-2-chloro-2-(4-chlorophenyl)ethyl acetate
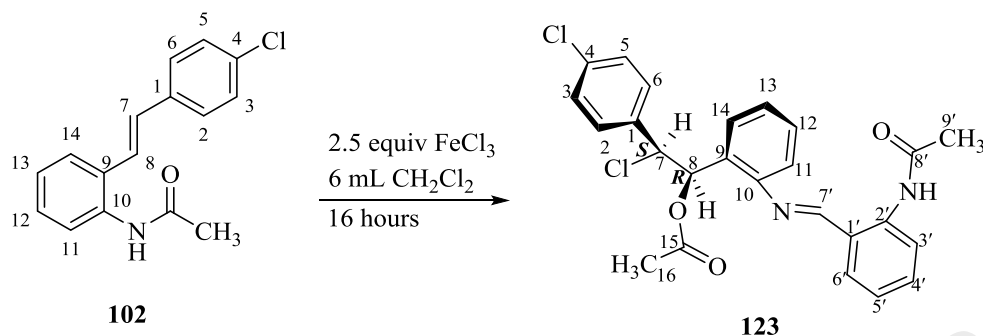
Compound **102** (0.084 g, 0.31 mmol) was dissolved in 6 mL of dichloromethane. Ferric chloride (0.130 g, 0.78 mmol) was added into the solution and capped with a rubber septum. It was left to stir until all **102** were consumed (checked via TLC). Saturated ammonium chloride was added and extracted with dichloromethane. Distilled water was used to wash, and dried over anhydrous sodium sulphate. Later, the solution was filtered and dried under reduced pressure to afford the crude product. Purification of the crude product by column chromatography (ethyl acetate/hexane 20:80) and extra step of separation by preparative TLC of silica backed glass (ethyl acetate/hexane 10:90) to afford (*1R,2S*)-1-(2-(((*E*)-2-acetamidobenzylidene)amino)phenyl)-2-chloro-2-(4-chlorophenyl)ethyl acetate **123** (0.029 g, 35% yield) as a white amorphous compound.

^{1}H NMR (CDCl$_3$, 400 MHz) δ: 6.96 (d, *J* = 8.7 Hz, 4H, H-2, H-3, H-5 and H-6), 5.25 (d, *J* = 9.0 Hz, 1H, H-7), 6.69 (d, *J* = 9.0 Hz, 1H, H-8), 7.49 (m, 1H, H-11), 7.28 (t, *J* = 8.0 Hz, 1H, H-12), 7.40 (t, *J* = 8.0 Hz, 1H, H-13), 6.86 (d, *J* = 8.0 Hz, 1H, H-14), 2.13 (s, 3H, CH$_3$, H-16), 8.79 (d, *J* = 7.6 Hz, 1H, H-3'), 7.49 (m, 1H, H-4′), 7.16 (t, *J* = 7.6 Hz, 1H, H-5′), 7.34 (d, *J* = 7.6 Hz , 1H, H-6′), 7.93 (s, 1H, H-7′), 2.29 (s, 3H, CH$_3$, H-9′), 12.01 (s, 1H, NH): ^{13}C NMR (CDCl$_3$, 100 MHz) : 135.2 (C-1), 129.4 (C-2), 128.3 (C-3), 122.8 (C-4), 128.3 (C-5), 129.4 (C-6), 63.7 (C-7), 72.7 (C-8), 134.6 (C-9), 149.2

(C-10), 128.6 (C-11), 126.4 (C-12), 130.2 (C-13), 118.3 (C-14), 169.4 (C-15), 21.1 (C-16), 120.5 (C-1′), 140.0 (C-2′), 119.9 (C-3′), 133.0 (C-4′), 122.8 (C-5′), 135.0 (C-6′), 164.5 (C-7′), 170.3 (C-8′), 25.6 (C-9′); HRMS (+ESI) [M+H]$^+$: found m/z 469.1108, $C_{25}H_{23}Cl_2N_2O_3$ requires m/z 469.1086.

3.6.3.4: (*1R,2S*)-1-(2-(((*E*)-2-acetamidobenzylidene)amino)phenyl)-2-chloro-2-(3-chlorophenyl)ethyl acetate
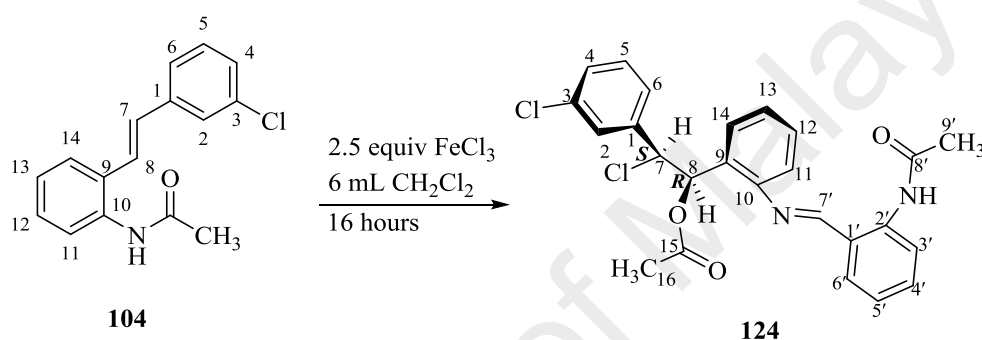
Compound **104** (0.084 g, 0.31 mmol) was dissolved in 6 mL of dichloromethane. Ferric chloride (0.130 g, 0.78 mmol) was added into the solution and capped with a rubber septum. It was left to stir until all **104** were consumed (checked via TLC). Saturated ammonium chloride was added and extracted with dichloromethane. Distilled water was used to wash, and dried over anhydrous sodium sulphate. Later, the solution was filtered and dried under reduced pressure to afford the crude product. Purification of the crude product by column chromatography (ethyl acetate/hexane 20:80) and extra step of separation by preparative TLC of silica backed glass (ethyl acetate/hexane 10:90) to afford (*1R,2S*)-1-(2-(((*E*)-2-acetamidobenzylidene)amino)phenyl)-2-chloro-2-(3-chlorophenyl)ethyl acetate **124** (0.034 g 40% yield) as a white amorphous.

^{1}H NMR (CDCl$_3$, 600 MHz) δ: 7.01 (brd t, J = 2.0 Hz, 1H, H-2), 7.05 (dt, J = 7.2 and 2.0 Hz, 1H, H-4), 6.85 (t, J = 7.2 Hz, 1H, H-5), 6.89 (d, J = 7.2 Hz, 1H, H-6) , 4.98 (d,

J = 8.2 Hz, 1H, H-7), 6.56 (d, J = 8.2 Hz, 1H, H-8), 7.57 (dd, J = 7.6 and 1.6 Hz, 1H, H-11), 7.35 (td, J = 7.6 and 1.6 Hz, 1H, H-12), 7.38 (dd, J = 7.6 and 1.6 Hz, 1H, H-13), 6.79 (dd, J = 7.6 and 1.6 Hz, 1H, H-14), 2.19 (s, 3H, CH$_3$, H-16), 8.84 (d, J = 7.6 Hz, 1H, H-3'), 7.51 (t, J = 7.6 Hz, 1H, H-4'), 7.16 (dt, J = 1.3 and 7.6 Hz, 1H, H-5'), 7.28 (dd, J = 1.3 and 7.6 Hz, 1H, H-6'), 7.71 (s, 1H, H-7'), 2.30 (s, 3H, CH$_3$, H-9') 12.01 (s, 1H, NH): ^{13}C NMR (CDCl$_3$, 150 MHz) : 138.7 (C-1), 128.2 (C-2), 134.1 (C-3), 128.9 (C-4), 129.1 (C-5), 126.2 (C-6), 64.9 (C-7), 73.5 (C-8), 130.4 (C-9), 149.0 (C-10), 126.7 (C-11), 126.8 (C-12), 130.2 (C-13), 118.7 (C-14), 169.3 (C-15), 21.0 (C-16), 120.1 (C-1'), 140.3 (C-2'), 120.1 (C-3'), 133.0 (C-4'), 122.6 (C-5'), 134.9 (C-6'), 164.6 (C-7'), 170.4 (C-8'), 25.5 (C-9'); HRMS (+ESI) [M+H]$^{+}$: found m/z 469.1093, C$_{25}$H$_{23}$Cl$_2$N$_2$O$_3$ requires m/z 469.1086.

3.6.3.5: (*1R,2S*)-1-(2-(((*E*)-2-acetamidobenzylidene)amino)phenyl)-2-chloro-2-(2-chlorophenyl)ethyl acetate

106   2.5 equiv FeCl$_3$ / 6 mL CH$_2$Cl$_2$ / 16 hours   **125**
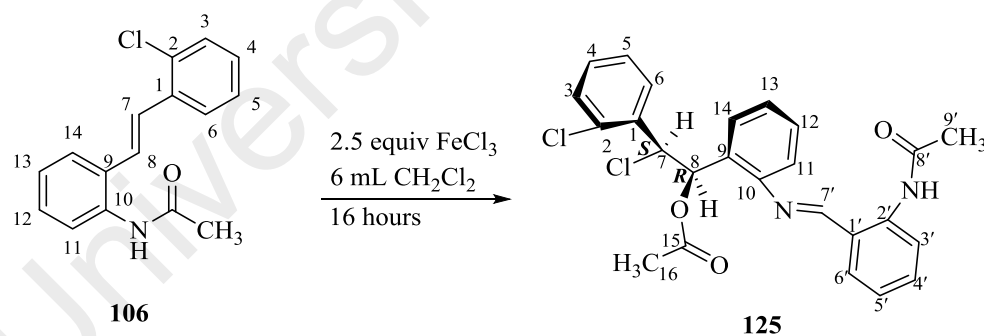
Compound **106** (0.084 g, 0.31 mmol) was dissolved in 6 mL of dichloromethane. Ferric chloride (0.130 g, 0.78 mmol) was added into the solution and capped with a rubber septum. It was left to stir until all **106** were consumed (checked via TLC). Saturated ammonium chloride was added and extracted with dichloromethane. Distilled water was used to wash, and dried over anhydrous sodium sulphate. Later the solution was filtered and dried under reduced pressure to afford the crude product. Purification of the crude

product by column chromatography (ethyl acetate/hexane 20:80) and extra step of separation by preparative TLC of silica backed glass (ethyl acetate/hexane 10:90) to afford (*1R,2S*)-1-(2-(((*E*)-2-acetamidobenzylidene)amino)phenyl)-2-chloro-2-(2-chlorophenyl)ethyl acetate **125** (0.030 g, 36% yield) as a white amorphous.

^{1}H NMR (CDCl$_3$, 600 MHz) δ: 7.56 (dd, *J* = 7.8 and 1.4 Hz, 1H, H-3), 6.76 (m, 1H, H-4), 6.99 (dt, *J* = 7.8 and 1.4 Hz, 1H, H-5), 7.09 (dd, *J* = 7.8 and 1.4 Hz, 1H, H-6) , 5.68 (d, *J* = 8.0 Hz, 1H, H-7), 6.69 (d, *J* = 8.0 Hz, 1H, H-8), 7.67 (dd, *J* = 7.6 and 1.3 Hz, 1H, H-11), 7.31 (dt, *J* = 7.6 and 1.3 Hz, 1H, H-12), 7.35 (dt, *J* = 7.6 and 1.3 Hz, 1H, H-13), 6.76 (m, 1H, H-14), 2.16 (s, 3H, CH$_3$, H-16), 8.83 (d, *J* = 8.2 Hz, 1H, H-3′), 7.51 (dt, *J* = 8.2 Hz, 1H, H-4′), 7.16 (dt, *J* = 7.6 and 1.3 Hz, 1H, H-5′), 7.27 (m, 1H, H-6′), 7.81 (s, 1H, H-7′), 2.31 (s, 3H, CH$_3$, H-9′) 11.95 (s, 1H, NH): ^{13}C NMR (CDCl$_3$, 150 MHz) : 134.8 (C-1), 129.8 (C-2), 131.1 (C-3), 126.6 (C-4), 129.6 (C-5), 129.0 (C-6), 60.6 (C-7), 72.5 (C-8), 132.6 (C-9), 148.9 (C-10), 128.1 (C-11), 126.4 (C-12), 130.1 (C-13), 118.7 (C-14), 169.3 (C-15), 21.0 (C-16), 120.6 (C-1′), 140.3 (C-2′), 120.1 (C-3′), 132.9 (C-4′), 122.5 (C-5′), 134.6 (C-6′), 164.7 (C-7′), 170.5 (C-8′), 25.5 (C-9′); HRMS (+ESI) [M+H]$^+$: found *m/z* 469.1061, C$_{25}$H$_{23}$Cl$_2$N$_2$O$_3$ requires *m/z* 469.1086.

3.6.3.6: (*1R,2S*)-1-(2-(((*E*)-2-acetamidobenzylidene)amino)phenyl)-2-(4-bromophenyl)-2-chloroethyl acetate

108   **126**
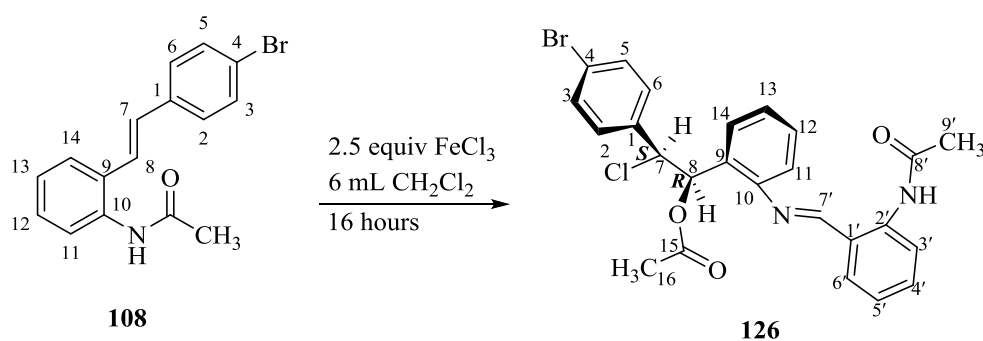
Compound **108** (0.098 g, 0.31 mmol) was dissolved in 6 mL of dichloromethane. Ferric chloride (0.130 g, 0.78 mmol) was added into the solution and capped with a rubber septum. It was left to stir until all **108** were consumed (checked via TLC). Saturated ammonium chloride was added and extracted with dichloromethane. Distilled water was used to wash it and dried over anhydrous sodium sulphate. Later, the solution was filtered and dried under reduced pressure to afford the crude product. Purification of the crude product by column chromatography (ethyl acetate/hexane 20:80) and extra step of separation by preparative TLC of silica backed glass (ethyl acetate/hexane 10:90) to afford (*1R,2S*)-1-(2-(((*E*)-2-acetamidobenzylidene)amino)phenyl)-2-(4-bromophenyl)-2-chloroethyl acetate **126** (0.037 g, 38% yield) as a white amorphous.

^{1}H NMR (CDCl$_3$, 400 MHz) δ: 6.96 (d, *J* = 7.7 Hz, 2H, H-2 and H-6), 6.81 (d, *J* = 7.7 Hz, 2H, H-3 and H-5), 4.97 (d, *J* = 9.1 Hz, 1H, H-7), 6.51 (d, *J* = 9.1 Hz, 1H, H-8), 7.58 (d, *J* = 6.4 Hz, 1H, H-11), 7.34 (m, 1H, H-12), 7.35 (m, 1H, H-13), 6.72 (d, *J* = 6.4 Hz, 1H, H-14), 2.19 (s, 3H, CH$_3$, H-16), 8.83 (d, *J* = 7.3 Hz, 1H, H-3′), 7.52 (t, *J* = 7.3 Hz , 1H, H-4′), 7.21 (t, *J* = 7.3 Hz, 1H, H-5′), 7.33 (m, 1H, H-6′), 7.43 (s, 1H, H-7′), 2.33 (s, 3H, CH$_3$, H-9′), 12.01 (s, 1H, NH): ^{13}C NMR (CDCl$_3$, 100 MHz) : 135.5 (C-1), 129.7 (C-2), 131.0(C-3), 122.5 (C-4), 131.0 (C-5), 129.7 (C-6), 65.1 (C-7), 73.5 (C-8), 130.4 (C-9), 149.2 (C-10), 130.3 (C-11), 126.7 (C-12), 118.7 (C-13), 126.5 (C-14), 169.4 (C-15), 21.0 (C-16), 120.5 (C-1′), 139.9 (C-2′), 134.9 (C-3′), 133.0 (C-4′), 122.7 (C-5′), 119.9 (C-6′), 164.5 (C-7′), 170.5 (C-8′), 25.5 (C-9′); HRMS (+ESI) [M+H]$^{+}$: found *m/z* 513.0592, C$_{25}$H$_{23}$BrClN$_2$O$_3$ requires *m/z* 513.0581.

3.6.3.7: (*1R,2S*)-1-(2-(((*E*)-2-acetamidobenzylidene)amino)phenyl)-2-(3-bromophenyl)-2-chloroethyl acetate (127) and

(*1S,2S*)-1-(2-(((*E*)-2-acetamidobenzylidene)amino)phenyl)-2-(3-bromophenyl)-2-chloroethyl acetate (128)

127 (32%)   **128** (15%)
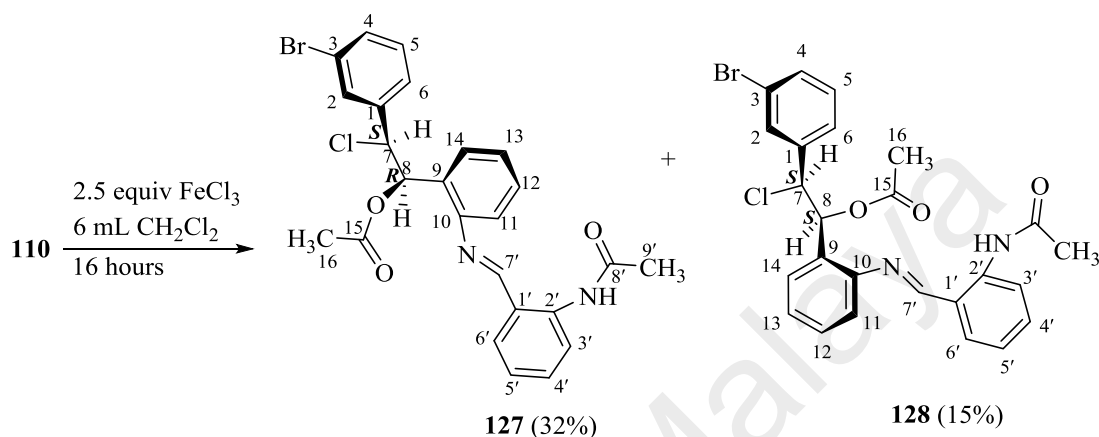
Compound **110** (0.098 g, 0.31 mmol) was dissolved in 6 mL of dichloromethane. Ferric chloride (0.130 g, 0.78 mmol) was added into the solution and capped with a rubber septum. It was left to stir until all **110** were consumed (checked via TLC). Saturated ammonium chloride was added and extracted with dichloromethane. Distilled water was used to wash, and dried over anhydrous sodium sulphate. Later the solution was filtered and dried under reduced pressure to afford the crude product. Purification of the crude product by column chromatography (ethyl acetate/hexane 20:80) and extra step of separation by preparative TLC of silica backed glass (ethyl acetate/hexane 10:90) to afford (*1R,2S*)-1-(2-(((*E*)-2-acetamidobenzylidene)amino)phenyl)-2-(3-bromophenyl)-2-chloroethyl acetate **127** (0.031 g, 32% yield) and (*1S,2S*)-1-(2-(((*E*)-2-acetamidobenzylidene)amino)phenyl)-2-(3-bromophenyl)-2-chloroethyl acetate **128** (0.015 g, 15% yield). Both compounds afforded as white amorphous.

127

^{1}H NMR (CDCl$_3$, 600 MHz) δ: 7.18 (s, 1H, H-2), 7.23 (d, J = 8.0 Hz, 1H, H-4), 6.83 (m, 1H, H-5), 6.98 (d, J = 8.0 Hz, 1H, H-6) , 4.99 (d, J = 8.0 Hz, 1H, H-7), 6.57 (d, J = 8.0 Hz, 1H, H-8), 7.60 (d, J = 7.3 Hz, 1H, H-11), 7.41 (t, J = 7.3 Hz, 1H, H-12), 7.37 (t, J = 7.3 Hz, 1H, H-13), 6.81 (m, 1H, H-14), 2.21 (s, 3H, CH$_3$, H-16), 8.87 (d, J = 7.8 Hz, 1H, H-3′), 7.53 (t, J = 7.8 Hz, 1H, H-4′), 7.19 (t, J = 7.8 Hz, 1H, H-5′), 7.32 (d, J = 7.8 Hz, 1H, H-6′), 7.74 (s, 1H, H-7′), 2.32 (s, 3H, CH$_3$, H-9′) 12.03 (s, 1H, NH): ^{13}C NMR (CDCl$_3$, 150 MHz) : 130.4 (C-1), 131.1 (C-2), 122.0 (C-3), 131.6 (C-4), 129.5 (C-5), 126.6 (C-6), 64.8 (C-7), 73.5 (C-8), 138.9 (C-9), 149.0 (C-10), 126.8 (C-11), 130.3 (C-12), 126.8 (C-13), 118.7 (C-14), 169.9 (C-15), 21.0 (C-16), 120.4 (C-1′), 140.2 (C-2′), 120.1 (C-3′), 133.0 (C-4′), 122.7 (C-5′), 134.9 (C-6′), 164.6 (C-7′), 170.4 (C-8′), 25.6 (C-9′); HRMS (+ESI) [M+H]$^+$: found m/z 513.0581, C$_{25}$H$_{23}$BrClN$_2$O$_3$ requires m/z 513.0581.

128

^{1}H NMR (CDCl$_3$, 600 MHz) δ: 7.16 (s, 1H, H-2), 7.16 (m, 1H, H-4), 6.92 (m, 1H, H-5), 7.03 (d, J = 7.7 Hz, 1H, H-6) , 5.23 (d, J = 4.0 Hz, 1H, H-7), 6.71 (d, J = 4.0 Hz, 1H, H-8), 7.50 (m, 1H, H-11), 7.33 (t, J = 8.0 Hz, 1H, H-12), 6.92 (m, 1H, H-13), 7.45 (m, 1H, H-14), 2.21 (s, 3H, CH$_3$, H-16), 8.82 (d, J = 8.0 Hz, 1H, H-3′), 7.52 (m, 1H, H-4′), 7.16 (m, 1H, H-5′), 7.38 (d, J = 8.0 Hz, 1H, H-6′), 8.07 (s, 1H, H-7′), 2.33 (s, 3H, CH$_3$, H-9′) 12.01 (s, 1H, NH): ^{13}C NMR (CDCl$_3$, 150 MHz) : 128.4 (C-1), 131.1 (C-2), 122.1 (C-3), 131.9 (C-4), 129.5 (C-5), 126.6 (C-6), 63.4 (C-7), 72.6 (C-8), 138.8 (C-9), 149.1 (C-10), 128.3 (C-11), 126.3 (C-12), 118.4 (C-13), 130.2 (C-14), 169.5 (C-15), 21.0 (C-16), 120.4 (C-1′), 140.1 (C-2′), 120.0 (C-3′), 133.0 (C-4′), 122.6 (C-5′), 134.7 (C-6′), 164.6 (C-7′), 170.2 (C-8′), 25.6 (C-9′); HRMS (+ESI) [M+H]$^+$: found m/z 513.0507, C$_{25}$H$_{23}$BrClN$_2$O$_3$ requires m/z 513.0581.

3.6.3.8: (1R,2S)-1-(2-(((E)-2-acetamidobenzylidene)amino)phenyl)-2-(2-bromophenyl)-2-chloroethyl acetate

112 → 2.5 equiv FeCl₃
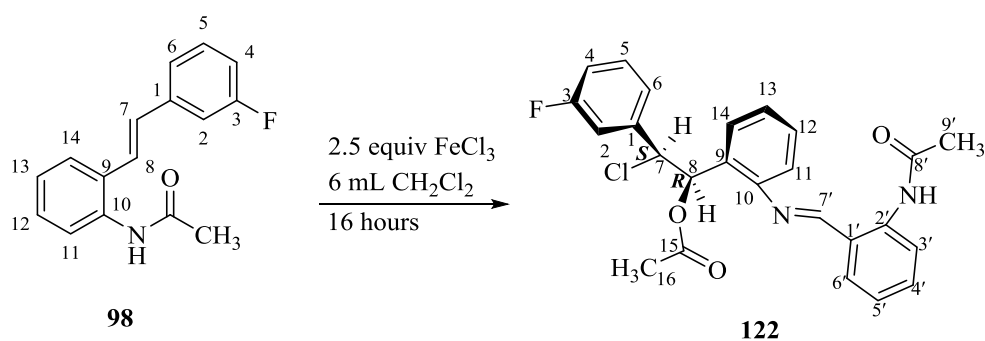6 mL CH₂Cl₂
16 hours → **129**
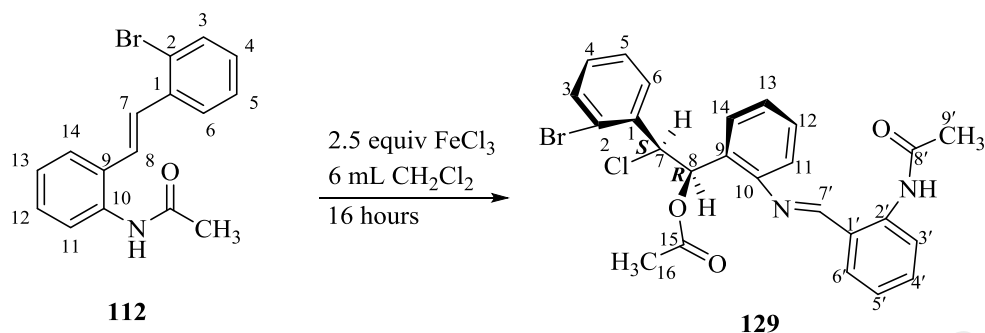
Compound **112** (0.098 g, 0.31 mmol) was dissolved in 6 mL of dichloromethane. Ferric chloride (0.130 g, 0.78 mmol) was added into the solution and capped with a rubber septum. It was left to stir until all **112** were consumed (checked via TLC). Saturated ammonium chloride was added and extracted with dichloromethane. Distilled water was used to wash, and dried under anhydrous sodium sulphate. Later, the solution was filtered and dried over reduced pressure to afford the crude product. Purification of the crude product by column chromatography (ethyl acetate/hexane 20:80) and extra step of separation by preparative TLC of silica backed glass (ethyl acetate/hexane 10:90) to afford (1R,2S)-1-(2-(((E)-2-acetamidobenzylidene)amino)phenyl)-2-(2-bromophenyl)-2-chloroethyl acetate **129** (0.037 g, 38% yield) as a white amorphous.

^{1}H NMR (CDCl₃, 600 MHz) δ: 7.27 (m, 1H, H-3), 6.89 (dt, J = 7.7 and 1.6 Hz, 1H, H-4), 6.78 (m, 1H, H-5), 7.56 (d, J = 7.7 Hz, 1H, H-6) , 5.67 (d, J = 8.1 Hz, 1H, H-7), 6.69 (d, J = 8.1 Hz, 1H, H-8), 7.70 (dd, J = 7.2 and 1.3 Hz, 1H, H-11), 7.31 (d, J = 7.2 Hz, 1H, H-12), 7.36 (dt, J = 7.2 and 1.3 Hz, 1H, H-13), 6.78 (m, 1H, H-14), 2.17 (s, 3H, CH₃, H-16), 8.83 (d, J = 8.0 Hz, 1H, H-3′), 7.51 (t, J = 8.0 Hz, 1H, H-4′), 7.16 (t, J = 8.0 Hz, 1H, H-5′), 7.27 (m, 1H, H-6′), 7.80 (s, 1H, H-7′), 2.32 (s, 3H, CH₃, H-9′) 12.04 (s, 1H, NH): ^{13}C NMR (CDCl₃, 150 MHz) : 136.3 (C-1), 122.9 (C-2), 132.3 (C-3),

130.0 (C-4), 127.2 (C-5), 131.3 (C-6), 62.9 (C-7), 72.5 (C-8), 129.2 (C-9), 148.8 (C-10), 128.4 (C-11), 126.4 (C-12), 130.3 (C-13), 118.7 (C-14), 169.3 (C-15), 21.0 (C-16), 120.7 (C-1′), 140.3 (C-2′), 120.1 (C-3′), 132.9 (C-4′), 122.5 (C-5′), 134.6 (C-6′), 164.6 (C-7′), 170.5 (C-8′), 25.5 (C-9′); HRMS (+ESI) $[M+H]^+$: found m/z 513.0361, $C_{25}H_{23}BrClN_2O_3$ requires m/z 513.0581.

3.6.4 General Procedure for Synthesis of Indolines

3.6.4.1: 1-(2-(4-methoxyphenyl)indolin-1-yl)ethanone
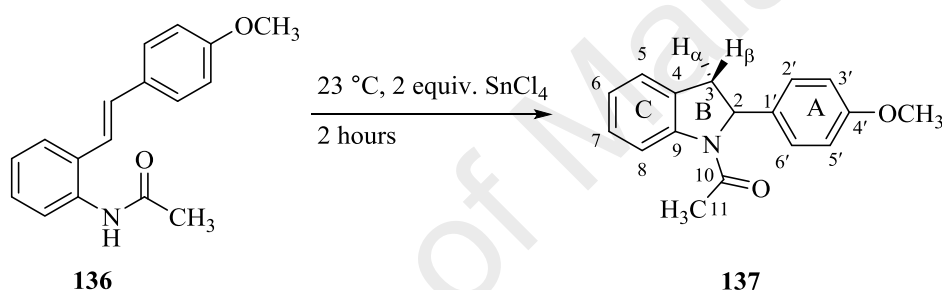
To a solution of compound **136** (0.100 g, 0.37 mmol) in toluene (8 mL) at 23 °C, tin (IV) tetrachloride (0.192 g, 0.74 mmol) was added and was left to stir for 2 hours. It was then diluted with ethyl acetate and quenched with methanolic solution of Et_3N (50 mL, 1 N). Later, the solution was extracted with ethyl acetate and washed with saturated NH_4Cl (3 x 30 mL) and brine (40 mL). The combined organic solution was dried with sodium sulphate anhydrous and filtered. It was dried under reduce pressure to afford the crude and purified through column chromatography (ethyl acetate/hexane 10:90) to afford 1-(2-(4-methoxyphenyl)indolin-1-yl)ethanone **137** (0.169 g, 55% yield) as a white solid.

^{1}H NMR (CDCl₃, 400 MHz) δ: 5.33 (d, J = 9.6 Hz, 1H, H-2), 2.95 (dd, J = 16.0 and 1.8 Hz, H-3α), 3.76 (m, 1H, H-3β), 7.05 (m, 1H, H-5), 7.05 (m, 1H, H-6), 7.25 (m, 1H, H-7), 8.31 (d, J = 8.2 Hz, 1H, H-8), 2.03 (s, 3H, CH₃, H-11), 7.05 (m, 1H, H-2′), 6.82 (d, J

= 8.7 Hz, H-3′), 6.82 (d, J = 8.7 Hz, 1H, H-5′), 7.05 (m, 1H, H-6′), 3.76 (s, 3H, CH$_3$); ^{13}C NMR (CDCl$_3$, 100 MHz) : 63.2 (C-2), 39.1 (C-3α), 39.1 (C-3β), 129.3 (C-4), 124.9 (C-5), 124.1 (C-6), 127.8 (C-7), 117.1 (C-8), 143.4 (C-9), 169.7 (C-10), 24.2 (C-11), 135.3 (C-1′), 126.3 (C-2′), 114.5 (C-3′), 159.2 (C-4′), 114.5 (C-5′), 126.3 (C-6′), 55.4 (OCH$_3$); HRMS (+ESI) [M+H]$^+$: found m/z 268.1393, C$_{17}$H$_{18}$NO$_2$ requires m/z 268.1338.

3.6.4.2: 1-(2-(4-fluorophenyl)indolin-1-yl)ethanone
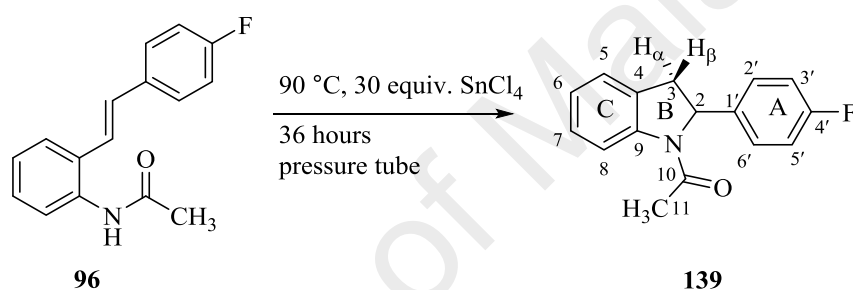
To a solution of compound **96** (0.094 g, 0.37 mmol) in toluene, tin (IV) tetrachloride (2.892 g, 0.0111 mol) was added and was left to stir for 36 hours in a pressure tube at 90 °C. After compound **96** was fully consumed (via TLC), it was then diluted with ethyl acetate and quenched with methanolic solution of Et$_3$N (50 mL, 1 N). Later, the solution was extracted with ethyl acetate and washed with saturated NH$_4$Cl (3 x 30 mL) and brine (40 mL). The combined organic solution was dried with sodium sulphate anhydrous and filtered. It was dried under reduce pressure to afford the crude and purified through column chromatography (hexane/ ethyl acetate, 80:20) to afford 1-(2-(4-fluorophenyl)indolin-1-yl)ethanone **139** (0.030 g, 32% yield) as a white solid.

^{1}H NMR (CDCl$_3$, 400 MHz) δ: 5.37 (d, J = 9.6 Hz, 1H, H-2), 2.95 (dd, J = 16.0 and 1.8 Hz, H-3α), 3.76 (dd, J = 16.0 and 9.6 Hz, 1H, H-3β), 7.13 (m, 1H, H-5), 7.05 (t, J = 8.0 Hz, 1H, H-6), 7.26 (t, J = 8.0 Hz, 1H, H-7), 8.31 (d, J = 8.0 Hz, 1H, H-8), 2.02 (s,

3H, CH$_3$, H-11), 6.98 (m, 1H, H-2′, H-6′), 7.13 (m, 2H, H-3′, H-5′); HRMS (+ESI) [M+H]$^+$: found *m/z* 256.1142, C$_{16}$H$_{15}$FNO requires *m/z* 256.1138.

3.6.4.3: 1-(2-(4-chlorophenyl)indolin-1-yl)ethanone

102　　　　　　　　　　　　　　　**140**
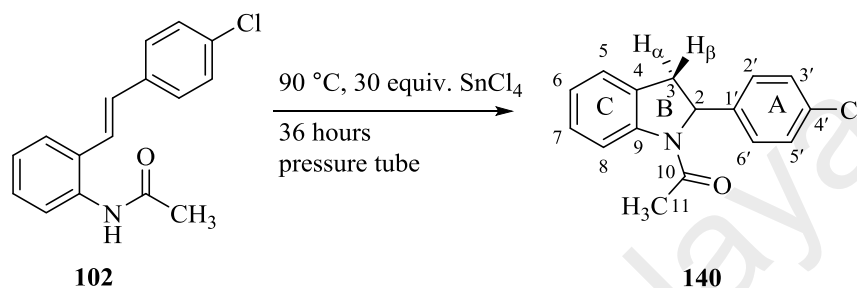
To a solution of compound **102** (0.101 g, 0.37 mmol) in toluene, tin (IV) tetrachloride (2.892 g, 0.0111 mol) was added and was left to stir for 36 hours in a pressure tube at 90 °C. After compound **102** was fully consumed (via TLC), it was then diluted with ethyl acetate and quenched with methanolic solution of Et$_3$N (50 mL, 1 N). Later, the solution was extracted with ethyl acetate and washed with saturated NH$_4$Cl (3 x 30 mL) and brine (40 mL). The combined organic solution was dried with sodium sulphate anhydrous and filtered. It was dried under reduce pressure to afford the crude and purified through column chromatography (hexane/ ethyl acetate, 80:20) to afford 1-(2-(4-chlorophenyl)indolin-1-yl)ethanone **140** (0.036 g, 36% yield) as a white solid.

^{1}H NMR (CDCl$_3$, 600 MHz) δ: 5.37 (d, *J* = 9.4 Hz, 1H, H-2), 2.94 (dd, *J* = 16.0 and 1.8 Hz, H-3α), 3.78 (m, 1H, H-3β), 7.11 (m, 1H, H-5), 7.06 (t, *J* = 7.7 Hz, 1H, H-6), 7.27 (m, 1H, H-7), 8.30 (d, *J* = 7.7 Hz, 1H, H-8), 2.03 (s, 3H, CH$_3$, H-11), 7.27 (m, 2H, H-2′, H-6′), 7.11 (m, 2H, H-3′, H-5′); ^{13}C NMR (CDCl$_3$, 150 MHz) : 62.9 (C-2), 38.9 (C-3α), 38.9 (C-3β), 133.7 (C-4), 124.9 (C-5), 124.3 (C-6), 127.9 (C-7), 117.1 (C-8), 143.1 (C-9), 169.3 (C-10), 24.1 (C-11), 141.6 (C-1′), 129.4 (C-2′), 126.4 (C-3′), 128.7 (C-4′),

126.4 (C-5′), 129.4 (C-6′); HRMS (+ESI) [M+H]$^+$: found m/z 272.0839, $C_{16}H_{15}ClNO$ requires m/z 272.0842.

3.6.4.4: 1-(2-(4-bromophenyl)indolin-1-yl)ethanone

108 **141**
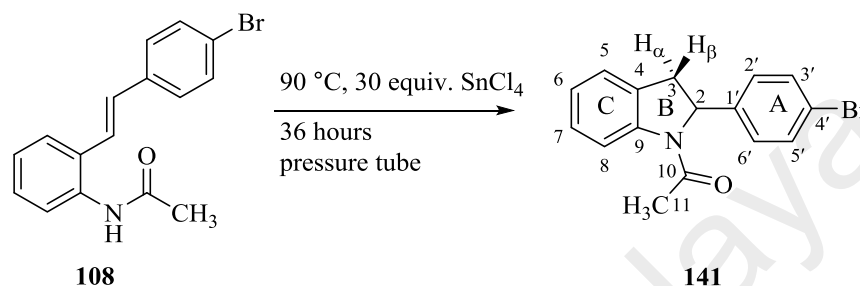
To a solution of compound **108** (0.101 g, 0.37 mmol) in toluene, tin (IV) tetrachloride (2.892 g, 0.0111 mol) was added and was left to stir for 36 hours in a pressure tube at 90 °C. After compound **108** was fully consumed (via TLC), it was then diluted with ethyl acetate and quenched with methanolic solution of Et_3N (50 mL, 1 N). Later, the solution was extracted with ethyl acetate and washed with saturated NH_4Cl (3 x 30ml) and brine (40 mL). The combined organic solution was dried with sodium sulphate anhydrous and filtered. It was dried under reduce pressure to afford the crude and purified through column chromatography (hexane/ ethyl acetate, 80:20) to afford 1-(2-(4-bromophenyl)indolin-1-yl)ethanone **141** (0.033 g, 28% yield) as a white crystal.

^{1}H NMR (CDCl$_3$, 400 MHz) δ: 5.27 (d, J = 9.5 Hz, 1H, H-2), 2.87 (d, J = 16.1 Hz, H-3α), 3.72 (m, 1H, H-3β), 7.34 (d, J = 7.56 Hz, 2H, H-2′, H-6′), 7.19 (t, J = 7.8 Hz, 1H, H-7), 7.06-6.96 (m, 4H, H-5, H-6, H-3′, H-5′), 8.23 (d, J = 7.7 Hz, 1H, H-8), 1.95 (s, 3H, CH$_3$, H-11), 7.27 (m, 2H, H-2′, H-6′). HRMS (+ESI) [M+H]$^+$: found m/z 316.0334, $C_{16}H_{15}BrNO$ requires m/z 316.0337.
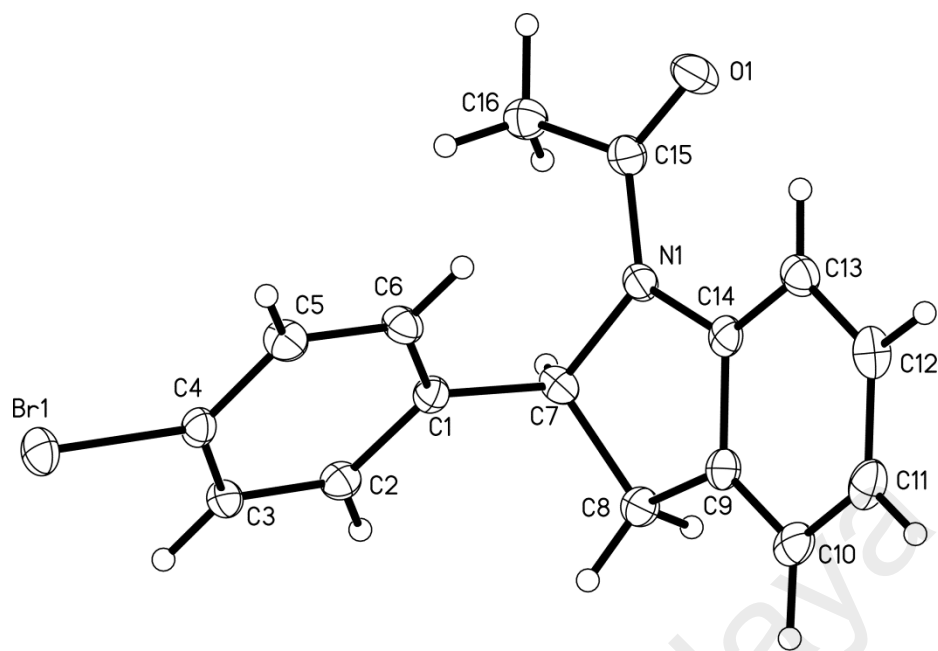
Figure 3.25: Ortep projection of single X-ray crystal of compound **141**

$C_{16}H_{14}BrNO$. M.p. 115-116 °C.

3.6.4.5: 1-(2-(3-fluorophenyl)indolin-1-yl)ethanone
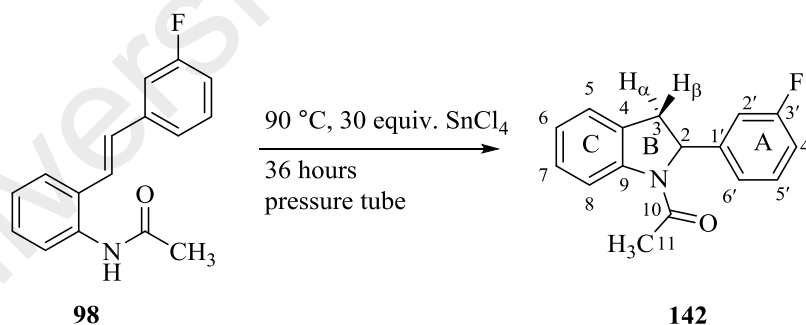
To a solution of compound **98** (0.094 g, 0.37 mmol) in toluene, tin (IV) tetrachloride (2.892 g, 0.0111 mol) was added and was left to stir for 36 hours in a pressure tube at 90 °C. After compound **98** was fully consumed (via TLC), it was then diluted with ethyl acetate and quenched with methanolic solution of Et_3N (50 mL, 1 N). Later, the solution was extracted with ethyl acetate and washed with saturated NH_4Cl (3 x 30 mL) and brine (40 mL). The combined organic solution was dried with sodium

sulphate anhydrous and filtered. It was dried under reduce pressure to afford the crude and purified through column chromatography (hexane/ ethyl acetate, 80:20) to afford 1-(2-(3-fluorophenyl)indolin-1-yl)ethanone **142** (0.033 g, 35% yield) as a white solid.

^{1}H NMR (CDCl$_3$, 400 MHz) δ: 5.38 (d, J = 9.4 Hz, 1H, H-2), 2.97 (d, J = 16 Hz, 1H, H-3α), 3.78 (m, 1H, H-3β), 6.97 (m, 1H, H-5), 7.05 (t, J = 7.6 Hz, 1H, H-6), 7.27 (m, 1H, H-7), 8.32 (d, J = 7.6 Hz, 1H, H-8), 2.04 (s, 3H, CH$_3$, H-9), 7.13 (m, 1H, H-2′), 6.97 (m, 1H, H-4′), 7.27 (m, 1H, H-5′), 6.87 (dt, J = 9.6 and 1.9 Hz, 1H, H-6′); ^{13}C NMR (CDCl$_3$, 100 MHz): 63.0 (C-2), 38.8 (C-3α), 38.8 (3β), 128.7 (C-4), 120.6 (C-5), 124.3 (C-6), 127.9 (C-7), 117.1 (C-8), 145.7 (C-9), 169.3 (C-10), 24.1 (C-11), 143.1 (d, J = 6.1 Hz, C-1′), 112.2 (d, J = 21.3 Hz, C-2′), 164.5 (d, J = 243.1 Hz, C-3′), 114.9 (d, J = 22.0 Hz, C-4′), 130.9 (d, J = 7.4 Hz, C-5′), 124.9 (C-6′); HRMS (+ESI) [M+H]$^+$: found m/z 256.1149, C$_{16}$H$_{15}$FNO requires m/z 256.1138.

3.6.4.6: 1-(2-(3-chlorophenyl)indolin-1-yl)ethanone
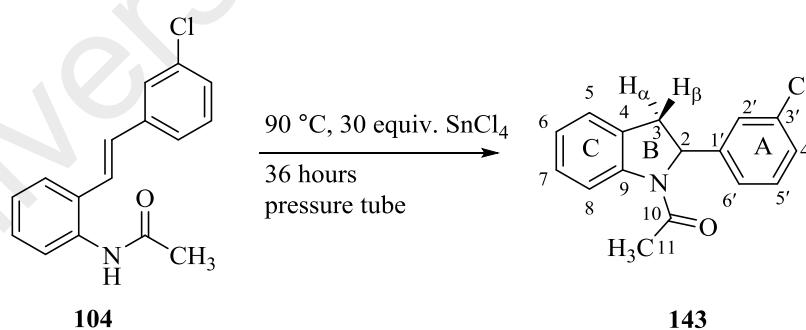
To a solution of compound **104** (0.101 g, 0.37 mmol) in toluene, tin (IV) tetrachloride (2.892 g, 0.0111 mol) was added and was left to stir for 36 hours in a pressure tube at 90 °C. After compound **104** was fully consumed (via TLC), it was then diluted with ethyl acetate and quenched with methanolic solution of Et$_3$N (50 mL, 1 N). Later, the solution was extracted with ethyl acetate and washed with saturated NH$_4$Cl (3

x 30 mL) and brine (40 mL). The combined organic solution was dried with sodium sulphate anhydrous and filtered. It was dried under reduce pressure to afford the crude and purified through column chromatography (hexane/ ethyl acetate, 80:20) to afford 1-(2-(3-chlorophenyl)indolin-1-yl)ethanone **143** (0.033 g, 33% yield) as a white solid.

^{1}H NMR (CDCl$_3$, 400 MHz) δ: 5.35 (d, J = 8.5 Hz, 1H, H-2), 2.97 (d, J = 16.0, H-3α), 3.79 (dd, J = 16.0 and 8.5 Hz, 1H, H-3β), 7.14 (m, 1H, H-5), 7.05 (m, 1H, H-6), 7.27 (d, J = 8.0 Hz, 1H, H-7), 8.31 (d, J = 7.5 Hz, 1H, H-8), 2.04 (s, 3H, CH$_3$, H-11), 7.14 (m, 1H, H-2′), 7.05 (m, 1H, H-4′), 7.27 (m, 1H, H-5′), 7.27 (m, 1H, H-6′); ^{13}C NMR (CDCl$_3$, 100 MHz) : 63.0 (C-2), 38.8 (C-3α), 38.8 (C-3β), 135.1 (C-4), 124.9 (C-5), 124.3 (C-6), 128.1 (C-7), 117.1 (C-8), 145.1 (C-9), 169.3 (C-10), 24.2 (C-11), 143.1 (C-1′), 131.3 (C-2′), 128.6 (C-3′), 125.8 (C-4′), 127.7 (C-5′), 130.0 (C-6′). HRMS (+ESI) [M+H]$^+$: found m/z 272.0844 C$_{16}$H$_{15}$ClNO requires m/z 272.0842.

3.6.4.7: 1-(2-(2-chlorophenyl)indolin-1-yl)ethanone
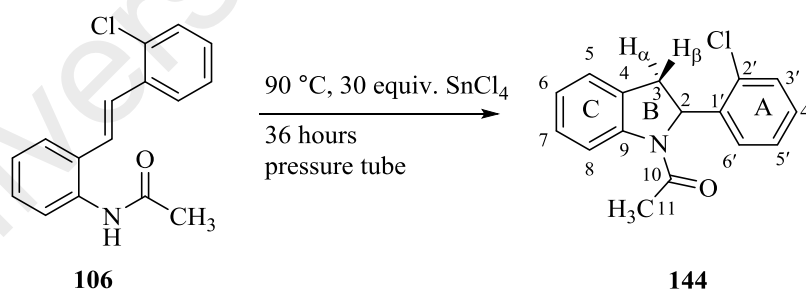
To a solution of compound **106** (0.101 g, 0.37 mmol) in toluene, tin (IV) tetrachloride (2.892 g, 0.0111 mol) was added and was left to stir for 36 hours in a pressure tube at 90 °C. After compound **106** was fully consumed (via TLC), it was then diluted with ethyl acetate and quenched with methanolic solution of Et$_3$N (50 mL, 1 N). Later, the solution was extracted with ethyl acetate and washed with saturated NH$_4$Cl (3 x 30 mL) and brine (40 mL). The combined organic solution was dried with sodium

sulphate anhydrous and filtered. It was dried under pressured to afford the crude and purified through column chromatography to afford 1-(2-(2-chlorophenyl)indolin-1-yl)ethanone **144** (0.035 g, 35% yield) as a white solid.

^{1}H NMR (CDCl$_3$, 400 MHz) δ: 5.77 (d, J = 9.0 Hz, 1H, H-2), 2.94 (d, J = 16.1, H-3α), 3.85 (dd, J = 16.1 and 9.0 Hz, 1H, H-3β), 7.13 (d, J = 7.7 Hz, 1H, H-5), 7.22 (t, J = 7.7 Hz, 1H, H-6), 7.28 (d, J = 7.7 Hz, 1H, H-7), 8.34 (d, J = 7.7 Hz, 1H, H-8), 2.00 (s, 3H, CH$_3$, H-11), 7.06 (d, J = 7.6 Hz, 1H, H-3'), 7.05 (dt, J = 7.6 and 1.0 Hz, 1H, H-4'), 7.16 (t, J = 7.6 Hz, 1H, H-5'), 7.43 (d, J = 7.6 Hz, 1H, H-6'); ^{13}C NMR (CDCl$_3$, 100 MHz) : 60.6 (C-2), 37.5 (C-3α), 37.5 (C-3β), 131.3 (C-4), 125.0 (C-5), 129.0 (C-6), 127.8 (C-7), 117.1 (C-8), 143.2 (C-9), 169.4 (C-10), 23.7 (C-11), 140.2 (C-1′), 131.3 (C-2′), 124.3 (C-3′), 125.8 (C-4′), 127.7 (C-5′), 129.9 (C-6′). HRMS (+ESI) [M+H]$^+$: found m/z 272.0849 , C$_{16}$H$_{15}$ClNO requires m/z 272.0842.

3.6.4.8: 1-(2-(2-bromophenyl)indolin-1-yl)ethanone
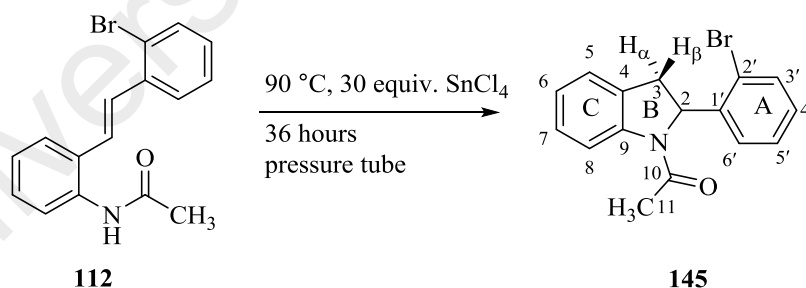
To a solution of compound **112** (0.101 g, 0.37 mmol) in toluene, tin (IV) tetrachloride (2.892 g, 0.0111 mol) was added and was left to stir for 36 hours in a pressure tube at 90 °C. After compound **112** was fully consumed (via TLC), it was then diluted with ethyl acetate and quenched with methanolic solution of Et$_3$N (50 mL, 1 N). Later, the solution was extracted with ethyl acetate and washed with saturated NH$_4$Cl (3 x 30 mL) and brine (40 mL). The combined organic solution was dried with sodium

sulphate anhydrous and filtered. It was dried under pressured to afford the crude and purified through column chromatography to afford 1-(2-(2-bromophenyl)indolin-1-yl)ethanone **145** (0.037 g, 32% yield) as a white solid.

^{1}H NMR (CDCl$_3$, 400 MHz) δ: 5.40 (d, J = 9.6 Hz, 1H, H-2), 3.81 (dd, J = 9.6 and 16.0 Hz, 1H, H-3β), 3.00 (dd, J = 1.8 and 16.0 Hz, 1H, H-3α), 7.33-7.25 (m, 3H, H-5, H-6 and H-7), 8.33 (d, J = 8.0 Hz, 1H, H-8), 7.06 (dt, J = 1.0 and 8.0 Hz, 1H, H-5'), 7.17 (m, 3H, H-3', H-4' and H-6'), 2.04 (s, 3H, CH$_3$); HRMS (+ESI) [M+H]$^+$: found m/z 316.0336, C$_{16}$H$_{15}$BrNO requires m/z 316.0337.

3.7   References

1   N. F. Thomas, S. S. Velu, J. F. F. Weber, K. C. Lee, A. H. A. Hadi, P. Richomme, D. Rondeau, I. Noorbatcha and K. Awang, *Tetrahedron*, 2004, **60**, 11733.

2   J. E. Plevyak, J. E. Dickerson and R. F. Heck, *J. Org. Chem.*, 1979, **44**, 4078.

3   D. Mc Cartney and P. J. Guiry, *Chem. Soc. Rev.*, 2011, **40**, 5122.

4   R. E. Buckles and N. G. Wheeler, *Org. Syntheses*, 1953, **33**, 88.

5   K. Ahmad, N. F. Thomas, M. R. Mukhtar, I. Noorbatcha, J. F. F. Weber, M. A. Nafiah, S. S. Velu, K. Takeya, H. Morita, C. G. Lim, A. H. A. Hadi and K. Awang, *Tetrahedron*, 2009, **65**, 1504.

6   K. Ferré-Filmon, L. Delaude, A. Demonceau and A. F. Noels, *Coord. Chem. Rev.*, 2004, **248**, 2323.

7   C. H. Kee, A. Ariffin, K. Awang, K. Takeya, H. Morita, S. I. Hussain, K. M. Chan, P. J. Wood, M. D. Threadgill, C. G. Lim, S. Ng, J. F. F. Weber and N. F. Thomas, *Org. Biomol. Chem.*, 2010, **8**, 5646.

8   C. C. C. Johansson Seechurn, M. O. Kitching, T. J. Colacot and V. Snieckus, *Angew. Chem. Int. Ed.,* 2012, **51**, 5062.

9   A. de Meijere and F. E. Meyer, *Angew. Chem. Int. Ed. Engl.,* 1994, **33**, 2379.

10 J. Tsuji, *Palladium Reagents and Catalysts - New Perspectives for the 21st Century*, John Wiley & Sons Ltd, Chichester, 2004.

11 T. Niu and Y. Zhang, *Tetrahedron Lett*, 2010, **51**, 6847.

12 M. J. O'Donnell and R. L. Polt, *J. Org. Chem.*, 1982, **47**, 2663.

13 I. Bauer and H. J. Knölker, *Chem. Rev.*, 2015, **115**, 3170.

14 X. Wu, A. P. Davis and A. J. Fry, *Org. Lett.*, 2007, **9**, 5633.

15 S. M. Halas, K. Okyne and A. J. Fry, *Electrochim. Acta*, 2003, **48**, 1837.

16 M. S. Paller, *The role of oxygen free radicals in acute renal failure*, in *Critical Care Nephrology*, ed. C. Ronco and R. Bellomo, Springer-Science+Business Media, Dordrecht, 1998, p. 557.

17 M. Hara, S. Samori, C. Xichen, M. Fujitsuka and T. Majima,, *J. Org. Chem.*, 2005, **70**, 4370.

18 F. D. Lewis, A. M. Bedell, R. E. Dykstra, J. E. Elbert, I. R. Gould and S. Farid, *J. Am. Chem. Soc.*, 1990, **112**, 8055.

19 T. Majima, S. Tojo, A. Ishida and S. Takamuku, *J. Org. Chem.*, 1996, **61**, 7793.

20 H. Togo, *Advanced Free Radical Reactions for Organic Synthesis*, Elsevier, Tokyo, 2004.

21 S. E. Denmark and L. Gomez, *Org. Lett.*, 2001, **3**, 2907.

22 I. Okamoto, H. Doi, E. Kotani and T. Takeya, *Tetrahedron Lett.*, 2001, **42**, 2987.

23 D. Benson, *Oxidation-Reduction Reactions Between Complexes of Different Metals*, in *Chemical Kinetics*, ed. C. H. Bamford and C. F. H. Tipper, Elsevier Publishing Company, Amsterdam, 1972, vol. 7, ch. 3, p. 175.

24 A. K. Holliday and A. G. Massey, *Non-aqueous Solvents in Inorganic Chemistry*. Pergamon Press, Oxford, 1965.

25 R. M. Silverstein, F. X. Webster and D. J. Kiemle, *Spectrometric Identification of Organic Compounds*, John Wiley and Sons, New Jersey, 2005.

26 C. A. G. Haasnoot, F. A. A. M. de Leeuw and C. Altona, *Tetrahedron*, 1980, **36**, 2783.

27 C. H. Kee, A. Ariffin, K. Awang, I. Noorbatcha, K. Takeya, H. Morita, C. G. Lim and N. F. Thomas, *Molecules*, 2011, **16**, 7267.

28 J. A. Connor, S. W. Leeming and R. Price, *J. Chem. Soc., Perkin Trans. 1*, 1990, 1127.

29 K. Ahmad, N. F. Thomas, M. F. Din, K. Awang and S. W. Ng, *Acta Crystallogr., Sect. E*, 2009, **E65**, o1289.

Chapter 4

Bioactivity Of Halogenated Acetamido Stilbenes And Structure Activity Relationship (SAR)

4.1   Introduction to Cancer

What is cancer? Cancer is the uncontrollable growth of the cells which contradict the control growth of a normal cell and the cells become a tumour. This tumour can transfer to other cell and cause morbidity, if left untreated, the patient may die. In Latin 'tumour' means swelling that occurred as the result of the abnormal growth of the mass cancer cells. The word tumour is used interchangeably with neoplasm meaning new cell growth. It was found that even five thousand year old mummies in Egypt and Peru were found to have tumours in their bones.[1] During that time, cancer was not understood and they have shorter lifespan.

The Greek physician Hippocrates (460-370BC) introduced the word 'cancer', it was from the greek word 'karcinos' meaning crab to describe the extensions going outward of the tumour from the central mass mimicking the shape of the crab.[1] It was reported in 2012, the death caused by cancer in the world was 8.2 million lives and lung cancer being the most prevalent with about 1.59 million lives.[2] Meanwhile cancer was the third cause of death after heart disease and Septicaemia in Malaysia in 2007. Lung cancer was the leading cancer in males while breast cancer in female population in Malaysia.[3]

Cancer can be classified into two; benign or malignant tumour. Benign tumours are abnormal growth of the cell and do not invade into other surrounding tissues and therefore does not metastasize. Their cells resemble the original tissues and most of them are harmless.

The cells are usually encapsulated by a membrane to separate from the surrounding normal tissues.[4] The growths of the cells are slow but it can reach into a considerable size. Due to the size, they may compress and damage other normal cells or press nearby optic nerves which can lead to blindness. Benign tumours of hormone producing gland such as thyroid, adrenal which put pressure locally may produce excessive amounts of their normal product, this will cause severe symptoms.[5]

Malignant tumours are abnormal cell growths that will metastasis from its primary site to invade surrounding cells. It will proliferate and kill normal cells. The tumour cells do not have well defined capsule and disorganised features. The cells invade through the blood system or lymphatic vessels.[1]

(a) Benign tumors are generally self-contained and localized and have a well-defined perimeter

They grow slowly, expanding outward from a central mass

They are dangerous when they compress surrounding tissues. A benign tumor near a blood vessel could restrict the flow of blood; in the abdomen it could impair digestion; in the brain it could cause paralysis

(b) Malignant tumors are not self-contained, and usually do not compress surrounding tissues. Their growth is an irregular invasion of adjacent cells

Although they may grow slowly, they are also capable of very rapid growth

They are not localized; in a process called metastasis they shed cells that travel through the bloodstream and infect tissues at other locations. They can even establish malignant growth in a different type of tissue: a breast cancer can spread to bone tissue, for example

Figure 4.1: Benign and malignant tumors (extracted from Almeida 2010).[1]

4.2   Types of Cancer

There are many type of cancer; the four predominant types are carcinomas, sarcomas, leukemias, and lymphomas. About 90% of human cancers are carcinomas, which arrived

from the epithelium of the glands, internal organs and body cavities. Sarcomas are the transformation of cells in connective tissue such as bone, fat, muscle, or cartilage.[1] Leukemias are cancers of the bone marrow, which leads to the over-production and early release of immature leukocytes (white blood cells).

4.3   Causes of Cancer

Causes of cancer are well documented and some of the examples will be discussed. Tobacco is well known cause of cancer especially with lung cancer. Tobacco is directly connected to smoking and most prevailing in male cancer patient who developed lung cancer. Tobacco contains nicotine which can cause mutation in the gene and the smoke from the tobacco can act as a promoter for chronic inflammation. Alcohol too is well associated with cancer but the mechanism in which alcohol causes the cancer is not clear, it is thought that acetaldehyde that is a break down product of the alcohol in the liver through enzymes alcohol dehydrogenase (producing acetaldehyde) and aldehyde dehydrogenase maybe is mutagenic towards the cell. Women who often consume two to five drinks of alcohol are more likely to develop breast cancer compare to those who does not consumed.[6]

Radiation is another well associated cause of cancer. Radiations from gamma ray and X-ray with high exposure rate destroy human tissues. Two famous world catastrophes that is the bombing of Hiroshima and Nagasaki and the explosion Chernobyl nuclear reactor led to a high amount of gamma rays being exposed to human. Survivors of these two events have died in the following years and some have developed solid tumours as a result of the mutation from the radiation. Infections also play a role in causing cancer. It is noted that most of cervical and liver cancers are initiated by viruses. *Helicobacter pylori*, a bacterium that causes chronic infection and ulcer in the stomach which can lead to gastric cancer.

Ultra-violet radiation is good for the health but also is a carcinogen. To absorb the UV light, the body produce melanocytes. An uncontrolled growth of melanocytes gives rise to a malignant tumour called melanoma. Several chemicals are known to be carcinogenic. Polycyclic aromatic hydrocarbons and 2,3,7,8-tetrachlorodi-benzo-p-dioxin (TCDD), is a potent mutagen.[5]

4.4   Stages of Cancer

A standard way to predict the treatment that is warranted and the course of the disease is described below [6];

Stage I : Long-term survival is from 70% to 90%. Primary tumour is limited to the organ of origin. There is no evidence of nodal or vascular spread. The tumour can usually be removed by surgical resection.

Stage II : Survival is 45% to 55%. Primary tumour has spread into surrounding tissue and lymph nodes immediately draining the area of the tumour (''first-station'' lymph nodes). The tumor is operable, but because of local spread, it may not be completely resectable.

Stage III: Survival is 15% to 25%. Primary tumour is large, with fixation to deeper structures. First-station lymph nodes are involved; they may be more than 3 cm in diameter and fixed to underlying tissues. The tumour is not usually resectable, and part of the tumour mass is left behind.

Stage IV: Survival is under 5%. Extensive primary tumour may be more than 10 cm in diameter. It has invaded underlying or surrounding tissues. Extensive lymph node involvement as occurred, and there is evidence of distant metastasis beyond the tissue of origin of the primary tumour.

4.5   Human Cancer

There are many types of human cancer and some of the most common ones are discussed briefly in the following sections.,[6-7]

4.5.1   Leukemias and Lymphomas

Leukemias and lymphomas are cancers arising from cells of the hematopoetic lineage (hence: hematological cancers). These cancers are diagnosed by blood and bone marrow tests. Leukemia is a cancer affecting leukocytes, cells that are grouped into two categories: lymphocytes and myelocytes. Early symptoms of leukemias are persistent fatigue or weakness, frequent infections, and easy bleeding or bruising.

4.5.2   Breast Cancer

Breast cancers are prominent disease among the females. Breast is the symbol of feminity among women. The malignant cells of the cancer are the epithelial of the lactiferous ducts. Early form of breast cancer is the ductal carcinoma *in situ* (DCIS) which can be detected by mammogram. It will later move on to more invasive stage that is the invasive ductal carcinoma (IDC).The symptoms are redness, swelling, dimpling, warmth of the breast and inverted nipple, or itchiness.

4.5.3   Colon cancer

Colon cancer is more prevalent in the developed nations. Colon is the lower part of the digestive system. Most of the cancer cells will start from the polyps which are benign and will turn malignant especially if there are adenomatous polyps. Patients who have *Ulcerative colitis* and Crohn's disease, increase the rate in developing colon cancer.

4.5.4 Lung Cancer

Lung cancer accounted for most mortality of cancer. It is mostly occur in smokers and predominantly male. Other factors contributing to lung cancer are environmental factor and genetic. Most often the cancer arises in the lining of the bronchi in the lung. Any toxic chemical in the air will enter into the body through the lung first. The cigarettes that smokers puff contain 40 known carcinogens and one piece of good news is his or her lung will recover after a number of years if the smoker stops early before the cancer developed. Other factor that contributes to lung cancer is the odourless but radioactive radon gas in area with high concentration of uranium in the soil. Asbestos which is a popular fire retardant material contribute to lung cancer and people who are exposed to it will have a higher risk of developing mesothelioma. Mesotheliomas have a high mortality rate. Symptoms that should be look at are coughing up blood, shortness of breath, persistent cough, constant chest, shoulder or back pain, hoarseness, recurrent bronchitis or pneumonia and bloody or rust-colored sputum (phlegm).

4.5.5 Prostate Cancer

Prostate cancer occurred in the male population and it is not really well understood the risk factors that cause this cancer. Several genes that play a progressive role have been identified. Testosterones stimulate the growth of prostate cells but they also increase the rate of growth of cancerous prostate cells. Benign prostatic hyperplasia (BPH) are among the symptom whereby the prostate enlarged that compress the urethra and developed difficulty starting or holding back the flow of urine, pain or burning during urination, a weak or interrupted urine flow, blood in the urine, an increased need to urinate and painful urination or impotency.

4.5.6   Cervical Cancer

Cervical cancer affects the reproductive organ of the female. The cancer grow very slowly in 2-10 years and among the symptoms that can be seen are vaginal bleeding or unusual discharge not associated with menstruation, bleeding between periods or after menopause or douching. These symptoms are not unique to cervical cancer, so it is better to have medical officer to examine the patient. Human papillomavirus (HPV) are associated with the development of cervical cancer.

4.6   Treatment for Cancer

There are many treatments in dealing with cancer. Three types of treatment will be briefly discussed; surgical procedure, radiation therapy and chemotherapy.[6-7]

4.6.1   Surgical Procedure

Surgical procedure is the removals of the tumour from a specific location in the body which have not metastasized. It offers the greatest hope in curing a patient from cancer completely. Firstly, a tissue sample is extracted for biopsy to determine whether the tumour is benign or malignant. The main purpose is to remove the entire tumour, if this is not possible due to the connectivity with other tissues or organs that might be affected if this procedure continued. A debulking surgery would be done to reduce the size of the tumour so that radiation or chemotherapy will be more effective when applied. If the tumour is pressing on specific nerves and causing pain, palliative surgery would be considered to reduce the pain of the patient. Other form of surgery that is being operated on patients is laser surgery whereby the intense heat of beam target and vaporizes the cancerous cells. Another form of surgery is

the cryo surgery that uses cold liquid nitrogen (−195.5 °C) to kill malignant cells. This cold treatment occasionally used on prostate, skin and cervical cancers.[1]

4.6.2 Radiation Therapy

Another common type of treatment is radiation therapy where 50-60% of cancer patient underwent this procedure. It uses X-ray to kill the tumour cells. The X-ray works by damaging the DNA of the cancer cell as it pass through it. This is done by minimizing the radiation effect on healthy cells that is close to the tumour cells. Radiation therapy can be delivered in single high dose or multiple small dosage of the radiation. External-beam radiation therapy (EBRT) shoots the radiation to the tumour from the outside while internal radiation therapy or brachytherapy uses radioactive pellets implant directly to the tumour or near it delivering the required dosage that is needed.

4.6.3 Chemotherapy

Chemotherapy is the uses of cytotoxic drug to target the tumour by moving around the body until it reaches the intended cancer cell. The advantage of the cytotoxic drug is that it will not only kill the solid tumour but also non-solid tumour (leukemias and lymphomas). Chemotherapy works by impairing the cancer cells to divide and proliferate. Choosing the right drugs depend on the type of cancer and stage. The use of drugs after surgery alleviates the chance of cancer to grow back. Combination of drugs are also used to treat cancer by hitting different target in the cancer cell, in what we call 'fractional killing' to increase the death of the cancer cells. Among the well-known drugs are 'Avastin' for colorectal, lung, breast, kidney and ovarian cancer, 'Herceptin' for breast cancer and 'Gardasil' for cervical cancer.

4.7   Cytotoxicity

The level of toxicity by which a substance can inflict damage onto cells is called cytotoxicity.[8] The damage will often result in cell death and there are two distinctive types of cell death. Firstly, necrosis is when the cell will prematurely die as a result of loss of membrane strength due to cell lysis.[9] While, apoptosis is a programmed cell death that follow a predictable and controlled pathway.[10]

Measuring the cell viability and cytotoxicity effects of the cancer cell caused by the therapeutic compound is usually done by assessing the integrity of the cell membrane.[11] Once the cell membrane is compromised, the use of dyes such as trypan blue and propidium iodide will cross inside the membrane into the intracellular components but would not affect the healthy cells.[12] Another common method used in measuring cytotoxicity is the Lactate Dehydrogenase assay (LDH). LDH is usually sequestered inside the cell but once the membrane integrity collapsed, it will venture out of the cell.[13] MTT assay uses 3-(4, 5-Dimethyl-2-thiazolyl)-2, 5-diphenyl-2H-tetrazolium bromide (MTT) is a popular type of cell viability measurement that depends on NAD(P)Hdependent oxidoreductase enzymes to reduce MTT to purple formazan.[14]

Cytotoxicity tests are the most popular preliminary examination to evaluate chemical compounds that could be potential cancer therapeutics.

4.8   Resveratrol

Resveratrol is a natural phenolic stilbene that is commonly found in grapes, berries and peanut. It usually acts as a phytoalexin to counter the stress from the environment and pathogen attack. In France, where the population consumed a lot of red wine and fatty food,

the incidences of heart related problems are small. This is due to the resveratrol in red wine that help the inhibition of LDL oxidation in human which are popularly known as the French Paradox.[15] This popularity has encouraged scientists to synthesize resveratrol and its analogues to test their bioactivity. Among the well-known properties of stilbene derivatives is its cytotoxicity properties toward cancerous cells. Fluoronated analogues of combretastatin A-4 were discovered to have good activity against K562 human myelogenous leukaemia cell-line, P388 murine leukaemia cell-line and SKMEL-5 human melanoma cell-line.[16] Sanoh et al. (2003) also reported good activity of stilbene derivatives against breast cancer cell (MCF-7). In another breast cancer cell line (MDA-MB-468), hydroxylated stilbenes showed good cytotoxicity against the cancer cell.[17] Stilbenes have also shown to be chemo preventive agents against colon cancer.[18]

It was also reported that stilbene has antiviral properties that it prevents initiation of hepatitis C virus RNA replication.[19] Other beneficial effect that stilbene possesses it is a neuroprotective agent and being experimented against the Huntington's disease.[20] Our group have also tested nine amido stilbenes against four cancer cell lines that are colon (HT29), liver (HepG2 and WRL-68) and blood (Jurkat and P388). One stilbene analogue has displayed potent cytotoxicity against colon (HT29) and blood (P388).
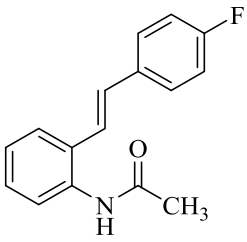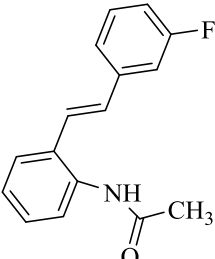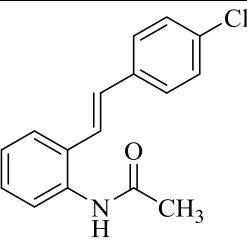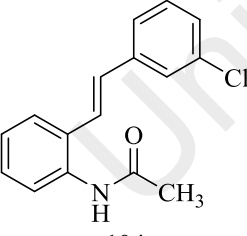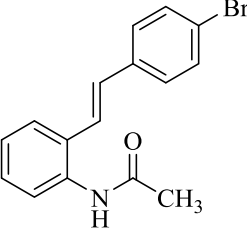
4.9   Results and Discussion

Five stilbenes were synthesized and evaluated against five cancer cells; colon cancer (HT-29), estrogen-sensitive breast cancer (MCF-7), estrogen-insensitive breast cancer (MDA-MB-231), prostate cancer (DU-145), pancreatic cancer (BxPC-3) and one normal human pancreatic cell (hTERT-HPNE) (Table 4.1). Testing on the colon cancer cell (HT-29) showed that stilbene **98** (IC_{50} = 11.40 μM) and **108** (IC_{50} = 15.92 μM) have good cytotoxic

activity while others were less effective. Stilbene **98** has a fluorin atom at the *meta* position and **108** have a bromine atom at *para* position. These two stilbenes displayed better result than cisplatin (IC_{50} = 30.61 µM) and resveratrol (IC_{50} = 72.90 µM). The estrogen-sensitive breast cancer cell (MCF-7) test result showed that stilbene **98** (IC_{50} = 32.52 µM) is almost two times more cytotoxic than cisplatin (IC_{50} = 55.04 µM) and nearly three times more than resveratrol (IC_{50} = 85.71 µM).

None of the tested stilbenes showed improved cytotoxic activity compared with control drugs when tested against pancreatic cancer cell (BxPC-3) and estrogen-insensitive breast cancer (MDA-MB-231). Stilbene **98** showed the most potent activity at IC_{50} = 16.68 µM better than the recognised drug vinblastin (IC_{50} = 20.31 µM) toward prostate cancer cell (DU-145). All of the tested stilbenes did not show any cyctotoxic activity against normal pancreatic cells (hTERT-HPNE) while the standard drugs (vinblastin, cisplatin, resveratrol) displayed otherwise. These findings suggest for the development of stilbene based drugs which are selective towards cancer cell which could reduce unwanted side-effects to patients.[21]

Table 4.1: Cytotoxic evaluation of halogenated acetamido stilbenes

Entry	IC$_{50}$ / µM (n = 3)					
	HT-29	MCF-7	Bx-PC-3	DU-145	MDA-MB-231	hTERT-HPNE
Vinblastin (positive control)	4.40 ± 2.70	21.00 ± 2.33	33.04 ± 2.14	20.31 ± 7.76	27.06 ± 6.05	22.81 ± 1.00
Cisplatin (positive control)	30.61 ± 2.34	55.04 ± 5.25	71.54 ± 5.36	22.68 ± 1.14	88.75 ± 12.10	42.53 ± 6.97
Resveratrol (control)	72.9 ± 2.4	85.71 ± 1.70	71.85 ± 1.55	107.92 ± 1.57	143.57 ± 12.12	82.69 ± 3.61
96	>200	>200	>200	>200	>200	>200
98	11.40 ± 7.35	32.52 ± 5.16	129.78 ± 4.36	16.68 ± 1.86	>200	>200
102	>200	97.00 ± 4.79	>200	>200	>200	>200
104	>200	>200	>200	>200	>200	>200
108	15.92 ± 3.85	>200	>200	>200	>200	>200

4.10 Conclusion

Stilbene **98** showed good and diverse cytotoxic activity against HT-29 (11.40 µM), MCF-7 (32.52 µM), Bx-PC-3 (129.78 µM) and DU-145 (16.68 µM), and more potent than resveratrol and cisplatin. All the stilbenes that were tested against the cancer cell lines, did not displayed any cytotoxicity against the normal pancreatic cell (hTERT-HPNE).

4.11 Experimental Section

Five cancer cell lines; colon (HT-29), breast (MCF-7) , prostate (DU-145), pancreatic (BxPC-3) and breast (MDA-MB-231); and one normal cell line, pancreatic (hTERT-HPNE) were selected for the cytotoxicity tests against the halogenated stilbenes. The National Cancer Institute (NCI) list of 60 cancer cell lines were used as a reference guideline for the chosen cancer cell lines for drug treatment and drug screening conditions according to NCI recommendations.[22] Cell lines were cultured in DMEM media supplemented with 2 mM L-glutamine, 2.5 µg/mL amphotericin B, 50 µg/mL gentamicin and 10% foetal bovine serum, maintained in a 37 °C humid atmosphere of 5% CO_2 cell incubator. hTERT-HPNE cell line was cultured in the same DMEM with 10 ng/mL human recombinant epithelial growth factor as recommended by ATCC.

DMSO was used to dissolve the stilbenes and drug standards (cisplatin, resveratrol and vinblastine) and DMEM media were used to dilute it to give a final DMSO concentration of less than 0.5% v/v. Around 5,000–10,000 cells per well were plated into 96-well microplates and maintained in the cell incubator for 24 h. Afterwards, samples amounting to 100 µL were introduced in triplicates to a final concentration of 0.1–200 µM. Insertion of drug standards at the final concentration of 0.03–2000 µM (cisplatin) 0.78–400 µM

(resveratrol) and 0.002–200 µM (vinblastine). After 48 hours of cell incubation, cell viability was determined according to the manufacturer protocol of a commercial MTS assay kit (CellTiter 96 ® AQueous One Solution, Promega). A quantity of 100 µL of DMEM media, followed by 20 µL per well of MTS reagent were used to revitalised the culture media. Incubation of 1–2 hours of the microplates was continued and absorbance of the formazan product was analysed on a microplate reader at 490 nm with 690 nm as the background wavelength (Infinite 200, Tecan, Mannedorf, Swizerland). Determination of IC_{50} of samples and drug standards were performed using dose-response curves, and statistical analysis using student's T-test ($p < 0.05$) was performed in Prism 5.02 software (GraphPad Software Inc., La Jolla, CA, USA).

4.12 References

1 C. A. Almeida and S. A. Barry, *Cancer*, Wiley-Blackwell, Oxford, 2010.

2 Cancer Research UK, *World Cancer Factsheet*, Cancer Research UK, London, 2014.

3 Z. A. Omar and N. S. Ibrahim Tamin, *National Cancer Registry, Malaysia*, Ministry of Health Malaysia, 2007.

4 H. Lüllmann, A. Ziegler, K. Mohr and D. Bieger, *Color Atlas of Pharmacology*, Thieme, Stuttgart, 2000.

5 R. Hesketh, *Introduction to Cancer Biology*. Cambridge University Press, Cambridge, 2013.

6 R. W. Ruddon, *Cancer Biology*, Oxford University Press, New York, 2007.

7 W. A. Schulz, *Molecular Biology of Human Cancers*, Springer, Dordrecht, 2005.

8 E. Hodgson, *A Textbook of Modern Toxicology*, John Wiley & Sons, New Jersey, 2004.

9 H. J. Rode, *Apoptosis, Cytotoxicity and Cell Proliferation*, Roche Diagnostics GmbH, Manheim, 2008.

10 Promega, *Apoptosis*, in *Protocols And Applications Guide*, ed. Promega, Promega Corporation, Madison, 2011.

11 Promega, *Cell Viability*, in *Protocols And Applications Guide*, ed. Promega, Promega Corporation, Madison, 2011.

12 T. L. Riss and R. A. Moravec, *Assay Drug Dev. Technol.*, 2004, **2**, 51.

13 T. Decker and M. L. Lohmann-Matthes, *J. Immunol. Methods*, 1988, **115**, 61.

14 M. V. Berridge, P. M. Herst and A. S. Tan, *Tetrazolium dyes as tools in cell biology: New insights into their cellular reduction,* in *Biotechnology Annual Review*, ed. M. R. El-Gewely, Elsevier, 2005, vol. 11, p. 127.

15 H. Arichi, Y. Kimura, H. Okuda, K. Baba, M. Kozawa and S. Arichi, *Chem. Pharm. Bull.*, 1982, **30**, 1766.

16 N. J. Lawrence, L. A. Hepworth, D. Rennison, A. T. McGown and J. A. Hadfield, *J. Fluorine Chem.*, 2003, **123**, 101.

17 C. J. Lion, D. A. Vasselin, C. H. Schwalbe, C. S. Matthews, M. F. Stevens and A. D. Westwell, *Org. Biomol. Chem.*, 2005, **3**, 3996.

18 A. M. Rimando and N. Suh, *Planta Med.*, 2008, **74**, 1635.

19 P. Gastaminza, S. M. Pitram, M. Dreux, L. B. Krasnova, C. Whitten-Bauer, J. Dong, J. Chung, V. V. Fokin, K. B. Sharpless and F. V. Chisari, *J. Virol.*, 2011, **85**, 5513.

20 G. M. Pasinetti, J. Wang, P. Marambaud, M. Ferruzzi, P. Gregor, L. A. Knable and L. Ho, *Exp. Neurol.*, 2011**, *232***, 1.

21 M. N. Azmi, M. F. M. Din, C. H. Kee, M. Suhaimi, K. P. Ang, K. Ahmad, M. A. Nafiah, N. F. Thomas, K. Mohamad, K. H. Leong and K. Awang, *Int. J. Mol. Sci.*, 2013**, 14**, 23369.

22 M. R. Boyd and K. D. Paull, *Drug Dev. Res.*, 1995**, 34**, 91-109.

Chapter 5

Quantitative Structure Activity Relationship (QSAR)

5.1 Introduction

Quantitative Structure Activity Relationship (QSAR) is the study of chemical compounds relationship on the activity of a biological cell, mostly disease cell.[1] This relationship is portrayed on mathematical equation that can be understood.[2] When was QSAR started is still undecided, but in 1868 a study on certain alkaloids on its biological activity before and after methylation of its nitrogen produced a conclusion that "physiological activity" is the function of the chemical constitution. At that time, chemical structure of compounds were still unknown so surely this relationship cannot be proven.[3] Entering a new century of 1900, independent study by Meyer and Overton have concluded a positive response between lipid solubility and effectiveness of the drugs that they were using, this have come to be known as Meyer-Overton theory of anesthesia. The compounds were tested on the solubility in partition of olive oil and water.[2, 4]

Work on QSAR started to pick up speed when Hansh published his work on the partition coefficient of water and *n*-octanol in correlation with biological activity of plant growth regulator.[5] The following year, Free et al. (1964) reported a mathematical model of the relationship between the biological activities with the modification of the analogues.[6] Langridge et al. in 1981 used the coordinates from the X-ray data to properly position the examined protein into the computer, atom by atom.[7] The colour graphic on computer have helped a lot in the understanding how well a small molecule can position itself inside a protein or enzyme. Computer programmes for calculating the QSAR models have been

developed and 3D models of the molecule have assisted in the understanding of the QSAR by using software such as COMFA,[8] Catalyst, DRAGON and Phase. In this research work, a QSAR study was attempted on 25 stilbene analogues to study the relationship between the structure and the activity manifested. The QSAR study in this research was done using Discovery Studio 3.0 software. The software was also known as Catalyst before this and was developed by BioCAD in1992.[9] Below is the workflow for the preparation of the 3D molecule before submitting to the Discovery Studio programme (Scheme 5.1).

Molecule in 3D

↓

Molecule PreOptimization
Using
Molecular Mechanics

↓

Conformational Analysis

↓

Molecule Optimization
Using
Semiemperical
Methods (PM7)
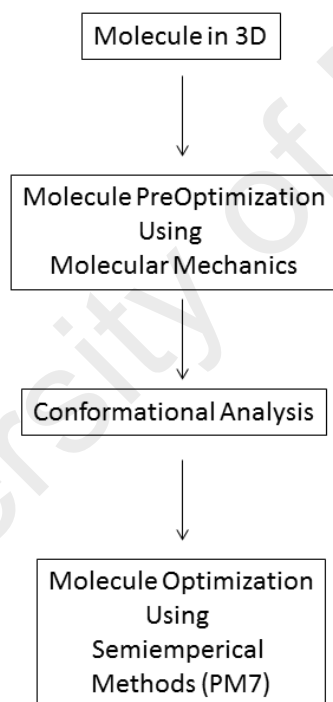
Scheme 5.1: Protocol for the preparation of 3D molecule

The QSAR study starts by preparing the 3D structure of each molecule using Chem3D and pre-optimization of the molecules was done using molecular mechanics MM2. Next, conformational analysis on the stilbene analogues was performed to find the global minimum for the analogues. Lastly, semiemperical method (PM7) was used for geometry optimization. Each step will be discussed briefly in the following subchapters.

5.1.1 Molecular Mechanics

Molecular mechanics use force field to calculate the total energy of the molecule using classical mechanics without computing the wave function or total energy density.[10] The model is based on assumption and one of this is the Born-Oppenheimer approximation. Other assumptions are that all the atoms in the molecule are ball and attached to each other with springs. So the balls will resist attempt to stretch or press the ball together, or bend the spring at an angle at which measurement it deem not 'natural'. In other words, it uses the mechanical model to find its minimum energy geometry. It does not involve any electron in the calculation.

The force field usually take the form of total energy:

$$\sum_{total} = \sum_{bonds} E\ stretch + \sum_{angles} E\ bends + \sum_{dihedrals} E\ torsion + \sum_{pairs} E\ non\ bond$$

Some of the force field that are commonly used: MM2, MM3, MM4, it have been parameterized based on the best quality experimental data and comprehensive, and these family of force field have been touted as the "gold standard". Other have force field are the

AMBER, CHARMM (Chemistry at Harvard Macromolecular Mechanic) and Merck molecular force field (MMFF).

5.1.2 Conformational Analysis

Molecules are not always static. In the course of time, molecules containing one or several single bond always moving, giving different isomers that is rotomers or conformers. Large amount of the conformers that are found are low-energy conformers.[11] The changes from one conformer to another depend on the rotation of the single bond or torsion angles. The most stable conformer gives the lowest energy surface because the movement of the angle influence the potential energy surface of the conformers. The population of the conformers depend on the potential energy surface and also the entropy of the molecules. From the Boltzmann distribution, we can calculate the population distribution of the conformers:

$$\frac{N_i}{N_{total}} = \frac{e^{-E_{rel}/RT}}{\sum_{k=1}^{N_{total}} e^{-E_k/RT}}$$

In determining the best conformer, a conformational search is done by increasing the torsion angles of the molecule. The degree of increment is the step size and from this formula the number of conformers can be calculated

Number of conformers = $(360/\text{step size})^n$

Usually the step size is 30°, so with a 360° rotation, 12 conformers are generated on a single torsion. If there is n number of torsion in a single molecule, 12^n of confomers are generated. A smaller step size can be used and larger size of conformers will be generated. Energies from the conformers will calculated and group according to the Boltzmann

distribution. In this conformational search, the Monte Carlo method is used whereby the new geometry (after minimisation) is accepted and used for the next perturbing step if the energy is lower than the previous ones or if the Boltzmann factor is larger than a random number between 0 and 1. A natural endpoint is not to be found in the random search as it will generate new conformations until no new ones can be found and this resulted each region of the conformers to be explored many times.[12,13]

5.1.3 Semiemperical Methods

Semiemperical methods derived from the combination of modify Hartree-Fock (*Ab-initio*) calculation with experiment.[14] The semiempirical methods are based on these three approximation schemes:

1) The exemption of the inner electron from the calculation

   This reduces the complexity of the calculation without effecting on the accuracy. The nucleus and inner electron are substituted by a parameterized function.

2) Minimum number of basis set

   It reduced the complexity of computation and only calculates the valence electron and requires minimum number of basis set.

3) Reduction of the two electron integrals

Modern semiemperical are founded on the modified neglect of differential overlap (MNDO) approach. The parameters in this method are attached various atomic types and are matched to replicate properties such as dipole moments, heats of formation, first ionization energies and geometrical variables. Latest versions of MNDO are the AM1, PM6 and the most used at the moment is PM7.[15,16]

5.2   QSAR Analysis

After the 3D molecules or ligands were prepared, these series or set of ligands were submitted into the Discovery Studio programme for the QSAR analysis. Below is the workflow for QSAR analysis (Scheme 5.2).
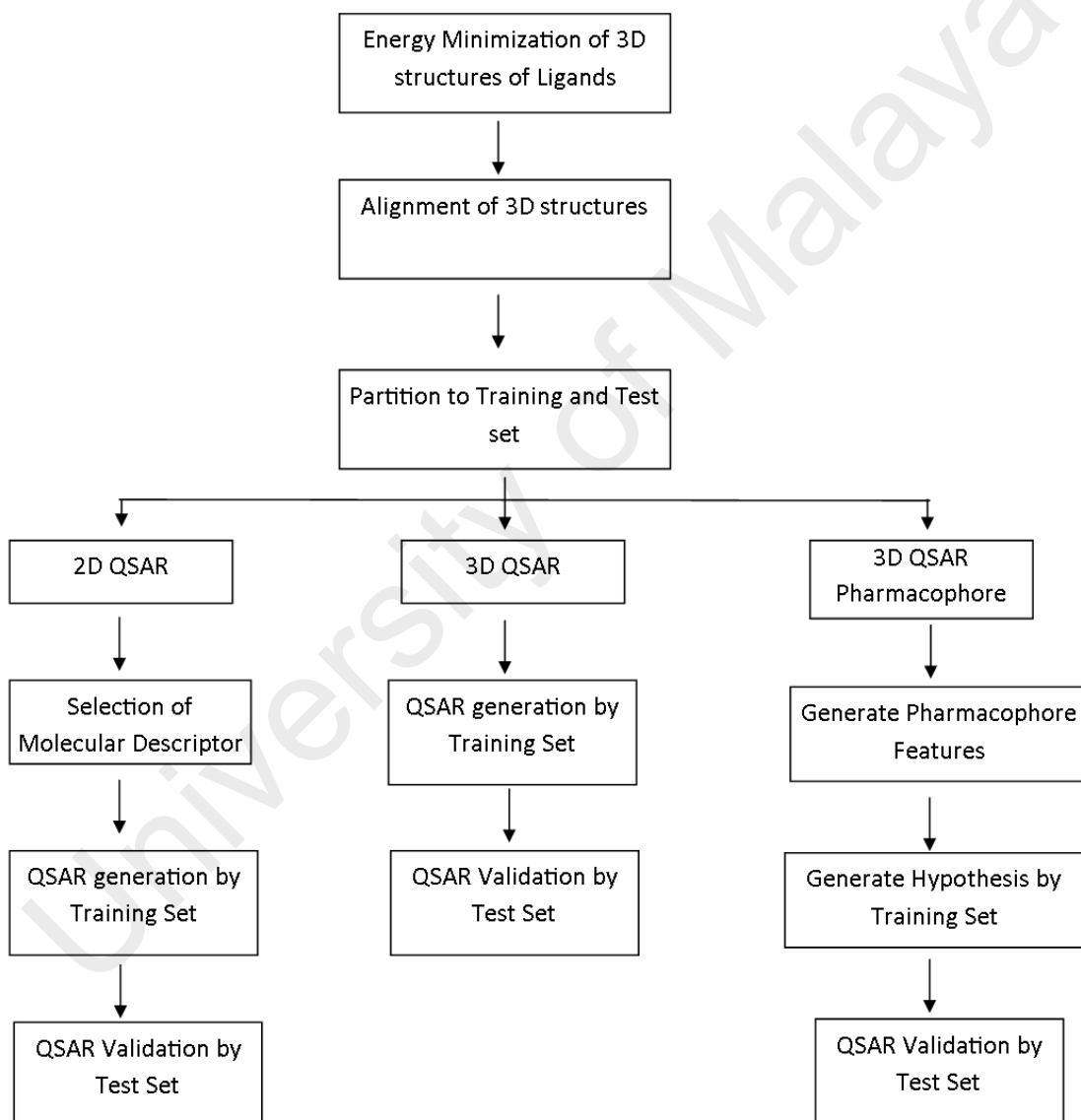
Scheme 5.2 : Workflow of QSAR Analysis

5.2.1 Data Analysis

Various techniques are applied to extract the primary information from the chemical data regarding the characteristics of the chemical compound. Data analyses also deal with the generation of secondary data like generation of models for the purpose of prediction. Several techniques such as multiple linear regression analysis and partial least square were discussed briefly in the following paragraphs.

5.2.1.1 Multiple Linear Regression Analysis

Between two variables, x and y, a correlation can be made using the Linear Regression Model.[10] It can be described by an equation of $y=ax + b$, a is the slope of the straight line while b is the intercept at y-axis. The objective of the line is to give the best prediction of y from x by accommodating the slope and the intercept. Reducing the sum of squares of the vertical distances of the points from the lines will give the best prediction. For Multiple Linear Regression Analysis, it uses more variables as given by the equation. The variable y is modelled analogously to the case of one input variable if given n input variable x_i. x_i should be uncorrelated.

$$y = a_0 + a_1x_1 + a_2x_2 + \ldots + a_nx_n$$

5.2.1.2 Partial Least Square (PLS) Method

Partial Least Square method is an interesting technique for QSAR as the features are highly correlated in building a predictive model. The model can relate two matrices X and Y as its objective. X and Y are calculated separately, the scores of matrix X are used to predict

the score of matrix Y. From there, it can predict Y. Determining the number of principal components for the regression is important selection in PLS.[17]

5.2.2 Model Evaluation

The model that has been established is evaluated before used to predict new molecules in QSAR.[18] A squared correlation coefficient, r^2 is calculated to evaluate how good is the model predicts the activity of the training set.

$$r^2 = 1 - \frac{\Sigma(p_{exp} - p_{calc})^2}{\Sigma(p_{exp} - p_{avg})^2}$$

p is potency values. This coefficient ranges from zero (no fit) to one (perfect fit).

After r^2 have been determined, it will be validated by method called "leave-one-out cross-validation". It is done by removing one data value (potency value) from the training set and the remaining data will be evaluated to predict the value that was left out. This method is called cross-validation r^2LOO.

$$r^2\text{LOO} = 1 - \frac{\Sigma(p_{exp} - p_{calc})^2}{\Sigma(p_{exp} - p_{avg})^2}$$

r^2 ranges from 0 (no fit) to 1 (perfect fit or prediction). It can be said that r^2 is a magnitude of the quality of the linear function to fit the training set data, r^2LOO is an indicator of the predictive power of the model. An external validation of the model is done by applying the model on a test set to assess the reliability of the model. A correlation coefficient q^2 is obtained, similar to the training set. The correlation coefficient for the training set and test set is then evaluated.

5.3   Results and Discussion

A total of 25 compounds of stilbene ligands were used in this calculation. The list of the stilbene ligands were divided into two sets; training set and test set. The training set contained 20 compounds (Figure 5.1 and Figure 5.2) while the test set contained 5 compounds (Figure 5.3). For QSAR studies, the compound of the stilbene analogues are usually called ligands.
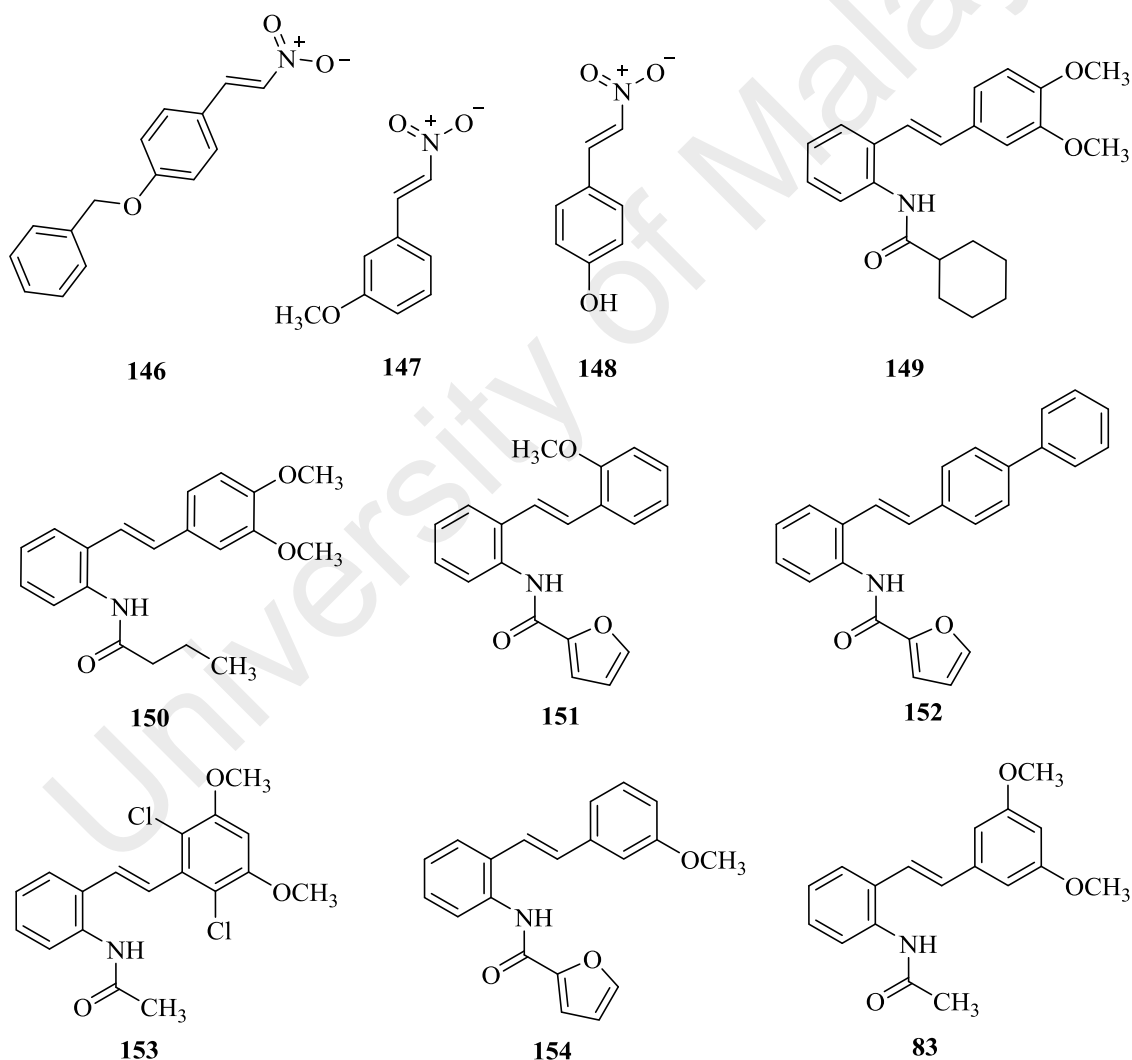
Figure 5.1: Training set ligands
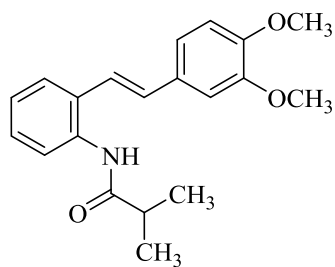
155
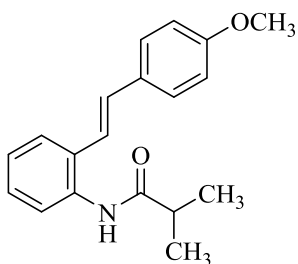
156
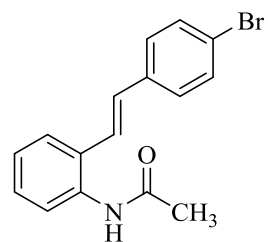
108
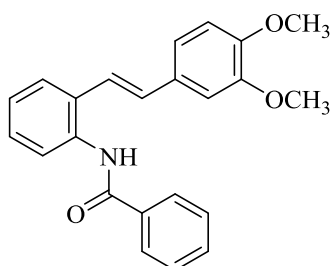
157
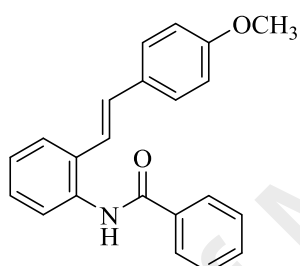
158
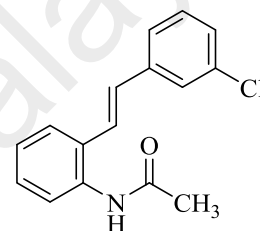
104
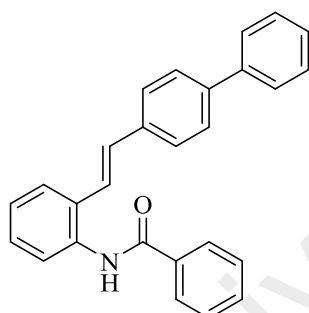
159
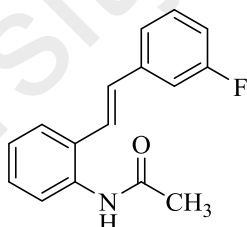
98
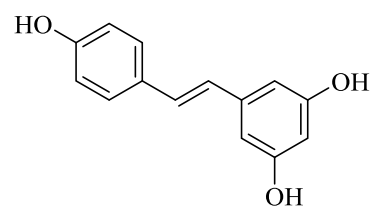
1
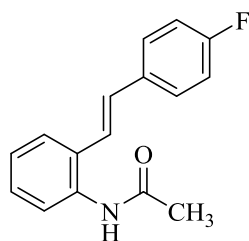
96

Figure 5.2: (continued) Training set ligands
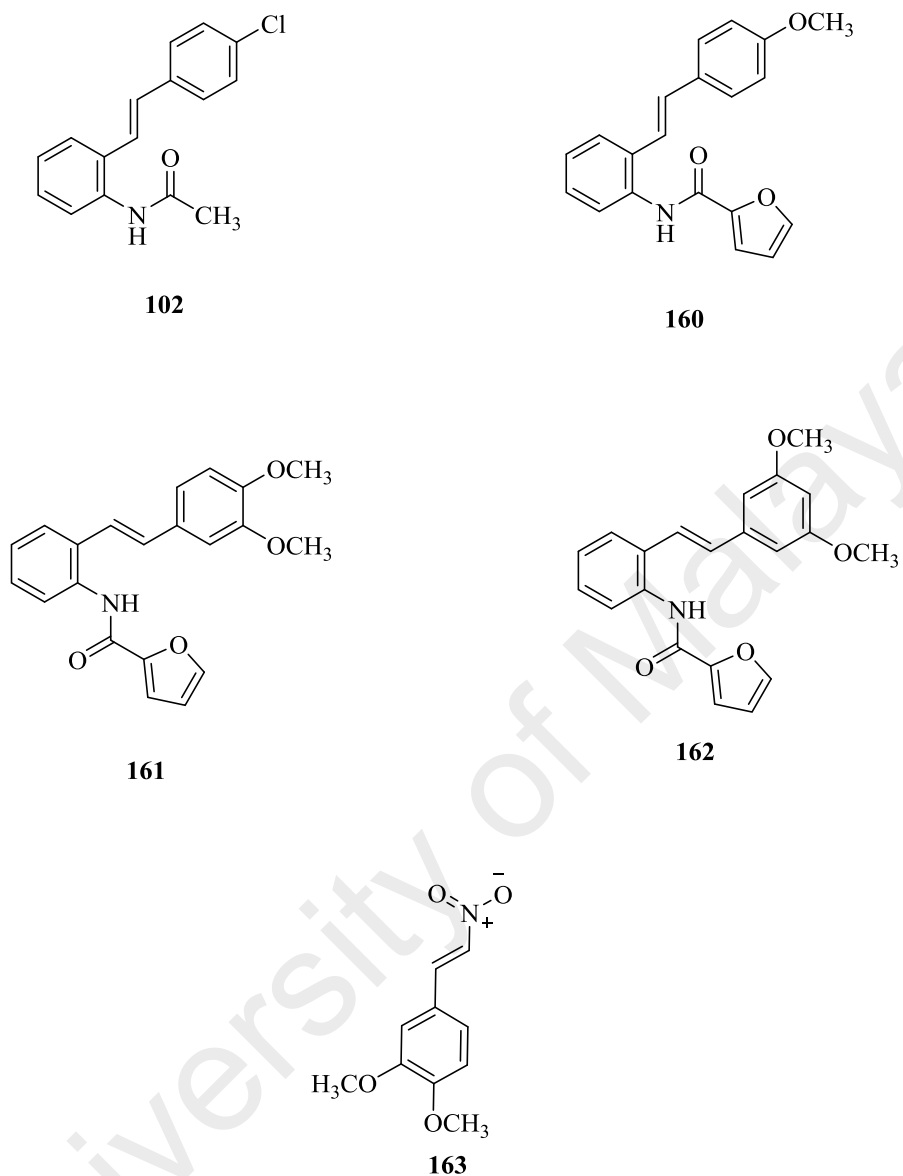
Figure 5.3: Test set ligands

Estrogen-insensitive breast cancer cell line (MDA-MB-231) was used for the cytotoxicity testing of the biological cell. Here are the complete IC_{50} values of MDA-MB-231 cell for the training and test set (Table 5.1). Three types of QSAR were studied; 2D QSAR,

3D QSAR and 3D QSAR Pharmacophore. A total of 25 compounds were used to study the QSAR run on Discovery Studio 3.0 by Accelerys.

Table 5.1 : IC$_{50}$ Values of stilbenes against estrogen insensitive-breast cancer cell line

(MDA-MB-231)

Entry	Compounds	IC$_{50}$ values(μM)
1	**146**	10.82
2	**147**	45.34
3	**148**	43.33
4	**149**	517.87
5	**150**	557.13
6	**151**	645.6
7	**152**	868.92
8	**153**	1,089.81
9	**154**	825.4
10	**83**	1,529.95
11	**155**	1,227.91
12	**156**	1,042.2
13	**108**	1,049.5
14	**157**	1,874.3
15	**158**	1,286.35
16	**104**	1,413.52
17	**1**	143.57
18	**159**	475.2
19	**98**	1,292.36
20	**96**	1,101.19
21	**163**	38.9
22	**162**	1,078.76
23	**102**	752.7
24	**161**	2,484.9
25	**160**	468.93

5.3.1 2D QSAR

The multiple linear regression (MLR) model was used to correlate the inhibitory activity of resveratrol analogues with various electronic, physicochemical, steric and structural molecular descriptors. Types of molecular descriptors that can be used are topological descriptors, dipole, ALogP, element counts, surface area and volume, molecular properties count and other descriptors.[19] Due to the large amounts of molecular descriptors, careful selection of suitable descriptors have been done to prevent chance correlation from occurring, eliminating highly correlated descriptors and excluding descriptors that have very broad training data. Correlation matrix was used as a quantitative model to discard any highly intercorrelated descriptors (Table 5.3). Also, the descriptor that affect the inhibitory activity of the resveratrol analogues can be deduced.[20] Descriptors that were chosen from various categories that influenced the activity of the compounds were ALogP, BIC, Dipole_mag, HBA_Count, IC, Molecular Fractional Polar SASA and NPlusO_Count. Descriptions of the molecular descriptors are provided in Table 5.2 according to the Accelrys manual.

Table 5.2 : Description of the molecule descriptors

Molecule Descriptors	Description
ALogP	Log of the octanol-water parition coefficient using Ghose and Crippen's method
BIC	Bonding information content
Dipole_mag	The strength and orientation behaviour of a molecule in an electrostatic field
HBA_Count	The number of hydrogen bond accepting gtoups in the molecule
IC	Information content
Molecular_Fractional PolarSASA	The ratio of the polar solvent accessible surface area divided by the total solvent accessible surface area
NPlusO_Count	The number of nitrogen and oxygen atoms in the molecule

Table 5.3 : Correlation matrix of biological activity with molecular descriptors

Property	ALogP	BIC	Dipole_mag	HBA_Count	IC	Molecular_ Fractional PolarSASA	NPlusO_ Count
ALogP	1						
BIC	-0.45	1					
Dipole_mag	0.10	-0.08	1				
HBA_Count	0.47	0.30	0.11	1			
IC	0.09	0.82	-0.08	0.70	1		
Molecular_ Fractional PolarSASA	-0.76	0.02	0.10	-0.54	-0.48	1	
NPlusO_ Count	-0.08	0.35	0.23	0.66	0.38	0.24	1

Correlation matrix was constructed for the chosen descriptor. In Table 5.3, the BIC and IC are intercorrelated with each other with a high value ($r = 0.82$) which is $r>0.7$. These descriptors were excluded as it does not affect the model. For Dipole_mag, it was also excluded as resveratrol analogues had implicit hydrogens and 3D descriptor calculation may not give useful results. ALogP and Molecular_FractionalPolarSASA showed high intercorrelation but in a negative value ($r = -0.76$). Only ALogP was discarded because when Molecular_FractionalPolarSASA was also discarded, the model gave a bad correlation to the inhibitory activity. After the exclusion, the model was left with 3 descriptors that have the most influence on the activity of the analogues. From here, multi linear regression (MLR) model was build using these 3 descriptors. The model was portrayed as follows:

Activity (Log IC$_{50}$) = $\quad$ 3.297 + 1.314 (**HBA_Count**) − 1.379 (**NPlusO_Count**) +

$\qquad$ 9.873 $\quad$ (**Molecular_FractionalPolarSASA**)

$\mathbf{n}$ = 20, r^2 = 0.92, r^2LOO = 0.873, q^2 = 0.839, RMS error = 0.168

The resveratrol analogue would be more cytotoxic towards the cancer cell when the value of 50% inhibitory concentration (log IC$_{50}$) is low. From the equation, the positive value of hydrogen bond acceptor group such as nitrogen, oxygen, carbonyl group, ester group, nitro group and phenol group will increase the value of the log IC$_{50}$. Increased numbers of nitrogen and oxygen in the molecules NPlusO_Count will lower the log IC$_{50}$ values. Molecular_FractionalPolarSASA descriptor exerted a greater influence on the inhibitory activity of analogues as the value is 10 times than other descriptors.
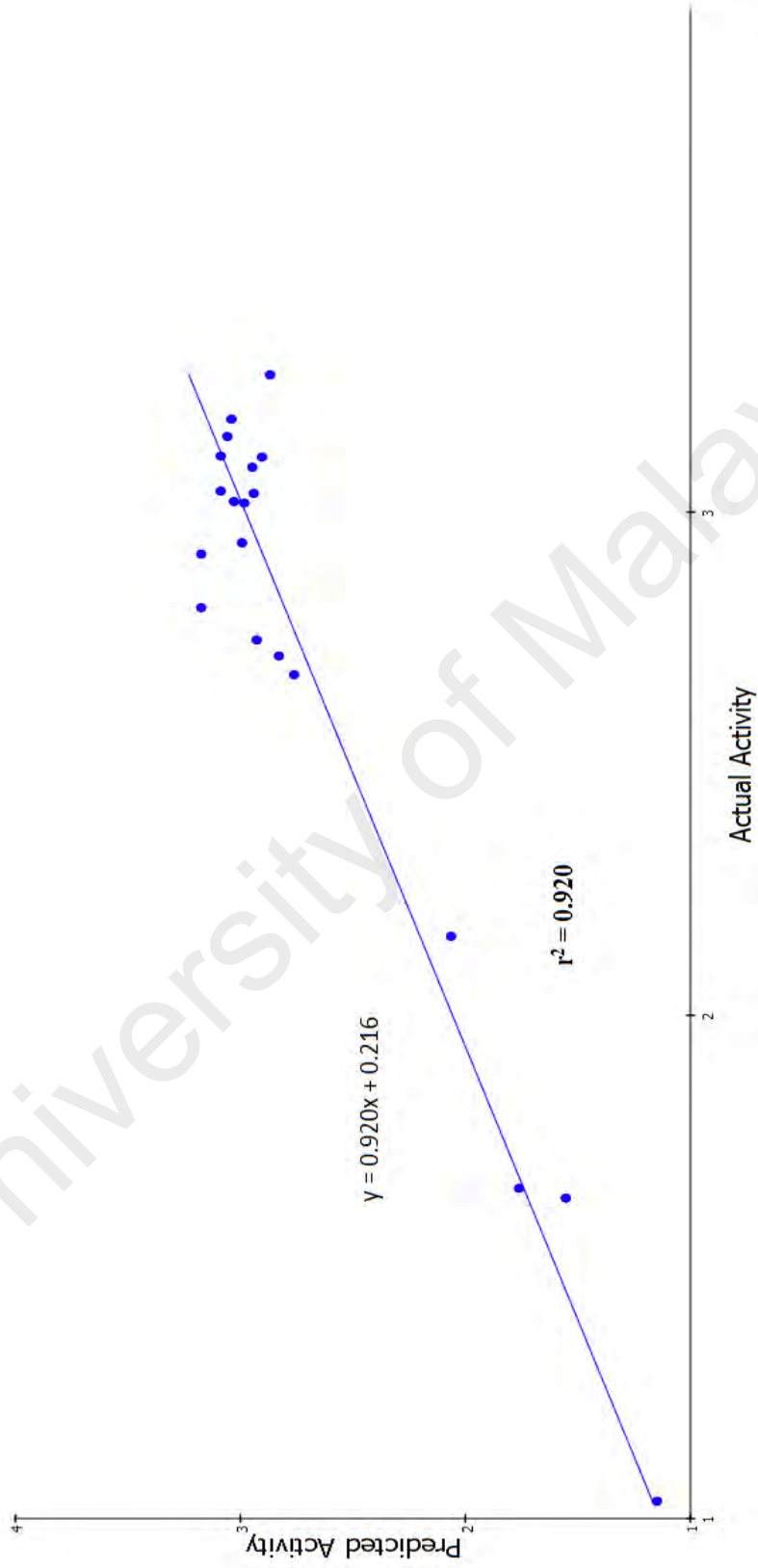
Figure 5.4: Plot of prediction versus actual activity for the training set

$y = 0.920x + 0.216$

$r^2 = 0.920$

Actual Activity

Predicted Activity

From Figure 5.4, it showed the r^2 for the training set is 0.920. This showed a high correlation value between the descriptor of the training set and the inhibitory activity of the analogues. This model is good enough to predict the activity of other compounds. Also, the low RMS error value 0.168, showed the high accuracy of the model. As seen from Table 5.4, the predicted IC_{50} of the training set for the ligands are almost the same as the actual activity. Ligand **146** has an IC_{50} value of 10.82 μM while the predicted value is 14.09 μM. The difference in IC_{50} values is not wide.

Another method to validate this model is the cross validation leave one out (LOO) method to ascertain the robustness of the model. The LOO is a method whereby one molecule is left out from dataset and the remaining data is evaluated of the predictive power of the model. This was done under a 21-fold cross validation (Figure 5.5). The correlation coefficient r^2LOO was 0.837 showed that the predictive power of the model is good.

Table 5.4 : Actual and predicted activity of the training set using the model

Compound	Actual IC_{50} (μM)	Predicted IC_{50} (μM)
1	143.57	115.68
96	1,101.19	1222.39
104	1,413.52	1141.80
151	645.6	1492.07
154	825.4	1492.07
152	868.92	982.38
159	475.20	577.30
157	1,874.30	737.45
149	517.87	673.35
155	1,227.91	884.52
150	557.13	845.22
156	1,042.20	960.31
158	1,286.35	800.61
83	1,529.95	1094.89
153	1,089.81	872.25
147	45.34	57.68
146	10.82	14.09
148	43.33	35.74
98	1,292.36	1222.39
108	1,049.50	1066.52
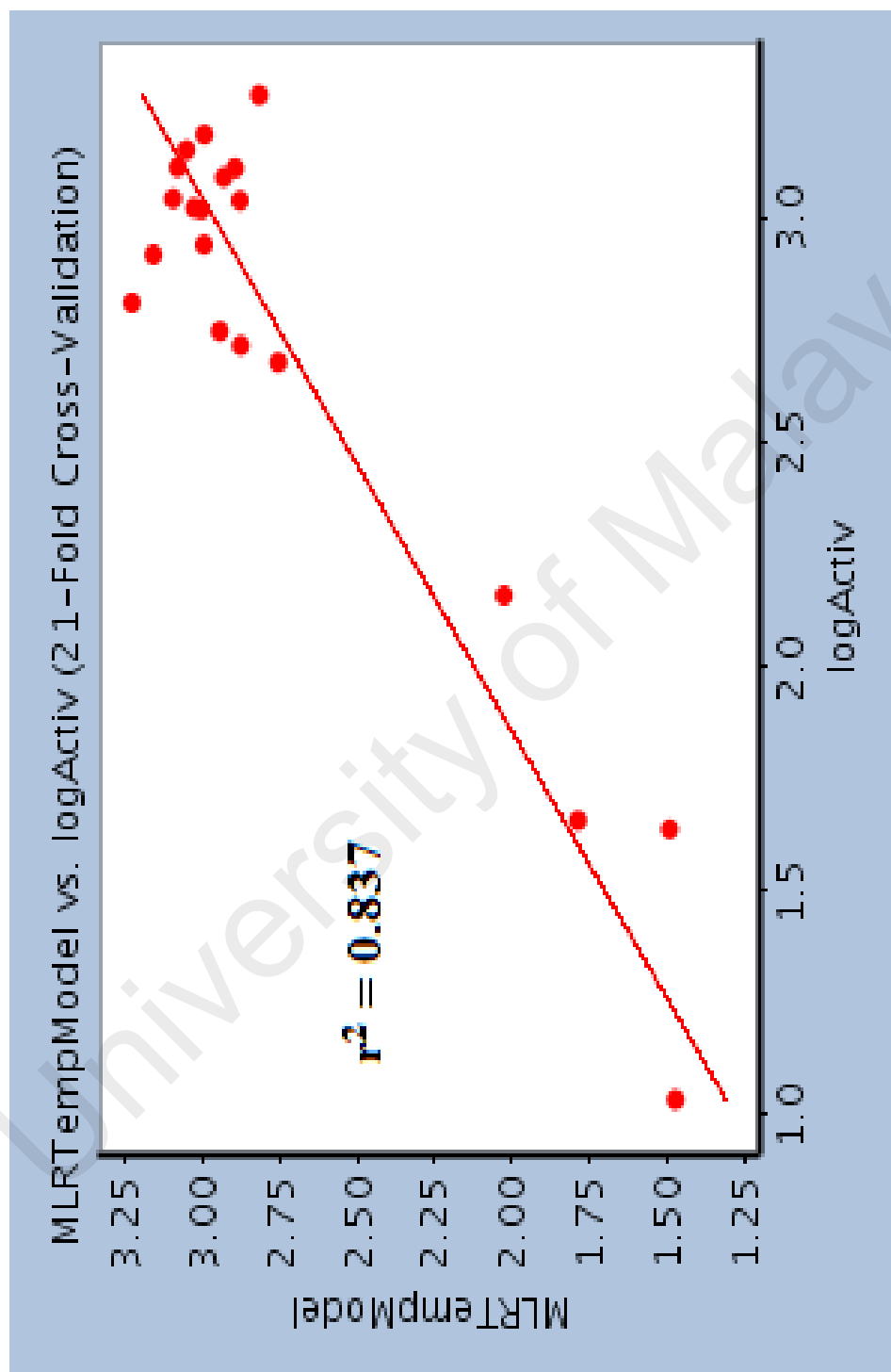
Figure 5.5: Plot of cross validation LOO of the MLR model

To determine if the model was good in predicting the activity of new compounds, it was evaluated against a test set. The test set contained 5 compounds which are different from the training set but have been tested on the same cancer cell. From Figure 5.6, the $q^2 = 0.839$ which showed a high correlation between the descriptors and the inhibitory activity of the analogues. In Table 5.5, the most potent ligand, **163** have an IC_{50} of 38.90 μM and predicted value is almost similar to the actual value with an IC_{50} of 39.53 μM. This validated the effectiveness of the model. It is proven that this MLR model can be utilized in predicting the inhibitory of a new untested compound.

Table 5.5 : Actual and predicted activity of the test set using the model

Compound	Actual IC_{50} (μM)	Predicted IC_{50} (μM)
102	752.70	1141.80
160	468.93	1492.07
161	2,484.90	1343.48
162	1,078.76	1343.48
163	38.90	39.53

Making sure that the model is fit and sound, a Y-scramble validation process was excuted.[21] We shuffle the activity value of the data set randomly and run again the MLR calculation and found that the r^2, q^2 and r^2 LOO value are different from the original value. This external validation process is important to prevent any chance correlation from occurring (Table 5.6).
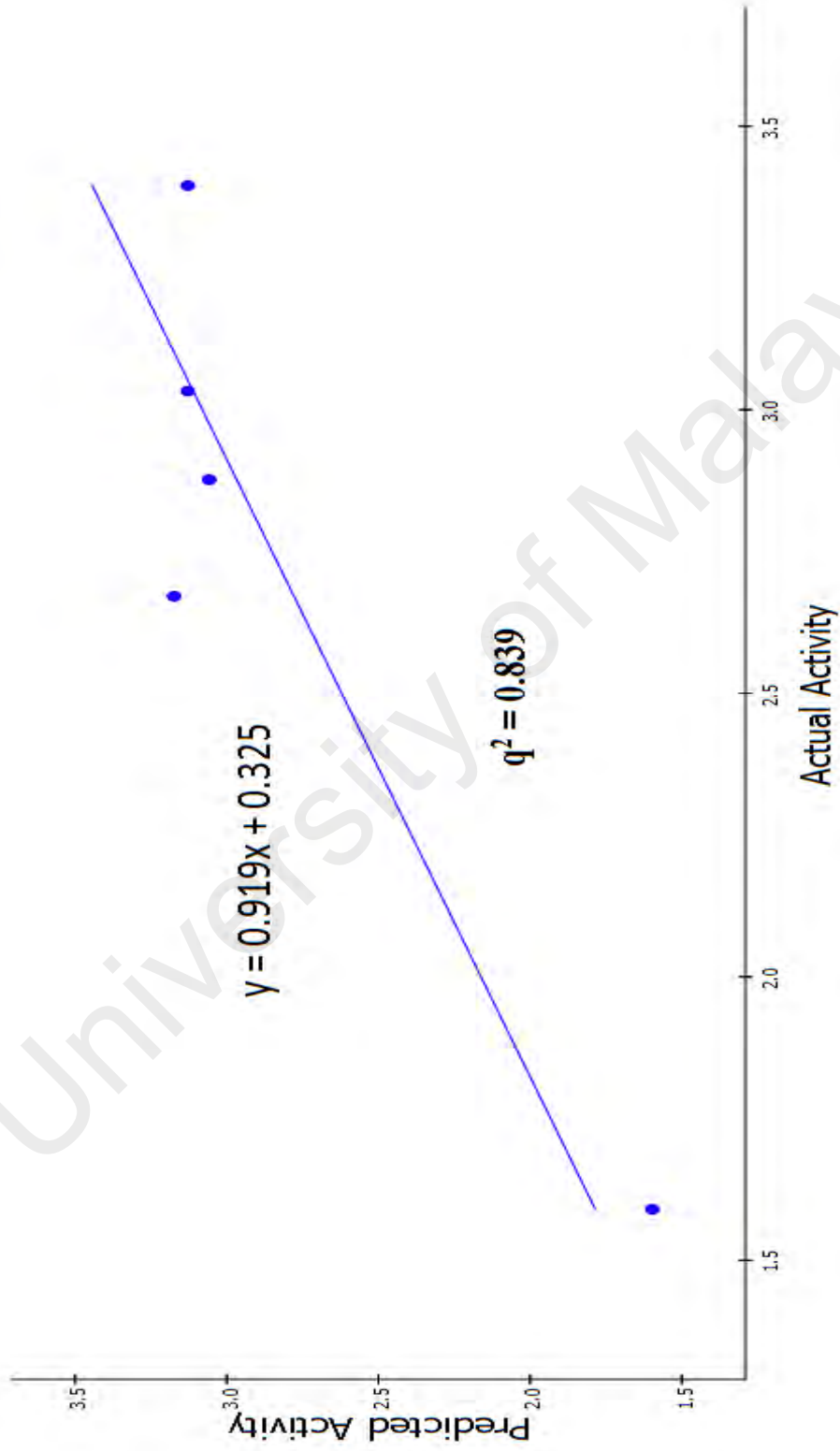
Figure 5.6: Plot of prediction versus actual activity for the test set

The plot shows:
$$y = 0.919x + 0.325$$
$$q^2 = 0.839$$

with axes labeled "Predicted Activity" (vertical) and "Actual Activity" (horizontal).

Table 5.6: Comparison between the original results of the MLR Model with the Y-scramble method

Y-scramble	r^2	r^2LOO	q^2
Original	0.920	0.837	0.839
Trial 1	0.407	0.183	-
Trial 2	0.504	0.225	-
Trial 3	0.349	0.134	-

5.3.1.1 Conclusion of 2D QSAR

The 2D QSAR showed that the model is robust with good correlation coefficient for the training set and test set with the value of r^2=0.920 and q^2=0.839. The model is able to predict the activity of new ligand with good accuracy.

5.3.2   3D QSAR

3D QSAR calculation was done to assess the correlation of the molecular field in a 3D grid by graphic visualisation for a clearer understanding.[22] The steric and electrostatic potential of the compounds were measured using this model. Before running the model, all of the analogues were aligned to the styrene skeleton which is the substructure of the stilbenes (Figure 5.7).
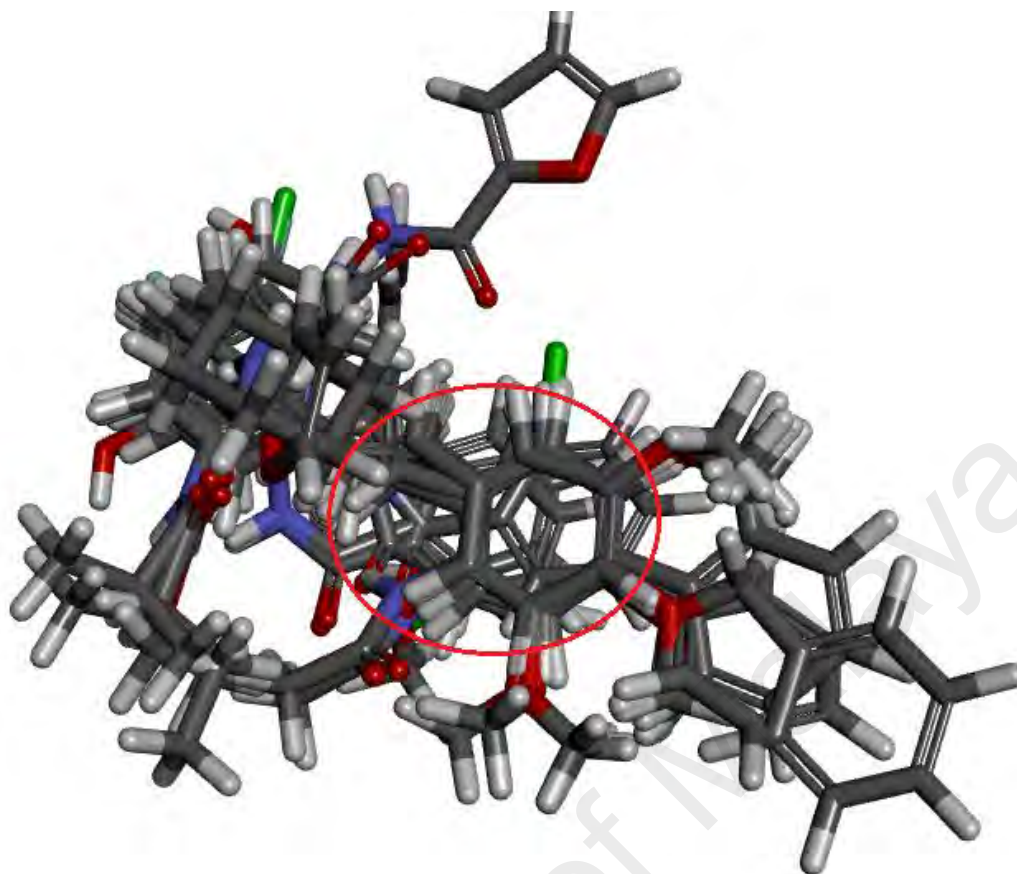
Figure 5.7: Alignment of stilbene analogues.

The algorithm that was used to construct this 3D QSAR model was the partial least square PLS model. From Figure 5.8, the GRID based diagram showed the electrostatic potential in graphical view of correlation that affect the activity of the ligands. The blue coloured contour map showed the positive electrostatic potential at different region of the structure of the ligands that by modifying the analogues with electropositive groups such as NH$_2$ at this region will increase the activity of the ligand. While the red coloured contour showed the negative electrostatic potential. By adding electronegative group such as OH, NO$_2$ and carboxyl into the analogues at the specified region, the activity of the ligand will increase.
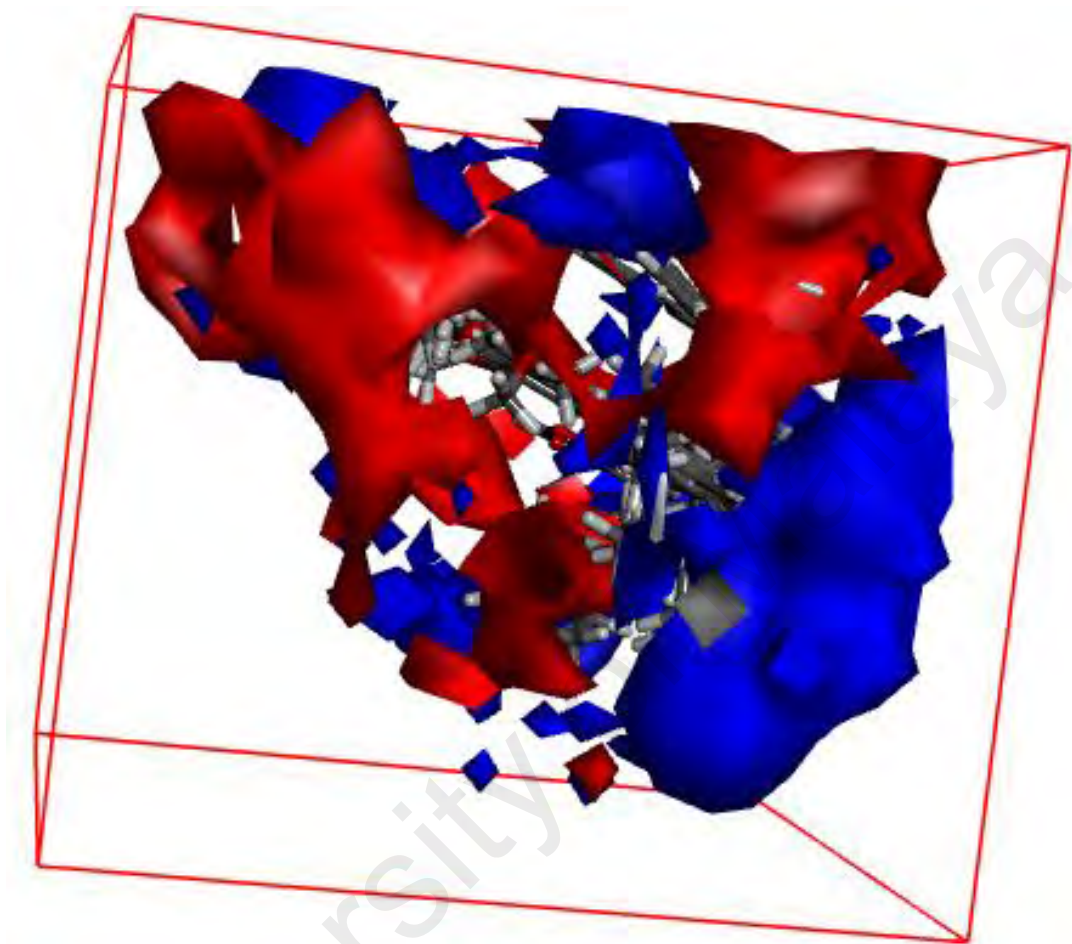
Figure 5.8: 3D QSAR model of the electrostatic potential in GRID based diagram.

From Figure 5.9, the green contour map showed positive Van der Waals interaction, whereby by adding bulky group in the yellow region, it will have profound increase in activity of the ligand. While the yellow contour showed that negative Van der Waals interaction at this region will increase the activity of the ligand.
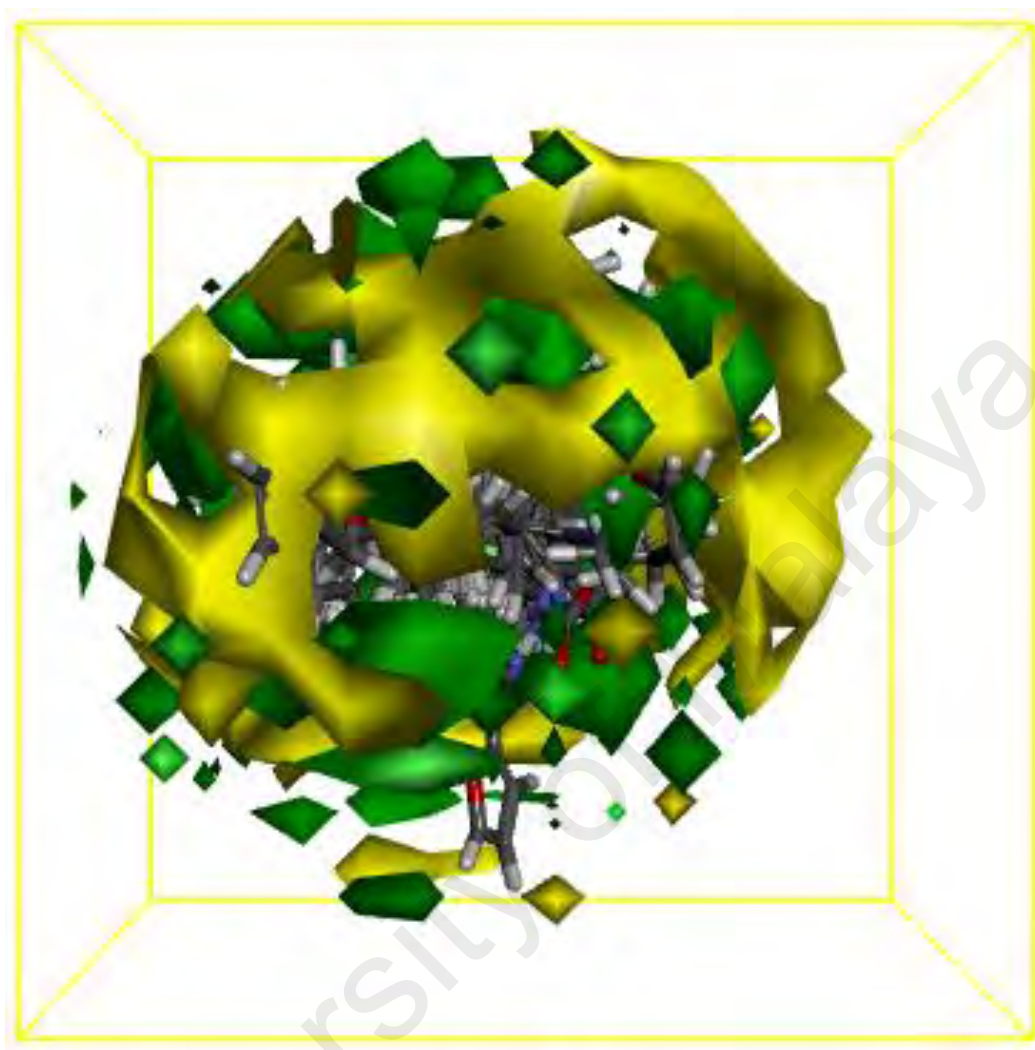
Figure 5.9: 3D QSAR model of the Van der Waals (steric) in GRID based diagram.

The graph correlation of the training set was calculated using the PLS and the correlation coefficient was very high $r^2 = 0.981$ (Figure 5.10). This implied that the 3D model was very robust and powerful. To verify the model is sturdy enough as it seemed, cross validation (21-fold) leave one out (LOO) was done on the model. However the result showed that correlation coefficient for the model r^2LOO is 0.333, which is very low value and showed that it is not a good model for predicting the activity of the ligand (Figure 5.11).
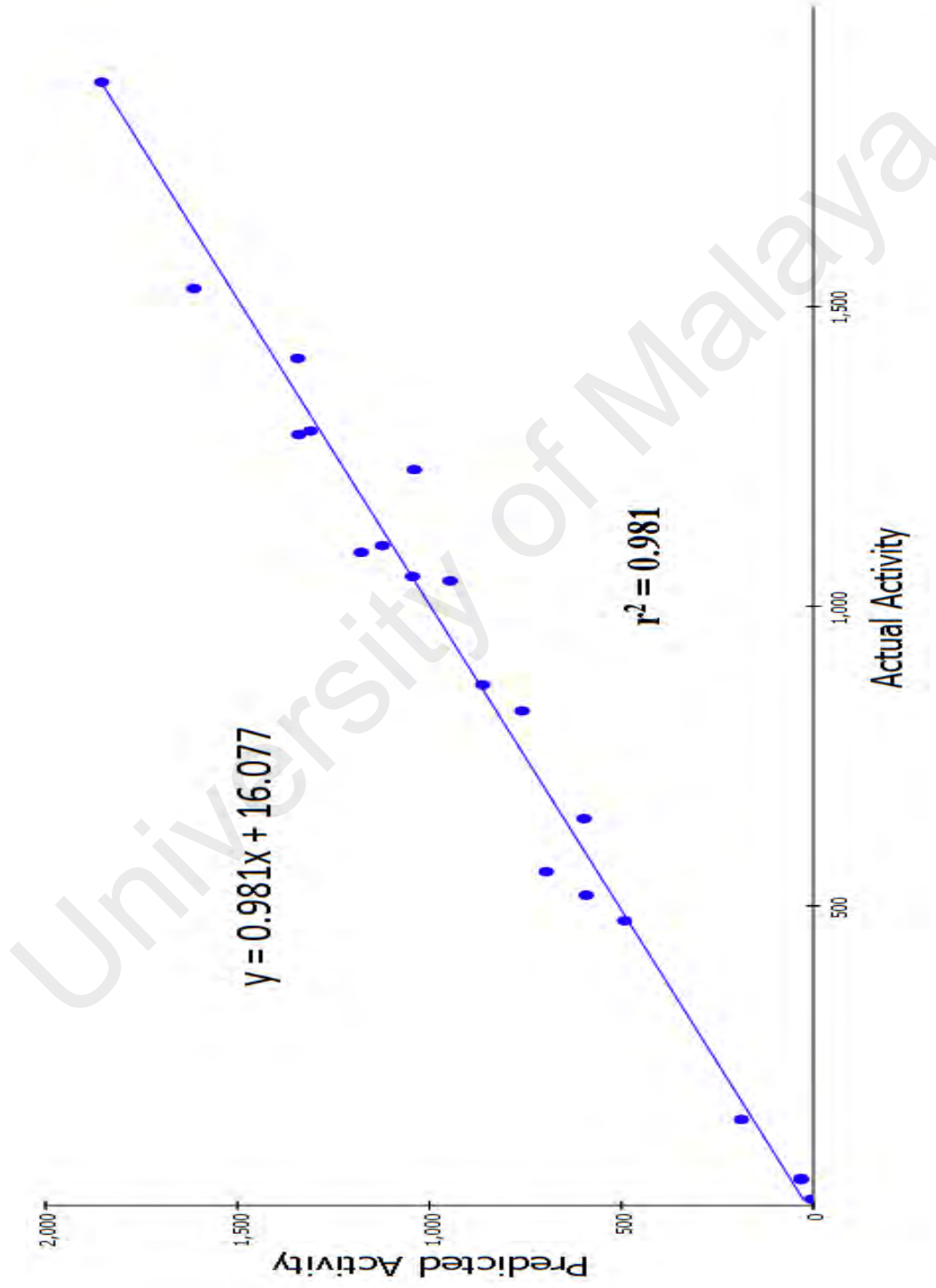
Figure 5.10: Plot of prediction versus actual activity for the training set.

y = 0.981x + 16.077

$r^2 = 0.981$

Actual Activity

Predicted Activity
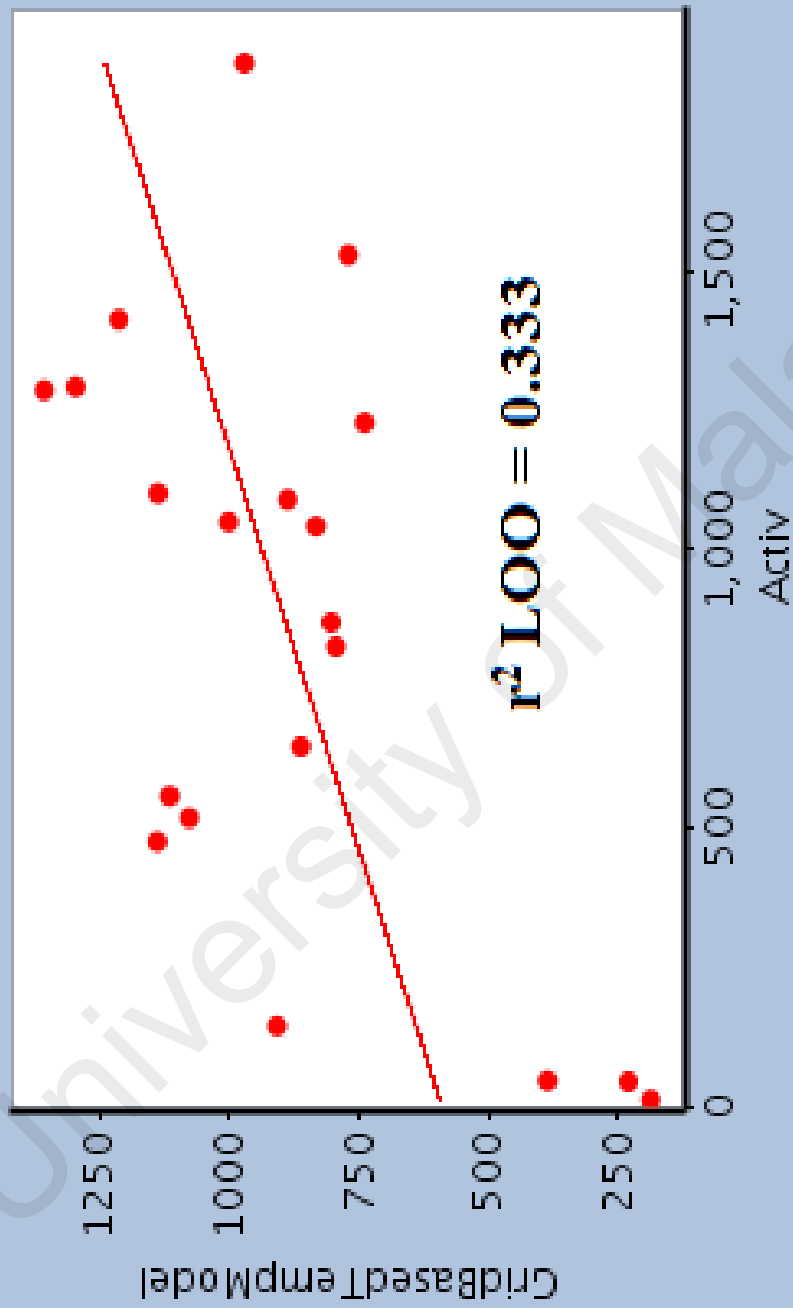
Figure 5.11 : Plot of cross validation LOO of the 3D QSAR model
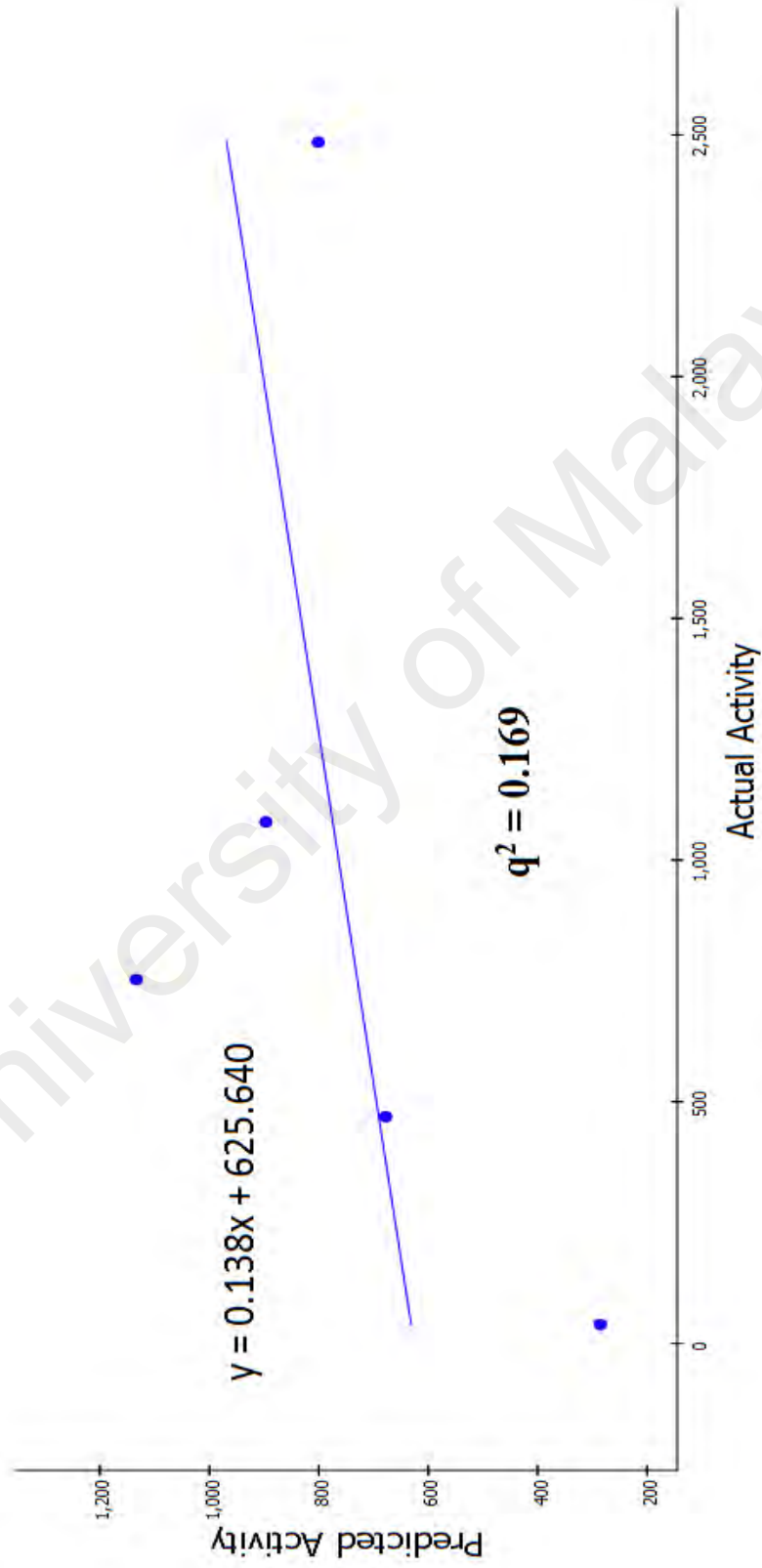
Figure 5.12 : Plot of prediction versus actual activity for the test set

In order to determine whether the model is still worthy of acceptance, an external validation on the model was carried by using the test set of the five ligands. Further disappointing result was received, the correlation coefficient q^2 for the test set was 0.169 (Figure 5.12), even lower than the r^2LOO = 0.333. Y-scramble was used to verify the integrity of this model by reshuffling the activity values of the analogues in the data set (Table 5.7).[21] The Y-scramble result showed that it was the same value as the model for the r^2. This suggested that there was no chance probability in the model and the r^2 was correct.

Table 5.7 : Comparison between the original results of the MLR Model with the Y-scramble method

Y-scramble	r^2	r^2LOO	q^2
Original	0.981	0.333	0.169
Trial 1	0.713	0.298	-
Trial 2	0.609	0.455	-
Trial 3	0.460	0.249	-

5.3.2.1 Conclusion of 3D QSAR

The 3D QSAR model has proven to be unsuitable for predicting the activity for new ligands. While the correlation coefficient for the training set was high r^2=0.981, the cross-validation have shown r^2LOO=0.333 which was low. Moreover, test set showed q^2=0.169 made the model an unreliable prediction tool.

5.3.3 3D QSAR Pharmacophore

Pharmacophore refers to the chemical common features of the molecule that gives activity of the ligands. The process of getting the 3D QSAR pharmacophore features started off with finding the best common pharmacophore features in the data set of analogues using the HipHop algorithm .[9] All of the analogues were aligned together to the structure of styrene which is a substructure of resveratrol. Then the common pharmacophore features that were shared by all of the analogues in the training set were determined.

The common pharmacophore features were hydrogen bond acceptor (HBA), hydrogen bond donor (HBD), hydrophobic and ring aromatic (RA). These four common pharmacophore features were used as parameter in calculating the 3D QSAR Pharmacophore of the training set and 3D QSAR Pharmacophore Generation protocol were selected in DS (Discovery Studio 3.0). Other parameter set is the minimum interfeature distance which was set to 1.00 Å, conformation generation was set to FAST, and the energy threshold was 10 kcal/mol. All other parameters were set to default.

The build-in HypoGen algorithm correlated the structure of the ligand with the activity to generate the pharmacophore model (hypotheses). The result from this calculation was 10 hypotheses. These hypotheses showed the best fit value of the training set and the pharmacophore features that were associated with the hypothesis (Table 5.8)

Table 5.8: Hypotheses of the training set

Hypothesis	r^2	Fit	rmsd	Total Cost	Null Cost Difference	Pharmacophore Feature
1	0.84	7.48	1.3461	76.34	85.35	HBA, HBA, Hydrophobic, RA
2	0.82	5.16	1.4529	82.00	79.69	HBA, HBA, Hydrophobic, RA
3	0.78	4.84	1.5707	86.21	75.48	HBA, HBA, Hydrophobic, RA
4	0.80	4.30	1.5339	86.36	75.33	HBA, HBA, Hydrophobic, RA
5	0.74	5.54	1.7121	89.51	72.18	HBA, HBA, Hydrophobic, RA
6	0.75	4.82	1.6800	89.82	71.87	HBA, HBA, Hydrophobic, RA
7	0.75	4.10	1.6757	91.43	70.26	HBA, HBA, Hydrophobic, RA
8	0.75	4.08	1.6792	91.58	70.10	HBA, HBA, Hydrophobic, RA
9	0.73	4.05	1.7562	94.31	67.38	HBA, HBA, Hydrophobic, RA
10	0.71	3.32	1.8211	95.67	66.02	HBA, HBA, RA

1) Null cost difference = Null Cost - Total cost ; (Null Cost = 161.687).

2) Hydrogen Bond Acceptor (HBA), Hydrogen Bond Donor (HBD), Hydrophobic and

Ring Aromatic (RA). rmsd= root mean square deviation.

163

From Table 5.8 it is shown that Hypothesis 1 is the best 3D QSAR pharmacophore model where the maximum fit value was the highest at 7.48 and the correlation coefficient r^2 was 0.84 for the training set was the highest (Figure 5.14). Cost analysis was applied to show the statistical significance of the hypotheses. The null cost difference (Null Cost - Total cost) was typically used to evaluate the hypotheses. The null cost difference for Hypothesis 1 was also high at 85.53 bits, whereby if the difference is 40-60 bits it shows that the probability is 90%. [23] This showed that Hypothesis1 probability was more than 95%. Hypotheses 1 has the lowest rmsd at 1.3461. The pharmacophore features that Hypothesis 1 maps are two hydrogen bond acceptor (HBA), one hydrophobic and one ring aromatic (RA) (Figure 5.13).
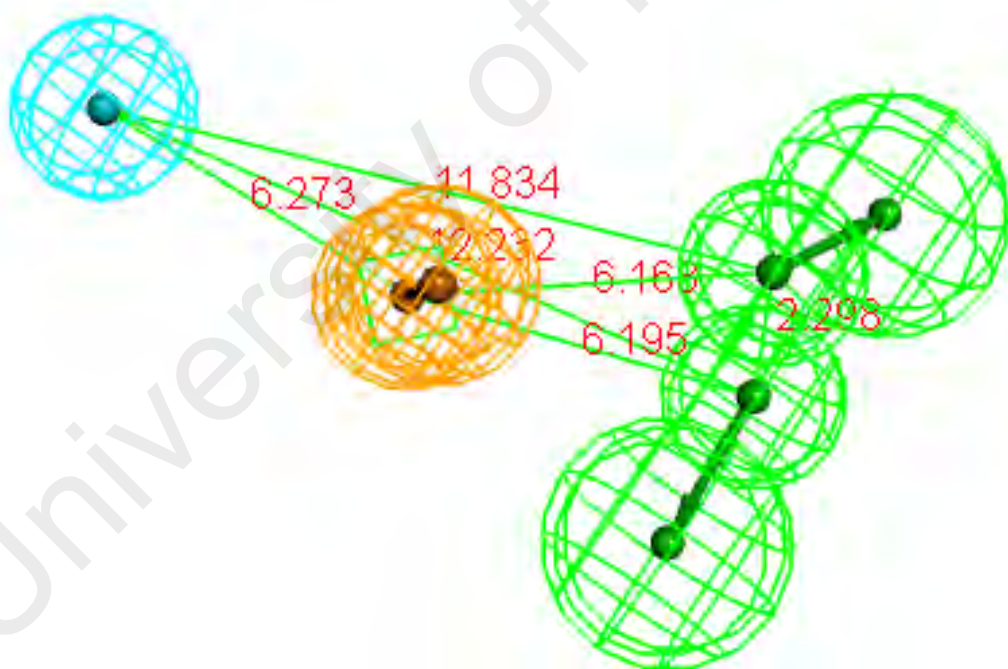
Figure 5.13: Pharmacophore features of Hypothesis 1 with the distance between the

features in Å (Green: HBA1, HBA2, Orange: Ring Aromatic, Cyan: Hydrophobic.

Color code can be found at Accelyris website)
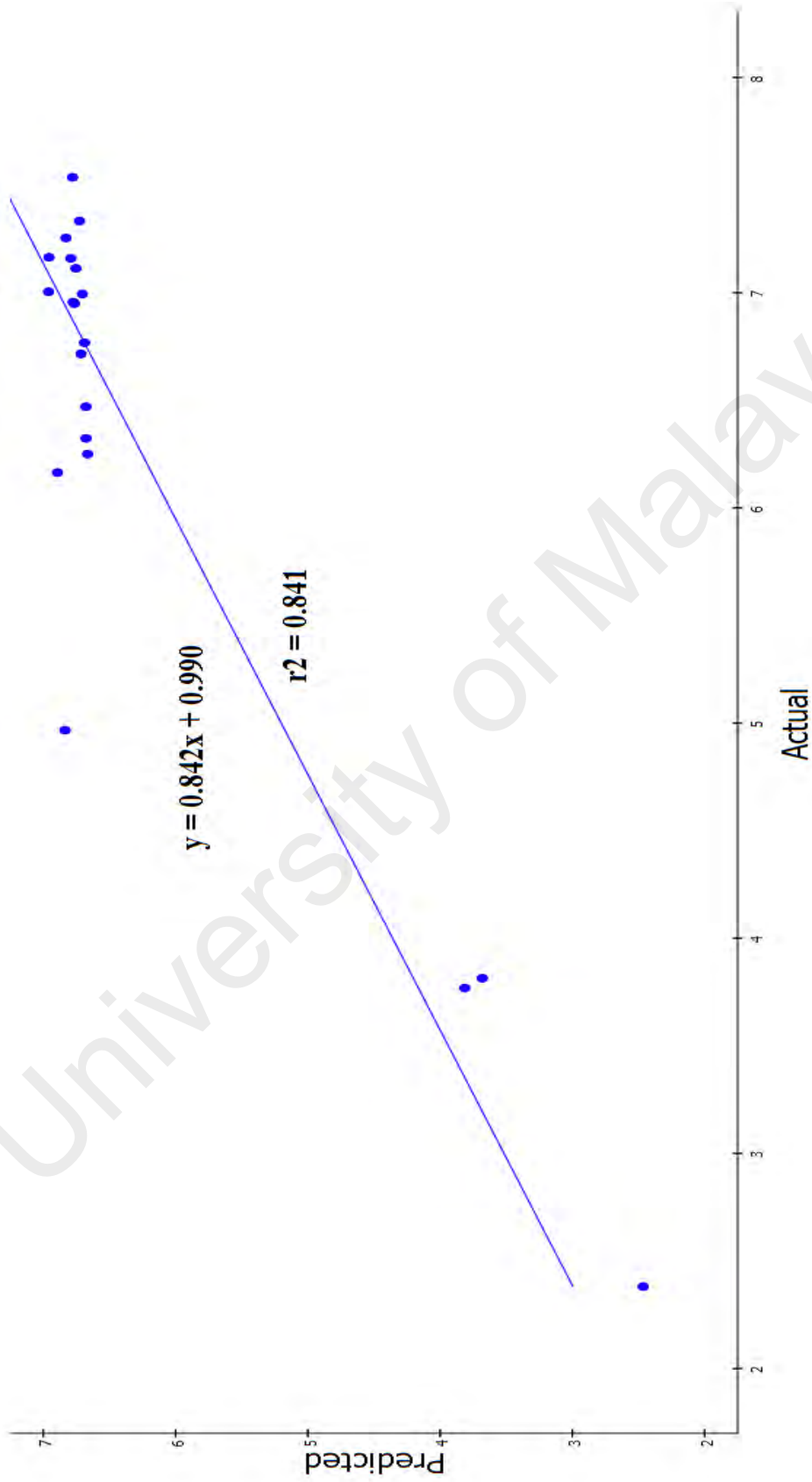
Figure 5.14 : Plot of prediction versus actual activity for the training set

$$y = 0.842x + 0.990$$

$$r2 = 0.841$$

Actual

Predicted

165

Table 5.9: Fit values, feature mapped and predicted values of the training set based on Hypothesis 1

Ligand	Actual activity (µM)	Predicted activity (µM)	Error	Fit value	Feature mapped	Status
146	10.82	11.75	+1.1	5.5618	HBA1,HBA2 Hydrophobic, RA	Active
147	45.34	39.67	-1.1	5.0336	HBA1,HBA2 RA	Moderately active
148	43.33	45.24	+1.0	4.9764	HBA1,HBA2 RA	Moderately active
149	517.87	783.39	+1.5	3.7381	HBA2, Hydrophobic	Moderately active
150	557.13	792.98	+1.4	3.7328	HBA2, Hydrophobic	Moderately active
151	645.6	793.83	+1.2	3.7323	Hydrophobic, RA	Moderately active
152	868.92	802.29	-1.1	3.7277	HBA2 Hydrophobic	Moderately active
153	1,089.81	815.71	-1.3	3.7205	Hydrophobic, RA	Moderately active
154	825.4	824.52	-1.0	3.7159	HBA2 Hydrophobic	Moderately active
83	1,529.95	833.51	-1.8	3.7111	Hydrophobic, RA	Moderately active
155	1,227.91	856.56	-1.4	3.6993	Hydrophobic, RA	Moderately active
156	1,042.2	866.50	-1.2	3.6943	Hydrophobic, RA	Moderately active
108	1,049.5	874.44	-1.2	3.6903	Hydrophobic, RA	Moderately active
157	1,874.3	878.51	-2.1	3.6883	Hydrophobic, RA	Moderately active
158	1,286.35	890.09	-1.4	3.6826	Hydrophobic, RA	Moderately active
104	1,413.52	923.27	-1.5	3.6667	Hydrophobic, RA	Moderately active
1	143.57	929.99	+6.5	3.6636	Hydrophobic, RA	Moderately active
159	475.2	984.57	+2.1	3.6388	Hydrophobic, RA	Moderately active
98	1,292.36	1,049.79	-1.2	3.6110	Hydrophobic, RA	Moderately active
96	1,101.19	1,053.27	-1.0	3.6095	Hydrophobic, RA	Moderately active

Hypothesis 1was used as a model to predict the activity of the 25 ligands training set (Table 5.9). Fit values for the ligands were calculated and the pharmacophore features were mapped onto the ligands using Hypothesis 1.[24] The error between the log value of the actual and predicted values of activity was also presented in Table 5.9. Ligand **146** showed the highest Fit value of 5.56, whereby the predicted activity of 11.75 μM was not far off from the actual value of 10.82 μM with a small error of +1.1. The ligand mapped all of the pharmacophore features of Hypothesis 1 (Figure5.15) which are two hydrogen bond acceptor (HBA1, HBA2), one hydrophobic and one ring aromatic (RA).
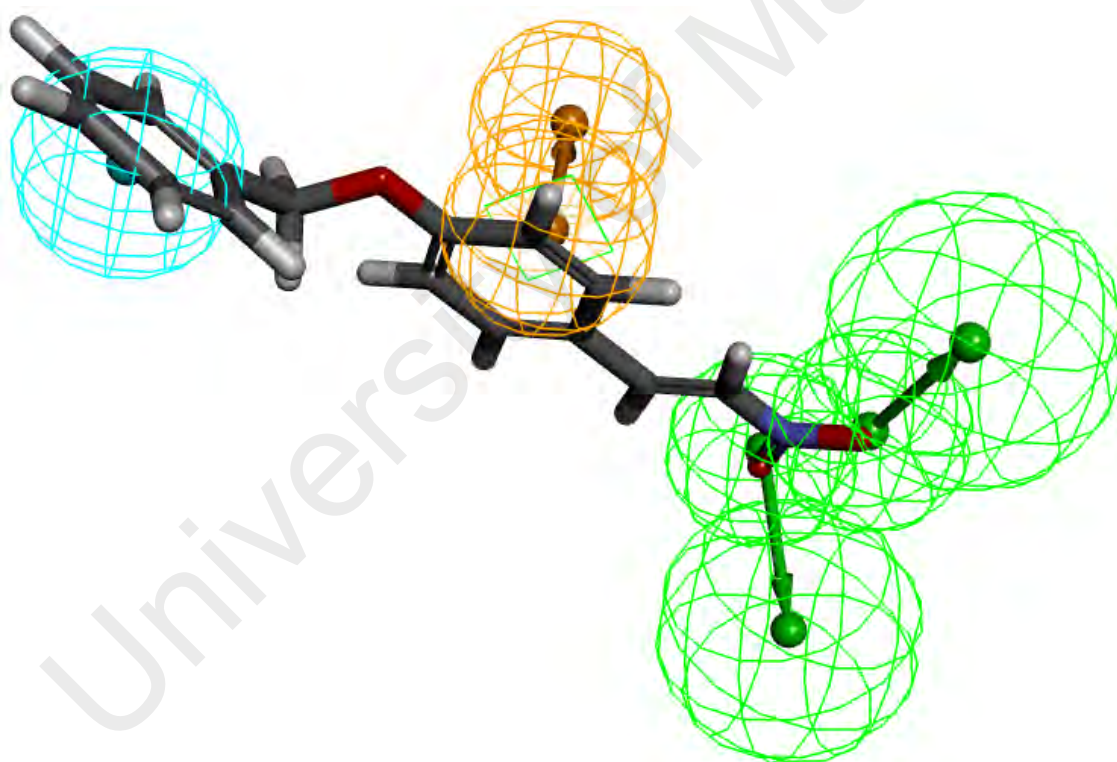
Figure 5.15: Pharmacophore features mapped on **146**

Compared **146** to the least active ligand **96**, the predicted value was 1,053.27 μM with the actual value of 1,101.19 μM. The ligand could only map two phamacophore features that are hydrophobic and ring aromatic (RA) while the two hydrogen bond acceptor (HBA1,HBA2) (Figure 5.16) was not aligned to the structure of ligand **96** thus the Fit value 3.61 was low.
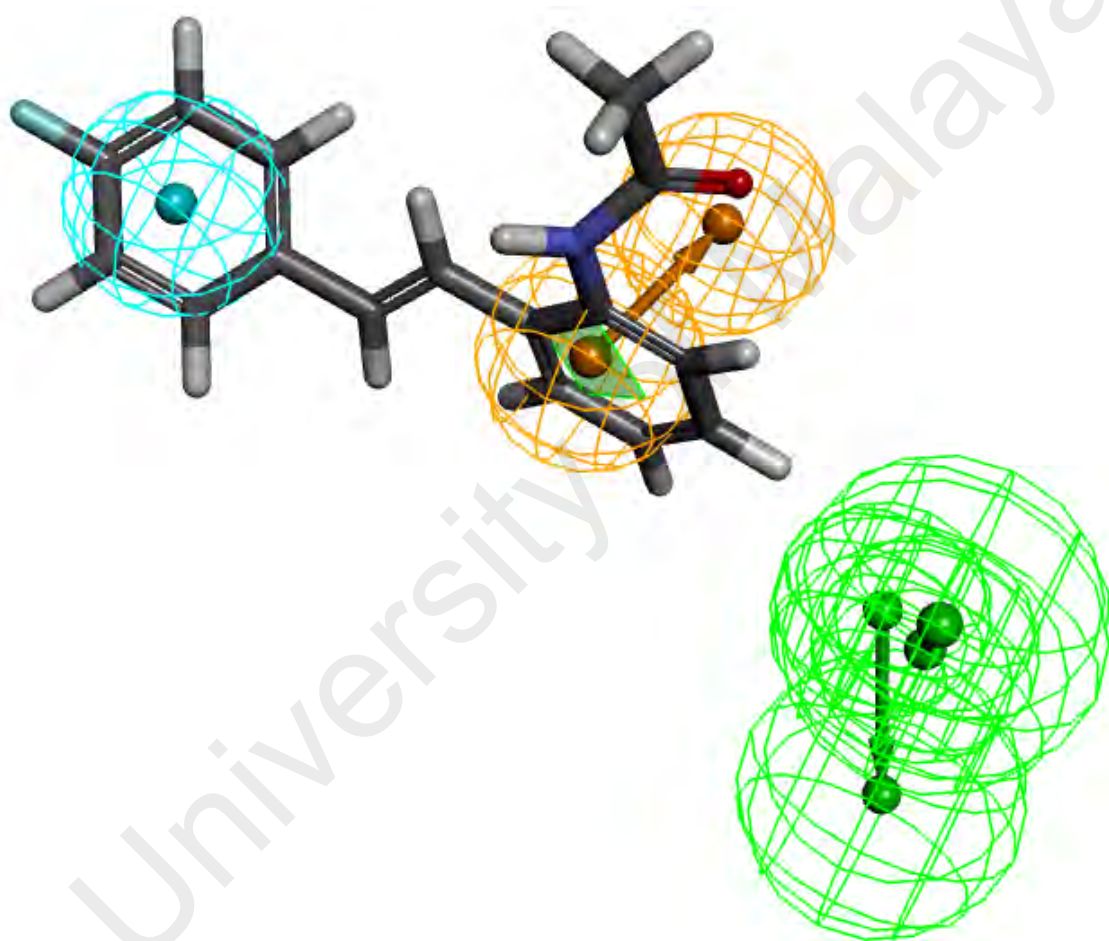
Figure 5.16: Pharmacophore features mapped on **96**

Then Hypothesis 1 was validated with the test set and resulted with $q^2 = 0.84$, this show the pharmacophore model was reliable and robust in predicting new compounds (Figure 5.17).
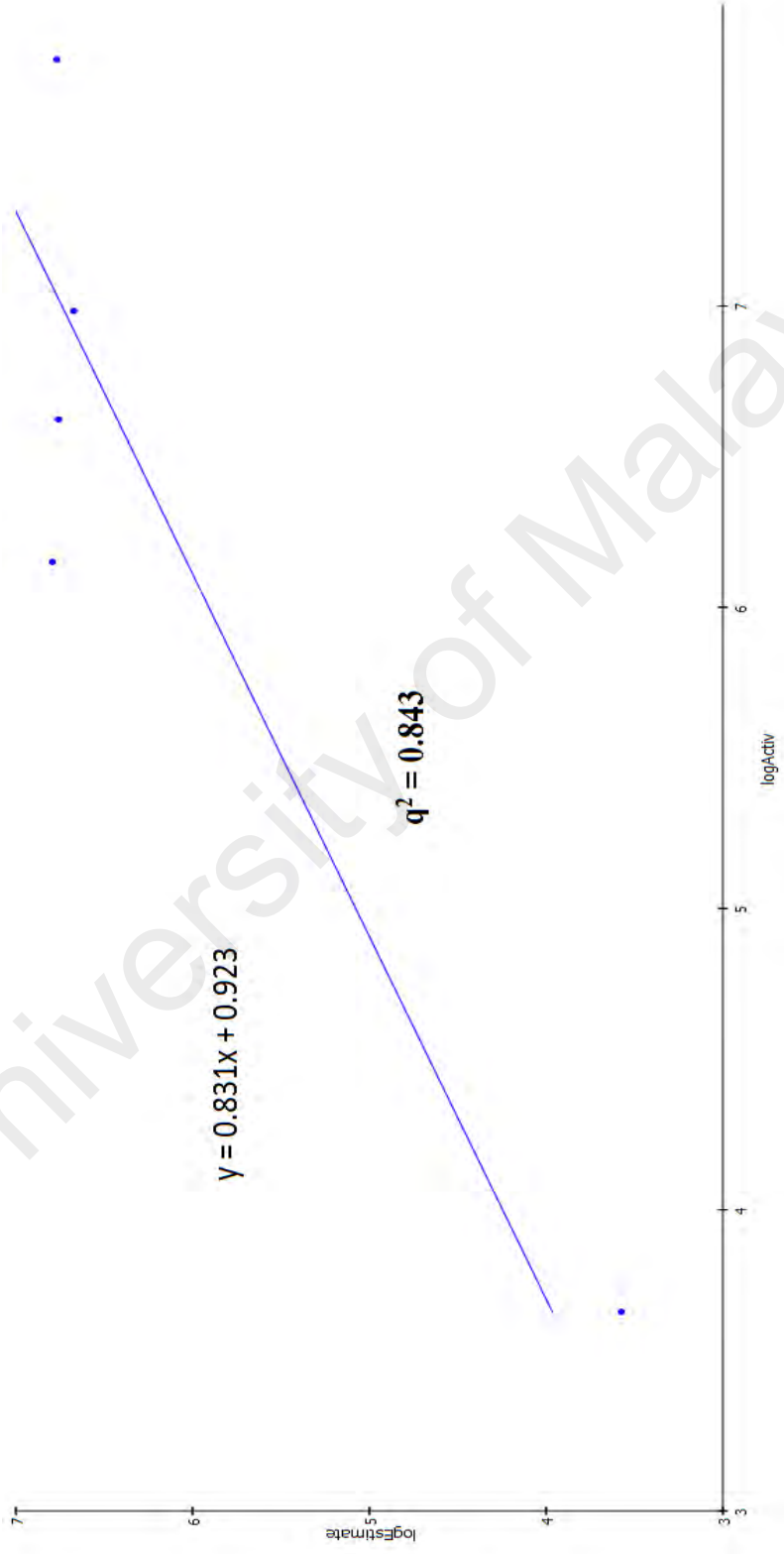
Figure 5.17 : Plot of prediction versus actual activity for the test set

$y = 0.831x + 0.923$

$q^2 = 0.843$

From Table 5.10, the most active compound, **163** displayed 38.9 µM compared with the predicted value of 35.68 µM. The predicted value was near to the actual value showing that the test model was good and reliable.

Table 5.10 : Test set values of actual and predicted IC_{50}

Compound	Actual IC_{50} (µM)	Predicted IC_{50} (µM)
102	752.7	861.25
160	468.93	891.53
161	2,484.90	869.82
162	1,078.76	790.03
163	38.9	35.68

A Y-scramble method was initiated on the training and test set to validate the model that no occurrence of chance probability exists. The result is shown in Table 5.11 and proved that Hypothesis 1 model was a very reliable model.

Table 5.11: Y-scramble for r^2

Y-scramble	r^2	q^2
Original	0.841	0.843
Trial 1	0.582	-
Trial 2	0.426	-
Trial 3	0.401	-

5.3.3.1 Conclusion of 3D QSAR Pharmacophore

Hypothesis 1 has shown to be the best Fit 7.48 with a high null cost difference of 85.53 bits implied high probability of prediction more than 90%. With a correlation coefficient of $r^2 = 0.841$ and $q^2 = 0.843$, this shows that this model is robust and good in predicting new ligand.

5.4   Conclusion

Three QSAR methods were carried out on the ligands to find which type is suitable in predicting the activity of the ligands. It is found that 2D QSAR was the most suitable method with the r^2 and q^2 showing high degree of correlation. While 3D QSAR have the highest r^2 of 0.981 but the test set was a failure with a very low q^2 value of 0.169 making it an unsuitable model. 3D QSAR Pharmacophore showed a very good value for r^2 of 0.841 with the q^2 0.843 a little bit higher than 2D QSAR. The 3D QSAR Pharmacophore have an advantage compared to 2D QSAR in that it showed the ligand in 3D structure with the pharmacophore features aligned to the ligand making it easier to visualize which part of the molecule that contribute to the pharmacophore.

Table 5.12 : r^2 and q^2 values of the three QSAR method

QSAR	r^2	q^2
2D QSAR	**0.920**	**0.839**
3D QSAR	0.981	0.169
3D QSAR Pharmacophore	**0.841**	**0.843**

5.5 References

1   H. Kubinyi, *Quant. Struct.-Act. Relat.*, 2002, **21**, 348.
2   C. Hansch, *J. Comput. Aided Mol. Des.*, 2011, **25**, 495.
3   A. Crum Brown and T. R. Fraser, *Trans. Roy. Soc. Edinburgh*, 1868, **25**, 151.
4   H. Meyer, *Arch. Exp. Pathol. Pharmakol.*, 1897, **38**, 336.
5   C. Hansch, R. M. Muir, T. Fujita, P. P. Maloney, F. Geiger and M. Streich, *J. Am. Chem. Soc.*, 1963, **85**, 2817.
6   S. M. Free and J. W. Wilson, *J. Med. Chem.*, 1964, **7**, 395.
7   R. Langridge, T. Ferrin, I. Kuntz and M. Connolly, *Science*, 1981, **211**, 661.
8   R. D. Cramer, D. E. Patterson and J. D. Bunce, *J. Am. Chem. Soc.*, 1988, **110**, 5959.
9   T. Langer and R. D. Hoffmann, *Pharmacophores and Pharmacophore Searches*, Wiley VCH, Weinheim, 2006.
10 D. C. Young, *Computational Chemistry: A Practical Guide for Applying Techniques to Real-World Problems,* John Wiley & Sons, New York, 2001.
11 H. D. Holtje and G. Folkerts, *Molecular Modeling : Basic Principles and Applications*, VCH, Weinheim, 1996.
12 A. R. Leach, *Molecular Modelling Principles and Applications*, Pearson Education Limited, Harlow, 2001.
13 F. Jensen, *Introduction to Computational Chemistry,* John Wiley and Sons, Chichester, 1999.
14 K. I. Ramachandran, G. Deepa and K. Namboori, *Computational Chemistry and Molecular Modeling,* Springer, Berlin, 2008.
15 A. Pedretti, L. Villa and G. Vistoli, *J. Comput. Aided Mol. Des.*, 2004, **18**, 167.
16 J. D. C. Maia, G. A. U. Carvalho, C.P. Mangueira, Jr., S. R. Santana, L. A. F. Cabral and G. B. Rocha, *J. Chem. Theory Comput.*, 2012, **8**, 3072.
17 H. van de Waterbeemd, *Advanced Computer-Assisted Techniques in Drug Discovery,* VCH, Weinheim, 1994.
18 B. A. Bunin, B. Siesel, G. A. Morales and J. Bajorath, *Chemoinformatics: Theory, Practice, and Products,* Springer, Dordrecht, 2007.
19 C. Enguehard-Gueiffier, S. Musiu, N. Henry, J. B. Veron, S. Mavel, J. Neyts, P. Leyssen, J. Paeshuyse and A. Gueiffier, *Eur. J. Med. Chem.*, 2013, **64**, 448.
20 S. O. Podunavac-Kuzmanovic, D. D. Cvetkovic, L. R. Jevric and N. J. Uzelac, *Acta Chim. Slov.*, 2013, **60**, 26.
21 C. Rucker, G. Rucker and M. Meringer, *J. Chem. Inf. Model.*, 2007, **47**, 2345.
22 Y.S. Yang, Q. S. Li, S. Sun, Y. B. Zhang, X. L. Wang, F. Zhang, J. F. Tang and H. L. Zhu, *Bioorg. Med. Chem.*, 2012, **20**, 6048.
23 A. H. Al-Nadaf and M. O. Taha, *J. Mol. Graph. Model.*, 2011, **29**, 843.
24 Y. K. Chiang, C. C. Kuo, Y. S. Wu, C. T. Chen, M. S. Coumar, J. S. Wu, H. P. Hsieh, C. Y. Chang, H. Y. Jseng, M. H. Wu, J. S. Leou, J. S. Song, J. Y. Chang, P. C. Lyu, Y. S. Chao and S. Y. Wu, *J. Med. Chem.*, 2009, **52**, 4221.

Chapter 6

Conclusion

A total of nine halogenated acetamido stilbenes (**96, 98, 100, 102, 104, 106, 108, 110, 112**) bearing electron-withdrawing group (F, Cl and Br) were synthesized through the Heck coupling. These halogenated acetamido stilbenes were then subjected to Lewis acid, $FeCl_3$. $FeCl_3$ is a known single electron oxidant whereby in this study, the $FeCl_3$ assisted in the transformation of the halogenated acetamido stilbenes into imines (**121, 122, 123, 124, 125, 126, 127, 128, 129**). Looking back on previous reports on $FeCl_3$ reactions on stilbenes, the products were mostly indolines, bisindolines and a unique indolostilbenes. Previous studies incorporated the electron donating group of methoxy in the stilbenes while this research focused on the electron withdrawing group on the stilbenes and reported interesting results on the formation of the imines. Another Lewis acid, $SnCl_4$ was studied on the reaction with the halogenated acetamido stilbenes. The $SnCl_4$ mediated reaction of stilbenes produced indolines (**139**, **140, 141, 142, 143, 144, 145**) and the electron donating and withdrawing group on the stilbenes also played a role in the reaction. Methoxy group (electron donating) helped to complete the reaction faster with mild conditions. The halogen electron-withdrawing group needed more time to complete the reaction on a harder reaction condition (see chapter 3.3.4).

Five halogenated acetamido stilbenes (**96, 98, 102, 104, 108**) were subjected to five cancer cells and one normal human cell; colon cancer (HT-29), estrogen-sensitive breast cancer (MCF-7), estrogen-insensitive breast cancer (MDA-MB-231), prostate cancer (DU-145), pancreatic cancer (BxPC-3) and normal pancreatic cells (hTERT-HPNE). Stilbene **98** displayed various and good cytotoxicity activity against MCF-7 (32.52 μM), HT-29 (11.40

μM), BxPC-3 (129.78 μM) and DU-145 (16.68 μM). Interestingly, it is not cytotoxic toward normal pancreatic cells (hTERT-HPNE). Quantitative Structure Activity Relationship (QSAR) studies were performed on 25 stilbene ligands. Three QSAR models; 2D QSAR, 3D QSAR and 3D QSAR Pharmacophore were undertook on the stilbene ligands. 3D QSAR Pharmacophore was seen as the best overall model for this QSAR study with an r^2= 0.841 and q^2=0.843, and with the graphic visualization of the chemical pharmacophore made it reasonably well understood.

Results from these studies can be used to further investigate and synthesize more compounds with potential cytotoxic activity based on the SAR and QSAR results. In addition further investigation can be pursued to investigate possible reaction of various amido stilbenes with Lewis acid apart from $FeCl_3$ and $SnCl_4$ to give a variety of new chemical product.

Publications

Peer-reviewed articles

1) Azmi, M.N., Din, M.F.M, Kee, C.H., Suhaimi, M., Ang, K.P., Ahmad, K., Nafiah, M.A., Thomas, N.F. Mohamad, K., Leong, K.H. and Awang, K. (2013). Design, Synthesis and Cytotoxic Evaluation of o-Carboxamido Stilbene Analogues. *Int. J. Mol. Sci.* , **14**, 23369-23389.

2) Ahmad, K., Thomas, N.F., Din, M.F.M, Awang, K. and Ng, S.W. (2009). *N'-{2-[2-(4-Methoxyphenyl)ethenyl]-phenyl}acetamide*. *Acta Crystallographica Section E - Structure Reports*, **E65**, o1289.

Oral presentation

1) Mohd Fadzli Md Din, Mohamad Nurul Azmi, Chin Hui Kee, Munirah Suhaimi, Ang Kheng Ping, Kartini Ahmad, Mohd Azlan Nafiah, Noel F. Thomas, Khalit Mohamad, Kok Hoong Leong and Khalijah Awang. *Synthesis and cytotoxic evaluation of stilbene analogues*.The 2nd International Conference of the Indonesian Chemical Society 2013 (20-23rd October 2013).